Francisco José Dinis de Sousa Fernandes Ganhão
Mestre

Energy-efficient Diversity Combining for Different Access Schemes in a Multi-Path Dispersive channel

Dissertação para obtenção do Grau de Doutor em
Engenharia Electrotécnica e Computadores

Orientador: Prof. Dr. Rui Dinis, FCT-UNL
Co-Orientador: Prof. Dr. Luis Bernardo, FCT-UNL

Júri:

Presidente: Prof. Dr. Paulo Pinto, FCT-UNL
Primeiro Arguente: Prof. Dr. António Grilo, Universidade de Aveiro
Segundo Arguente: Prof. Dr. Adão Silva, IST-UL
Vogal: Prof. Dr. Nuno Souto, ISCTE-IUL

FACULDADE DE CIÊNCIAS E TECNOLOGIA
UNIVERSIDADE NOVA DE LISBOA

Janeiro, 2014

Energy-efficient Diversity Combining for Different Access Schemes in a Multi-Path Dispersive channel

To my Mother
and Late Grandmother

Acknowledgements

The last four years remarked perhaps the best years of my life where I withstood immense life lessons, some of them quite life changing, while others contributed for a better self. Obviously, no man or woman can complete his or hers *Sistine Chapel* without relying in his or hers support group. I was fortunate enough in the last four years to be surrounded by top performers, as well as philosophers, but most importantly by my friends and family.

First of all, I would like to share my gratitude towards my supervisors, they were kind enough to take me *under their wing* and give me insightful lessons from research. Professor *Luis Bernardo* was always helpful, kind and patient, and never stopped to amaze me with his knowledge – wealthy and deep knowledge that you cannot meet its end. Professor *Rui Dinis* was always cheerful and pragmatic, plus, nothing seems to stop him from moving forward – in a good sense. I am very thankful and honored for their support.

Professors *Rodolfo Oliveira* and *Paulo Pinto* were always helpful when needed, both had a sixth sense to spot inaccuracies and grammatical sentences that did more harm than good – without their help our published work would be indeed poorer and perhaps unpublished.

Professor *Marko Beko* had a small but important role in my late *PhD* student publications, I would like to thank him for his work.

Professor *Paulo Montezuma* was always helpful and entertaining to talk with for most of the time – our random encounters in the corridor were always instructional about history and other matters related to society.

Professor *Pedro Amaral*, despite not contributing directly to this thesis, he had an important role during my *MSc.* thesis, without him I believe I would not have pursued a *PhD* degree. Plus, it was always interesting to talk about *outside* subjects from research with him.

Professor *Mário Macedo* parted too soon and I would like to remember his contributions before passing away – he will be always remembered.

Despite not being from our *beloved* campus, Professor *Paulo Pereira* had a small but important role in my early *PhD* student publications, I would like to thank him for his input.

Professor *Manuel Esquível* taught me the basics of *Stochastic Processes* in a pragmatic manner and I will fondly miss those classes during my first years as a graduate student. In my point-of-view every engineering student should learn *Stochastic Processes* with him!

Most importantly, I would like to appreciate and show gratitude towards the *Fundação para a Ciência e Tecnologia* for enabling me to pursue my *PhD* degree with a scholarship awarded by personal merit – despite this, difficult times are coming for Portuguese research in terms of funding, which is sad.

Besides the Professors who had an impact during the last four years, my fellow *PhD* colleagues also played an important role. Dr. *Miguel Pereira* had a great impact for the last four years, first because my work *inherits his legacy*; second, he had a crucial role in managing our room's network, a task I believe I am not befitted as much as I want to; third, it is sad to see him go for newer ventures, he was an integral part of the team. *Miguel Luis* has been a close colleague for several years and it has been great to see us both *grow* in the the world of research; without him, staying up late working would not be as fun as it is, besides I am thankful for making great singing duets and for learning Stochastic Processes with him – our mutual need for helping each other's work has been the most satisfying experience for the last five years. *José Lima* was also a positive influence outside of research, without him I would not think *outside of the box*, quite literally, I admire him for his entrepreneurial attitude. *Miguel Luzio* has been a great influence for the last four years (and more), he is well rounded in most aspects of life and very knowledgeable about his trade, without him I would not have experienced life to the fullest in an RV van while traveling in North American soil – I am thankful for that experience, besides being one of my closest friends. *Fábio Silva* has always been empathetic, even though he had little time and for that I am very grateful. *Slavisa Tomic* has played an integral part of my last years as a *PhD* student, I am grateful and honored to meet such a *courageous and integer* individual – always cracking jokes and always ready to help you, there is not any better combination than that. Other honorable mentions from our campus are: *João Melo*, *Pedro Magalhães*, *Gonçalo Luis*, *Rui Lopes*, *Michael Figueiredo*, *Edinei Santin*, *Ivan Yuri*, *António Furtado*, *Rui Rodrigues*, *Filipe Casal Ribeiro*, *Filipa Lourenço*, *Ali Shaarbaf* and *Hugo Viana*.

Colleagues are important, but friends are also an integral part of our lives. *Filipe Dias* during my first years as a *PhD* student was very empathetic and supportive in difficult times and for that I am very grateful. *Ricardo Gomes* has always been a voice of *reasoning* and always made *insightful* points about my life. *Hugo Lopes* has also played an important role for the last two to three years, always with his feet in the ground and reminding me that things are perhaps simpler than they are. *Sérgio Dias*, despite his *Bohemian* approach to life, has been of great help, without him I would be seriously burnout during my last summer as a *PhD* student. Other honorable mentions: *Susana Rolo*, *Filipa Ruiz*, *Susana Mata*, *Raquel Reis*, *Mariana Oliveira*, *António Rocha*, *Pawel Pankiewicz*, *João Costa* and *Dalila Forte*.

My cats, *PeeWee and Tofu*, were also an integral part of my distracting writing!

Finally, and most importantly I am thankful for the emotional support of my Mother and Grandmother; sadly the passing of my Grandmother left me emotionally wounded, but allowed me to rethink better about my life, she will be sorely missed.

For all of those that I forgot – *Sorry for forgetting about you!*.

To all of you, thank you!

Francisco Ganhão

Abstract

The forthcoming generation of mobile communications, 5G, will settle a new standard for a larger bandwidth and better Quality of Service (QoS). With the exploding growth rate of user generated data, wireless standards must cope with this growth and at the same time be energy efficient to avoid depleting the batteries of wireless devices. Besides these issues, in a broadband wireless setting QoS can be severely affected from a multipath dispersive channel and therefore be energy demanding.

Cross-layered architectures are a good choice to enhance the overall performance of a wireless system. Examples of cross-layered Physical (PHY) - Medium Access Control (MAC) architectures are type-II Diversity Combining (DC) Hybrid-ARQ (H-ARQ) and Multi-user Detection (MUD) schemes. Cross-layered type-II DC H-ARQ schemes reuse failed packet transmissions to enhance data reception on posterior retransmissions; MUD schemes reuse data information from previously collided packets on posterior retransmissions to enhance data reception. For a multipath dispersive channel, a PHY layer analytical model is proposed for Single-Carrier with Frequency Domain Equalization (SC-FDE) that supports DC H-ARQ and MUD. Based on this analytical model, three PHY-MAC protocols are proposed. A cross-layered Time Division Multiple Access (TDMA) scheme that uses DC H-ARQ is modeled and its performance is studied in this document; the performance analysis shows that the scheme performs better with DC and achieves a better energy efficiency at the cost of a higher delay. A novel cross-layered prefix-assisted Direct-Sequence Code Division Multiple Access (DS-CDMA) scheme is proposed and modeled in this document, it uses principles of DC and MUD. This protocol performs better by means of additional retransmissions, achieving better energy efficiency, at the cost of higher redundancy from a code spreading gain. Finally, a novel cross-layered protocol H-ARQ Network Division Multiple Access (H-NDMA) is proposed and modeled, where the combination of DC H-ARQ and MUD is used with the intent of maximizing the system capacity with a lower delay; system results show that the proposed scheme achieves better energy efficiency and a better performance at the cost of a higher number of retransmissions.

A comparison of the three cross-layered protocols is made, using the PHY analytical model, under normalized conditions using the same amount of maximum redundancy. Results show that the H-NDMA protocol, in general, obtains the best results, achieving a good performance and a good energy efficiency for a high channel load and low Signal-to-Noise Ratio (SNR). TDMA with DC H-ARQ achieves the best energy efficiency, although presenting the worst delay. Prefix-assisted DS-CDMA in the other hand shows good delay results but presents the worst throughput and energy efficiency.

Keywords. NDMA; DS-CDMA; TDMA; H-ARQ; Multipacket Reception; Multi-user Detection; H-NDMA; EPUP; Analytical Performance; IB-DFE; PHY-MAC; Cross-layer.

Resumo

A próxima geração de comunicações móveis, 5G, irá estabelecer um novo *standard* para uma largura de banda maior e melhor qualidade de serviço. Com o ritmo de crescimento explosivo de conteúdo gerado por utilizadores, os *standards* de comunicações sem fios devem acompanhar este crescimento e ao mesmo tempo serem energeticamente eficientes de forma a evitar que as baterias dos dispositivos móveis se esgotem. Para além destes problemas, num contexto de banda larga sem fios, a qualidade de serviço pode ser seriamente comprometida por um canal multi-percurso dispersivo e extremamente exigente em termos energéticos.

As arquitecturas com optimização entre camadas (cross-layer) são uma boa opção para a melhoria de desempenho de um sistema sem fios. Como exemplos de arquitecturas com optimização entre as camadas PHY e MAC temos H-ARQ de tipo II com *Diversity Combining* (DC) e esquemas de *Multiple User Detection* (MUD). Esquemas com DC H-ARQ de tipo II reutilizam as transmissões de pacotes com erros para melhorar a recepção de dados em retransmissões posteriores; esquemas MUD reutilizam os dados de pacotes com erros, derivado a uma colisão de pacotes, para melhoria da recepção de dados em retransmissões posteriores. Para um canal multi-percurso dispersivo, é proposto para a camada PHY um modelo analítico para SC-FDE que suporta DC H-ARQ e MUD. Com base neste modelo analítico, são propostos três protocolos PHY-MAC. Um esquema de controlo *Time Division Multiple Access* (TDMA) que usa DC H-ARQ é modelado e o seu desempenho é estudado neste documento; a análise de desempenho mostra que este esquema tem melhor desempenho com DC e que consegue uma eficiência energética melhor a custo de um atraso maior. Um esquema inovador, *Direct Sequence Code Division Multiple Access* (DS-CDMA) com prefixo cíclico, é proposto e modelado neste documento. O esquema utiliza princípios de DC e MUD. O protocolo tem um melhor desempenho com retransmissões adicionais e é energeticamente eficiente a custo de um ganho de código de espalhamento. Finalmente, é proposto e modelado um protocolo inovador, *H-ARQ Network Diversity Multiple Access* (H-NDMA), sendo combinados H-ARQ e MUD com o intuito de maximizar a capacidade de sistema com menor atraso; o desempenho do sistema mostra que o protocolo é energeticamente eficiente e com melhor desempenho a custo de um maior número de retransmissões.

Uma comparação entre os três protocolos é feita recorrendo ao modelo analítico da camada PHY, sob condições normalizadas para a mesma quantidade de redundância. Resultados mostram que o esquema H-NDMA obtém no geral os melhores resultados, especialmente um bom desempenho e uma boa eficiência energética para um canal saturado e uma relação sinal-ruído baixa. TDMA com DC H-ARQ consegue a melhor eficiência energética, apesar de apresentar piores resultados em termos de atraso de recepção de dados. DS-CDMA com prefixo cíclico mostra um bom desempenho de atraso, mas no entanto, tem os piores resultados em termos de energia e de débito.

Contents

List of Figures

List of Tables

Acronyms

ACK ACKnowledgment 16

ARQ Automatic Repeat reQuest 53

ATM Asynchronous Transfer Mode 21

AWGN Additive White Gaussian Noise 58

BEB Binary Exponential Backoff 16

BER Bit Error Rate 25

BS Base Station 1

B-NDMA Blind NDMA 26

BPSK Binary Phase Shift Keying 58

BTMA Busy Tone Multiple Access 15

CA Collision Avoidance 29

CC Code Combining 24

CDMA Code Division Multiple Access 2

C-NDMA Cooperative NDMA 27

CP Cyclic Prefix 11

CPI Cyclic Prefix Insertion 11

CRC Cyclic Redundancy Check 91

CRDSA Collision Resolution Diversity Slotted ALOHA 30

CSI Channel State Information 29

CSMA Carrier Sense Multiple Access 15

CTS Clear to Send 15

DA Demand Assignment 15

DARPA Defense Advanced Research Projects Agency 30

DC Diversity Combining 2

DCF Distributed Coordinated Function 16

DFE Decision Feedback Equalization 11

DFT Discrete Fourier Transform 36

DFWMAC Distributed Foundation Wireless MAC 16

DIFS Distributed Inter-Frame Space 16

DPMA Dual Power Multiple Access with Multipacket Reception using Local CSI 29

DQRUMA Distributed-Queueing Request Update Multiple Access 20

DSA++ Dynamic Slot Assignment ++ 20

DS-CDMA Direct-Sequence CDMA 10

DTMC Discrete Time Markov Chain 70

DTMP Disposable Token MAC Protocol 18

EC Equal Channel 38

ECPR Equal Channel with Phase Rotation 38

EPUP Energy per Useful Packet 54

E-SSA Enhanced Spread Spectrum ALOHA 30

EY-NPMA Elimination Yield - Non-Preemptive Multiple Access

FAMA Fixed Assignment Multiple Access 15

FDD Frequency Divison Duplexing 13

FDE Frequency Domain Equalization 1

FDMA Frequency Division Multiple Access 18

FEC Forward Error Correction 8

FF-NDMA Feedback-Free NDMA 28

FFT Fast Fourier Transform 11

FH-NDMA Frequency Hopping NDMA 28

F-RAMA Fair Resource Auction Multiple Access 17

FRMA Frame Reservation Multiple Access 19

H-ARQ Hybrid-ARQ 2

HAP High Altitude Platform 24

H-NDMA H-ARQ NDMA 3

IB-DFE Iterative Block Decision Feedback Equalization 1

ICA-NDMA Independent Component Analysis NDMA 27

ICI Inter-Code Interference 25

IDMA Interference Division Multiple Access 30

IEEE Institute of Electrical and Electronics Engineers 3

IFFT Inverse Fast Fourier Transform 11

IR-ARQ Incremental Redundancy ARQ 28

IS Idle Signal 16

ISA Idle Signal with Acknowledgment 17

ICI Inter-Chip Interference 25

ISI InterSymbol Interference 11

ISMA Idle Sense Multiple Access 16

LDPC Low Density Parity Code 7

LTE Long Term Evolution 1

LOS Line of Sight 8

MAC Medium Access Control 1

MACA Multiple Access with Collision Avoidance 15

MAI Multiple Access Interference 4

MAP Maximum a Posteriori 63

MASCARA Mobile Access Scheme based on Contention and Reservation for ATM 20

MC-CDMA Multi-Carrier CDMA 10

MIMO Multiple Input Multiple Output 8

MMSE Minimum Mean Square Error 9

MSE Mean Square Error 40

MPR Multipacket Reception 14

MQSR MultiQueue Service Room 29

MT Mobile Terminal 1

MUD Multi-user Detection 2

NACK Negative ACK 17

NASA National Aeronautics and Space Administration 20

NAV Network Allocation Vector 16

NDMA Network-assisted Diversity Multiple Access 2

OFDM Orthogonal Frequency Division Multiplexing 8

OFDMA Orthogonal Frequency Division Multiple Access 8

QPSK Quadrature Phase Shift Keying 41

OSI Open Systems Interconnection 23

PAPR Peak to Average Power Ratio 1

PDAMA Packet-Demand Assignment Multiple Access 19

PDF Probability Density Function 76

PER Packet Error Rate 33

PHY Physical 1

PIC Parallel Interference Cancellation 9

PRMA Packet Reservation Multiple Access 19

PS Polling Signal 17

QAM Quadrature Amplitude Modulation 11

QoS Quality of Service 1

RAMA Resource Auction Multiple Access 16

RAP Randomly Addressed Polling 16

RI-BTMA Receiver Initiated - Busy Tone Multiple Access 15

R-ISMA Reservation ISMA 17

RRA Random Reservation Access 15

RRA-ISA Random Reservation Access - Independent Stations Algorithm 19

RS Reed-Solomon 24

RSSI Received Signal Strength Information 29

RTS Request To Send 15

RTT Round-Trip Time 56

S-ALOHA Slotted ALOHA 14

SC Single-Carrier 12

SC-FDE Single-Carrier with Frequency Domain Equalization 11

SC-FDMA Single-Carrier FDMA 1

SDMA Space Division Multiple Access 30

SIC Successive Interference Cancellation 9

SICTA Successive Interference Cancellation Tree Algorithm 28

SIFS Short Inter-Frame Space 16

SINR Signal-to-Interference-plus-Noise Ratio 25

SISO Single Input Single Output 8

SNR Signal-to-Noise Ratio 1

SP Shifted Packet 38

SRUC Split Reservation Under Collision 21

SUD Single User Detection 9

TCM Trellis Coded Modulation 6

TDD Time Division Duplexing 13

TDMA Time Division Multiple Access 2

UC Uncorrelated Channel 38

WSN Wireless Sensor Network 17

ZF-DF Zero Forcing - Decision Feedback 9

List of Symbols

General Symbols

PHY Layer Equalization Symbols

$s_{n,p}$ nth time domain symbol from Mobile Terminal p 36

$Y_k^{(l)}$ lth frequency domain transmission for a symbol k 36

$\rho_{n,p}^{I\ (i-1)}$ pth *in-phase* coefficient element from $\mathbf{P}^{(i-1)}$ 45

$\rho_{n,p}^{Q\ (i-1)}$ pth *quadrature* coefficient element from $\mathbf{P}^{(i-1)}$ 45

$\sigma_{n,p}^{2\ (i)}$ Time domain mean error variance for an iterative receiver at the ith iteration for the pth Mobile Terminal 46

$L_{n,p}^{I\ (i-1)}$ In-phase log likelihood ratio 45

$L_{n,p}^{Q\ (i-1)}$ Quadrature log likelihood ratio 45

TDMA Symbols

α_1 TDMA model generic packet arrival rate 56

$\hat{b}$ Multi-rate estimated bit sequence 63

$\hat{b}_{\Pi}$ Multi-rate estimated interleaved bit sequence 63

$\hat{s}_n$ TDMA's AWGN symbol estimation 59

$\mathcal{D}^T$ Transmission delay per packet for a TDMA context 56

$\mathcal{D}_{service}$ TDMA's Packet's service duration 56

$\mathcal{Q}_{min}$ TDMA's minimum success probability 58

$\mathcal{S}_{min}^*$ TDMA's minimum goodput 58

$\nu_n^{(i)}$ TDMA's AWGN channel noise at the ith attempt 58

Φ^T Energy per useful packet for an H-ARQ TDMA context 55

Π_1 TDMA Multi-rate permutation function 63

$A(z)$ Z-transform of a_m 56

a_m TDMA's probability of arriving m packets during a slot 56

$BER_T(l)$ TDMA's BER for the lth packet transmission. 54

D_{max} TDMA's maximum delay 58

E_c Energy per encoded bit 63

$G(D)$ TDMA multi-rate encoding transfer function 63

L_c Channel reliability factor 63

L_{ap} *A priori* decoded information function 63

L_{b_t} Output function of the soft-input and soft-output decoders 63

L_T Number of TDMA slots per frame 54

N_{sys}^T Number of transmissions per packet for an H-ARQ TDMA context 55

$P_{1,0,1}$ TDMA's probability of having one packet inside the Mobile Terminal's queue 57

$p_{suc}^{(l)}$ H-ARQ TDMA's probability of receiving a packet, from a given mobile terminal, with success at the lth transmission. 54

Q_x H-ARQ TDMA's probability of receiving a packet with errors after $x-1$ transmissions. 54

R_T Maximum number of TDMA transmissions per packet 54

S^* TDMA's channel goodput 56

S^*_{sat} TDMA's saturated goodput 56

S^T Normalized TDMA throughput 112

s_n TDMA's data symbol in the time-domain 58

X_T TDMA's number of packets in the queue 56

y^s Multi-rate systematic observations 63

$y^{p,i}$ Multi-rate parity observations from the ith encoder 63

$y_n^{(i)}$ Symbol received by the TDMA base station at the ith transmission 58

E_{bmax} TDMA's maximum bit energy 58

CDMA Symbols

${}^{C}\mathbf{F}_{k,p}^{(i)}$ Feedforward coefficients for the ith iteration regarding a DS-CDMA context 73

χ H-ARQ DS-CDMA collection of DTMC system states 76

χ^n nth iteration of a random process χ 76

χ_e Random variable of the number of idle terminals 76

χ_e^n nth iteration of a random process regarding χ_e 76

χ_l Random variable of the number of terminals transmitting data at the lth H-ARQ stage 76

χ_l^n nth iteration of a random process regarding χ_l for an lth H-ARQ stage 76

${}^{(i)}\mathbf{F}_{k,p}^{(l)}$ Feedforward coefficients for the ith iteration and lth transmission, for MT p, regarding a DS-CDMA context 73

${}^{(i)}F_{k,p}^{(k,l)}$ Feedforward coefficients for the ith iteration, lth transmission and kth chip, for MT p, regarding a DS-CDMA context 73

$\mathbf{C}_{m,p}$ mth chip from $\mathbf{C}_p$ assigned to Mobile Terminal p 72

$\mathbf{C}_p$ Spreading sequence vector assigned to Mobile Terminal p 72

$\mathbf{H}_k^C$ kth frequency domain channel realization from all terminals and transmissions 72

$\mathbf{H}_{k,p}^C$ Group of channel responses after spreading all transmissions of the kth symbol from mobile terminal p 72

$\mathbf{N}_k^C$ kth frequency domain channel noise for all transmissions 72

$\mathbf{Y}_k^C$ kth symbol received at the frequency domain 72

$\mathcal{D}^C$ System delay for a DS-CDMA context 77

$\mathcal{N}^C$ Number of packet transmissions to deliver a packet 78

Φ^C Energy per useful packet for an H-ARQ DS-CDMA context 78

π_χ Steady-state distribution of χ 77

ϑ Collection of possible system state values 76

ϑ^n nth iteration of ϑ values 76

ϑ_l Number of users in the lth H-ARQ stage 71

ϑ_l^n nth iteration of ϑ_l 76

I Number of idle users 71

I^n nth iteration of I 76

K Spreading factor 10

$N_k^{(m,l)}$ Channel noise concerning the spread kth symbol for a given mth chip 72

N_{sys}^C Number of packet transmissions for an H-ARQ DS-CDMA context 77

p_{err}^l Average packet error rate of mobile terminals at the lth H-ARQ stage 76

p_{QE}^C Probability of a MT having an empty queue, regarding an H-ARQ DS-CDMA system 76

p_{suc}^C Success probability of an H-ARQ DS-CDMA system at the R_Cth H-ARQ stage 78

R_C Maximum number of H-ARQ retransmissions for a DS-CDMA context 70

Tx Random variable regarding the number of packet retransmissions 77

$\mathbf{H}_{k,p}^{(l)\ \ddagger}$ Channel response of the lth transmission after spreading the kth symbol from mobile terminal p 72

$\mathbf{H}_{k,p}^{(l)\ \dagger}$ Group of channel responses before Code Division Multiplexing spreading for the lth transmission of the kth symbol 72

$\mathbf{N}_k^{(l)\ddagger}$ Channel noise concerning all the transmissions for the kth spread symbol 72

$\mathbf{Y}_k^{(l)\ddagger}$ kth symbol received at the frequency domain from an lth transmission 72

$H_{k,p}^{(m,l)\dagger}$ Channel response of the mth chip before spreading for the lth transmission of the kth symbol 72

NDMA Symbols

$\Delta\left(\Psi^{(R_N)}\right)$ Epoch's duration based on $\Psi^{(R_N)}$ 92

$\frac{E_b}{N_0}{}_{max}^{p}$ Bit energy over noise ratio at Mobile Terminal p for the highest transmission power 97

$\left(\frac{E_b}{N_0}\right)_{max}$ Highest bit energy over noise ratio at the base station 97

$\Omega_P^{(l)}$ NDMA's System state for l H-ARQ transmissions and P colliding users 91

$\overline{h_{ir}^2}$ Second moment of an irrelevant epoch's duration 95

$\overline{h_{ir}}$ First moment of an irrelevant epoch's duration 95

$\overline{h_r^2}$ Second moment of a relevant epoch's duration 95

$\overline{h_r}$ First moment of a relevant epoch's duration 95

Φ^N Energy per useful packet for an H-NDMA context 96

$\Psi^{(l)}$ Random vector of the system state up to the lth H-ARQ slot 91

$\psi_k^{(l)}$ kth random variable from $\Psi^{(l)}$ of the number of terminated transmissions up to the lth H-ARQ slot 91

Chapter 1

Introduction

The wireless communications' industry is an important economic sector that thrives year after year [Tim11] - civilians and corporations rely more and more in Internet based services, from chat services, to e-mail, video streaming, web browsing, video calls, gaming, etc. Mobile carriers expect to increase their profits from premium services that rely heavily on broadband and Quality of Service (QoS). Wireless broadband *on the go* is a required feature these days [ER10] and considering that mobile data is growing at an explosive rate [Lia], some precautions must be taken to fully comply with the users' demands. Future technology should take these requirements into account, especially to value the users' experience.

Furthermore, the form factor of Mobile Terminals (MTs), i.e. laptops and cellphones/smartphones, have become smaller, cheaper and more attractive, appealing to a mass market. Nevertheless, current wireless standards (Long Term Evolution (LTE)) are still energy inefficient [GJV13], since MTs waste their batteries' energy after a short period of time - the *obvious* solutions in recent years have been to increase the batteries' capacity and to improve the MTs' software. On top of this, when difficult transmission conditions persist (low Signal-to-Noise Ratio (SNR) scenario or a deep fade in the wireless channel), the QoS is hard to guarantee and therefore MTs have to waste more energy to ensure a successful reception at their local Base Station (BS) cell.

Single-Carrier FDMA (SC-FDMA), which uses Single Carrier with Frequency Domain Equalization (SC-FDE), has been proposed for LTE's uplink communication [FAea02], since it has a low Peak to Average Power Ratio (PAPR) - which makes sense from a Mobile Terminal (MT) point of view, since MTs are energy constrained devices. Nevertheless, Frequency Domain Equalization (FDE) at the BS should be appropriately configured, since a severely dispersive channel can severely affect data reception and therefore lead to a higher energy consumption. The Iterative Block Decision Feedback Equalization (IB-DFE) technique [BDFT10] has been proposed to deal with highly dispersive channels under difficult transmission conditions; the technique enhances data reception, using iterative equalization principles, and therefore better energy savings at the MTs. Unfortunately, modeling SC-FDE equalization techniques is fairly complicated at the Physical (PHY) layer, since closed loop formulas are inexistent; besides, the simulation of SC-FDE equalization techniques would be very useful for Medium Access Control (MAC) layer simulations as well as for upper layers.

Regardless of the PHY layer, wireless Medium Access Control (MAC) solutions are typically very rigid, i.e. the PHY-MAC interaction is usually inexistent [SRK03]. Classical MAC techniques usually discard packet copies with errors. Thankfully a cross-layered technique can enhance packet reception by reusing

the packet copies with errors - when a given application uses two (or more) layers that are strongly interconnected in their design, it is referred to as a cross-layered application [SRK03]. A known cross-layered technique is soft combining Hybrid-ARQ (H-ARQ) that combines the several packet copies with errors to enhance data reception on posterior retransmissions [LY82, Kal90] - for such scheme to work, both PHY and MAC layers need to be strongly interconnected. In this thesis type II Diversity Combining (DC) H-ARQ [LY82], a variation of soft combining H-ARQ, is considered.

When traditional MAC schemes employ type II DC H-ARQ technique, their performance is significantly improved, with examples such as Time Division Multiple Access (TDMA) [LY82, Kal90] and slotted Code Division Multiple Access (CDMA) [AGTT05, TA07]. The first one multiplexes MTs in the time domain, where MTs take turns to transmit their packets and the latter multiplexes MTs through the use of orthogonal spreading codes. For a broadband setting, where packets are transmitted in the time domain, TDMA can use SC-FDE at the uplink; CDMA, on the other hand, when employing FDE is denominated as prefix-assisted DS-CDMA at the uplink - prefix-assisted DS-CDMA is an SC-FDE variant that uses time-domain spreading.

Unfortunately, employing DC H-ARQ for traditional access schemes also comes at the price of wasted resources, i.e. idle resources or too much redundancy in use. Network-assisted Diversity Multiple Access (NDMA), a cross-layered PHY-MAC protocol [TZB00, ZT02], attempts to diminish idle resources by using Multi-user Detection (MUD) principles, where for a collision of J packets it asks for $J-1$ retransmissions from each MT to resolve packet collisions. Despite performing quite well for a random access scenario, NDMA has a poor performance when interference conditions are extremely high, e.g. low SNR and/or a deep fade.

To make things worse, academic research in terms of cross-layered PHY-MAC architectures is usually focused in one layer and less in the other, e.g. detailed PHY receiver implementation with sparse modeling of the MAC layer or a detailed MAC implementation with a simplistic PHY layer model.

It is important to note that the models developed in this thesis are general in terms of the technology in use, since one of the main objectives of this thesis is to achieve energy efficiency for wireless communications in general.

1.1 Research Goals

Regarding the context of this thesis, the following research goals were defined below.

- Study existing techniques that enhance packet reception under difficult transmission conditions and improve energy efficiency at the MTs.
- Design a cross-layered architecture that should improve packet reception and energy efficiency at the MTs.
- Select an appropriate PHY layer receiver and extract an analytical model that is easily applicable to MAC layer simulations.
- Model the MAC layer combined with the PHY layer receiver.
- Implement the PHY-MAC layer design in a network simulator.
- Compare the analytical model with the network simulator's results.
- Benchmark the cross-layered architecture with others.

- Disseminate the obtained results in relevant scientific conferences and journals.

1.2 Research Question & Hypothesis

Given the presented context of this thesis, the following research question is posed below

Is it possible to achieve energy efficient wireless communications under strict Quality of Service (QoS) requirements with a proper PHY-MAC architecture?

The presented document enunciates the following hypothesis below

Energy efficient wireless communications can be achieved using a combination of type II DC H-ARQ with NDMA that comply with existing QoS requirements.

1.3 Contributions

The contributions of this thesis are enumerated below.

- A PHY layer model, for linear and iterative equalization regarding SC-FDE, that is easily applicable to MAC layer simulations without requiring PHY layer simulations beforehand. The model and its respective results, in chapter 3, were published in [GDBO12].
- A TDMA model that correlates the expended energy per useful packet for a given QoS when employing DC H-ARQ. The cross-layered TDMA approach, in chapter 4, was published in [GPB$^+$10a, GPB$^+$10b].
- A novel slotted prefix-assisted DS-CDMA model that uses DC H-ARQ that is thoroughly detailed at both PHY and MAC layers; the protocol performance is also correlated with the expended energy per useful packet. The slotted prefix-assisted DS-CDMA model, in chapter 5, is partially published in [GVBD13].
- A novel NDMA protocol variant, named H-ARQ NDMA (H-NDMA), that uses DC H-ARQ to improve the protocol performance; the model of the proposed protocol takes in consideration the optimal parameters that improve energy efficiency. The H-ARQ NDMA (H-NDMA) protocol, in chapter 6, was published in [GPB$^+$11a, GPB$^+$13], and was also a *runner-up* for best paper award in [GPB$^+$11b].
- A comparison of the aforementioned techniques using the proposed PHY layer model, in chapter 7, will be submitted for the Institute of Electrical and Electronics Engineers (IEEE) Communications Magazine in a foreseeable future.

Regarding the scope of this thesis, the H-NDMA protocol was also extended for a satellite network scenario with stringent QoS requirements, more specifically for a demand access scheme in [GBD$^+$12, GBB$^+$13] and a random/scheduled access scheme in [VGB$^+$13]. However, these were minor contributions when compared to the others included in this document, and therefore considered out of scope.

1.4 Document's Structure

The document is structured in a total of eight chapters as enumerated in the paragraphs below.

Chapter 2 overviews a comprehensive set of PHY layer and MAC layer techniques that tackle channel errors and/or Multiple Access Interference (MAI) when several MTs access the wireless medium.

Chapter 3 proposes an analytical model for two SC-FDE equalization schemes at the PHY layer: linear and iterative equalization. The proposed model *eases* the process of evaluating a cross-layered PHY-MAC protocol without the need of computing PHY layer simulations beforehand. Plus, the analytical model is presented in a simple and versatile way.

Chapter 4 studies a cross-layered DC H-ARQ TDMA MAC performance model. The model portrays several metrics: the expended energy per useful packet, the goodput and the packet delay. An optimization problem is also posed, based on the performance model, to compute the optimal parameters that satisfy a given QoS.

Chapter 5 studies a novel wireless PHY-MAC DC H-ARQ prefix-assisted DS-CDMA model where several metrics are extracted: the delay, throughput and the expended energy per useful packet. The proposed system model attempts to improve the energy efficiency for a given QoS requirement, especially for difficult transmission conditions, i.e. low Signal-to-Noise Ratio (SNR).

Chapter 6 proposes a new NDMA protocol variant. The protocol uses additional DC H-ARQ transmissions to enhance the system performance. An analytical model is derived for the system throughput, packet delay and expended energy per useful packet.

Chapter 7 compares the performances of TDMA, slotted prefix-assisted DS-CDMA and H-NDMA, employing DC H-ARQ. The three protocols are compared in a fair way using an iterative equalization scheme at the PHY layer.

Finally, chapter 8 presents this document's conclusions.

Chapter 2

Literature Review

Wireless communication systems have to rely on an extensive array of techniques to cope with channel errors or collisions; these techniques could be employed either at the Physical (PHY) or Medium Access Control (MAC) level, or at both levels. Without these techniques, wireless communication systems would be extremely energy inefficient and would difficultly adapt to demanding Quality of Service (QoS) requirements. Considering that there is an increasing demand for mobile spectrum [CW10] in such a lucrative business for mobile operators [Tim11], communication systems are continuously evolving to satisfy the needs of customers - cheap, energy efficient and QoS-aware communication systems are needed for future mobile communications.

The current chapter presents a comprehensive literature review of current trends and challenges from communication systems. Section 2.1 overviews known coding schemes for reliable data transmission. Section 2.2 presents diversity schemes. Section 2.3 introduces PHY layer techniques for Multi-user Detection (MUD). Section 2.4 grasps future modulation schemes. Section 2.5 overviews Medium Access Control (MAC) schemes. Section 2.6 briefs Physical (PHY)-Medium Access Control (MAC) cross-layered schemes. Section 2.7 overviews the conclusions of this chapter.

2.1 Error Control Coding

Data sent on the wireless channel is subject to errors for various reasons, such as multipath fading, shadowing, atmospheric precipitation, among other reasons. MTs rely on channel coding to circumvent data errors. *Shannon* [Sha48] made the first breakthrough on this field, allowing researchers to study the physical channel capacity, i.e. the maximum rate at which data is reliably sent. Shannon's theorem states that for a given transmission rate R_a less or equal than the channel capacity C_a, there is a coding scheme that allows data transmission with a small error probability; if R_a is higher than the channel capacity C_a, there is no reliable coding scheme. However, the theorem does not state which coding scheme is appropriate for a given context. Based on *Shannon*'s theorem it is possible to increase spectral efficiency, η^s, i.e. the average number of transmitted bits per signalling interval T_s, at the cost of a higher bit energy noise ratio, E_b/N_0, where E_b is the average bit energy and N_0 is the average channel noise [CHIW98]; however to decrease E_b/N_0, a lower η^s is required.

A comprehensive study of channel coding is made by *Costello et al* in [CHIW98] and [CF07].

The current section is divided in various topics of channel coding: section 2.1.1 presents algebraic coding, section 2.1.2 briefly overviews probabilistic coding and section 2.1.3 presents turbo-codes.

2.1.1 Algebraic Coding

Algebraic coding dominated the first decades of channel coding. A thorough explanation is given in [Pet61, Ber68, Lin70, PJ72, MS77, Bla83]. Algebraic coding regards the construction of a linear (n, d, k) block code over the *Galois* field $\mathbb{F}_2$; the (n, d, k) block code is a 2^k binary code of n codewords, where d is the *Hamming* distance [Ham50], i.e. the minimum coordinates that differ between two codewords.

The main purpose of algebraic coding is to maximize the *Hamming* distance d, such that it is possible to minimize the number of errors within a codeword. A code with a minimum distance d can correct at most $(d-1)/2$ errors. Algebraic codes in general cannot approach the maximum channel capacity, also known as *Shannon*'s channel capacity.

At the receiver, a maximum likelihood decision is performed, trying to match the closest codeword to the received signal. *Costello et al* emphasizes that to obtain better results, *soft* decoding decisions should be used instead of *hard* decoding decisions, i.e. the decision is based on the value of the received signal instead of a two-level quantization decision.

2.1.2 Probabilistic Coding

Contrarily to algebraic coding, that aims to maximize the minimum Hamming distance for a given code, probabilistic coding aims to find classes of codes that optimize the average performance of coding and decoding. Probabilistic coding, uses *soft*-decoding information as input of intermediate decoding stages. Coding schemes inherent to this concept are: convolutional codes, product codes, concatenated codes, trellis-coded modulation and trellis decoding of code blocks. More information of probabilistic coding can be found in [WJ65, Gal68, GCCC81, LC04, JZ99, RU08].

Convolutional codes were first studied by *Elias* [Eli55, Gal05]. The structure of these codes are similar to a Markov finite-state process of k inputs and n outputs.

Product codes were also invented by *Elias* [Eli54]. As the name implies, they are the product of two block codes (n_1, d_1, k_1) and (n_2, d_2, k_2) with a resulting block code $(n_1 n_2, d_1 d_2, k_1 k_2)$. These codes can achieve an arbitrary low error, but without taking full advantage of the channel capacity.

Coding on narrow-band systems implies the use of nonbinary codes. For such conditions, there are spherical lattice coding [CS88] and trellis-coded modulation technique [Ung82]. The most popular technique is Trellis Coded Modulation (TCM), where redundancy is obtained by expanding the signal constellation with the same bandwidth. *Ungerboeck* [Ung82] discovered that doubling the constellation size is enough to obtain redundancy, where minimum Euclidean distance is used instead of the Hamming distance for design criterion. These codes can be optimally decoded with a *Viterbi* decoder [CF07].

2.1.3 Turbo-codes

Turbo-coding is the latest breakthrough in terms of channel coding. Since its discovery it has been used in most communication systems [CF07]. *Berrou et al* [BGT93] presented this new class of coding declaring that it could achieve near Shannon channel capacity with modest complexity. Their work took

advantage of repeated decoding, using an iterative feedback as a form of additional redundancy. The model presented in [BGT93] used a systematic recursive convolutional encoding scheme and a pseudo-random interleaver that made the coding scheme *random-like*. This random property is important in the sense that the codewords distance is randomly distributed, which according to [CF07] is better than maximizing the minimum distance between codewords. However, turbo-codes have a poor minimum distance performance; *Breiling* [Bre04] discovered that the minimum distance increases logarithmically with the interleaver length.

Low Density Parity Code (LDPC) was also rediscovered as a turbo-code scheme, first invented by *Gallager* [Gal63] and later studied by *Spielman et al* [SS96] and *MacKay et al* [MN95]. An LDPC is commonly represented by a bipartite graph, where each code symbol is defined by a node type and each parity symbol check is defined by a second node type. A symbol node and a parity check node are connected by an edge if the corresponding symbol is involved with the parity check [Tan81]. With LDPC coding, the edges increase linearly with the block length. *Richardson et al* [RSU01] proved that using LDPC coding, it is possible to achieve near Shannon channel capacity, outperforming traditional turbo-coding schemes.

2.1.4 Comments

Channel coding has evolved in various forms since *Shannon*'s work on channel capacity [Sha48]. Due to the latest breakthroughs on channel coding, by means of turbo-coding, advances on this field of study have stagnated in terms of channel capacity; nonetheless, *Costello et al* emphasizes the importance of improving channel coding and decoding complexity of turbo-codes [CF07]. For energy constrained devices, turbo-coding might be unsuitable due to their complexity; other variations of channel coding should be used. Furthermore, turbo-codes suffer of a low *error-floor*; for these cases LDPC could be appropriate. Algebraic codes are somewhat simpler, but cannot attain Shannon's channel capacity. Probabilistic coding does obtain good results but not as good as turbo-coding.

2.2 Diversity Techniques

Error-control coding is important to ensure reliable communication, but diversity techniques also improve data reception. The current section overviews diversity techniques that complement error-control coding. While error-control coding relies on additional redundancy of the codewords, diversity techniques rely on the redundancy from several copies of the same data symbol. Diversity techniques can be employed in several domains: frequency, spatial and time domains. *Beaulieu* [Bea03] lightly introduces diversity combining techniques. If data replicas are sufficiently spaced, i.e. in frequency, space or time, their statistical properties can be considered independent of each other. *Brennan* [Bre55] introduced the concept of diversity and explained how to process different data replicas. The following sub-sections briefly introduce each type of diversity techniques. Section 2.2.1 introduces frequency diversity, section 2.2.2 presents spatial diversity and section 2.2.3 handles time diversity.

2.2.1 Frequency Diversity

Frequency diversity implies the transmission of the same data symbol over multiple carriers [DGea02]. Each copy of the data symbol must be sufficiently separated at the frequency domain to ensure inde-

pendent fading. The difference between each carrier must be greater than the coherence bandwidth of the system. This way the receiver is able to combine the data symbol copies from independent fading channels. However, such scheme could be difficult to implement for a narrow-band system, besides the increased complexity at both the receiver and the emitter [DGea02]. Contrarily to a time diversity technique, it does not require an higher delay to successfully transmit a data block, though it requires an efficient spectrum allocation for each data block copy. However, for unlicensed frequency bands, this technique is inadequate [LL07]. A technique that uses frequency diversity and overcomes some of the problems associated with frequency diversity is Orthogonal Frequency Division Multiple Access (OFDMA), through Orthogonal Frequency Division Multiplexing (OFDM) [LJC85] - this technique has become a standard for current communication systems that adopt wideband communications, i.e. 3GPP-Long Term Evolution (LTE). OFDMA multiplexes data symbols over multiple *orthogonal* subcarriers to achieve frequency diversity and thus better spectral efficiency. This technique will be further discussed in section 2.4.

2.2.2 Spatial Diversity

Spatial diversity implies the use of multiple antennas either at the receiver or the emitter when emitting data symbols [Ala98]; a well known example of such scheme is the Multiple Input Multiple Output (MIMO) technique [Sha06]. The MIMO technique takes advantage of multipath signals, where antennas are spaced enough, such that it diminishes the correlation between the received signals. It has become a standard for WiMax and 3GPP-Long Term Evolution (LTE) [CFea10]. Besides diversity, MIMO is also capable of increasing a system's transmission rate while maintaining the same spectrum by sending parallel streams of data [CFea10, Sha06]. The main advantage over traditional antenna schemes, such as Single Input Single Output (SISO), is the ability of extending the radio range and taking advantage of other multipath components without *interpreting* them as noise. Nonetheless, it requires a modestly complex design for an increasing number of antennas [Sha06].

Besides MIMO, it is also possible to introduce spatial diversity from relay terminals that are available for a given Mobile Terminal (MT) [CFRP00, Mat87]. While taking advantage of multipath components, a MT could also receive the Line of Sight (LOS) signals from available relay terminals. This way the system capacity increases, but such scheme requires an efficient resource allocation [Mat87].

2.2.3 Time Diversity

Time diversity is achieved when a data symbol is transmitted more than once at different time instants spaced by a given coherence time. Symbol copies are then stored for further processing. There are channel control techniques such as Type II Hybrid-ARQ (H-ARQ)/Forward Error Correction (FEC) [LY82] that make use of time diversity to enhance data reception, either by data symbols concatenation where long codewords are formed or by repeating data symbol copies at different instants. These techniques will be further explained in section 2.6.1.

2.2.4 Comments

Diversity techniques are a great solution to enhance data communication alongside with error control coding. Time diversity techniques are appropriate when the delay requirements of a given application

are suitable for an increasing number of retransmissions. Diversity at the frequency domain can overcome higher delays at the cost of a larger bandwidth; furthermore, a standard technique for wideband communications such as OFDM achieves a good spectral efficiency when considering frequency diversity. Regarding spatial diveristy, it does not degrade an application delay requirements or requires an higher bandwidth; it takes advantage of multiple multipath components of the received signal, despite demanding a complex receiver structure, MIMO techniques have become standard for WiMax, 3GPP-LTE, IEEE 802.11n and 802.11ac.

2.3 Multi-user Detection Techniques

Multi-user Detection (MUD) is the ability of discerning data symbols from multiple interfering users [Mos96, Ver86]. MUD was first devised by *Verdu* [Ver86] using a maximum likelihood estimator, however it was too complex. Suboptimal schemes have been devised since then. According to *Moshavi* [Mos96], MUD techniques can be categorized in two types: linear detection and subtractive interference detection.

Linear detectors apply a linear mapping to the soft output of a conventional detector to reduce Multiple Access Interference (MAI), i.e. interference from other users. The most popular linear detectors are the decorrelating detector [Sch79, KHI83] and the Minimum Mean Square Error (MMSE) detector [XSR90]. The decorrelating detector applies the inverse correlation matrix to the matched filter bank outputs. The MMSE detector applies a modified inverse correlation matrix at the matched filter bank outputs, obtaining better results than the decorrelating detector. Unfortunately linear detectors are too complex to implement [Mos96].

Subtractive interference detection techniques [Hol94, Koh94] make separate estimates of the MAI of each user and subtract some or all the MAI for each user. This technique can employ several stages, where performance is improved at each successive stage. Subtractive techniques are easier to implement than linear detection techniques [Mos96]. Subtractive interference techniques can be organized in three types: Successive Interference Cancellation (SIC), Parallel Interference Cancellation (PIC) and Zero Forcing - Decision Feedback (ZF-DF).

SIC schemes [Vit90, ea90] employ a serial approach to subtract the MAI; at each stage, SIC schemes regenerate the received signal and subtract the MAI for each user [Mos96]. Contrary to SIC, PIC subtracts the MAI in parallel for each user [ea90, VA90]. Regarding ZF-DF [DH93b, DH93a, KKB96, JB95], it performs linear preprocessing followed by SIC detection; the linear preprocessing usually employs a decorrelating decision feedback detector, which decorrelates the user data and the SIC operation subtracts the interference in descending order based on the MT signal strength.

SIC techniques perform better on fading environments than PIC techniques, despite that PIC techiques are well suited on power-controlled environments [PH94, WDH96]. The ZF-DF technique requires complex computations, opposite to the aforementioned techniques [Mos96]. Nonlinear detectors have the disadvantage of requiring reliable estimates of the channel.

Code Division Multiple Access (CDMA) [HP97, ASO97] from a MUD perspective can be used to multiplex several users in a synchronous way and from a Single User Detection (SUD) perspective it can be used as a diversity technique that copes with channel errors. To separate MTs, CDMA assigns orthogonal signature codes to each MT; when MTs transmit data packets, they spread each data symbol from their packets and send the spread packets in a synchronous way - this can be achieved in the

frequency domain [HP97], time domain [ASO97], or in both domains [YH05]; the CDMA technique for the frequency-domain is denominated as Multi-Carrier CDMA (MC-CDMA), while for the time-domain it is denominated as Direct-Sequence CDMA (DS-CDMA).

For an orthogonal code of K chips, CDMA has the ability to multiplex up to K MTs - for instance, considering a packet of N bits, CDMA will convolute each data bit to a sequence of K chips that is further modulated and then transmitted into the wireless medium. At the end of the convolution function results a packet with $N \times K$ chip symbols. Regarding MC-CDMA, data chips are modulated in different sub-carriers, while DS-CDMA modulates data in the time-domain. Figure 2.1 illustrates the differences between both techniques, assuming a spreading gain of K.

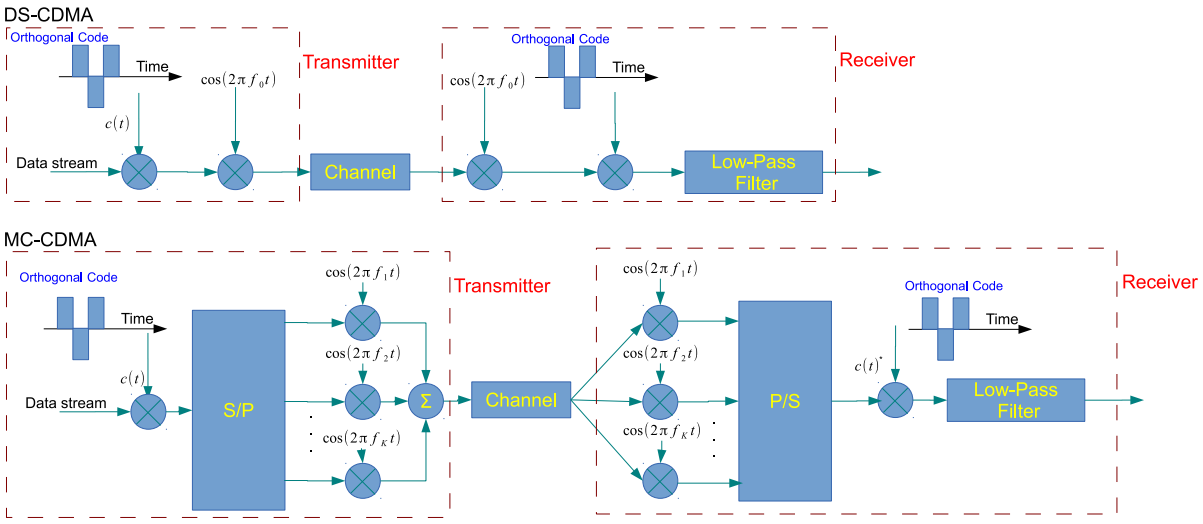

Figure 2.1: DS-CDMA and MC-CDMA comparison.

At the receiver, once the data chips are demodulated, the reverse operation is ensued, where each set of K chips are input into a deconvolution block and then filtered to retrieve the original data symbols. From a SUD or from a non-saturated system perspective (i.e. there are less MTs than the number of spreading sequence signatures), data chips can be used to enhance data reception, since these provide additional redundancy that enhance packet reception at the receiver [SD11].

CDMA has similar concepts that are close to MUD and to diversity techniques, but it can be further enhanced with those techniques as well, either for better MT separation and/or error mitigation [SD11]. Despite CDMA's advantages, it lacks flexibility in terms of channel utilization, especially when the wireless channel has fewer MTs than chip signature sequences or when the channel is overloaded with MTs.

MUD techniques are becoming quite popular since *Verdu*'s work [Ver86]. For more recent works refer to [TZB00, ZT02, DCB+09].

MUD techniques have the advantage of coping with multiple users accessing the channel, taking also advantage of diversity techniques to diminish the MAI seen from each user at each decoding stage; these techniques require further work for non-linear implementations for channel estimation.

2.4 Future Broadband Modulation Techniques

Data transmission for a WiMax/3GPP-LTE system can be severely affected by multipath propagation, since InterSymbol Interference (ISI) can affect several data symbols [ea99, FAea02]. To cope with severe multipath propagation and support high data rates, there are two capable solutions for data modulation: Orthogonal Frequency Division Multiplexing (OFDM) and Single-Carrier with Frequency Domain Equalization (SC-FDE).

OFDM [LJC85] transmits several modulated subcarriers in parallel; each one occupying a narrow bandwidth. With this modulation technique, equalization is required at the frequency domain, which is advantageous for frequency selective fading [FAea02]. The subcarriers are generated by means of the Inverse Fast Fourier Transform (IFFT) at the emitter on blocks of M data symbols. To extract the subcarriers at the receiver, a Fast Fourier Transform (FFT) operation is performed. The FFT block should be four to ten times larger than the channel impulse response to diminish the block overhead from the Cyclic Prefix Insertion (CPI) operation. The Cyclic Prefix (CP) is the repetition of the last data symbols in a block to avoid ISI and to make the received block look periodic, which is essential for the FFT operation. OFDM has a high Peak to Average Power Ratio (PAPR), since an OFDM signal is the sum of a large number of slowly modulated subcarriers [FAea02]. The OFDM technique must employ a power amplifier with a large backoff to remain linear over the range of the signal envelope [SG01]. Another problem concerning OFDM is that data packets must have the same size as FFT blocks, or be a multiple, otherwise some bits in the FFT block may not be used.

Regarding the SC-FDE technique, data is sent at a high rate through a modulated single carrier, e.g. using Quadrature Amplitude Modulation (QAM), with equalization at the frequency domain. According to *Sari et al* [SKJ94, SKJ95], SC-FDE has the same performance and low complexity as OFDM; OFDM and SC-FDE share most of the same processing operations. Contrary to OFDM, SC-FDE has a reduced PAPR envelope signal, requiring less demanding amplifiers. Furthermore, the complexity at the emitter is reduced when compared to OFDM. Similarly to OFDM, a cyclic prefix is also appended to each FFT block. At the receiver, an IFFT is performed to return the equalized signal at the time domain before attempting the data symbol detection. According to *Qureshi* [Qur85], Decision Feedback Equalization (DFE) gives better performance than linear equalization. *Falconer et al* [FAea02] suggest a hybrid time-frequency domain equalization technique.

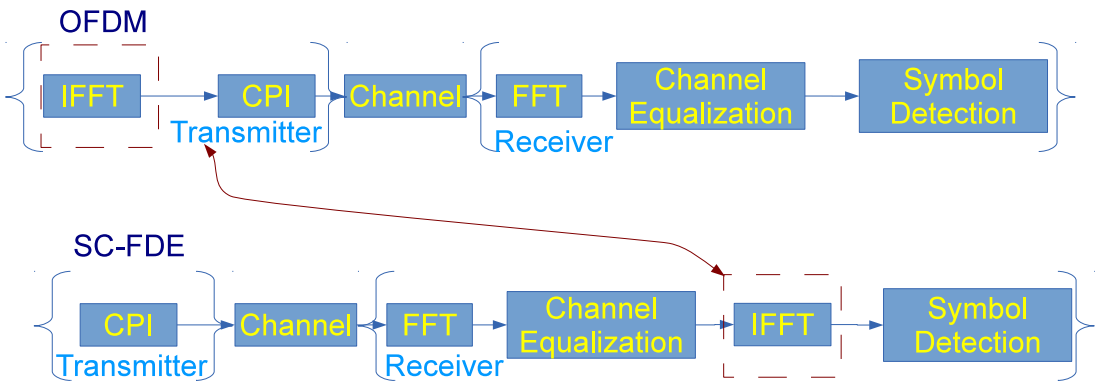

Figure 2.2: OFDM and SC-FDE comparison.

Figure 2.2 illustrates in a schematic the difference between both techniques, where CPI stands for the CP insertion. Both systems, OFDM and SC-FDE, differ by an IFFT operation; the OFDM technique uses the IFFT operation at the emitter to multiplex data in multiple subcarriers while the SC-FDE technique

uses the IFFT at the receiver to convert the FDE signals to the time domain. According to *Falconer et al* [FAea02], both systems can coexist as a dual-mode system; a Base Station (BS) could use an OFDM transmitter and a Single-Carrier (SC) receiver, while the MT uses an OFDM receiver and an SC transmitter. This configuration has the advantage of keeping most of the signal processing complexity at the BS. As aforementioned, SC in terms of energy saving is better than OFDM, which is good for energy constrained MTs.

In terms of broadband transmission, both DS-CDMA and MC-CDMA were generically named prefix-assisted DS-CDMA and prefix-assisted MC-CDMA respectively due to the introduction of a cyclic-prefix to each system, similar to SC-FDE and OFDM [AGTT05]. For example, SC-FDE is equivalent to a prefix-assisted DS-CDMA system with spreading $K = 1$, while OFDM is equivalent to a prefix-assisted MC-CDMA system with spreading $K = 1$. Both DS-CDMA and MC-CDMA for a broadband context have very similar performances, according to *Adachi et al* [AGTT05], as long as the FDE is appropriately applied; however, for the uplink and similar to SC-FDE, prefix-assisted DS-CDMA has a better PAPR than MC-CDMA.

From a MUD perspective, *Dinis et al* studied an iterative SIC equalization technique named Iterative Block Decision Feedback Equalization (IB-DFE) applied to a SC-FDE [DCB+07] context. This technique performs successive iterations to remove channel interference and residual errors at the symbol level, up to a maximum number of iterations.

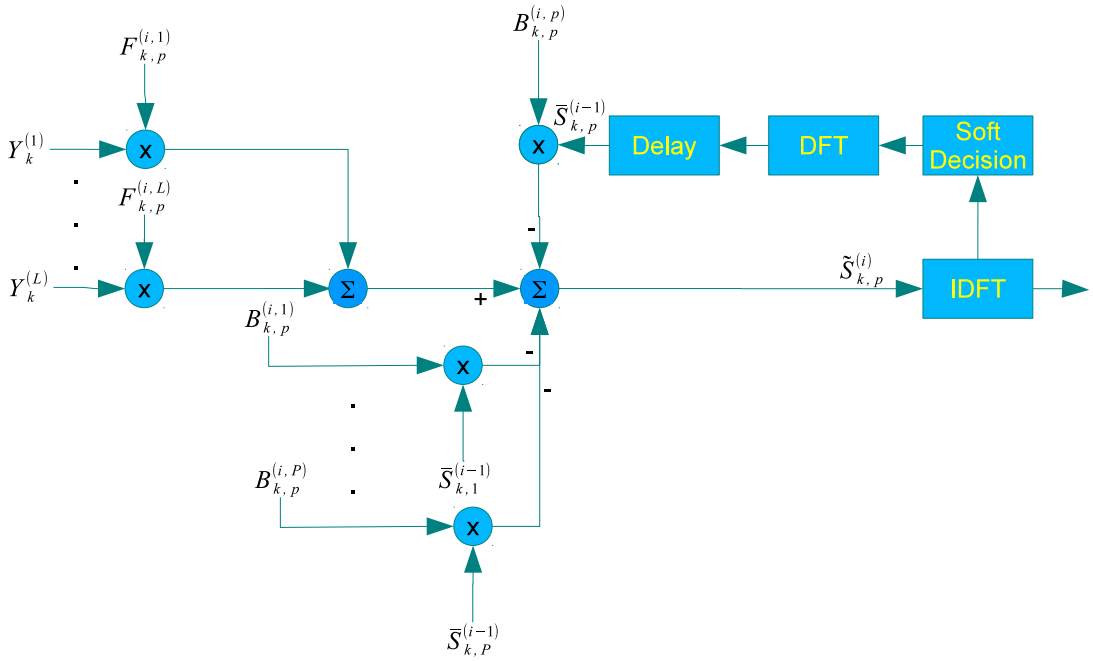

Figure 2.3: IB-DFE equalization technique for L packet copies and P MTs.

Figure 2.3 illustrates the structure of the IB-DFE technique to equalize a packet symbol from a MT p, assuming that P MTs transmitted L packet copies, where $L \geq P$ and $p \in [1, \ldots, P]$; the L packet copies are used to enhance packet reception, similar to Diversity Combining (DC) [PBD+12], which will be explained in section 2.6.1. For an iteration i, the L symbol copies $\mathbf{Y}_k = [Y^{(1)}, \ldots, Y^{(L)}]$ at the receiver are combined to retrieve MT's p packet symbol, where thanks to the feed-forward coefficients $\mathbf{F}_{k,p}^{(i)} = [F_{k,p}^{(i,1)}, \ldots, F_{k,p}^{(i,L)}]$ and the feedback coefficients $\mathbf{B}_{k,p}^{(i)} = [B_{k,p}^{(i,1)}, \ldots, B_{k,p}^{(i,P)}]$ the channel interference and the residual errors are diminished. $\tilde{S}_{k,p}^{(i)}$ and $\bar{S}_{k,p}^{(i-1)}$ are the symbol estimation for the current iteration and the soft decision estimation from the previous iteration respectively. The role of the $\mathbf{B}_{k,p}^{(i)}$ coefficients is to remove the residual ISI and other kinds of interference based on the $\bar{S}_{k,p}^{(i-1)}$ estimation, while the

$\mathbf{F}_{k,p}^{(i)}$ coefficients remove the ISI at the beginning of the equalization procedure. The IB-DFE technique demonstrates promising qualities for MUD applied to SC-FDE. This technique will be further studied in chapter 3.

2.5 Medium Access Control Schemes

Medium Access Control (MAC) schemes are important in a wireless medium to coordinate MTs eligible for packet transmission. The basics on MAC schemes are studied on [Tan03, GL00, Int02]. Since the wireless medium is a *broadcast* medium, multiple MTs might contend the wireless channel and interfere with each other [GL00]. The design of the access scheme is crucial, since it should enhance the throughput of the system and diminish the interference between users. Multimedia applications play a big role on the telecommunications scene, where users demand stringent requirements in terms of QoS and bitrate. With the advent of future mobile communication systems, an adequate contention for the wireless medium is essential.

Data transmission can be either half-duplex or full-duplex; half-duplex communication implies that the uplink and downlink cannot be used simultaneously while a full-duplex communication allows simultaneous uplink and downlink transmission. Half-duplex communication at the time domain is known as Time Division Duplexing (TDD) and full-duplex communication at the frequency domain is regarded as Frequency Divison Duplexing (FDD).

Wireless MAC schemes are logically divided in two types: Distributed and Centralized schemes [GL00]. A distributed wireless MAC scheme allows the sharing of the medium between MTs without a pre-existing infrastructure. In a distributed network, all MTs should work at the same frequency band, therefore MTs operate in TDD. On the other hand, centralized wireless MAC schemes are an extension to wireline networks; a Base Station (BS) serves as an interface between the wireless and wireline networks. The BS may control the MTs uplink according to the QoS requirements. A centralized MAC scheme can operate with TDD or FDD modes.

Wireless MAC protocols can be seriously affected by multipath propagation and channel errors as aforementioned. More specifically, distributed wireless MAC schemes can also be affected by location-dependent carrier sensing [Stü00]. Knowing that the transmitted signal power decays with the power-law of the distance, MTs at a given distance might have difficulties sensing the transmitted signal. On carrier-sensing protocols there are three types of issues that make difficult the medium access: hidden and exposed MTs, and channel capture. An hidden MT C is within the range of a destination B, but out of the range of a sender A [Bha97]. Suppose that MT A sends data to B; MT C, assuming that the channel is idle, might interfere with a new transmission to B. An exposed MT is complementary to an hidden MT; an exposed node C is within the range of sender A but out of reach of destination B. This way, MT C does not interfere with A's transmission, however C cannot transmit data to MTs outside the range of B. With exposed MTs, the bandwidth is underutilized [Bha97, GL00]. Channel capture occurs when a MT C is able to receive simultaneously the transmissions from MTs A and B, however A's transmission power is higher than B's transmission power. If A and B transmit data simultaneously then B's transmission might be unnoticed and A's message can be successfully decoded [Bha97, GL00, GS87, Gea89, RGS87].

Figure 2.4 shows a taxonomy of MAC protocols from *Gummalla et al* [GL00]. As mentioned before, MAC protocols can be generically classified as distributed or centralized; centralized protocols can be further classified as random access, guaranteed access, hybrid access, fixed access and adaptive access.

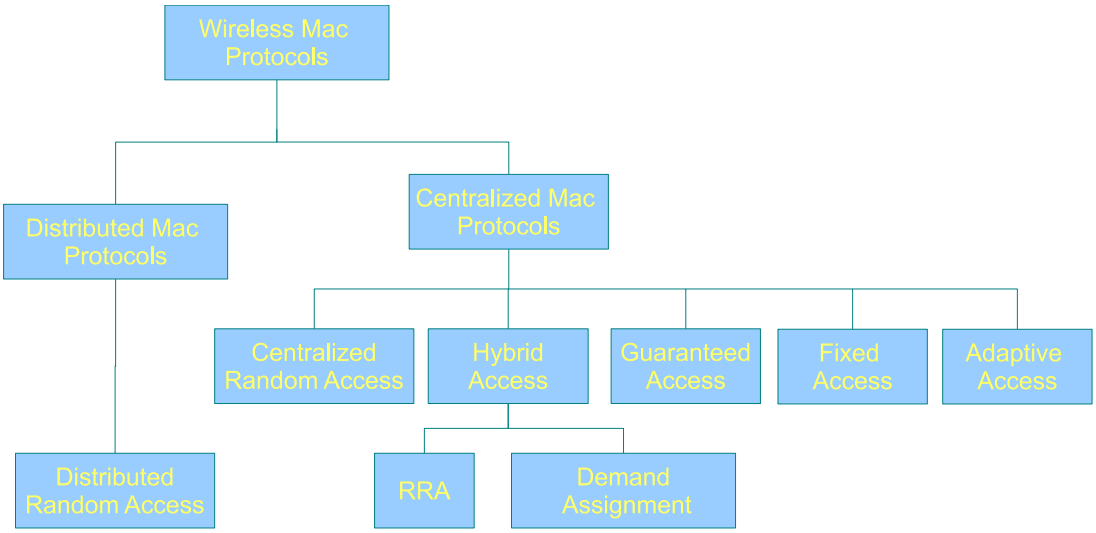

Figure 2.4: Wireless MAC taxonomy [GL00].

Random access

A random access protocol, as the name implies, specifies a contention algorithm to be used by the MTs when transmitting to the wireless medium; a transmission is successful if only one MT transmits, otherwise the obtained result is usually garbled data (except for Multipacket Reception (MPR) systems [LE05]). ALOHA [Abr70, Abr73] was the first protocol for packet radio that introduced the concept of a random access protocol. On the ALOHA protocol, a MT transmits data to the wireless medium when packets arrive to its buffer; if a collision occurs, it waits a random period of time. The maximum throughput of the protocol is 18%; a centralized slotted access version (i.e. controlled by a BS) of the protocol, Slotted ALOHA (S-ALOHA), achieves a throughput of almost 37% [GL00]. The S-ALOHA protocol is exemplified in figure 2.5, with four MTs: A, B, C and D. A BS signals the MTs the beginning of each slot, any MT with packets will attempt to transmit in the wireless medium. As observed at the second slot, MTs B, C and D fail to transmit their packets, so each MT will wait a random amount of time slots before transmitting again.

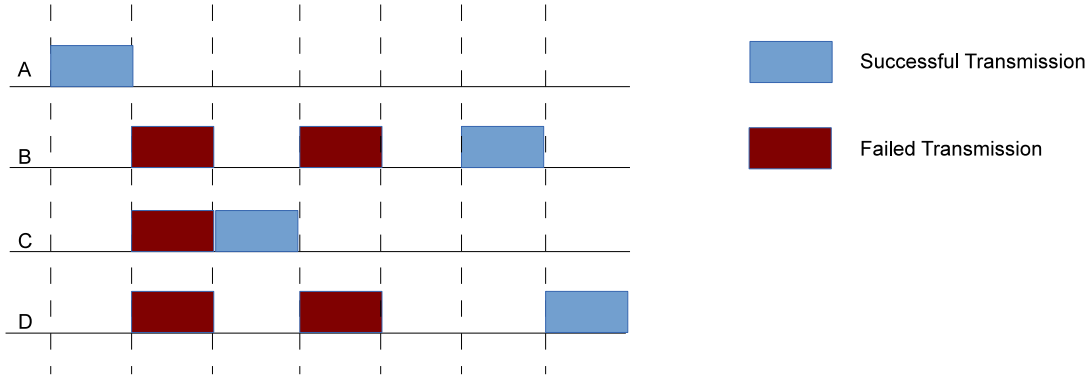

Figure 2.5: Slotted ALOHA example with four MTs: A, B, C and D.

Guaranteed access

Regarding guaranteed access protocols, MTs access the medium in an organized way, e.g. round-robin. The MTs access can be configured by a *master-slave* setup, where the master polls the slaves for data, or the MTs access is made by token-passing. Currently, token-passing protocols are not commonly

used, since these are prone to errors upon the failure of the token reception [GL00].

Hybrid access

Hybrid access protocols are based on request-grant processes, where MTs contend the channel to reserve slots or bandwidth, to send data. A BS allocates the required resources and sends a grant to a requesting MT. Hybrid access protocols are further classified as Random Reservation Access (RRA) and Demand Assignment (DA). In RRA protocols, the BS reserves upstream bandwidth based on users requests, while on DA protocols, the BS controls upstream bandwidth based on QoS constraints.

Fixed and adaptive access

Peyravi [Pey99] extends *Gummala*'s classification for centralized MAC protocols with two additional categories: Fixed Assignment Multiple Access (FAMA) and adaptive protocols. FAMA protocols statically assign bandwidth to each MT regardless of their activity; adaptive protocols attempt to diminish the number of contention slots in the medium by switching between random access or reservation access dynamically.

Sections 2.5.1 and 2.5.2 overview distributed and centralized MAC protocols respectively.

2.5.1 Distributed MAC Protocols

Distributed MAC protocols rely on carrier sensing and collision avoidance, except the ALOHA system and its derivatives. Location-dependent carrier sensing implies the existence of hidden and exposed MTs. Carrier Sense Multiple Access (CSMA) protocols [GL00] plays an important role regarding hidden/exposed MTs. On a half-duplex system, MTs cannot sense the channel while they are transmitting. Some sort of information must be used to avoid collisions, either using an out-of-band signal or an handshaking procedure. Below, collision avoidance mechanisms and distributed random access protocols are described.

Collision Avoidance Mechanisms

Busy Tone Multiple Access (BTMA) [TK75] is an example of collision avoidance using out-of-band signalling to prevent hidden MTs. A MT that *listens* to a transmission, emits a *busy* tone; any MT that *listens* the busy tone does not initiate a transmission. This solution solves the hidden MT problem, but increases the number of exposed MTs. Receiver Initiated - Busy Tone Multiple Access (RI-BTMA) diminishes the number of exposed MTs by emitting the busy tone after decoding the message at the intended receiver. According to *Gummala et al* it takes a long time to emit the busy tone [GL00] due to the decoding phase; RI-BTMA does not eliminate the hidden MT problem.

Multiple Access with Collision Avoidance (MACA) [Kar90] attempts to minimize the hidden MT problem by using a three-way handshake system. A MT that has data to send, transmits a Request To Send (RTS) packet. All stations within one hop delay their transmissions. The destination responds with a Clear to Send (CTS) packet; all MTs within one hop from the destination also delay their transmissions. Once the transmitting MT receives the CTS packet, it initiates data transmission. Enhancements to this technique can be found in [Bha97].

Distributed Random Access Protocols

The current section regards distributed random access protocols. Carrier Sense Multiple Access (CSMA) attempts to transmit data only when it senses that the channel is idle, otherwise it waits a random period of time. If the channel is idle, the protocol attempts to acquire the channel and if successful the protocol sends a data packet; afterwards the protocol waits for an acknowledgment [GL00]. A known example of a CSMA protocol is the Distributed Foundation Wireless MAC (DFWMAC) used as the basic Distributed Coordinated Function (DCF) protocol for the IEEE 802.11 [Cea96]. The DFWMAC consists of a four-way handshake. A MT with data waits a random period of time; this time is decremented while the channel is idle. Once the waiting period expires, the MT attempts to acquire the channel with a RTS packet. The destination MT replies with a CTS. Afterwards the source MT transmits its packet, named DATA. If the packet is received without errors, the destination acknowledges with an ACKnowledgment (ACK). If the ACK is not received, then it is assumed that the packet was lost, implying an additional transmission from the source MT. On the occasion that the RTS failed, the sending MT doubles its waiting period. This contention method is known as the Binary Exponential Backoff (BEB). The DFWMAC has distinct waiting periods; before attempting a RTS request, the sending MT must sense the channel during a Distributed Inter-Frame Space (DIFS). A Short Inter-Frame Space (SIFS) waiting time is used between the RTS and CTS, between a CTS message and a data packet and before an ACK transmission. The SIFS interval is shorter, such that the destination MT takes priority when sending an ACK. All MTs that hear the RTS or CTS messages backoff during a Network Allocation Vector (NAV) time. The NAV is included in each RTS/CTS/DATA message.

Another example of a CSMA protocol is the Elimination Yield Non-Preemptive Multiple Access (EY-NPMA) [ETS95]. The contention phase of the protocol has two sub-phases: An elimination phase and a yield phase. During the elimination phase, MTs may transmit during a slotted random period of time, afterwards MTs sense the channel. If the channel is busy, MTs abort their transmission, otherwise a node moves to the yield phase. If no transmission occurs during the yield phase, the node starts data transmission. The number of slots' distribution for the elimination phase is chosen to ensure a single packet transmission, i.e. only one MT transmits with a probability close to 1.

From these ad-hoc mechanisms, DFWMAC has the highest throughput when compared to EY-NPMA. In terms of QoS, EY-NPMA performs better [GL00].

2.5.2 Centralized MAC Protocols

Opposite to distributed MAC protocols, in centralized MAC protocols the coordination is made at the BS. All communications must go through the BS; it is assumed that all MTs can talk and hear the BS, so there are no hidden or exposed MTs. Centralized protocols can be classified in five types: random, fixed, guaranteed, hybrid and adaptive.

Centralized Random Access Protocols

Examples of centralized random access protocols are: Idle Sense Multiple Access (ISMA) [WMF93], Randomly Addressed Polling (RAP) [CL93] and Resource Auction Multiple Access (RAMA) [Ami93, Ami92].

On ISMA, carrier sense is performed at the BS. When the channel is idle, the BS sends a broadcast message Idle Signal (IS). MTs with data to send transmit with a given probability p. On a collision

occurrence, the BS broadcasts an IS again; otherwise, if a transmission was successful, then it transmits an Idle Signal with Acknowledgment (ISA). The protocol performs poorly when a collision occurs; Reservation ISMA (R-ISMA) [Wea66] solves this problem by using small reservation packets instead of data packets. Once the BS successfully receives a reservation from a MT, it sends a Polling Signal (PS) message back to the MT, then the MT transmits its respective data message.

MTs in RAP use orthogonal pseudo-random codes to contend the medium simultaneously. The BS receives and decodes all transmitted codes, requiring a Code Division Multiple Access (CDMA) receiver [Hol94]. Afterwards the BS polls each transmitted code; the MTs that transmitted the polled code, transmit their data packet. If a collision occurs a Negative ACK (NACK) is sent, otherwise an ACK is sent.

On RAMA each MT has a b-bit identification. Collision resolution is based on a symbol-by-symbol transmission of the MT's identification. During the contention phase, MTs transmit their identifier, the BS transmits to all MTs the identifier it heard symbol-by-symbol; if the symbol identifier heard by the BS does not match the MT's identification, then the MT backs off from the wireless channel. It is assumed that the channel performs an OR operation on a symbol collision. In RAMA, if a MT has data to transmit, a communication slot is always used. The protocol might starve MTs with lower identifications, making the protocol unfair. Fair Resource Auction Multiple Access (F-RAMA) [PM96] addresses the problem by selecting a random symbol at the BS during the contention period.

From the discussed protocols, RAMA has the highest throughput with an unfair approach as opposed to RAP and ISMA. Nonetheless RAMA might starve the channel.

Distributed and Random Access Control Discussion

Parameter	DFWMAC	EY-NPMA	ISMA	RAP	RAMA
Coordination	Ad-hoc	Ad-hoc	Central	Central	Central
Throughput	0.7	0.45	0.75	0.8	0.84
Delay	10ms	20ms	20ms	5ms	-
Collision resolution	Exponential backoff	Geometric backoff	p-persistent	Random backoff	Deterministic
Fairness	Unfair	Unfair	Fair	Fair	Unfair
QoS	No	Partial	No	No	No

Table 2.1: Comparison of random access protocols [GL00].

Table 2.1 compares the distributed and centralized random access protocols according to [GL00]. From this table, it is possible to conclude that random access protocols may be unfair due to various reasons: existence of hidden/exposed nodes for distributed access or unfair reservation mechanisms. Furthermore, it should be noted that the throughput and delay values were not normalized between both types of random access, either way both types of protocols are very difficult to compare - for example, distributed random access protocols are used when it is difficult to structure a network (e.g. a Wireless Sensor Network (WSN) [YMG08]) while with a centralized network MTs are associated to a BS that coordinates the medium.

Fixed Assignment Multiple Access

As aforementioned, Fixed Assignment Multiple Access (FAMA) protocols statically assign bandwidth regardless of a MT's activity, i.e. if it has packets or not. This is achievable by assigning *even* pieces of bandwidth to each MT [Pey99]. There are various methods to assign bandwidth, either at the time

domain, Time Division Multiple Access (TDMA), at the frequency domain, Frequency Division Multiple Access (FDMA) or using orthogonal codes, Code Division Multiple Access (CDMA)[Hol94].

FAMA protocols are effective when the number of MTs is small and MTs have predictable traffic patterns.

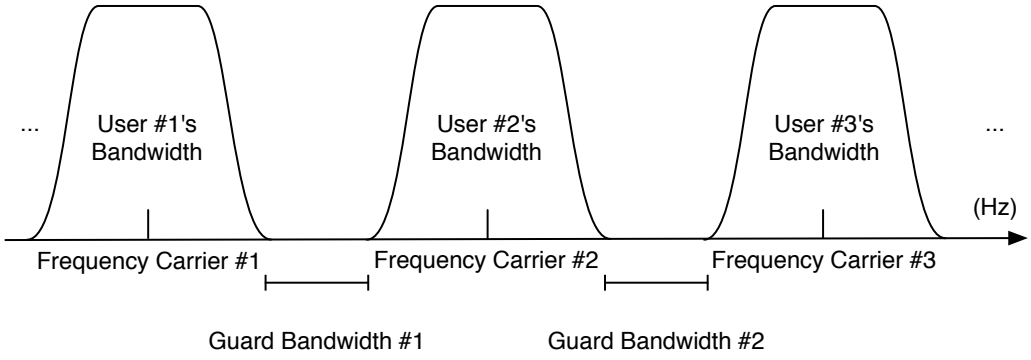

Figure 2.6: FDMA illustration.

FDMA, illustrated in figure 2.6, does not require any kind of coordination since each MT has its own band, however it can be wasteful if the channel load is uneven; for example, an idle MT is wasting bandwidth when other MTs could use it. Two currently known schemes based on OFDM and SC-FDE, that expand the notion of FDMA, and efficiently use the spectrum are Orthogonal Frequency Division Multiple Access (OFDMA) [SS05] and Single-Carrier FDMA (SC-FDMA) [MLG06] respectively; these schemes multiplex MTs by assigning to each one a given subset of subcarriers.

Figure 2.7: TDMA illustration.

TDMA, illustrated in figure 2.7, has a better throughput [Pey99], but still, MTs have to wait a fixed channel time before transmitting any data. With bursty traffic, TDMA has a poor performance since idle slots could be used for transmission.

Regarding CDMA, MTs can transmit data in a slotted manner without the need to contend for the wireless channel by means of orhtogonal spreading sequence codes [Hol94]; nonetheless, as referred in section 2.3, MTs are restricted to a fixed spreading sequence rate [Pey99] that limits the spectrum efficiency.

Guaranteed Access Protocols

Guaranteed access protocols are polling protocols that attempt to minimize bandwidth waste from channel outage [GL00]. The channel is tested with a control handshake. If it is successful, then it is assumed that a good channel exists between a MT and a BS.

Zhang et al [ZA91] propose a round-robin polling scheme for transmission requests. A MT with data responds to a polling message from the BS with a request, or a KEEP ALIVE message when it does not have any data to transmit. Afterwards the BS proceeds with data polling according to each MT's request. *Zhang* proposes that the BS must poll each MT periodically with a coherence time T, to ensure that after time T the channel has changed enough to affect data transmission.

Disposable Token MAC Protocol (DTMP) [HA93] on the other hand discards the poll-request phase, and proceeds to a poll-data cycle phase directly.

Acampora et al [AK97] proposed a protocol with three phases: polling phase, request phase and data phase. The BS first identifies the active MTs by polling each active MT's identifier; an active MT reiterates the identifier if it has data to transmit. Afterwards, the BS echoes the identifier back so that all MTs know the active MTs order. During the request phase, all active MTs send their requests to the BS. Afterwards the BS polls the MTs for data transmission.

These protocols have similar performance [GL00] for error-free channels; however, these protocols do not support QoS and multimedia applications.

Hybrid Access Protocols

A hybrid access protocol blends the concept of a random access protocol and the deterministic features of a polling protocol. Hybrid access protocols can be further categorized in two classes: Random Reservation Access (RRA) and Demand Assignment (DA).

■ Random Reservation Access (RRA) protocols

RRA protocols attempt to multiplex data stochastically on a TDMA basis. These protocols were studied to support data services on cellular networks [GL00]. The uplink is structured as a time-slotted system and organized into frames. The frame size is chosen such that it supports a single voice packet for each frame. Subsequently each data packet fits one time slot. The downlink from the BS to the MTs is a broadcast channel. A RRA protocol is composed of a random access component and a reservation component. A MT with data to transmit uses a random access protocol to attempt transmission. The reservation component is described by the BS rules that define the uplink slots for MTs that successfully contended the channel. Examples of RRA protocols are Packet Reservation Multiple Access (PRMA) [Gea89, WG93], Random Reservation Access - Independent Stations Algorithm (RRA-ISA) [ACD88, BDN97] and Packet-Demand Assignment Multiple Access (PDAMA) [PRC86].

PRMA was designed to multiplex speech and data on cellular networks [Gea89, WG93]. A MT with backlogged voice data contends the channel with probability p. If successful it reserves the following slots for the voice stream until the end of the talk [Nan90]. MTs with data packets contend in a similar fashion, but opposed to voice traffic, data traffic is not reserved. Voice traffic and data traffic have different access probabilities [Nan90]. *Wong et al* designed a PRMA protocol that allows limited slot reservations for data traffic. *Wong* defined a maximum reservation threshold to avoid starvation. Mixing data and voice traffic degrades the performance of the PRMA protocol [Nan90]. Frame Reservation Multiple Access (FRMA) [NY95] attempts to enhance PRMA contention algorithm by separating both voice and data slots. *PRMA++* [DeV93] separates data and voice channels to improve the PRMA contention bandwidth. Each uplink frame consists of request slots and information slots. MTs contend during the request slots using S-ALOHA; based on successful requests, the BS grants information slots to MTs. *Bianchi et al* [BBFM97] designed an extension to PRMA with QoS. When contending for the medium, MTs send their QoS requirements; based on this information the BS schedules the uplink transmissions according to the delay and traffic rate. It guarantees the next transmission opportunity to the MT with the closest deadline.

RRA-ISA uses the Independent Stations Algorithm [ACD88, BDN97]. The algorithm distributes access rights to MTs to enhance the throughput from slot to slot [GL00]. It is similar to a BS polling a subset of MTs, where the subset is chosen in order to maximize the probability of a single transmission in a slot. The BS based on past history, computes the probability that a MT has a packet to transmit. The algorithm can make a good prediction if the upstream traffic is well characterized.

PDAMA is a protocol developed by the National Aeronautics and Space Administration (NASA) [PRC86]. PDAMA's frame structure consists of a leader control slot, a guard slot and reservation mini-slots. The leader slot is transmitted by the BS and it has acknowledgments for previously reserved slots and frame time allocation for other stations. The guard slot ensures that all stations hear the BS before attempting reservations. A MT that is inserted into the network for the first time transmits its identification during the guard slot; if no collision occurs, the MT can hear its own transmission and determine the RTT. On a collision situation, the MT uses a random backoff algorithm [Tan03]. During the reservation mini-slots, MTs use S-ALOHA for contention. There are three types of reservations: urgent mode, long message mode and digitized mode. On urgent mode, a MT requests an information subframe to transmit data; it can also request subframes for digitized voice. On long message mode, as the name implies, the MT reserves enough subframes for long messages. On digitized mode, frames are allocated for digitized voice, allowing full-duplex communication.

Parameter	PRMA	RRA-ISA	FRMA	PDAMA
Duplex operation	FDD	TDD/FDD	TDD	TDD/FDD
Data Delay	1.6s	32ms	40ms	-
Collision resolution	p-persistent	Group polling	p-persistent	S-ALOHA
Priority in access	Yes	Yes	Yes	Yes
QoS	No	Partial	Voice-only	Partial

Table 2.2: Comparison of RRA protocols [GL00, Pey99].

Table 2.2 compares the different protocols according to [GL00, Pey99]. According to *Gummala* [GL00], FRMA has the best performance; RRA-ISA also performs good when the number of MTs is small, otherwise it performs as good as PRMA. PDAMA achieves a good performance since it supports QoS to some extent - it differentiates the types of reservations for a high RTT network (e.g. satellite network).

RRA protocols are a good choice for an unsaturated wireless network that needs some sort of QoS control to achieve a better throughput and delay without wasting the available resources if MTs are idle; however, with a saturated network load RRA protocols can be heavily affected.

■ Demand Assignment (DA) protocols

DA protocols allocate bandwidth to MTs according to their QoS constraints [GL00]. QoS requirements are hard to achieve with random access protocols, since every packet must contend for access. There are three phases on a DA protocol: request, scheduling and data transmission. The request phase is used to send a MT's QoS requirements. Additional requests can be further processed with additional data transmissions instead of contending for the channel. Based on these requirements, the BS schedules the uplink transmissions. At the end MTs transmit their data. Examples of DA protocols are: Distributed-Queueing Request Update Multiple Access (DQRUMA) [KLE95], Mobile Access Scheme based on Contention and Reservation for ATM (MASCARA) [Mea98], and Dynamic Slot Assignment ++ (DSA++) [Pet96].

DQRUMA assumes an FDD approach for the uplink and downlink. The uplink has a request channel and

a packet transmission channel; the request channel is used for contention requests, while the packet transmission channel, as the name implies, is used to transmit data. MTs can also use the packet transmission channel to piggyback requests when outstanding data is present. At the downlink, an ACK message is sent confirming the contention of the current uplink slot and stating the MTs eligible to transmit data at the next uplink slot. If a collision occurs during the contention period, the MT waits a random period of time and tries again.

MASCARA uses variable time frames. Each frame consists of three distinct periods: broadcast, reserved and contention. The broadcast period is used to announce the structure of the current time frame and the scheduled uplink transmissions. The reserved period is composed of two sub-periods: a downlink sub-period where the BS sends data and the uplink sub-period where MTs send data. The contention period is used to send requests to the BS. S-ALOHA is used to send requests; the BS uses a leaky-bucket token scheme to schedule the uplink period.

DSA++ takes advantage of a fixed TDMA structure for the uplink, carrying fixed-size Asynchronous Transfer Mode (ATM) cells, where slots can be either marked for reservation or contention. The downlink is also slotted, where each slot carries data and a MAC message. The MAC message contains an acknowledgment from the previous uplink slot and the reservation for the next uplink slot. Contention slots are sub-divided into mini-slots. Based on all requests, the BS schedules the uplink transmissions, taking into account specific connection parameters such as mean data rate, peak data rate, queue length and waiting period from the first cell at the queue. The scheduling algorithm prioritizes the requests and assigns the next slot according to the MTs priority.

Parameter	DQRUMA	MASCARA	DSA++
Duplex operation	FDD	TDD	FDD
Maximum throughput	0.92	0.78	0.82
Average delay	10 slots	300 slots	10 slots
Collision resolution	Binary stack	S-ALOHA	Ternary Splitting
QoS	Yes	Yes	Yes

Table 2.3: Comparison of DA protocols [GL00].

Table 2.3 compares the different DA protocols according to [GL00]. DA protocols in general outperform other protocol classes in terms of multimedia traffic [GL00]. In terms of throughput, DQRUMA has the best performance. MASCARA, despite being the slowest of the three due to TDD operation, does not have limitations in terms of framing structure between the uplink and downlink timings, contrary to the other DA protocols [GL00]. DA protocols are a perfect fit for delay-sensitive applications, however these protocols can be very complex to implement and should be very robust for time-sensitive applications.

Adaptive Protocols

Peyravi extends the MAC protocol notation from figure 2.4 with adaptive protocols [Pey99]. Adaptive protocols can control the number of MTs that contend the channel to reduce conflicts or to switch dynamically from random access to reservation mode. These protocols can perform well for asymmetric traffic [Pey99]. Examples of adaptive protocols are: The Adaptive Tree Walk protocol [Tan03], URN protocol [Tan03] and Split Reservation Under Collision (SRUC) [BF78].

The Adaptive Tree Walk protocol [Tan03] organizes MTs as leafs of a binary tree. On a successful transmission in a given slot, MTs are authorized to transmit at the following slot. Otherwise, if a collision occurs, on the following slot only the MTs from the left subtree are authorized to transmit data, the tree

is searched in-depth to locate MTs that are ready to transmit. The search can begin farther, if q ready stations are uniformly distributed; the optimal level to begin searching is $log_2(q)$.

A URN protocol [Tan03] gives sequential permission to groups of MTs to contend the channel using S-ALOHA. Under light-load it operates similarly to the ALOHA protocol and under heavy load it operates as TDMA. Under light load, a large number of MTs have channel access rights, whereas for heavy load the number of MTs with access rights is reduced.

SRUC [BF78] divides slots into a control part and a data part. The data subslots can be either in reserved mode or random mode. Random mode operates the same way as S-ALOHA. Upon data collision, the data subslot becomes reserved until all collided packets have been successfully transmitted. The control subslot informs about MTs involved in a collision. Access to the control subslots are contention-free. Previously contended MTs do not mix with new ones. SRUC combines S-ALOHA with reservation protocols, switching between them according to the state of the channel. SRUC divides MTs into groups. Slots are then combined to a time frame so that all MTs have an information entry after a corresponding number of frames.

According to [Pey99], adaptive MAC protocols are ideal when confronted with a variable traffic load and also with topological changes; however these protocols are very complex to implement and need to be robust in terms of the access control mechanisms. Despite the complexity, these protocols have a very high throughput and low delay which makes them suitable for stringent QoS requirements. As an ending remark, SRUC outperforms the other adaptive protocols mentioned in this section [Pey99], being the most stable and scalable of all three.

2.5.3 Comments

	Random access	Guaranteed	RRA	DA	Adaptive
Infrastructure	Distributed/Centralized	Centralized	Centralized	Centralized	Centralized
Scalability	Low-Medium	Low	Medium	High	High
Delay at low load	Good	Medium	Medium	Medium	Medium
Delay at high load	Poor	Medium	Medium	Good	Good
QoS support	Poor	Poor	Medium	Very High	High
Complexity	Low	Low	Low	High	High

Table 2.4: Comparison of the different classes of protocols [GL00, Pey99].

Several *traditional* MAC architectures were presented for wireless communications. Each one suits specific characteristics for distributed or centralized networks. A centralized architecture should be suitable for *asymmetric* QoS requirements that varies greatly from light to heavy traffic. So a BS that can manage the MTs' needs is a requirement of great importance. Table 2.4 summarizes the MAC protocols' classes discussion.

A centralized random access protocol can be interesting if the channel load is light, but under a heavy load, and/or large RTTs, MTs should know how to act according to the channel's load; therefore, better channel coordination is needed. A FAMA scheme can be useful for a channel under a heavy load, but it wastes too much bandwidth under light load conditions - OFDMA and SC-FDMA waste less bandwidth though. Guaranteed access protocols can minimize this effect, by polling MTs with data to send, but considering an immense number of MTs, it is unfeasible due to the RTT between polling all MTs and informing which users can transmit data.

Regarding hybrid protocols, DA protocols fit considerably well under strict QoS requirements; it requires

a robust implementation of the BS, since a substantial overhead is required for connection establishment and scheduling. RRA protocols are someway in between random access protocols and DA protocols, but not as good as the latter. DA protocols seem appropriate as long as the BS is reliable and robust.

Adaptive protocols do not take into account QoS requirements of each MT, but are better adapted to asymmetric traffic than random centralized architectures or FAMA architectures. According to *Peyravi* [Pey99], these protocols are not as good as hybrid implementations in terms of delay versus throughput, but are a good option.

The employment of *sophisticated*, yet complex, MAC protocols can be useless for stringent QoS requirements if these schemes cannot cope with high throughputs under difficult transmission conditions, e.g. channel errors, or packet collisions; such difficult conditions lead to even higher delays. Furthermore, a wide array of PHY layer techniques that cope with packet errors exist, especially for packet collisions - due to this fact, *traditional* MAC schemes can be *stale* in terms of performance; the following section will present cross-layered PHY-MAC designs that overcome *traditional* MAC schemes disadvantages. The design of a PHY-MAC protocol that can cope with packet collisions or errors could be extremely valuable for asymmetric traffic loads without wasting channel resources and therefore enhancing existing designs that perform poorly without any QoS control.

2.6 PHY-MAC Cross-layered Designs

According to the Open Systems Interconnection (OSI) reference model, layers do not share information with each other. *Shakkotai et al* emphasizes the opposite [SRK03], referring the importance of sharing information from lower layers to enhance the performance of higher layers on a wireless context. Based on the PHY layer information, the maximum channel capacity can be achieved based on the diversity gain, according to [SRK03]; however, there is not an optimal cross-layered design, it depends on the embedded algorithms of the MAC and PHY layers. Cross-layered implementations focused on Hybrid-ARQ (H-ARQ) and MUD are discussed on this section. Section 2.6.1 refers to cross-layered TDMA MAC implementations with H-ARQ; section 2.6.2 studies CDMA MAC implementations with H-ARQ; section 2.6.3 overviews MAC implementations using MUD techniques, focusing mainly in Network-assisted Diversity Multiple Access (NDMA) techniques.

2.6.1 TDMA with type-II H-ARQ techniques

A TDMA MAC protocol is suitable for delay-based QoS applications, i.e. for a given maximum delay; a BS can reuse the information from an unsuccessful packet to enhance the reception on subsequent retransmissions [PBD+10].

Figure 2.8 illustrates a type II H-ARQ example with two MTs: A and B. Packets from MTs A and B are represented as $A_i^{(j)}$ and $B_k^{(l)}$ respectively; subscripts i/k represent the MT's packet identifier and superscripts j/l the number of transmissions for packets i/k. MTs A and B transmit a packet in the first TDMA frame; A fails to transmit its packet, henceforth the BS will ask MT A to retransmit its packet at the following frame. At the second frame, the BS recovers A's packet based on $A_1^{(1)}$ and $A_1^{(2)}$. If the wireless channel suffered a deep fade during the second frame, the BS would ask MT A to re-transmit its packet at the following frame; this behavior would repeat up to a maximum number of packet re-transmissions to enhance packet reception with the available packet copies.

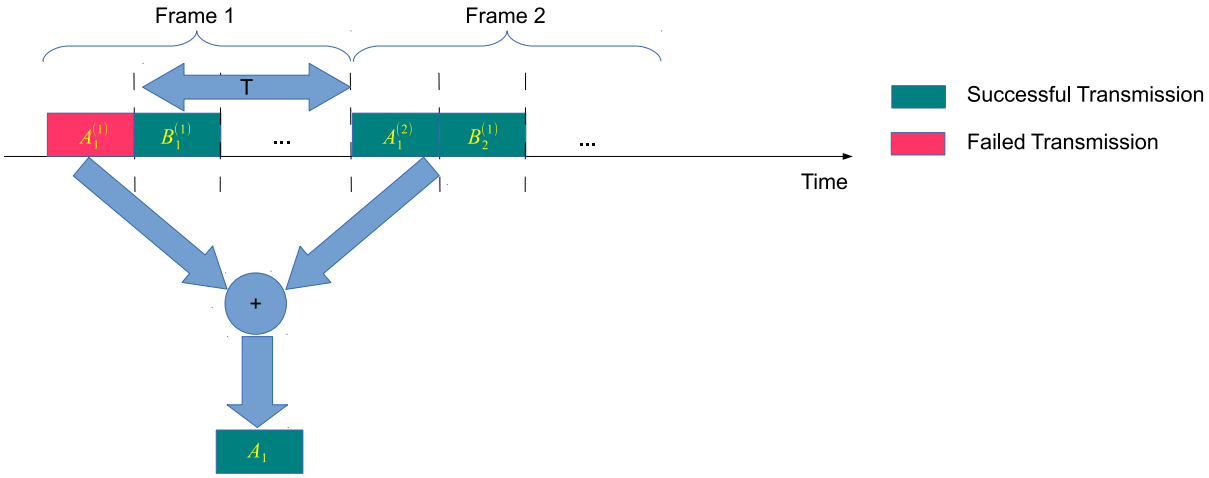

Figure 2.8: TDMA with H-ARQ example with two MTs: A and B.

Type II H-ARQ techniques can be broadly organized as Code Combining (CC) and Diversity Combining (DC) techniques. CC techniques [LY82, Cha85, Hag88, GDE99, VST+05, VSW05] concatenate data block copies that form long codewords; the technique relies on a powerful punctured error correcting code, where successive retransmissions of a given data block improve data reception. DC techniques [Ben85] combine the copies of a given data symbol, providing a robust scheme for data detection. DC techniques are simpler to implement and are much more efficient than CC techniques [DCM08].

ARQ error control for TDMA was first analyzed by *Saeki* for three variations [SR82]: Stop-and-Wait, Block and Selective Repeat. *Kallel* analyzed the maximum throughput performance employing convolutional coding with code combining for Selective Repeat [Kal90]. *Kallel* concludes that employing code combining has a good throughput performance for high channel error rates. *Jun-Bae et al* studied the queuing model of a type-II hybrid ARQ with convolutional coding for error correction on a Markovian channel [JBSQNHea05b, JBSQNHea05a]. The system is modeled with a Poisson inter-arrival message process, though lacking a generic approach towards the system modeling. *Badia et al* studied the performance of type-II H-ARQ Reed-Solomon (RS) erasure codes for Selective Repeat [BLZ08]. *Pereira et al* extended *Saeki*'s model [SR82] for an SC-FDE context, where the BS employs a DC technique. *Pereira*'s extended model has the advantage of being generic for any message arrival process for a unsaturated network. *Quaglieri et al* studied the benefits of using a type-II H-ARQ technique on a High Altitude Platform (HAP) link in terms of energy efficiency [QSCea05]; the authors concluded that there is an expected trade-off in terms of throughput degradation if it is intended to diminish the MTs energy consumption. Nevertheless, the aforementioned research lacks a correlation study between the packet error rate, the expected delay and the required energy to send a packet. *Lin* studied error control with H-ARQ using parity retransmission [LY82]; the research proves that it is possible to achieve high-speed data communication for high round trip times. The research lacks a complete study of the expected delay.

2.6.2 CDMA with type-II H-ARQ techniques

Wireless Code Division Multiple Access (CDMA) packet-data-oriented systems have been an hot research topic for the last decades, attracting contributions with the design and analysis of physical-layer receiver algorithms aimed at either the PHY layer performance (focused in minimizing the PER, e.g. [Ver86]) or the system-level throughput performance (depending upon the logical-layer protocols, includ-

ing the MAC and ARQ protocols, e.g. [CF07]). A small number cover a quantitative understanding of the joint effects of the PHY and MAC layers on the throughput performance (e.g. [LWZ04, LZ09]).

Takeda and Adachi [TA07] analyzed the use of turbo coded H-ARQ for multicoded DS-CDMA considering a MMSE turbo equalization to mitigate the effect of the residual Inter-Chip Interference (ICI); the authors verified that their equalization technique improved the system throughput, since it could suppress ICI for a higher coding gain. Similarly with the same conclusions, *Chafnaji et al* [CAISV12] investigated MMSE FDE-based iterative turbo packet combining for prefix-assisted DS-CDMA aided by MIMO. The Iterative Block Decision Feedback Equalization (IB-DFE) technique was studied by *Silva and Dinis* for a prefix-assisted DS-CDMA system under the MMSE criterion [DSG07a, SD06, DS06b], showing better Bit Error Rate (BER) results for each succeeding iteration of this technique, especially when compared to a linear equalization technique.

Regarding solutions to improve the BER with H-ARQ, *Letaief et al* proposed a power control algorithm that was used with outer RS and inner convolutional codes for DS-CDMA that satisfies the BER of differentiated QoS requirements [LM02]. Adaptive modulation coding combined with H-ARQ was also analyzed by *Garg* to improve the average BER performance [GA06].

Works that attempt to model the access control with H-ARQ have simplified channel models that rely on the Signal-to-Interference-plus-Noise Ratio (SINR) (e.g. [SW95, BGB97, ZWL99, PV00, LWZ04, LZ09]). For most works (e.g. [WPS09]), the receiver performance is modeled by a threshold value that defines the minimum SINR above which the receiver satisfies the QoS requirements. Approximated values are calculated for the receiver's BER (e.g.[LS04, LWZ04]), using average interference estimation. However, the BER depends on the distributions of the number of transmitted packets and the transmission power [DV06]. A closer connection is needed between the physical and logical layer models to have a better precision regarding the MAC performance model.

Some H-ARQ models considered a constant transmission rate for all MTs and modeled the H-ARQ performance with DC for the average SINR (e.g. [SW95]). *Bigloo et al* [BGB97] modeled a DS-CDMA H-ARQ system with DC, assuming that the composite packet arrivals (including both new arrivals and retransmissions) in different slots are independent and identically Poisson.

Multidimensional Markov chain models were used for the system dynamics in [ZWL99, PV00, LWZ04]. The average BER is obtained from steady-state probabilities by solving a fixed-point equation [PV00] or applying the renewal-reward theorem [LWZ04]. Until now, most of the authors assumed that the number of MTs transmitting during the H-ARQ transmissions remained constant for an average number of colliding MTs.

Sun and Shi [SS07] analyzed the asymptotic performance of large CDMA random access systems using H-ARQ, where the ratio of the number of users and the spreading, each tending to infinity, converges to a constant. The study shows that the throughput, packet delay, transmission and waiting times, and the spectral efficiency can be obtained from the packet detection probability.

Levorato and Zorzi proposed a work regarding the performance of CDMA with H-ARQ [LZ09] for spatially distributed interfering signals. It describes the distribution of the number of decoded packets at a given stage using an embedded chain of a semi-Markov process in function of the node's distribution and error probability.

The steady-state distributions for the interference and throughput are obtained using a recursive algorithm, based on the model defined in [LS04] for a SIC receiver; the BER is obtained for a Gaussian approximation. The analytical model for the system behavior is rather complex and does not consider

the interference of all concurrent transmissions from all transmission stages at a given instant.

The presented models for the joint-performance of CDMA at the PHY and MAC layers, are either too focused on one layer or the other, i.e. presenting detailed PHY-layer results but limited results at the MAC-layer or detailed MAC performance results using simplified PER models. Furthermore, CDMA even with H-ARQ has system-wise issues in terms of spectral efficiency, since it uses more redundancy than it needs for a low channel access rate - i.e. the spreading code's length is higher than the number of active MTs transmitting data.

2.6.3 Multipacket Reception Access Control Techniques

Multipacket Reception (MPR) techniques take advantage of signal processing techniques to separate collided signals from multiple users on a structured random access wireless context [TZB00, ZT02, LE05]. *Ghez et al* studied this multipacket reception capability on a S-ALOHA context [GVS88] without much emphasis on the receiver's design. *Luo and Ephremides* studied the relationship of throughput, delay and stability regions of MPR [LE05]; this work discovered that the asymptotic capacity region follows closely the throughput region. MPR can be achieved from multiple manners: spread-spectrum techniques such as CDMA; spatial diversity techniques as aforementioned with MIMO; and time diversity. This section is mostly focused in time diversity techniques.

Network Diversity Multiple Access Protocols

Tsatsanis et al introduced Network-assisted Diversity Multiple Access (NDMA), where collided packets are used to extract their respective signals on forthcoming re-transmissions [TZB00]. If P MTs send data on a given time slot, they will have to re-send their data $P-1$ times to separate each MT's packet. The BS receives the collided packets and stores them for future decoding. Similarly to an H-ARQ type-II technique, packets are not discarded to enhance data reception. *Tsatsanis*' work uses DC as a diversity technique. According to *Tsatsanis*, using an NDMA technique ensures better resource usage than fixed-resource techniques such as TDMA, CDMA or FDMA, since MTs re-use idle resources. The number of slots required to transmit data when collisions occur with NDMA are the same as when no collisions occur for a traditional access scheme. *Tsatsanis*' work, for an enormous number of MTs accessing the wireless medium, can become problematic without an appropriate backoff scheme.

Figure 2.9 illustrates an example of the NDMA protocol with two MTs: A and B. The BS coordinates the wireless medium in a slotted manner and signals MTs at the beginning of an epoch; MTs with packets in their queue will transmit them at the beginning of the epoch, if collisions are detected then the BS will notify the MTs to retransmit at the beginning of the next slot. This behavior is illustrated at the fourth epoch (slots four and five). New packet transmissions during an epoch are not allowed.

Tsatsanis' work was later extended for multipath dispersive channels [ZT02], by means of a blind collision resolution algorithm that employs rotational invariance and factor analysis techniques - this approach is named Blind NDMA (B-NDMA). Data detection is possible through a rank test for blind multiplicity detection. This approach was proposed to avoid the use of orthogonal identification codes that are required in the original NDMA, since the size of orthogonal identification codes grows linearly with the number of users; therefore B-NDMA improves the channel utilization and the system capacity, as well as avoiding synchronization errors. Contrary to NDMA, it requires $(P+1)$ transmissions for P colliding packets.

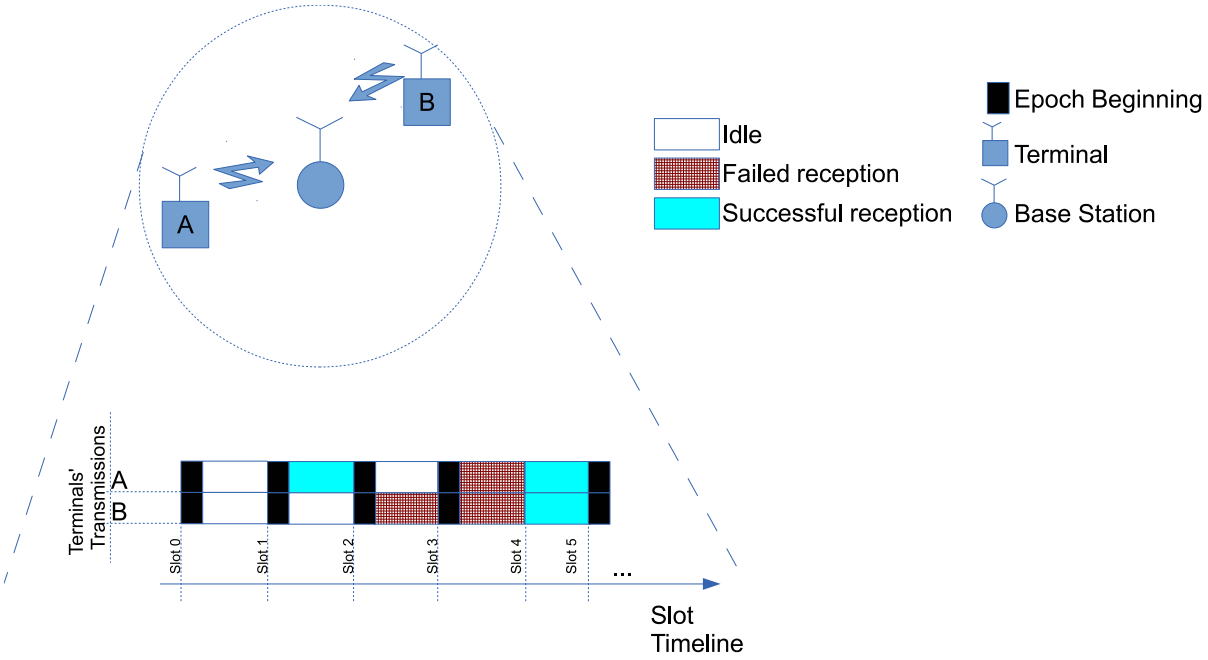

Figure 2.9: NDMA example with two MTs.

Özgul and Deliç introduced Independent Component Analysis NDMA (ICA-NDMA) [ÖD06], an extension to NDMA that attempts to solve collisions through independent component analysis, which is another way to accomplish the collision resolution in a blind way similar to B-NDMA, and it can work in quasi-static fading channels without requiring any kind of phase control. ICA-NDMA performs data detection by combining a minimum description length criterion and a variation of the rank test method. Nevertheless, ICA-NDMA requires at least $(P + 2)$ transmissions for P colliding MTs.

Lin and Petropulu [LP05] extended the NDMA protocol for a cooperative setting, named Cooperative NDMA (C-NDMA). In C-NDMA, there are non-regenerative relays that retransmit the received signal after a collision slot. This way, the BS can retrieve the original packets, without needing to ask for more re-transmissions from the original sources, though implying the additional complexity of having well positioned relays; in practice C-NDMA resembles a MIMO system that achieves better throughput results than NDMA.

Yao et al [YYL+10] also proposed a cooperative solution based on B-NDMA, where a cooperative transmission epoch is triggered once a collision occurs, and at each slot only one MT, randomly selected by the BS, forwards the garbled data from the collision slot if the MT was idle, otherwise it sends its own packet; through interference cancellation methods the BS is able to recover the collided packets. Although this work does not study the PHY layer performance, it achieves an higher throughput than B-NDMA.

Pereira et al [PBD+09] extended *Tsatsanis*' work. Their work allows a number of J MTs contending the wireless medium higher than the maximum number of decodable packets P, with an appropriate backoff mechanism; *Pereira*'s research is employed with half-duplex radios. A p-persistent NDMA MAC technique is employed, where each MT's packet has the same duration. The BS at the beginning of a control frame sends a medium access probability, p, to control the number of MTs contending the channel. This work uses a SIC technique, Iterative Block Decision Feedback Equalization (IB-DFE), from [DCB+07] to separate the MTs' packets.

Samano-Robles et al proposed a p-persistent NDMA protocol, assuming an infinite population of MTs

[SRGM06]. Their work was later extended, under a QoS context, where the false probability of estimating the transmission multiplicity influences the incurred delay for a given throughput, i.e. overestimating the number of required retransmissions [SRGM07]; to ensure different levels of QoS, an optimal mean of active slots is estimated to comply with throughput-delay requirements. *Samano-Robles et al* also studied NDMA with tree splitting algorithms and studied the optimum number of MTs that should access the wireless medium to retransmit data [SRGM08a]. This work was extended for a thorough study concerning an infinite population [SRGM08b]. To diminish the number of redundant retransmissions, *Samano-Robles et al* propose that MTs should cooperate to inform a BS about the collision multiplicity under *deep* fading conditions. For low traffic conditions, MTs should relay their received packet header information to the BS [SRGM08c]. For an high traffic load, *Samano-Robles et al* suggest that the BS should take full advantage of all retransmissions to estimate the collision multiplicity from a sequential approach [SRGM08c]. *Samano-Robles et al* proposed an NDMA solution with imperfect detection using CSMA, where CSMA improves the detection of the MTs' packets and NDMA can be used to solve the hidden MT problem [SRGM09].

Dimic and Sidiropoulos proposed Frequency Hopping NDMA (FH-NDMA) [DS03] that consists on a distributed concept, i.e. ad-hoc, applied to NDMA, where nodes are organized into clusters, and each cluster works under the NDMA protocol combined with a pseudo-random frequency hopping scheme on a per-slot basis.

Madueño and Vidal also contributed with an ad-hoc version of NDMA named as Feedback-Free NDMA (FF-NDMA) [MV05a] that does not require any feedback from the receiver, forcing MTs to retransmit data packets over a fixed number of R slots. The authors also proposed to combine spatial diversity, i.e. MIMO, with time diversity to enhance packet reception [MV05b].

Nam et al combined MPR with H-ARQ similar to NDMA [NGEG07], naming their protocol Incremental Redundancy ARQ (IR-ARQ), where the BS asks for additional re-transmissions to mitigate channel fading and diminish MTs co-interference; IR-ARQ resorts to punctured codes for additional retransmissions, working in a similar way to CC.

Successive Interference Cancellation Tree Algorithm

Yu and Giannakis developed the Successive Interference Cancellation Tree Algorithm (SICTA) [YG05], based on *Tsatsanis*' work [TZB00]. SICTA resolves collisions based on a conventional tree structure, retaining the signals from collided packets and employing a SIC technique. With a regular tree algorithm [Tan03], packet collisions are resolved according to the tree structure. The SICTA implementation achieves a maximum throughput of 0.693, opposite to a maximum throughput of a standard tree algorithm with 0.346. Despite the improvement over a regular tree algorithm, it is possible to achieve better results with an NDMA algorithm [PBD$^+$09]. Also related to tree algorithms, *Gau and Chen* proposed a tree splitting algorithm that supports up to P MTs contending the channel. If more than P users contend the channel, then a tree algorithm is employed to limit the number of contending MTs [GC08], where the throughput performance is directly related to the number of MTs present on the wireless medium.

Celik et al MAC Protocol for Spatially Distributed Nodes

Celik et al studied the effect of channel capture on a structured wireless network, for standard backoff algorithms, with spatially distributed MTs around a BS for an MPR (CDMA) context [CZKM10]. *Celik*'s work suggests that the transmission probability of a distant MT should be larger than nearby MTs; with

this insight the network throughput can be increased. The backoff model, named *Alternative Model*, decreases the transmission probability after a successful transmission and increases it after an unsuccessful transmission. Contrary to previous works, *Celik*'s research does not assume power control; this work concludes that it is not possible to use common CSMA/Collision Avoidance (CA) algorithms on an MPR context [Cea96]. Nevertheless,*Celik*'s work could consider other factors for the backoff algorithm, such as power and congestion control.

Dual Power Multiple Access

Yim et al developed the Dual Power Multiple Access with Multipacket Reception using Local CSI (DPMA) scheme [YMMZ09] under the context of a structured random access channel. Their work contrary to other MPR proposals does not store *soft* information from collided packets for further processing, local Channel State Information (CSI) and Received Signal Strength Information (RSSI) measurements are used to simplify the receiver's design. Based on Channel State Information (CSI), power levels at the receiver are limited to two values to enhance SIC. For example, two colliding packets with different power levels can be successfully decoded if the ratio between the received signal from the MT with the highest signal strength and the Signal-to-Interference-plus-Noise Ratio (SINR) of the channel plus the received signal from the MT with the lowest signal strength, is higher than a given decoding threshold. If more users are involved, the receiver is able do decode the packet from a user with the highest signal strength when up to P users with a lower signal strength are involved; the remaining MTs with the lower signal strength should contend the channel with different power levels according to a pilot sequence from the BS.

Multi-Queue Service Room

Zhao et al proposed an adaptive MPR protocol for an heterogeneous structured network with a finite population [ZT03]. The protocol is named MultiQueue Service Room (MQSR). The proposed protocol assumes that it is possible to handle users with distinct QoS requirements. Assuming a slotted design for the random access, the protocol infers each MT's QoS requirements based on previous channel outcomes; based on each MT's QoS requirements, the BS defines which users have access to the wireless medium. The protocol achieves maximum throughput with heavy traffic and small delay with light traffic. MTs with packets to transmit contend the channel; if their packets are not acknowledged, these will be retransmitted the next time the MTs have access to the channel. *Zhao*'s work assumes the knowledge of the total number of users, the number of users per group of QoS, the traffic load, and the CSI; these factors are invariant of time. MTs enter a *service room* - *Zhao*'s work considers a service room with multiple queues, each queue regards a group with certain QoS requirements. The *service room* consists of an access set and a waiting room; a MT stays inside the service room until the BS detects a successful reception of the MT's packet or the MT's buffer is empty when it enters the *service room*. A processed MT goes to the end of its queue, i.e. the queue concerning a given QoS requirement. MTs outside of the *service room* enter the waiting room at the beginning of the next slot. The BS then decides which MTs enter the access set. The MQSR complexity is exponential when the number of MTs grows [ZT04]. *Zhao et al* implemented a simpler algorithm, that divides the time axis in transmission periods [ZT04]. Based on the MT's access probability and its load, the size of the access set is chosen to minimize the duration of the transmission period. The disadvantage of this scheme is the excessive use of signaling, which might not be useful on an error prone downlink channel.

Collision Resolution Diversity Slotted Aloha

Concerning a satellite context, *Casini et al* proposed the Collision Resolution Diversity Slotted ALOHA (CRDSA) access scheme [CGdRH07, GdRH09]. The CRDSA assumes that MTs send two replicas of the same packet at a random time within a time frame. Packet collisions are solved through interference cancellation. *Casini et al* assumed a slotted access such as S-ALOHA. The successful recovery of one of the packets will be used to solve a possible collision from the other packet. CRDSA is strongly dependent from the channel estimation of each packet; to estimate the channel, each received packet has a pseudo-random preamble to obtain the channel's estimate for a given MT. *Oscar Herrero and Riccardo de Gaudenzi* propose an enhanced version of Spread Aloha [Rob72], i.e. MTs contend the channel asynchronously, where MTs contend with the same spreading code [dRHG08, GdRH09]. MTs only contend the channel when SINR conditions are favorable to enhance the SIC performance; the authors name the SIC technique Enhanced Spread Spectrum ALOHA (E-SSA).

Distributed MPR algorithms

Guo et al studied the capacity of a distributed access algorithm with MPR [GWW09]. As expected, when compared to a single reception case, a distributed MPR access scheme has a higher channel capacity; it depends on the number of transmitters and flows to fully utilize the channel.

Eisenberg et al proposed the Defense Advanced Research Projects Agency (DARPA) Interference Division Multiple Access (IDMA) protocol [ECSN07]. IDMA is presented over a distributed context, where distributed synchronization and scheduling is applied. According to the authors, IDMA is robust to near-far interference, without the need of an infrastructure. The IDMA protocol proposes an RTS/CTS scheme. The IDMA frame structure consists of four zones: RTS, CTS, DATA and ACK. The RTS zone consists of RTS slots. The CTS zone consists of CTS slots, the number of CTS slots is equal to the number of RTS slots. The DATA zone may consist of one or more DATA slots, where each slot may be used by more than one MT. The ACK zone consists of one or more acknowledgement slots, each one might be used by more than one MT. Both DATA and ACK zones employ MUD. If the number of MTs is less than the number of available RTS slots, then one CTS and RTS slots are assigned to each MT. Both the DATA and ACK zones are assigned to MTs according to the IDMA scheduling mechanism. All MTs have the same scheduling algorithm.

Babich and Comisso analyzed a mathematical framework that assumes MPR under an 802.11 distributed network [BC10]. The framework assumes the knowledge of the backoff decreasing probability and the conditional packet failure probability. A slotted CSMA scheme is assumed, where the maximum backoff is the same as the retry limit. The cross-layer implementation can sustain up to a maximum of P transmissions, but still using the collision avoidance mechanism. A transmission slot is considered unsuccessful if there are more than P transmissions. The use of error correcting codes supports the use of longer slots with collisions, though it does not introduce any improvements in terms of throughput for ideal channel conditions. Enabling an MPR approach for a distributed 802.11 context holds the problem of how to estimate the number of sources.

Ying Zhang proposed an MPR Space Division Multiple Access (SDMA) architecture for a structured network, where MTs contend the wireless medium for multiple rounds until there are enough MTs to transmit data simultaneously [Zha10]. *Ying Zhang*'s work studies the optimal threshold to stop the contention period and start data transmission. The optimal threshold corresponds to a tradeoff between contention overhead and channel utilization. Compared to other MPR works, most of them only have

one contention period, underutilizing the channel's capacity. This work was also tested with 802.11. *Ying Zhang et al* found that using MAC protocol techniques that enable concurrent transmissions from multiple users, scale super-linearly, i.e. the system throughput increases as the Multipacket Reception capability increases [ZLC08, ZZL09].

2.6.4 Comments

PHY-MAC cross-layered solutions, when well-implemented, can enhance the performance of the overall system. It is important to overcome the limitations of traditional MAC schemes that do not take advantage from advanced techniques like error coding, diversity, among others. Cross-layered solutions using H-ARQ schemes combined with TDMA or CDMA techniques are great when considering QoS requirements that demand a bounded delay and jitter; subsequent packet retransmissions can improve the overall throughput of the system, though with a higher delay. A cross-layered solution such as H-ARQ combined with TDMA or CDMA, wastes channel resources when the traffic load is low. MPR schemes, and particularly, NDMA access schemes are a good proposal to reach the maximum capacity of the channel. With light to medium traffic load, NDMA schemes are a good solution when multiple MTs are contending the wireless medium. However, under heavy traffic conditions, NDMA schemes might not be a good solution if MTs do not have an appropriate backoff mechanism. A combination of both H-ARQ with NDMA could provide a good solution that enhances the reception performance of the NDMA system with additional retransmissions, as long as the QoS and energy requirements of the MTs are attended; a careful and simple design of the PHY and MAC layers should improve the overall performance in terms of throughput, energy requirements and delay.

2.7 Conclusions

The current chapter described a comprehensive bibliography concerning the theme of this thesis. Section 2.1 overviews error control coding and it is concluded that turbo-coding can achieve near Shannon capacity, though its complexity might be unsuitable for energy-constrained devices. Section 2.2 presents alternative or complementary techniques to error-coding, named diversity techniques. These techniques can be used on various domains: time, frequency and space. The use of these techniques depends on various requirements: bandwidth, delay, or complex transmitter/receiver structures. From these diversity techniques, it is possible to achieve MUD by employing interference cancellation techniques. These interference cancellation techniques require further work in terms of non-linear interference. Section 2.4 has some comments concerning future modulation techniques, namely OFDM and SC-FDE, where both complement each other, especially for structured networks, where a BS employs an OFDM transmitter and an SC-FDE receiver, and at the MT the opposite design structure. Section 2.5 briefs traditional MAC schemes and their respective taxonomy. Centralized MAC schemes are appropriate to coordinate MTs actions within the wireless channel, though the MAC scheme should be adequate for strict QoS requirements for a given number of MTs; so a structured network where MTs contend for their access seems appropriate for asymmetric traffic loads. Section 2.6 overviews cross-layered PHY-MAC schemes that perform better when compared to a *traditional* MAC scheme - though a cross-layered scheme should be carefully designed, so that the access scheme is not overly complex for a given number of MTs. The PHY-MAC cross-layered design should attend the MTs throughput, delay and energy constraints.

Chapter 3

Physical Layer Equalization Methods for SC-FDE

3.1 Introduction

Wireless broadband systems are expected to have high transmission rates and high power efficiency. As aforementioned in the previous chapter, the multipath propagation channel can be strongly selective, due to high transmission rates, leading to severe time-distortion effects. OFDM and SC-FDE with frequency-domain processing are appropriate techniques for high transmission rates over severely time-dispersive channels. OFDM suffers from high envelope fluctuations, making it power inefficient at the uplink; SC-FDE on the other hand has lower envelope fluctuations. In addition, the SC-FDE performance can be further enhanced with an iterative equalization method such as IB-DFE at the receiver. Because of the aforementioned reasons, the SC-FDE technique is the foundation of this thesis at the PHY level.

Cross-layered PHY-MAC protocols need to be thoroughly studied at both PHY and MAC layers. These layers should be strongly inter-connected to take advantage from each other's key-attributes - e.g., for DC purposes, when errors occur at the receiver, the MAC layer should *order* the PHY layer to hold the current data block symbols to enhance data reception; at the next data block copy reception, the PHY receiver will combine the symbols from both receptions and if successful, it will pass the data block to the MAC layer, otherwise it warns the MAC layer and waits for additional *commands* from the latter.

Besides the strong inter-connection between PHY and MAC layers, the performance of MUD and DC techniques at the MAC level are usually difficult to study, mostly because there are no closed formulas for the Bit Error Rate (BER) and Packet Error Rate (PER) in a SC-FDE context. In general, average BER and PER values are obtained from extensive PHY layer simulations and then used by the MAC simulator under very specific conditions, e.g., perfect power control. A viable option would be to implement the physical layer in the MAC simulator, although this would significantly increase the simulations' complexity and duration. A better solution would be the application of simple BER/PER formulas for the MAC performance simulator.

The main objective of this chapter is to study simple analytical BER/PER models for SC-FDE, assuming DC and/or MUD, using two FDE methods: linear equalization and IB-DFE equalization; for a Gaussian characterization of the signals at the FDE output, it is possible to obtain simple BER/PER performance formulas [PDN10, CDM11]. The analytical models are studied for a wide range of application scenarios

that combine DC and MUD; these models also consider retransmission techniques that avoid channel correlation between data block retransmissions.

The analytical models provided in this chapter are used in posterior chapters, except for chapter 4; in addition, these models are further extended in chapter 5 for a prefix-assisted DS-CDMA system.

The work presented in this chapter was accepted for publication in [GDBO12].

This chapter is structured as follows: section 3.2 characterizes the SC-FDE receiver capabilities. Section 3.3 introduces alternative retransmission techniques for DC purposes. Section 3.4 analyzes the receiver design for DC and MUD and provides an analytical model for their performance evaluation. Finally, section 3.5 briefly comments this chapter's conclusions.

3.2 Receiver Design Characterization

Devising an analytical model that comprises the application of DC and MUD for several simulation scenarios can be cumbersome. Therefore, the analytical model should be simple and versatile enough for different MAC schemes. This section characterizes the receiver design and sub-section 3.2.1 introduces a mathematical abstraction of data reception at the BS.

Picturing the performance of a regular NDMA system, a BS typically asks for $L = P$ retransmissions from P colliding terminals; despite the typical performance of NDMA, a BS could ask for additional packet copies in a similar way to DC H-ARQ to overcome difficult transmission conditions (e.g., a channel deep-fade) as shown in figure 3.1 for two MTs.

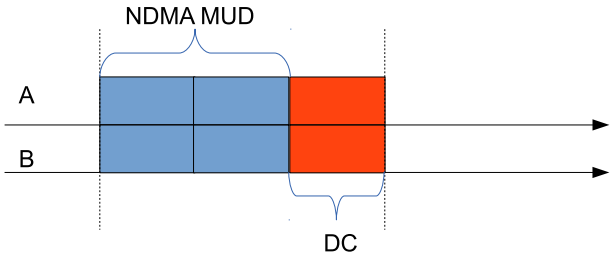

Figure 3.1: NDMA DC H-ARQ example for two MTs.

Since this thesis studies MAC schemes with DC H-ARQ it is important to assert a PHY layer model that is easily used in a general manner. For example, TDMA with DC at the PHY-level is *roughly* equivalent to an NDMA epoch with more than one packet transmission from a single MT. The same logic is fairly *similar* for a DS-CDMA system, i.e. a single packet reception with CDMA for a spreading factor K is equivalent to K TDMA DC packet copies; though, for DS-CDMA with DC H-ARQ it is not so straightforward, since it depends on the number of packet transmissions L, which means that there are $L \times K$ equivalent TDMA DC transmissions. In a nutshell, the PHY analytical model should present itself as a consistent framework across the different MAC protocols in this thesis. Figure 3.2 illustrates the aforementioned equivalence for single packet reception for $L = 4$ DC transmissions and a spreading code $K = L$.

From a PHY layer perspective MTs access the wireless uplink channel in a slotted manner using SC-FDE, where packets arrive synchronously at the BS. MTs are low resource battery operated devices, whereas the BS is a high resource device that can use DC to cope with packet errors due to poor propagation conditions or MUD due to collisions; or both techniques when conditions apply. Packets

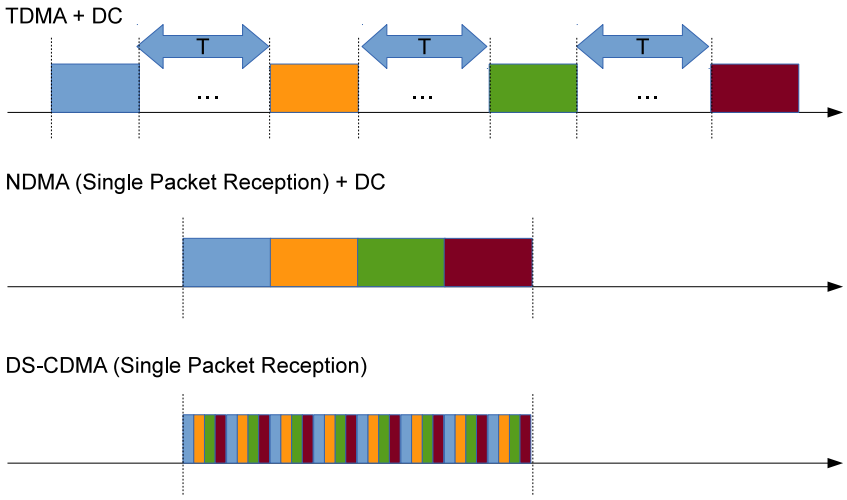

Figure 3.2: Equivalence between TDMA with four DC transmissions, NDMA for single packet reception with $L = 4$ DC transmissions and DS-CDMA also for single packet reception with a spreading code of $K = L$.

from each MT have the same duration - the duration of a time slot. Perfect channel estimation and synchronization are assumed, and on top of that colliding packets in each slot arrive simultaneously, which means that perfect time advance mechanisms exist to compensate different propagation times. Finally, the nature of the presented receiver leads to some delay since a pair of DFT and Inverse DFT per MT is performed. However, this is a function of the digital signal processing capabilities of the receiver, which are usually high for the uplink.

As a side note, for CP assisted block transmission techniques such as SC-FDE, a slightly extended CP can be used to absorb residual time-of-arrival errors, which means that it can be regarded as a time shift in the equivalent channel impulse response and, therefore, the FDE can cancel it, provided that a good channel estimation exists (a requirement for SC-FDE). On the other hand, using IB-DFE [BDFT10], it is possible to estimate and cancel residual carrier synchronization errors with proper modifications [AD04, DAPN10], even when multiple terminals have different carrier synchronization errors [DS06a], leading to a similar performance to perfect carrier synchronization.

An important assumption of this chapter is that the BS is capable of detecting the number of MTs, P, transmitting during a slot - for this chapter, and for the sake of simplicity there are at most P MTs transmitting in each slot. MTs can be recognized by specific orthogonal IDs, that only need to be transmitted once in a MUD situation, provided that the terminals are successfully identified. The size of these IDs grows with the number of terminals. To reduce the inherent overheads to these IDs the number of terminals that can register in a given slot must be limited, ensuring that the BS is able to support all terminals in the wireless medium.

Regardless of the MAC protocol, it is assumed that the PHY receiver handles L packet transmissions.

For a NDMA MAC protocol that supports DC H-ARQ, the BS must signal at the end of P packet transmissions from P MTs, which MTs succeeded and which MTs failed. For those who have failed, the BS can ask for additional copies and acknowledge their reception at the end of each subsequent slot in an H-ARQ basis - so an epoch will end until all packets are received, or when the PHY layer reaches its maximum H-ARQ capacity, $L = (P + R_N)$; R_N is the maximum number of DC H-ARQ transmissions for NDMA. The pth MT involved in a collision may retransmit its data packet $L_p - 1$ times during an epoch, where different L_p values may be used for MTs with different signal to noise ratios. The epoch's number

of PHY transmissions is $L = \max_{1 \leq p \leq P}\{L_p\}$.

Furthermore, in NDMA [ZT02, DMB+09], it was shown that a minimum of $L = P$ packet transmissions are required when P MTs are involved in a collision with perfect constant average power control at the reception. Considering that P MTs access simultaneously the channel with different transmission power gains $|\xi_v|$, with v ranging from 1 up to a maximum of N_{Gain}, the BS can ask fewer retransmissions than P, using the IB-DFE technique from [DCB+07].

The models proposed in this chapter are capable of providing the BER and PER for the aforementioned scenarios.

3.2.1 Problem Formulation

The current section introduces the formulation of the received signals at the BS and how these signals are handled regardless of the MAC layer. A data packet in the time domain from a MT p is $\{s_{n,p}; n = 0, ..., N-1\}$, and its respective frequency domain counterpart is $\{S_{k,p}; k = 0, \ldots, N-1\}$, i.e. the Discrete Fourier Transform (DFT) of $\{s_{n,p}; n = 0, \ldots, N-1\}$. Assuming that P MTs transmit simultaneously during L slots, the received content at the BS is $\{\mathbf{Y}_k; k = 0, \ldots, N-1\}$, where $\mathbf{Y}_k = \left[Y_k^{(1)}, \ldots, Y_k^{(L)}\right]^T$. The received content depends on the L channel realizations of the MTs $\mathbf{H}_k = [\mathbf{H}_{k,1}, \ldots, \mathbf{H}_{k,P}]^T$, where $\mathbf{H}_{k,p} = \left[H_{k,p}^{(1)}, \ldots, H_{k,p}^{(L)}\right]$, the MTs transmissions $\mathbf{S}_k = [S_{k,1}, \ldots, S_{k,P}]^T$, and the channel noise $\mathbf{N}_k = \left[N_k^{(1)}, \ldots, N_k^{(L)}\right]^T$. So,

$$\mathbf{Y}_k = \mathbf{H}_k^T \mathbf{S}_k + \mathbf{N}_k. \tag{3.1}$$

The expanded expression of $\mathbf{Y}_k$ is

$$\begin{bmatrix} Y_k^{(1)} \\ \vdots \\ Y_k^{(L)} \end{bmatrix} = \begin{bmatrix} H_{k,1}^{(1)} & \ldots & H_{k,P}^{(1)} \\ \vdots & \ddots & \vdots \\ H_{k,1}^{(L)} & \ldots & H_{k,P}^{(L)} \end{bmatrix} \begin{bmatrix} S_{k,1} \\ \vdots \\ S_{k,P} \end{bmatrix} + \begin{bmatrix} N_k^{(1)} \\ \vdots \\ N_k^{(L)} \end{bmatrix}. \tag{3.2}$$

If a MT p for a given transmission l has an attenuation gain, $|\xi_{l,p}|$, then $H_{k,p}^{(l)}$ should be replaced by $|\xi_{l,p}|\, H_{k,p}^{(l)}$. Also, if MT p does not transmit for a given slot l then $H_{k,p}^{(l)} = 0$.

Since the error rate models are dependent of the channel realizations $\mathbf{H}_k$ and the SNR, this chapter's objective is to present a function that computes both the BER and PER based on $\mathbf{H}_k$ and the SNR. This function should be generic and apply to any system that employs DC, MUD, SIC, or any combination of these techniques. This function should be independent of the MAC protocol used, since the MAC protocol behaviour can be modeled in $H_{k,p}^{(l)}$. A DC system is modeled with $P = 1$ and with $H_{k,p}^{(l)} = 0$ for l above the last retransmission. MUD systems have $P > 1$ and these may have $H_{k,p}^{(l)} = 0$ when retransmissions are suppressed for successfully received packets. Systems that control the transmission power can be modeled by setting the $|\xi_{l,p}|$ values.

Figure 3.3 exemplifies the range of applications of the proposed work. A structured wireless network is represented with three MTs, A, B and C that transmit data to a BS. The MTs are radially distributed around the BS, where A and B are closer to the BS, and C is the farthest MT in terms of distance. Both A and B have the same attenuation gain $|\xi_1|$, and C has an attenuation gain $|\xi_2|$. It is assumed that $|\xi_2| << |\xi_1|$. Figure 3.3 also illustrates a series of six epochs delimited by black bars. The first epoch has a successfully transmitted packet from MT A. The second epoch, has two slot transmissions from MT B, where the first transmission of MT B's packet was unsuccessful; regarding the second slot,

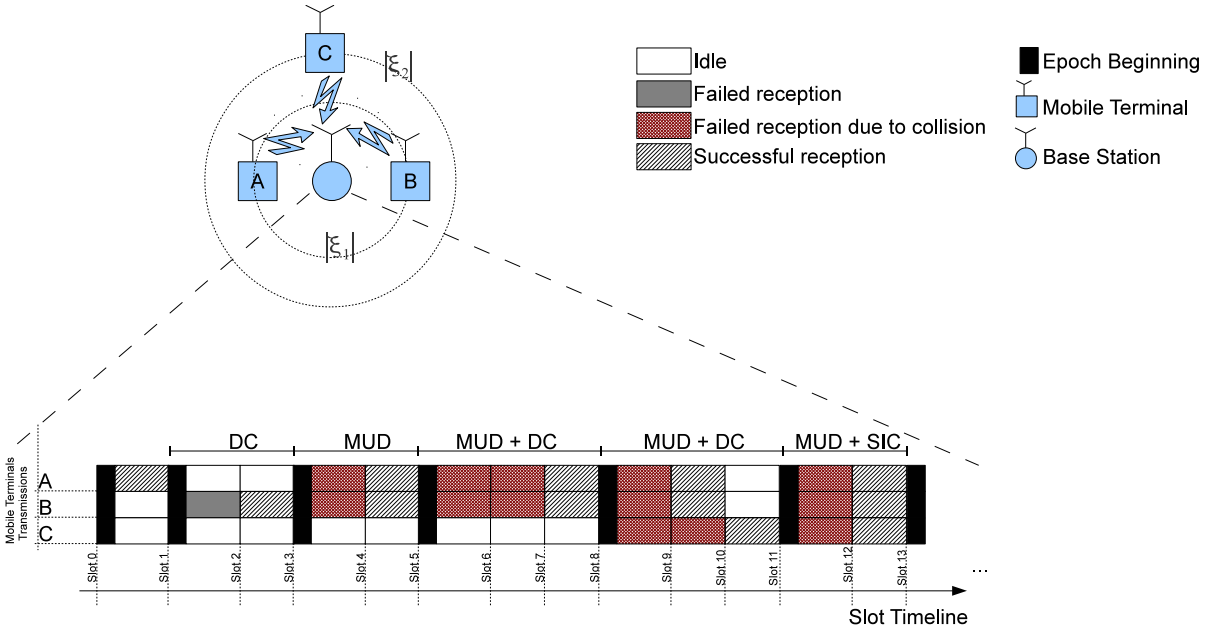

Figure 3.3: Time sequence of a series of epochs that involve Diversity Combining, Multiuser Detection and the hybrid of both schemes.

MT B retransmits the same packet, where the DC technique was used to successfully decode MT B's packet from both transmissions. The third epoch shows a MUD situation, where MTs A and B transmit data on the first slot, a second transmission is requested to enhance the reception of both packets, at the end of the second slot both packets are successfully received. The fourth epoch illustrates an hybrid combination of MUD with DC, where a third transmission is requested to both A and B to ensure a successful reception. Regarding the fifth epoch, all MTs access simultaneously the channel, where the BS is able to decode the information from MTs A and B, but asks for a third transmission from MT C to improve data reception, since MT C's attenuation is the highest. The sixth epoch illustrates a situation assuming the employment of a SIC technique such as IB-DFE, where the three MTs access the wireless medium. Only two time slots are required to transmit data, since IB-DFE is able to resolve packet collisions when the number of transmissions is smaller than the number of MTs, as long as the SNR between MTs is separated enough[YMMZ09]; however, such situation can require an increased computational time.

The analytical model proposed in this chapter is easily applied to any situation illustrated above, which makes the proposed work quite versatile, without relying on previous simulations of the physical medium to test the MAC protocols' performance. The model allows a precise estimation of the PER, simplifying the performance estimation for system level models, which run on top of the PHY layer.

3.3 Alternative Retransmission Techniques

When data blocks are retransmitted, chances are that the wireless channel remained the same since the first transmission, therefore there are retransmission techniques that enhance data reception under these conditions. The current section presents a brief overview of alternative retransmission techniques that the proposed analytical model supports.

There are two extreme cases concerning the channel conditions when packets are retransmitted. In

one case, which will be denoted Uncorrelated Channel (UC), the channel is completely uncorrelated for different retransmission attempts. In the other case, which will be denoted Equal Channel (EC), the channel remains fixed for all retransmission attempts. If packets are transmitted under the UC condition, then all packet retransmissions from each MT are uncorrelated, i.e. the channel response for a MT p regarding a transmission l of a given packet symbol, $H_{k,p}^{(l)}$, is uncorrelated from previous transmission attempts. Although it is desirable to have small channel correlations between transmission attempts for both DC and MUD schemes, this condition is not achieved in most practical scenarios, unless there is a fast channel variation (high Doppler effects) or long intervals between retransmissions. The EC condition is not desirable when retransmissions are needed, but it is very common in practical scenarios - if a deep fade persists for all retransmission attempts in a given sequence of data symbols then those data symbols are most likely irretrievable without any type of error correcting techniques.

It would be desirable to have small equivalent channel correlations under EC conditions. This is especially important for MUD to avoid an ill-conditioned matrix inversion. To cope with EC conditions this paper considers the following retransmission techniques: Equal Channel with Phase Rotation (ECPR) [ZT02] and EC with Shifted Packet (SP) [DMB$^+$09].

With the ECPR technique, different phase rotations are employed for the transmitted data at different retransmission attempts. Assuming that θ_p is a fixed phase for MT p and δ_l is an offset for each transmission then a phase rotation $(\theta_p + \delta_l)^l$ is applied for the lth retransmitted data packet, which is formally equivalent to have $H_{k,p}^{(l)} = H_{k,p}^{(1)} \exp(j(\theta_p + \delta_l)^l)$. By performing the phase rotations, the matrix inversions required for MUD are well conditioned. However, with ECPR the magnitude of $H_{k,p}^{(l)}$ is unchanged, therefore the DC technique in such conditions is ineffective.

An alternative method to reduce the channel correlation between different transmission attempts is to employ the SP technique. With the SP technique a cyclic shift ζ_l is performed on the frequency-domain samples of the lth retransmitted block. For example, if a MT attempts to retransmit a block, it performs a cyclic shift of $\zeta_2 = N/2$, if the reception fails, it re-transmits with a cyclic shift $\zeta_3 = N/4$, $\zeta_4 = 3N/4$, $\zeta_5 = N/8$, $\zeta_6 = 3N/8$, etc. These cyclic shifts are odd multiples of $N/2$; $N/4$; $N/8$ and so on. Figure 3.4 exemplifies the SP technique for three transmissions, where the transmitted block sub-carriers are shifted.

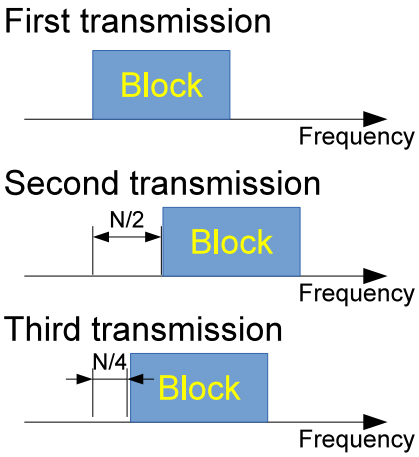

Figure 3.4: Example of the SP technique for three transmissions.

The SP operation is formally equivalent to perform a cyclic shift to the channel response of a given MT, i.e., $H_{k,p}^{(l)} = H_{(k+\zeta_l) \bmod N,p}^{(1)}$. This is especially efficient with time-dispersive channels, where the frequency response changes substantially from subcarrier to subcarrier. This technique can be interesting

not just to avoid ill-conditioned matrix inversions in MUD but also to avoid deep in-band fades in DC. Figure 3.5 illustrates the SP technique for two transmissions, where the channel sub-carriers are shifted by half.

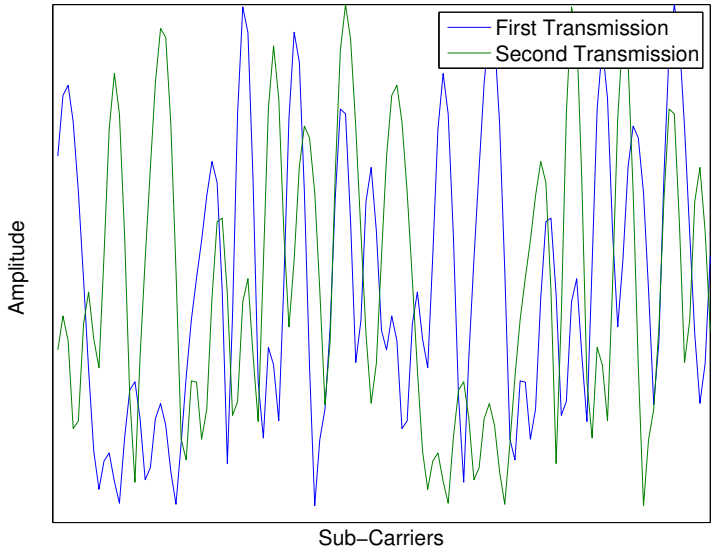

Figure 3.5: Illustration of the SP technique for two transmissions regarding its respective sub-carriers.

3.4 Equalization Model for SC-FDE

The analytical model of the receiver design is a uniform representation from models [DCM09] and [DCB+09]. This chapter assumes that the overall interference that affects the symbol estimation has a Gaussian behavior, either for linear or iterative equalization methods in subsections 3.4.1 and 3.4.2 respectively. The performance model evaluates the BER and PER for a given ratio of the bit energy, E_b, over the average channel noise, N_0; the performance model is presented in a generic way that can be easily extended to any particular case as long as the system assumptions are respected.

For each equalization method, performance results are illustrated, exemplifying a highly dispersive channel [MS98], with uncorrelated Rayleigh fading for each path and MT. The simulation results were computed through *Monte Carlo* simulations using the *MATLAB* software [Mat11].

3.4.1 Linear Receiver

The current section analyzes a linear receiver structure for SC-FDE and its respective results. The results section overviews the retransmission techniques from section 3.3.

Design

The linear receiver decodes the MTs L transmissions, where the estimated data symbol from a MT p is $\tilde{S}_{k,p} = \mathbf{F}_{k,p}^{T}\mathbf{Y}_k$. $\mathbf{F}_{k,p}^{T} = \left[F_{k,p}^{(1)}, \ldots, F_{k,p}^{(L)}\right]$ are the feedforward coefficients.

For $\mathbf{\Gamma}_p = [\Gamma_{p,1} = 0, \ldots, \Gamma_{p,p} = 1, \ldots, \Gamma_{p,P} = 0]^T$, the Mean Square Error (MSE), $\mathbb{E}\left[\left|\tilde{S}_{k,p} - S_{k,p}\right|^2\right]$, of $S_{k,p}$ is

$$\begin{aligned}\mathbb{E}\left[\left|\tilde{S}_{k,p} - S_{k,p}\right|^2\right] &= \mathbb{E}\left[\left|\mathbf{F}_{k,p}^T\mathbf{Y}_k - S_{k,p}\right|^2\right] \\ &= \mathbb{E}\left[\left|\left(\mathbf{F}_{k,p}^T\mathbf{H}_k^T - \mathbf{\Gamma}_p\right)\mathbf{S}_k\right|^2\right] + \mathbb{E}\left[\left|\mathbf{F}_{k,p}^T\mathbf{N}_k\right|^2\right].\end{aligned} \tag{3.3}$$

Expanding (3.3) results

$$\begin{aligned}\left(\mathbf{F}_{k,p}^T\mathbf{H}_k^T - \mathbf{\Gamma}_p\right)\mathbb{E}\left[\mathbf{S}_k\mathbf{S}_k^H\right]\left(\mathbf{F}_{k,p}^T\mathbf{H}_k^T - \mathbf{\Gamma}_p\right)^H + \\ \mathbf{F}_{k,p}^T\mathbb{E}\left[\mathbf{N}_k\mathbf{N}_k^H\right]\mathbf{F}_{k,p}^* \quad .\end{aligned} \tag{3.4}$$

$\mathbb{E}\left[\mathbf{S}_k\mathbf{S}_k^H\right]$ and $\mathbb{E}\left[\mathbf{N}_k\mathbf{N}_k^H\right]$ are respectively

$$\begin{aligned}\mathbb{E}\left[\mathbf{S}_k\mathbf{S}_k^H\right] &= 2\sigma_S^2\mathbf{I}_P, \\ \mathbb{E}\left[\mathbf{N}_k\mathbf{N}_k^H\right] &= 2\sigma_N^2\mathbf{I}_L,\end{aligned}$$

where σ_S^2 and σ_N^2 are the transmitted symbol's variance and the noise variance, respectively.

To obtain the MMSE, the optimal $\mathbf{F}_{k,p}$ coefficients need to be computed, so subjecting the MSE to $\gamma_p = \frac{1}{N}\sum_{k=0}^{N-1}\sum_{l=1}^{L}F_{k,p}^{(l)}H_{k,p}^{(l)} = 1$ is formally equivalent to the gradient of the Lagrange function applied to (3.3) where

$$\nabla\mathcal{L} = \nabla\left(\mathbb{E}\left[\left|\tilde{S}_{k,p} - S_{k,p}\right|^2\right] + (\gamma_p - 1)\lambda_p\right), \tag{3.5}$$

From the following set of equations,

$$\begin{cases}\nabla_{\mathbf{F}_{k,p}}\mathcal{L} = 0 \\ \nabla_{\lambda_p}\mathcal{L} = 0\end{cases}, \tag{3.6}$$

$\nabla_{\mathbf{F}_{k,p}}\mathcal{L} = 0$ is represented by

$$2\sigma_S^2\mathbf{H}_k^H\mathbf{H}_k\mathbf{F}_{k,p} - 2\sigma_S^2\mathbf{H}_k^H\mathbf{\Gamma}_p + 2\sigma_N^2\mathbf{F}_{k,p} + \frac{1}{N}\lambda_p\mathbf{H}_k^H\mathbf{\Gamma}_p = 0, \tag{3.7}$$

and $\nabla_{\lambda_p}\mathcal{L} = 0$ by $\gamma_p = 1$. The optimal $\mathbf{F}_{k,p}$ coefficients are

$$\mathbf{F}_{k,p} = \left(\mathbf{H}_k^H\mathbf{H}_k + \frac{2\sigma_N^2}{2\sigma_S^2}\mathbf{I}_L\right)^{-1}\mathbf{H}_k^H\mathbf{\Gamma}_p\left(1 - \frac{1}{2N\sigma_S^2}\right). \tag{3.8}$$

For a single MT p transmitting data, i.e. without collisions, for a given transmission l, results

$$F_{k,p}^{(l)} = \frac{\gamma_p H_{k,p}^{(l)\,*}}{\frac{\sigma_N^2}{\sigma_S^2} + \sum_{l=1}^{L}\left|H_{k,p}\right|^2}. \tag{3.9}$$

From (3.3) and (3.8), results

$$\sigma_p^2 = \frac{1}{N^2}\sum_{k=0}^{N-1}\mathbb{E}\left[\left|\tilde{S}_{k,p} - S_{k,p}\right|^2\right]. \tag{3.10}$$

Assuming the Gaussian behavior of the overall interference η_k that affects the symbol estimation, in

accordance to [CC09], the symbol error probability P_s for a QPSK constellation is denoted by

$$P_s \simeq 2 \times BER_p\left(\eta_k > \sqrt{E_b}\right) = 2 \times BER_p\left(\frac{\eta_k}{\sigma_p} > \sqrt{\frac{E_b}{\sigma_p^2}}\right) \simeq 2Q\left(\sqrt{\frac{E_b}{\sigma_p^2}}\right), \tag{3.11}$$

where $Q(x)$ is the well known Gaussian error function. Assuming that $E_b = 1$, the BER for a given MT p is

$$BER_p \simeq Q\left(\frac{1}{\sigma_p}\right). \tag{3.12}$$

It should be noted that the results from BER_p are heavily conditioned to the simulated channel realizations.

Similarly, it is possible to generalize the same expression for M^2-QAM constellations with Gray mapping and minimum distance between symbols (i.e., the real and imaginary parts of the symbols are $\pm 1, \pm 3, ..., \pm(M-1)$), so the BER is approximately given by

$$BER_p \simeq \frac{2}{\log_2(M)}\left(1 - \frac{1}{M}\right) Q\left(\frac{1}{\sigma_p}\right). \tag{3.13}$$

For an uncoded system with independent and isolated errors, the PER for a fixed packet size of M bits is

$$PER_p \simeq 1 - (1 - BER_p)^M. \tag{3.14}$$

Performance Results

The current section describes the evaluation of the analytical model for a linear receiver structure. A highly dispersive channel [MS98], with uncorrelated Rayleigh fading for each path and MT for a total of 32 ray paths/MT is considered. The performance results also consider data blocks with $N = 256$ uncoded Quadrature Phase Shift Keying (QPSK) symbols, where each block occupies a $4\mu s$ time slot.

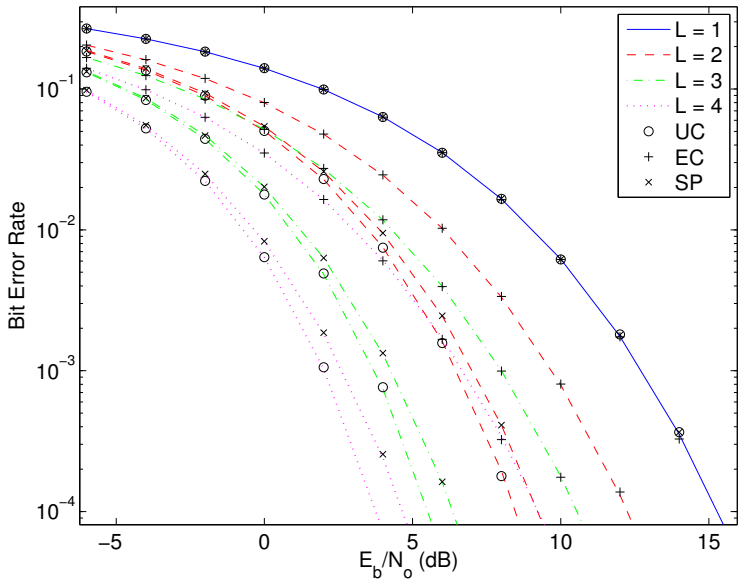

Figure 3.6: BER performance for the DC technique for a linear receiver structure.

Figure 3.6 analyzes the DC scheme up to $L-1$ packet retransmissions. The lines correspond to the analytical calculus of the BER, while the markers are the simulation values. Clearly, the proposed analytical model is very accurate for the various conditions and techniques. The BER diminishes considerably for a given E_b/N_0 when a higher number of transmissions is involved. Moreover the SP technique has a close performance to the UC condition. It should be noted that the EC results are enhanced for a higher number of transmissions due to the combination of energy from each transmission.

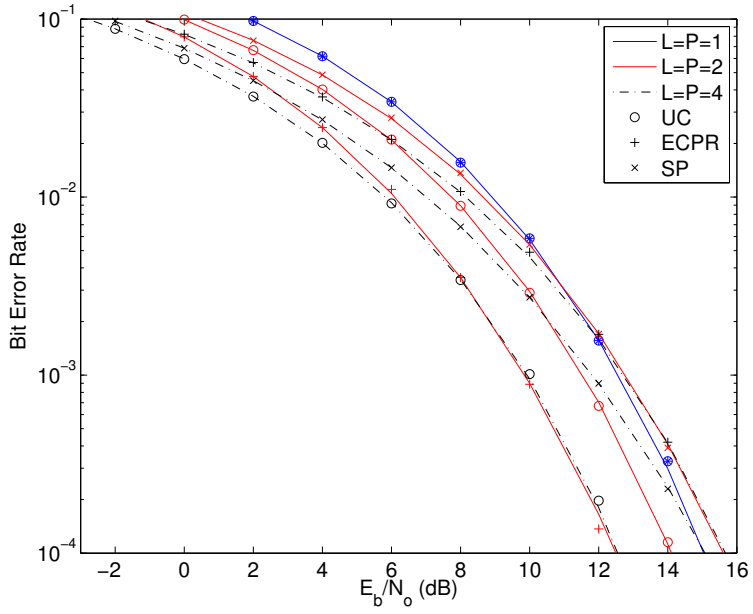

Figure 3.7: BER performance for MUD, concerning the UC condition, and the ECPR and SP separation techniques for a linear receiver structure.

Figure 3.7 compares the BER for the UC, ECPR and SP for MUD, up to $P = L$ collisions. The lines correspond to the theoretical BER, while the markers are the simulation values; once again the analytical model is very accurate. When P increases, the performance degrades for all retransmission techniques except for the UC condition. Considering the UC condition for a BER of 10^{-4}, it is possible to achieve an E_b/N_0 gain of 2dB between $P = 1$ and $P = 4$ collisions. The stored energy from each transmission does improve data reception, despite the increasing interference when compared to the DC technique. Moreover, the UC condition does achieve a reasonable performance for $P = 4$ collisions when compared to the ECPR technique with $P = 2$ collisions. In most cases the SP technique outperforms the ECPR technique.

Figure 3.8 illustrates the BER performance of the MUD scheme for $P = L = 4$, with distinct gains $|\xi_p|$, where p corresponds to the pth MT. For this scenario, $|\xi_1| = 0$dB, $|\xi_2| = -6$dB, $|\xi_3| = -3$dB and $|\xi_4| = -1.25$dB. The lines are the analytical values and the markers are the simulated ones. Once again, it is noticeable the precision of the analytical model. As expected the MT with $|\xi_2|$ has the worst performance, while the MT with $|\xi_1|$ has the best performance. Finally the curves show that in some cases the MT with $|\xi_4|$ can outperform the MT with $|\xi_1|$, when different transmission conditions are considered.

Figure 3.9 illustrates the BER performance for the hybrid combination of the MUD with DC when the number of transmissions L is higher or equal to the number of collisions P using the SP separation technique - for $L > P$, $L = 6$ and $P = [1, 2, 3, 4]$, and for $L = P$, $P = [1, 2, 3, 4]$. Comparing both cases

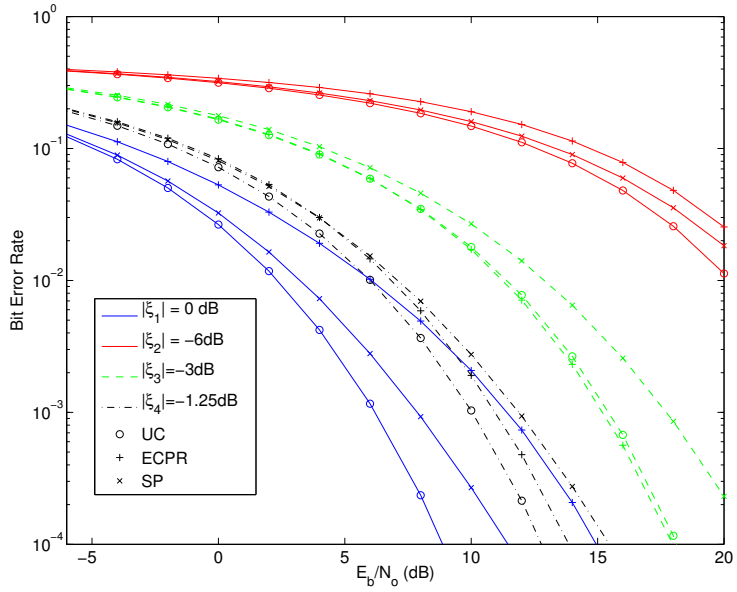

Figure 3.8: BER performance for MUD, concerning the UC condition, and the ECPR and SP separation techniques for different transmitting powers, regarding a linear receiver structure.

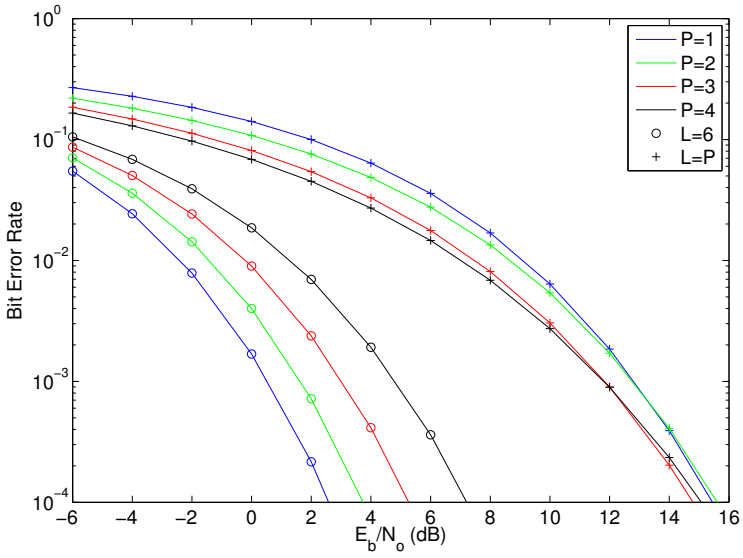

Figure 3.9: BER performance for the MUD technique, regarding $L = P$ and $L > P$, for a linear receiver structure using the SP retransmission technique.

when $L = P$ and $L > P$, the MUD technique achieves a remarkable performance when the BS asks for *extra* retransmissions from all MTs, outperforming the regular case where $L = P$.

Figure 3.10 illustrates the BER performance for the DC technique when employing the 16-QAM constellation combined with the SP technique. It is noticeable how well the analytical model portrays the simulation values, though slightly inaccurate for low E_b/N_0. As expected, the performance of the linear DC technique is enhanced for an increasing number of transmissions. These results can be generically applied to other constellations as well as other configurations for the linear equalization technique.

Figure 3.11 illustrates the PER performance for the hybrid combination of MUD with DC, where $P =$

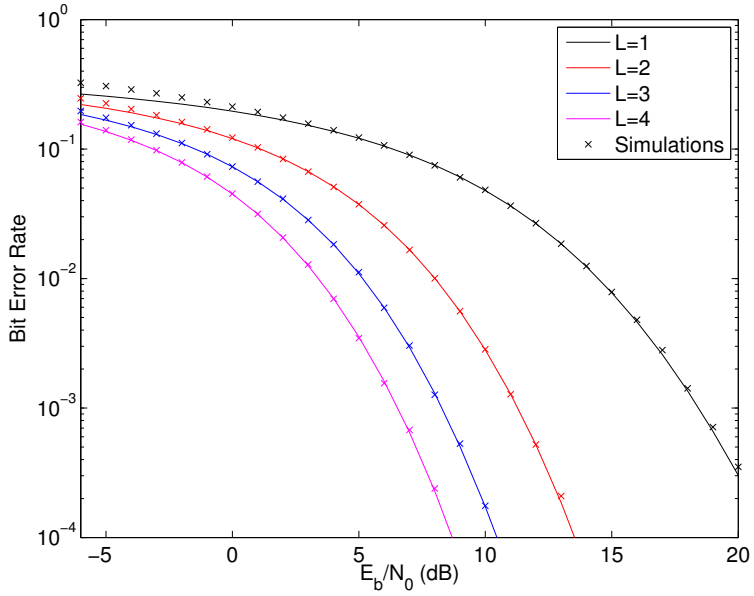

Figure 3.10: 16-QAM BER performance for the DC technique, for $P = 1$ and $L = [1, 2, 3, 4]$ for a linear receiver structure regarding the SP transmission technique.

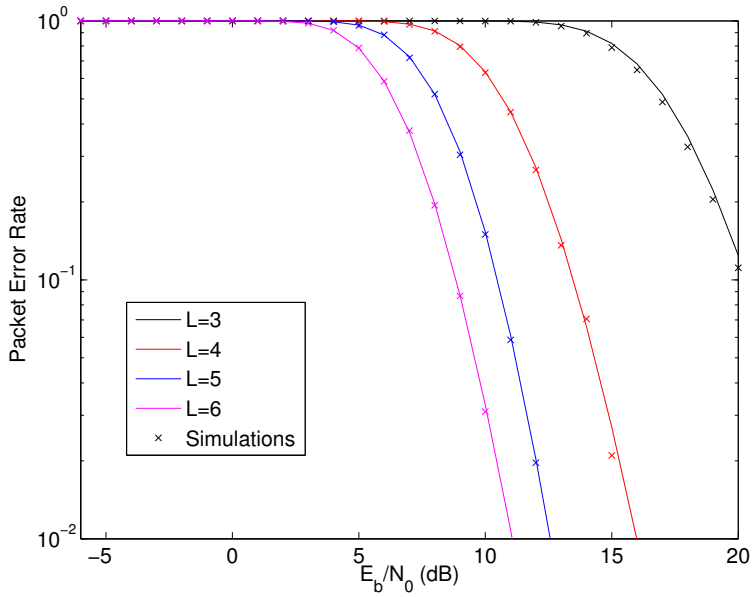

Figure 3.11: 16-QAM PER performance for the MUD technique, for $P = 3$ and $L = [3, 4, 5, 6]$ for a linear receiver structure regarding the SP transmission technique.

3 and $L = [3, 4, 5, 6]$, for a 16-QAM constellation and the SP technique. The analytical model can decently portray the PER with good accuracy. Furthermore, for an increasing number of transmissions the performance of the hybrid combination of MUD with DC is enhanced. As aforementioned, these results can be generically applied to other constellations as well as other configurations for the linear equalization technique.

3.4.2 Iterative Receiver

The current section analyzes the IB-DFE receiver structure model and its respective results.

Design

The IB-DFE receiver decodes the MTs L transmissions up to N_{iter} iterations. The estimated data symbol, $\tilde{S}_{k,p}^{(i)}$, for a given iteration i and MT p is

$$\tilde{S}_{k,p}^{(i)} = {\mathbf{F}_{k,p}^{(i)}}^{T}\mathbf{Y}_k - {\mathbf{B}_{k,p}^{(i)}}^{T}\bar{\mathbf{S}}_k^{(i-1)}, \tag{3.15}$$

where ${\mathbf{F}_{k,p}^{(i)}}^{T} = \left[F_{k,p}^{(i,1)}, \ldots, F_{k,p}^{(i,L)}\right]$ are the feedforward coefficients and ${\mathbf{B}_{k,p}^{(i)}}^{T} = \left[B_{k,p}^{(i,1)}, \ldots, B_{k,p}^{(i,P)}\right]$ are the feedback coefficients. $\bar{\mathbf{S}}_k^{(i-1)} = \left[\bar{S}_{k,1}^{(i-1)}, \ldots, \bar{S}_{k,P}^{(i-1)}\right]^T$ are the soft decision estimates from the previous iteration for all MTs. $\bar{\mathbf{S}}_k^{(i-1)}$ can be related to the symbols hard decisions, $\hat{\mathbf{S}}_k^{(i-1)}$, where according to [DSG07b] and [DGE03] results

$$\bar{\mathbf{S}}_k^{(i-1)} \simeq \mathbf{P}^{(i-1)}\hat{\mathbf{S}}_k^{(i-1)} \tag{3.16a}$$

$$\hat{\mathbf{S}}_k^{(i-1)} = \mathbf{P}^{(i-1)}\mathbf{S}_k + \mathbf{\Delta}_k \tag{3.16b}$$

$\mathbf{P}^{(i-1)} = diag\left(\rho_1^{(i-1)}, \ldots, \rho_P^{(i-1)}\right)$ are the correlation coefficients and $\mathbf{\Delta}_k = \left[\Delta_k^{(1)}, \ldots, \Delta_k^{(P)}\right]^T$ is a zero mean error vector that is independent from the $\mathbf{S}_k$ vector. For more information on $\bar{\mathbf{S}}_k^{(i-1)}$ and $\hat{\mathbf{S}}_k^{(i-1)}$ calculus refer to [DGE03, BT02, GTDE07]. Expanding $\rho_p^{(i-1)}$ for a given MT p, assuming a QPSK constellation, according to [GTDE07] results

$$\rho_p^{(i-1)} = \frac{1}{2N}\sum_{n=0}^{N-1}\left|{\rho_{n,p}^{I}}^{(i-1)}\right| + \left|{\rho_{n,p}^{Q}}^{(i-1)}\right|, \tag{3.17}$$

so that

$${\rho_{n,p}^{I}}^{(i-1)} = tanh\left(\frac{\left|{L_{n,p}^{I}}^{(i-1)}\right|}{2}\right), \tag{3.18a}$$

$${\rho_{n,p}^{Q}}^{(i-1)} = tanh\left(\frac{\left|{L_{n,p}^{Q}}^{(i-1)}\right|}{2}\right), \tag{3.18b}$$

where

$${L_{n,p}^{I}}^{(i-1)} = \frac{2}{{\sigma_{n,p}^{2}}^{(i-1)}}Re\left\{\tilde{s}_{n,p}^{(i-1)}\right\}, \tag{3.19a}$$

$${L_{n,p}^{Q}}^{(i-1)} = \frac{2}{{\sigma_{n,p}^{2}}^{(i-1)}}Im\left\{\tilde{s}_{n,p}^{(i-1)}\right\}, \tag{3.19b}$$

where $\tilde{s}_{n,p}^{(i)}$ is the time-domain estimation of $s_{n,p}$ and

$${\sigma_{n,p}^{2}}^{(i-1)} = \frac{1}{2N}\sum_{n'=0}^{N-1}\left|\hat{s}_{n',p}^{(i-1)} - s_{n',p}\right|^2. \tag{3.20}$$

$\hat{s}_{n,p}^{(i)}$ is the hard estimation of $s_{n,p}$. For the first iteration, i.e. $i = 1$, $\bar{\mathbf{S}}_k^{(i-1)}$ is a null vector and $\mathbf{P}^{(i-1)}$ is a null matrix. Assuming that $\mathbf{R}_S$, $\mathbf{R}_N$ and $\mathbf{R}_\Delta$, are respectively, the correlation of $\mathbf{S}_k$, $\mathbf{N}_k$ and $\mathbf{\Delta}_k$, where

$$\mathbf{R}_S = \mathbb{E}\left[\mathbf{S}_k \mathbf{S}_k^H\right] = 2\sigma_S^2 \mathbf{I}_P, \tag{3.21a}$$

$$\mathbf{R}_N = \mathbb{E}\left[\mathbf{N}_k \mathbf{N}_k^H\right] = 2\sigma_N^2 \mathbf{I}_L, \tag{3.21b}$$

$$\mathbf{R}_\Delta = \mathbb{E}\left[\mathbf{\Delta}_k \mathbf{\Delta}_k^H\right] \simeq 2\sigma_S^2 \left(\mathbf{I}_P - \mathbf{P}^{(i-1)} \mathbf{P}^{(i-1)^T}\right). \tag{3.21c}$$

σ_S^2 is the symbol's variance and σ_N^2 is the noise's variance. Assuming that

$$\alpha_{k,p}^{(i)} = \mathbf{F}_{k,p}^{(i)} \mathbf{H}_k^T - \mathbf{B}_{k,p}^{(i)} \mathbf{P}^{(i-1)} \mathbf{P}^{(i-1)^T} - \mathbf{\Gamma}_p, \tag{3.22a}$$

$$\beta_{k,p}^{(i)} = \mathbf{B}_{k,p}^{(i)^T} \mathbf{P}^{(i-1)}, \tag{3.22b}$$

the MSE, $\mathbb{E}\left[\left|S_{k,p} - \tilde{S}_{k,p}^{(i)}\right|^2\right]$, of $S_{k,p}$ is

$$\mathbb{E}\left[\left|S_{k,p} - \tilde{S}_{k,p}^{(i)}\right|^2\right] = \mathbb{E}\left[\left|\Xi_{k,p}^{(i)} - \Upsilon_{k,p}^{(i)}\right|^2\right], \tag{3.23}$$

where $\Xi_{k,p}^{(i)} = \mathbf{F}_{k,p}^{(i)^T} (\mathbf{H}_k^T \mathbf{S}_k + \mathbf{N}_k)$ and $\Upsilon_{k,p} = \mathbf{B}_{k,p}^{(i)^T} \mathbf{P}^{(i-1)} (\mathbf{P}^{(i-1)^T} \mathbf{S}_k + \mathbf{\Delta}_k) + \mathbf{\Gamma}_p \mathbf{S}_k$.

Expanding (3.23) results

$$\begin{aligned}
&\mathbb{E}\left[\left|S_{k,p} - \tilde{S}_{k,p}^{(i)}\right|^2\right] = \\
&\mathbb{E}\left[\left|\left(\mathbf{F}_{k,p}^{(i)^T} \mathbf{H}_k^T - \mathbf{B}_{k,p}^{(i)^T} \mathbf{P}^{(i-1)} \mathbf{P}^{(i-1)^T} - \mathbf{\Gamma}_p\right) \mathbf{S}_k\right|^2\right] \dots \\
&+ \quad \mathbb{E}\left[\left|\mathbf{B}_{k,p}^{(i)^T} \mathbf{P}^{(i-1)} \mathbf{\Delta}_k\right|^2\right] + \mathbb{E}\left[\left|\mathbf{F}_{k,p}^{(i)^T} \mathbf{N}_k\right|^2\right] = \\
&\alpha_{k,p}^{(i)^*} \mathbf{R}_S \alpha_{k,p}^{(i)^T} + \mathbf{F}_{k,p}^{(i)^H} \mathbf{R}_N \mathbf{F}_{k,p}^{(i)} \dots \\
&+ \quad \beta_{k,p}^{(i)^*} \mathbf{R}_\Delta \beta_{k,p}^{(i)^T}.
\end{aligned} \tag{3.24}$$

To compute the MMSE, the optimal $\mathbf{F}_{k,p}^{(i)}$ and $\mathbf{B}_{k,p}^{(i)}$ coefficients need to be computed, so subjecting the MSE to $\gamma_p^{(i)} = \frac{1}{N} \sum_{k=0}^{N-1} \sum_{l=1}^{L} F_{k,p}^{(i,l)} H_{k,p}^{(l)} = 1$ is formally equivalent to the gradient of the Lagrange function applied to (3.24). So

$$\nabla \mathcal{L} = \nabla \left(\mathbb{E}\left[\left|S_{k,p} - \tilde{S}_{k,p}^{(i)}\right|^2\right] + \left(\gamma_p^{(i)} - 1\right) \lambda_p^{(i)}\right), \tag{3.25}$$

From the following set of equations,

$$\begin{cases} \nabla_{\mathbf{F}_{k,p}^{(i)}} \mathcal{L} = 0 \\ \nabla_{\mathbf{B}_{k,p}^{(i)}} \mathcal{L} = 0 \\ \nabla_{\lambda_p^{(i)}} \mathcal{L} = 0 \end{cases}, \tag{3.26}$$

$\nabla_{\mathbf{F}_{k,p}^{(i)}} J = 0$ is

$$\mathbf{H}_k^H \mathbf{R}_S \mathbf{H}_k \mathbf{F}_{k,p}^{(i)} - \mathbf{H}_k^H \mathbf{R}_S \mathbf{P}^{(i-1)} {\mathbf{P}^{(i-1)}}^T \mathbf{B}_{k,p}^{(i)} - \mathbf{H}_k^H \mathbf{R}_S \ldots + \mathbf{R}_N \mathbf{F}_{k,p}^{(i)} + \frac{1}{N} \mathbf{H}_k^H \lambda_p^{(i)} \mathbf{\Gamma}_p = 0, \tag{3.27}$$

$\nabla_{\mathbf{B}_{k,p}^{(i)}} J = 0$ is

$$\left(\mathbf{P}^{(i-1)} {\mathbf{P}^{(i-1)}}^T \mathbf{R}_S + \mathbf{R}_\Delta \right) \mathbf{B}_{k,p}^{(i)} = \mathbf{R}_S \mathbf{H}_k \mathbf{F}_{k,p}^{(i)} - \mathbf{R}_S \mathbf{\Gamma}_p, \tag{3.28}$$

and $\nabla_{\lambda_p^{(i)}} J = 0$ when $\gamma_p^{(i)} = 1$. So the optimal coefficients are

$$\begin{cases} \mathbf{B}_{k,p}^{(i)} = \mathbf{H}_k \mathbf{F}_{k,p}^{(i)} - \mathbf{\Gamma}_p \\ \mathbf{F}_{k,p}^{(i)} = \mathbf{\Lambda}_{k,p}^{(i)} \mathbf{H}_k^H \mathbf{\Theta}_{k,p}^{(i)} \end{cases}. \tag{3.29}$$

$\mathbf{\Lambda}_{k,p}^{(i)} = \left(\mathbf{H}_k^H \left(\mathbf{I}_P - \mathbf{P}^{(i-1)} {\mathbf{P}^{(i-1)}}^T \right) \mathbf{H}_k + \frac{\sigma_N^2}{\sigma_S^2} \mathbf{I}_L \right)^{-1}$ and $\mathbf{\Theta}_{k,p}^{(i)} = \left(\mathbf{I}_P - \mathbf{P}^{(i-1)} {\mathbf{P}^{(i-1)}}^T \right) \mathbf{\Gamma}_p - \frac{\lambda_p^{(i)}}{2\sigma_S^2 N} \mathbf{\Gamma}_p$. For a single MT p transmitting data, i.e. without collisions, results

$$B_{k,p}^{(i)} = \sum_{l=1}^{L} F_{k,p}^{(i,l)} H_{k,p}^{(l)} - 1, \tag{3.30a}$$

$$F_{k,p}^{(i,l)} = \frac{\gamma_p^{(i)} {H_{k,p}^{(l)}}^*}{\frac{\sigma_N^2}{\sigma_S^2} + \sum_{l=1}^{L} \left| H_{k,p}^{(l)} \right|^2}. \tag{3.30b}$$

From (3.24), and the optimal $\mathbf{F}_{k,p}^{(i)}$ and $\mathbf{B}_{k,p}^{(i)}$ coefficients from (3.29), it is possible to compute the MMSE. Considering that

$$\sigma_p^{2(i)} = \frac{1}{N^2} \sum_{k=0}^{N-1} \mathbb{E} \left[\left| \tilde{S}_{k,p}^{(i)} - S_{k,p} \right|^2 \right], \tag{3.31}$$

and $Q(x)$ as the Gaussian error function, according to [CC09] and similar to the previous section, the BER of MT p at the ith iteration for a QPSK constellation is

$$BER_p^{(i)} \simeq Q\left(\frac{1}{\sigma_p{}^{(i)}} \right). \tag{3.32}$$

Although the linear frequency-domain receiver can be employed with any constellation, the presented iterative receiver is specific for a QPSK constellation. The iterative receiver can be extended to other constellations by employing the generalized IB-DFE receiver concept of [DMSS10]. So analogous to section 3.4.1, the BER for other constellations can be extracted. For instance, for M^2-QAM constellations with Gray mapping and minimum distance between symbols (i.e., the real and imaginary parts of the symbols are $\pm 1, \pm 3, ..., \pm(M-1)$), the BER is approximately given by

$$BER_p^{(i)} \simeq \frac{2}{\log_2(M)} \left(1 - \frac{1}{M} \right) Q\left(\frac{1}{\sigma_p{}^{(i)}} \right). \tag{3.33}$$

For an uncoded system with independent and isolated errors, the PER for a fixed packet size of M bits is

$$PER_p^{(i)} \simeq 1 - (1 - BER_p^{(i)})^M. \tag{3.34}$$

Performance Results

The current section regards the performance evaluation of the analytical model for an IB-DFE receiver structure. Contrary to section 3.4.1, this section only considers the UC condition. Nevertheless, the analytical model is still valid for other retransmission scenarios, namely when the SP technique is employed [DMB+09]. A highly dispersive channel [MS98], with uncorrelated Rayleigh fading for each path and MT for a total of 32 ray paths/MT is considered. The performance results also consider data blocks with $N = 256$ uncoded Quadrature Phase Shift Keying (QPSK) symbols, where each block occupies a $4\mu s$ time slot.

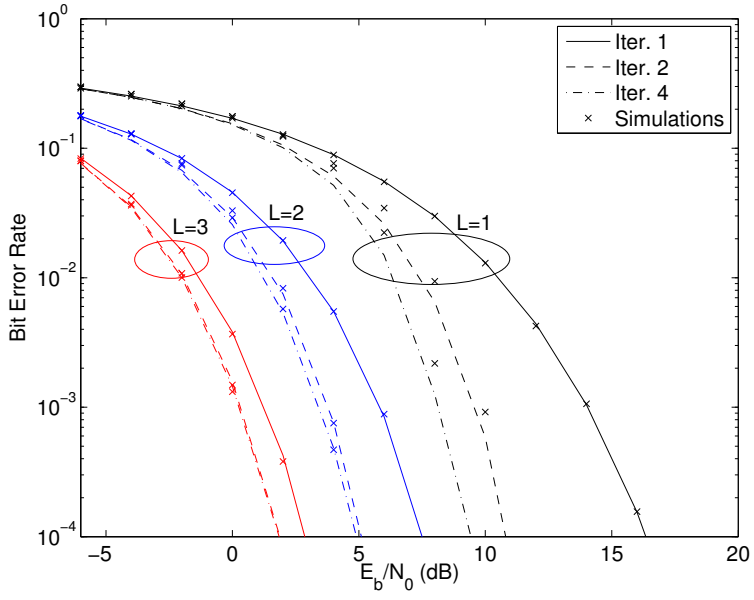

Figure 3.12: DC technique up to 4 iterations and $L = [1, 2, 4]$.

Figure 3.12 depicts the Bit Error Rate (BER) performance for the DC case for a single MT, with $L = [1, 2, 4]$ transmissions and up to four iterations of the IB-DFE technique. From this figure, it is possible to observe that the IB-DFE technique enhances data reception for an increasing number of iterations, though for $L \geq 2$ there are not many differences between the second and the fourth iterations. The analytical model is slightly inaccurate for fewer transmissions, i.e. $L = 1$, and on succeeding iterations, mostly due to the fact that each iteration introduces residual errors in the analytical model.

Figure 3.13 evaluates the BER analytical tool performance for $P = 2$ MTs, employing a traditional MUD scheme where $P = L = 2$ and the hybrid of MUD with DC where $L = 4 > P = 2$. The IB-DFE technique has a good performance up to 4 iterations when $P = L$; for $L > P$, the IB-DFE technique enhances data reception but marginally after the second iteration. The analytical tool has a good accuracy for multiple MTs accessing the channel, though on succeeding iterations for fewer transmissions, i.e. $L = 2$, it is possible to observe a slight inaccuracy to portray the IB-DFE technique.

Figure 3.14 illustrates the MUD scheme performance for two groups of MTs radially distributed around the BS, where $P = 4$ MTs. The first group has two MTs, closer to the BS, where $|\xi_1| = 0$dB; the remaining MTs from the second group have $|\xi_2| = -6$dB. For $L = 3$ transmissions, it is possible to

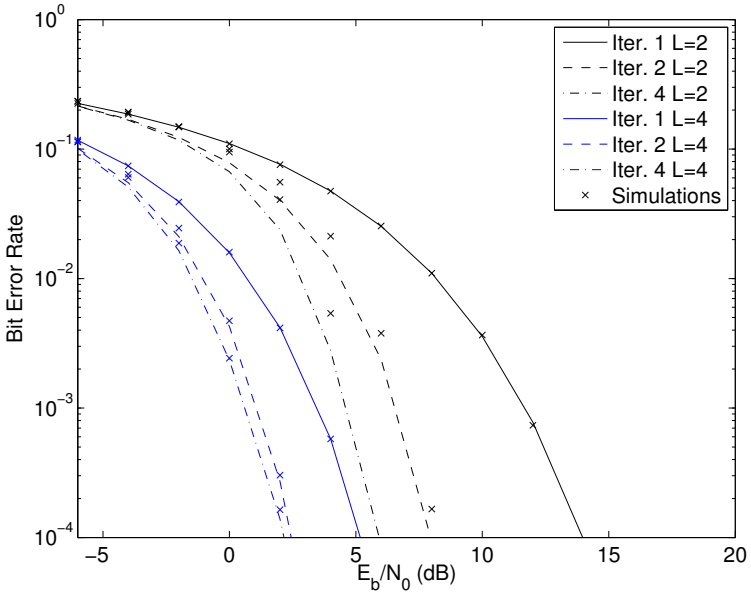

Figure 3.13: MUD for $P = 2$ MTs, $L = [2, 4]$ and up to 4 iterations for an iterative receiver structure.

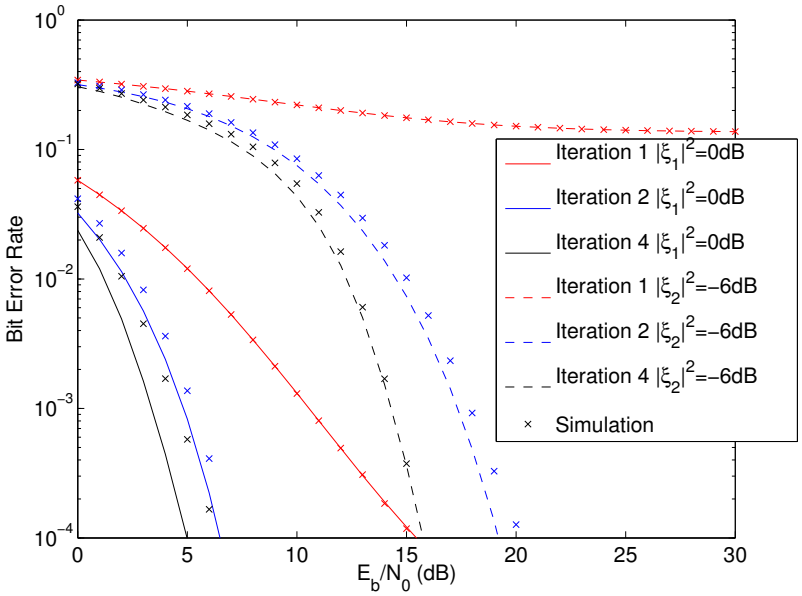

Figure 3.14: MUD for $P = 4$ MTs, two of them with $|\xi_1| = 0$dB and the remaining MTs with $|\xi_2| = -6$dB, with $L = 3$ transmissions and up to 4 iterations regarding an iterative receiver structure.

decode data blocks from $P = 4$ MTs accessing the channel, where the IB-DFE technique achieves a good performance up to four iterations. From this figure it is possible to observe that the analytical model performs quite well; however, with fewer transmissions than P and the existence of non-uniform transmission powers, the analytical model has a noticeable degradation for 0dB, starting from the second iteration.

Figure 3.15 evaluates the PER analytical tool performance for the same scenario of Figure 3.13. The theoretical PER values computed from (3.34) were compared with the simulation values. Likewise the BER results, there is a good match between the theoretical and simulated PER values, though with a

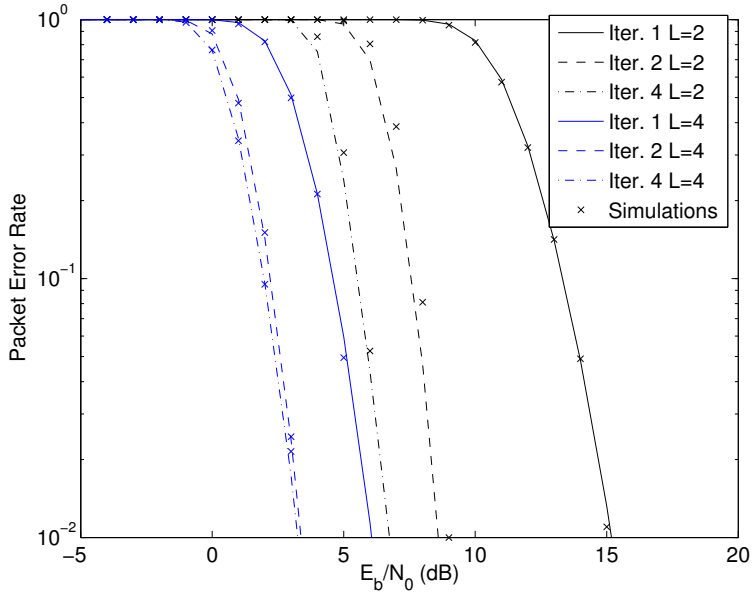

Figure 3.15: MUD for $P = 2$ MTs, $L = [2, 4]$ and up to 4 iterations regarding an iterative receiver structure.

slight inaccuracy for $L = P$ for succeeding iterations. This inaccuracy could be explained by the fact that each succeeding iteration introduces some residual error to the analytical model, though with $L > P$ this inaccuracy is indeed smaller.

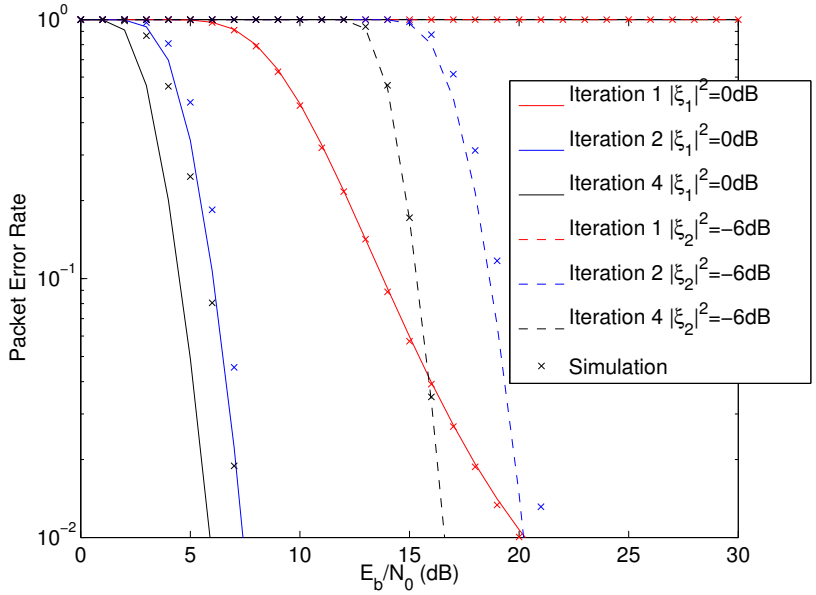

Figure 3.16: MUD for $P = 4$ MTs, two of them with $|\xi_1| = 0$dB and the remaining MTs with $|\xi_2| = -6$dB, with $L = 3$ transmissions and up to 4 iterations regarding an iterative receiver structure.

Figure 3.16 illustrates the PER performance for the same scenario of Figure 3.14. Similarly to the BER results, the analytical model performs decently, though there is a noticeable difference between the analytical values and the simulation values starting from the second iteration for $|\xi_2| = 0$dB. This difference, once again, could be explained by the inability of the analytical model to faithfully portray the

IB-DFE behavior for $L < P$, especially when non-uniform transmission powers are considered, hence amplifying the residual error of the IB-DFE scheme when estimating the BER and consequently the PER.

The differences between the theoretical values and the simulation values were quite noticeable for the IB-DFE scheme, especially when $L < P$ and with non-uniform transmission powers on succeeding iterations. This is due to two reasons: The Gaussian approximation of the FDE output and the overestimation of the FDE coefficients. These effects were already observed in [PDN10, CDM11], though in most cases the proposed analytical model has a good performance.

3.5 Conclusions

The current chapter considered two SC-FDE equalization schemes: linear equalization and iterative equalization. An analytical model was proposed, to compute the BER and PER performances for DC and MUD schemes, that is relatively simple and versatile. In fact, it is suitable for DC and MUD schemes, as well as hybrid schemes that combine both DC and MUD; the analytical model can be employed to study scenarios with non-homogeneous transmitting powers for each MT; different channel conditions concerning retransmission techniques can also be studied using the proposed analytical model. A set of simulation results showed that the proposed analytical model provides accurate BER and PER results in a wide range of scenarios, although presenting some inaccuracy for iterative equalization, mostly because of residual errors that are not portrayed in the analytical model. Anyway, the proposed work can be very helpful in MAC layer simulations that study the impact of using DC and MUD techniques.

Chapter 4

Type II H-ARQ Time Division Multiple Access Model

4.1 Introduction

TDMA as a MAC protocol presents itself as a *rigid* centralized MAC scheme, since each slot is assigned to a MT; such scheme can be very helpful when the channel is fully loaded, i.e. MTs always have a packet to transmit at each TDMA frame, and/or especially for stringent QoS requirements. However, when conventional Automatic Repeat reQuest (ARQ) techniques are employed, the transmission delay can be very high and the throughput very low for difficult channel conditions. Besides these problems, a MT will use a higher transmission power to overcome difficult channel conditions, which can quickly deplete the MT's battery.

As aforementioned in chapter 2, the employment of a type II DC H-ARQ technique can ameliorate the overall performance of the TDMA scheme, where both techniques will work as a cross-layered scheme; the ability of combining data block symbols from all packet transmissions at the BS will improve the throughput, delay and the expended energy per packet.

Cui et al studied the effect of type II H-ARQ in a TDMA MAC scheme [CGB05] and discovered that the E_b/N_0 ratio, for a given PER requirement, diminishes for an increasing number of transmissions; since packet copies are stored and combined at the BS, the energy from each packet is used to enhance the system performance, which leads to a lower energy transmission on subsequent retransmissions. *Quaglieri et al* [QSCea05] reveals that there is a performance trade-off between energy efficiency and throughput when employing type II H-ARQ with TDMA. However, this work does not study an effective way to cope with *hard* QoS requirements. It should be remarked that cross-layered type II H-ARQ TDMA MAC protocols studied in chapter 2 do achieve a better energy efficiency, however, these protocols/studies do not pinpoint a performance correlation between energy efficiency and QoS.

The current chapter models a TDMA MAC system with type II H-ARQ and poses an optimization problem: to seek the optimal PHY and MAC parameters that achieve energy efficiency and at the same time cope with QoS requirements. The model performance will be tested for two PHY layer scenarios: a WSN scenario and a High Altitude Platform (HAP) scenario; both scenarios are studied under an AWGN channel. The WSN scenario is studied with a simple DC receiver for BPSK modulation [Ben85] and the HAP scenario is studied with a multi-rate CC receiver [BDMP95]. The SC-FDE DC receiver model from

chapter 3 will be later studied with TDMA, in chapter 7, for benchmark purposes against DS-CDMA and NDMA; both DS-CDMA and NDMA will also take advantage of DC.

The work presented in this chapter was accepted for publication in [GPB+10a, GPB+10b].

The current chapter is organized as follows: section 4.2 overviews the assumptions of a TDMA MAC protocol with type II H-ARQ and studies the performance model; section 4.3 studies the model optimization; section 4.4 analyzes how well the model behaves for a WSN and a HAP; finally, section 4.5 regards this chapter's conclusions.

4.2 TDMA with Type II H-ARQ Performance Analysis

The wireless channel is composed by a BS that coordinates the MTs access in a slotted manner. Time is divided into equal length slots, each slot with the duration of a data packet. Each data packet transmission is synchronized at the beginning of a slot. It is assumed that suitable time synchronization and slot scheduling protocols are running (e.g. [BOP+07]) to ensure that each slot is assigned to a single MT and that no interference exists between slots.

Each MT has one slot per TDMA frame. A frame contains $(1 + L_T)$ slots, with $L_T \geq 1$, representing the group of slots allocated to other stations and for TDMA supporting protocols. When the BS detects errors in a packet, it asks for its retransmission. Both the BS and the MT give up after the $(R_T - 1)$th retransmission attempt.

A performance analysis of a TDMA protocol with H-ARQ is done at this section, where several metrics are studied: the MAC reception success and failure probabilities in section 4.2.1; the expended Energy per Useful Packet (EPUP) in section 4.2.2; the goodput in section 4.2.3; and the delay in section 4.2.4.

4.2.1 MAC Reception Failure and Success Probabilities

The probability of receiving a packet with success at the BS is given by $p_{suc}^{(l)}$, $0 \leq p_{suc}^{(l)} \leq 1$, where l, $1 \leq l \leq R_T$, is the number of transmissions for a given packet. The probability $p_{suc}^{(l)}$ depends on the successful reception of every bit, assuming that each bit is i.i.d.. Assuming a fixed size of M bits per packet, then

$$p_{suc}^{(l)} = \left(1 - BER_T(l)\right)^M , \tag{4.1}$$

where $BER_T(l)$ is TDMA's BER probability for an lth transmission. The probability of having $x-1$ failed transmissions is denoted by

$$Q_x = \prod_{l=1}^{x-1} \left(1 - p_{suc}^{(l)}\right) . \tag{4.2}$$

Both $p_{suc}^{(l)}$ and Q_x will be used in the remaining subsections.

4.2.2 Energy per Useful Packet (EPUP)

The modeling of the expended EPUP has to consider the transmission energy to send a data packet over the wireless medium and the energy from the MT's circuitry. *Cui et al* [CGB05] proposed an energy

model for uncoded M-QAM, however, this model does not take into account the acknowledgement costs that depend on the MAC layer design. The model from [CGB05] is summarized in this section.

The model from *Cui et al* assumes that a MT works in a multimode basis: when a MT has a packet to transmit the circuitry works in active mode for a duration T_{on}; when there is no signal to transmit it works in sleep mode; and when switching from sleep mode to active mode, there is a transient mode that lasts for a duration T_{tr}. [CGB05] shows that the energy consumption per packet is approximately given by

$$E_p \approx (1+\beta_T)P_tT_{on} + P_cT_{on} + 2P_{syn}T_{tr}, \tag{4.3}$$

where P_c denotes the total circuit energy consumption for the active mode (including the digital-to-analog and analog-to-digital converters, the bandpass filters, the intermediate frequency amplifiers, and the low noise amplifier for the transmitter); P_{syn} defines the power consumption of the frequency synthesizers; and $\beta_T = P_{amp}/P_t$ is the ratio between the power consumption of the power amplifier, P_{amp}, and the transmitted power, P_t. β_T can be also characterized as $\beta_T = (\nu_P/\varpi_P - 1)$ with ϖ_P as the drain efficiency of the radio frequency power amplifier and ν_P as the peak-to-average-power ratio. Although ϖ_P increases with the transmitted power [WHY06], for the sake of simplicity a constant value is considered for $\varpi_P = 0.35$ as in [CGB05]. Assuming the κth-power path-loss model at distance d (meters), the transmission power is expressed as

$$P_t = P_rG_1d^{\kappa}M_l, \tag{4.4}$$

where P_r is the received power at the BS, M_l is the link margin gain compensating the hardware process variations and other additive noise, and G_1 is the gain factor at $d = 1$ m. $\kappa = 3.5$ and $G_1 = 30$dB will be assumed for free-space propagation.

For an AWGN, the power spectral density is $\sigma_C^2 = \frac{N_0}{2} = -174$dBm/Hz for a given bandwidth B, and based on the E_b/N_0 ratio, equation (4.4) and $P_r = \frac{ME_b}{T_{on}}$, the expended energy for each packet is defined as

$$E_p \approx (1+\beta_T)G_1d^{\kappa}M_lME_b + P_cT_{on} + 2P_{syn}T_{tr}. \tag{4.5}$$

The EPUP, denoted Φ^T, measures the average transmitted energy for a correctly received packet. It depends on the expected number of transmissions per packet $\mathbb{E}[N_{sys}^T]$ and the packet's success rate, and is given by:

$$\Phi^T = \frac{\mathbb{E}[N_{sys}^T]E_p}{1 - Q_{R_T+1}}. \tag{4.6}$$

Assuming that R_T is the maximum number of transmissions for a given packet, $E[N_{sys}^T]$ is obtained as

$$\mathbb{E}[N_{sys}^T] = \sum_{i=1}^{R_T}\left[i\, p_{suc}^{(i)}Q_i\right] + R_TQ_{R_T+1}. \tag{4.7}$$

4.2.3 Goodput

The mean duration of a packet's service time counts the number of slots used to transmit a packet or to cancel its transmission after $(R_T - 1)$ retries. For a single slot per frame it counts the duration of the frames and is equal to

$$\mathbb{E}[\mathcal{D}_{service}] = (L_T + 1)\,\mathbb{E}[N_{sys}^T]. \tag{4.8}$$

Let S_{sat}^* be the channel's saturation goodput. It is limited by the packet's mean service time and by the packet's success probability, and is given by

$$S_{sat}^* = \frac{1 - Q_{R_T+1}}{\mathbb{E}[\mathcal{D}_{service}]}. \tag{4.9}$$

The channel goodput, S^*, is proportional to the mean number of packet arrivals per slot, denoted by α_1, as long as the channel is not saturated.

$$S^* = \begin{cases} S_{sat}^*, & \alpha_1 \geq 1/S_{sat}^* \\ \alpha_1 \left(1 - Q_{R_T+1}\right), & \alpha_1 < 1/S_{sat}^* \end{cases}. \tag{4.10}$$

4.2.4 Delay Analysis

The packet delay $\mathbb{E}[\mathcal{D}^T]$, for a TDMA with type-II H-ARQ protocol, was derived in [PBD+12] for an SC-FDE receiver; the model is briefly summarized in this section.

The number of packet arrivals per slot at a MT's buffer are i.i.d. random variables, defined by a stochastic process a_m. a_m denotes the probability of arriving m packets during a slot; $A(z)$ is a_m's z-transform. α_1 defines the mean number of packet arrivals per slot and α_2 denotes the second order moment of packet arrivals per slot. The model assumes that the Round-Trip Time (RTT) is lower than the frame duration. It can be shown, as in [PBD+12], that

$$\mathbb{E}[\mathcal{D}^T] = \frac{\mathbb{E}[X_T]}{\alpha_1} + \frac{1}{2}, \tag{4.11}$$

where $\mathbb{E}[X_T]$ denotes the mean number of packets in the MT's queue. $\mathbb{E}[X_T]$ can be computed as

$$\mathbb{E}[X_T] = \frac{f_2(1)\,g_1(1) - f_1(1)\,g_2(1)}{2g_1^2(1)}, \tag{4.12}$$

where

$$\begin{aligned} f_1(1) =& P_{1,0,1}\Bigg[1 + \alpha_1\Bigg(1 - p_{suc}^{(1)} - Q_{R_T}\left[(R_T - 1)(L_T + 1) + \right. \\ & \left. 1\right] - \sum_{l=2}^{R_T-1} p_{suc}^{(l)} Q_l\left[(l-1)(L_T+1)+1\right]\Bigg)\Bigg], \end{aligned} \tag{4.13}$$

$$g_1(1) = 1 - (L_T + 1)\,\alpha_1\left[p_{suc}^{(1)} + Q_{R_T}R_T + \sum_{l=2}^{R_T-1} l \times p_{suc}^{(l)} Q_l\right], \tag{4.14}$$

$$
\begin{aligned}
f_2(1) =& P_{1,0,1}\Bigg[2\alpha_1 + \alpha_2\left(1 - p_{suc}^{(1)}\right) - Q_{R_T}\left[(R_T - 1)\right. \\
& \left.(L_T + 1) + 1\right]\left[(R_T - 1)(L_T + 1)\alpha_1^2 + \alpha_2\right] - \\
& \sum_{l=2}^{R_T - 1} p_{suc}^{(l)} Q_l \left[(l-1)(L_T+1)+1\right]\left[(l-1)\right. \\
& \left.(L_T + 1)\alpha_1^2 + \alpha_2\right]\Bigg],
\end{aligned} \tag{4.15}
$$

$$
\begin{aligned}
g_2(1) =& -p_{suc}^{(1)}(L_T+1)\left(L_T\alpha_1^2 + \alpha_2\right) - \\
& Q_{R_T} R_T (L_T+1)\left(\left[R_T(L_T+1) - 1\right]\alpha_1^2 + \alpha_2\right) - \\
& \sum_{l=2}^{R_T-1} p_{suc}^{(l)} Q_l l (L_T+1)\left[\left(l(L_T+1) - 1\right)\alpha_1^2 - \alpha_2\right].
\end{aligned} \tag{4.16}
$$

$P_{1,0,1}$ is the probability of having one packet in the MT's queue waiting for transmission, given that it will be transmitted at the next slot allocated to the MT. $P_{1,0,1}$ can be expressed as

$$
P_{1,0,1} = \left[\left(1 + \sum_{l=2}^{R_T} Q_l\right)\frac{\varphi_z}{\omega_z} - \sum_{l=2}^{R_T} Q_l\right]^{-1}, \tag{4.17}
$$

where

$$
\begin{aligned}
\varphi_z =& 1 + \alpha_1\left(1 - p_{suc}^{(1)} - Q_{R_T}\left[(R_T - 1)(L_T+1) + 1\right] - \right. \\
& \left. \sum_{l=2}^{R_T-1} p_{suc}^{(l)} Q_l \left[(l-1)(L_T+1)+1\right]\right)
\end{aligned} \tag{4.18}
$$

and

$$
\omega_z = 1 - (L_T+1)\alpha_1\left[p_{suc}^{(1)} + Q_{R_T}R_T + \sum_{l=2}^{R_T-1} l \times p_{suc}^{(l)} Q_l\right]. \tag{4.19}
$$

The $P_{1,0,1}$ equation is very useful to model the mean H-ARQ TDMA delay for any packet arrival distribution, as long as $A(z)$ is defined. The following section validates the proposed models, assuming that packet arrivals are governed by a Poisson process, so

$$
A(z) = e^{-\lambda(1-z)}, \quad A'(1) = \alpha_1 = \lambda, \quad A''(1) = \alpha_2 = \lambda^2. \tag{4.20}
$$

Notice, that a packet departures the system after a failed transmission with probability Q_{R_T+1}. Therefore, the delay must be only considered if the success rate $(1 - Q_{R_T+1})$ satisfies the application requirements.

4.3 System Optimization

Equation (4.6) can tend to infinity for very low and for very high E_b/N_0 values. Φ^T increases when less packet transmissions are successful for low E_b/N_0 because Q_{R_T+1} tends to one; Φ^T also increases when the transmission power increment is not compensated by a reduction on the error rate (Q_{R_T+1})

or on the mean number of packet transmissions ($E[N_{sys}^T]$), for high E_b/N_0 values. However, the E_b/N_0 value that minimizes Φ^T may not satisfy the application requirements.

The QoS offered by a channel is influenced by R_T. The maximum packet transmission delay is equal to $D_{max} = (L_T + 1)R_T$ slots. A higher R_T allows the use of a lower transmission power to achieve the same packet transmission success probability ($1 - Q_{R_T+1}$), however, it introduces a higher packet transmission delay variation. R_T must be set to the highest possible value tolerated by the application's delay and jitter requirements.

Given R_T and the packet arrival distribution $A(z)$, Φ^T should be bounded by the following four constraints: a minimum goodput value, S_{min}^*; a maximum delay value, D_{max}; a minimum packet transmission success probability, $\mathcal{Q}_{min}$; and a maximum bit energy at the MT, E_{bmax}. Using (4.6), (4.10) and (4.11), the optimization model can be written as

$$\begin{aligned} &\text{minimize} \quad \Phi^T \\ &\text{subject to} \quad (S_{sat}^* \geq S_{min}^*) \wedge \left(E\left[\mathcal{D}^T\right] \leq D_{max}\right) \wedge (1 - Q_{R_T+1} \geq \mathcal{Q}_{min}) \wedge (E_b \leq E_{b_{max}}) . \end{aligned} \tag{4.21}$$

4.4 Model Performance

The current section evaluates the H-ARQ TDMA model for two receiver configurations: an uncoded Binary Phase Shift Keying (BPSK) constellation receiver and a multi-rate code receiver for a QPSK constellation. The first receiver, in section 4.4.1, is studied for a WSN topology; the second receiver, in section 4.4.2, is studied for a HAP configuration. For each receiver, the model performance was simulated with previously computed BER results using the *MATLAB* [Mat11] software; MAC simulations were performed using the *ns-2* simulator [Inf07]. Despite the use of different receiver configurations, it should be noted that the EPUP performance for a HAP scenario has negligible expended energy concerning a BS's electrical circuitry since the transmission distance is very high, contrarily to a WSN scenario that has small distances comprehended between 10m and 100m.

4.4.1 DC Receiver for an AWGN with BPSK

A BPSK DC receiver for an Additive White Gaussian Noise (AWGN) scenario, that regards a WSN topology, is studied in this section section and its respective results are also analyzed.

Receiver Model

The DC receiver in this section is characterized in the time domain. Data is transmitted in fixed size packets, defined as $\{s_n; n = 0, 1, \ldots, M-1\}$, where s_n is a data symbol selected from the BPSK constellation. When the BS detects errors in a packet, it asks for its retransmission but stores the signal associated to each transmission attempt. The received signal associated to the ith transmission attempt is sampled as $\left\{y_n^{(i)}; n = 0, 1, \ldots, M-1\right\}$, where

$$y_n^{(i)} = s_n + \nu_n^{(i)}, \tag{4.22}$$

where $\nu_n^{(i)}$ denotes the channel noise, with variance σ_ν^2.

For a BPSK constellation $s_n = \pm b_n = \pm 1$ and a fixed channel, the estimates of s_n, $\hat{s}_n$, can be made based on the sign of $y_n = \sum_{i=1}^{l} y_n^{(i)}$ for l transmission attempts.

Assuming uncorrelated noise for the different transmission attempts results

$$y_n = \sum_{i=1}^{l} y_n^{(i)} = l b_n + \nu_n^{eq}, \tag{4.23}$$

where $\nu_n^{eq} = \sum_{i=1}^{l} \nu_n^{(i)}$ has variance $l\sigma_\nu^2$. Therefore, after the combination of the l symbol copies, the BER will be

$$BER_T(l) = Q\left(\sqrt{\frac{2E_b}{N_0} l}\right). \tag{4.24}$$

Model Performance

The current section presents a performance analysis of the proposed system model. It is assumed that a TDMA frame lasts $(L_T + 1) = 8$ slots, where the wireless terminals generate packets with a constant length of $M = 256$ bits based on a Poisson process with $\lambda = 1/40$ packets/slot. Table 4.1 lists the parameters' configuration for the H-ARQ TDMA model.

Parameter	Value
P_c	164.998 mW
P_{syn}	50 mW
ϖ_P	0.35
T_{on}	0.026s
T_{tr}	5μs
B	10KHz
M	256 bit
G_1	30 dB
κ	3.5
M_l	40 dB
σ_C^2	-174 dBm/Hz

Table 4.1: Simulation parameters for a WSN.

The model's performance is compared against simulation results; an H-ARQ TDMA simulator was implemented based on the ns-2 simulator [Inf07]. $p_{suc}^{(l)}$ is a mean-ergodic process, where the PER is modeled up to 10 transmissions per packet. For each simulation, $p_{suc}^{(l)}$ was used as an input matrix parameter for a given value of E_b/N_0. The PER results are shown in figure 4.1, showing a gain of 3dB with a single retransmission ($R_T = 2$) for a $PER = 10^{-1}$. The additional gain decreases for the subsequent retransmissions; in this case there is a total gain of 10dB for $R_T = 10$ transmissions per packet.

Figures 4.2 and 4.3 illustrate the variation of the $EPUP$ with E_b/N_0 for a transmission distance of respectively $d = 10$m and $d = 100$m. The figures depict the analytical and simulated Φ^T values for a conventional ARQ technique, using up to $R_T = 2$ transmissions of the same packet, and for the DC H-ARQ technique with $R_T = [2, 3, 4, 10]$ transmissions. The analytical values were calculated using (4.6) and the simulated values were measured from the average of total transmissions per successful packet for a given E_b/N_0. Results show that the simulated values follow the analytical model, therefore validating the presented model. The figures show that the H-ARQ energy efficiency does depend on the transmission distance. The H-ARQ technique does not improve Φ^T for $d = 10$m when compared to a conventional ARQ technique; the circuit power consumption is almost the same order of magnitude

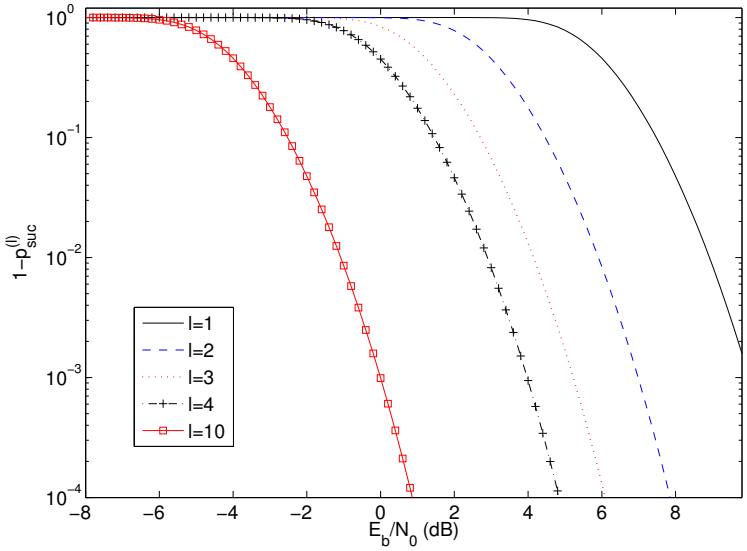

Figure 4.1: $1 - p_{suc}^{(l)}$ performance.

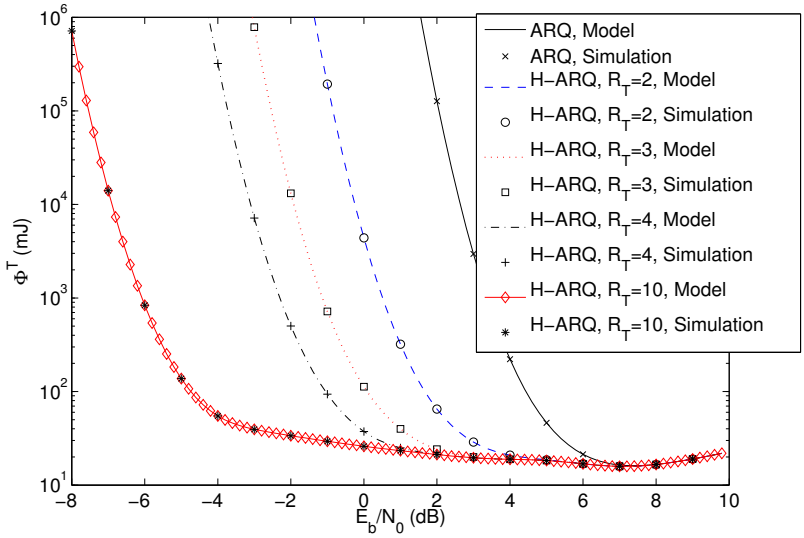

Figure 4.2: Φ^T performance for ARQ up to $R_T = 2$ and H-ARQ up to $R_T = 10$, regarding a distance of $d = 10$ m.

as the transmission power. The minimum Φ^T is always achieved with a single packet transmission. On the other hand, H-ARQ allows a significant $EPUP$ reduction for $d = 100$m with lower E_b/N_0 values; the statement is valid as long as the number of transmissions R_T increases. For $d = 100$m the minimum Φ^T occurs for the minimum E_b/N_0 value where almost no errors occur (see Figure 4.4).

Figure 4.4, shows the performance of the success probability $1 - Q_{R_T+1}$, and figure 4.5 illustrates the performance of $\mathbb{E}[\mathcal{D}^T]$. Once more, it is noticeable that the analytical values accurately model the proposed system. The analytical values of $1 - Q_{R_T+1}$ were obtained from (4.2); as for $E[D]$, they were obtained from (4.11). It is perceivable that the delay for ARQ and for the proposed H-ARQ system with $R_T = 2$ is the same; however the success probability $1 - Q_{R_T+1}$ is different, favoring the proposed H-ARQ system. It should be taken into account that as R_T increases for the proposed model, the expected delay for a given packet is also higher; nonetheless, the energy spent transmitting a packet

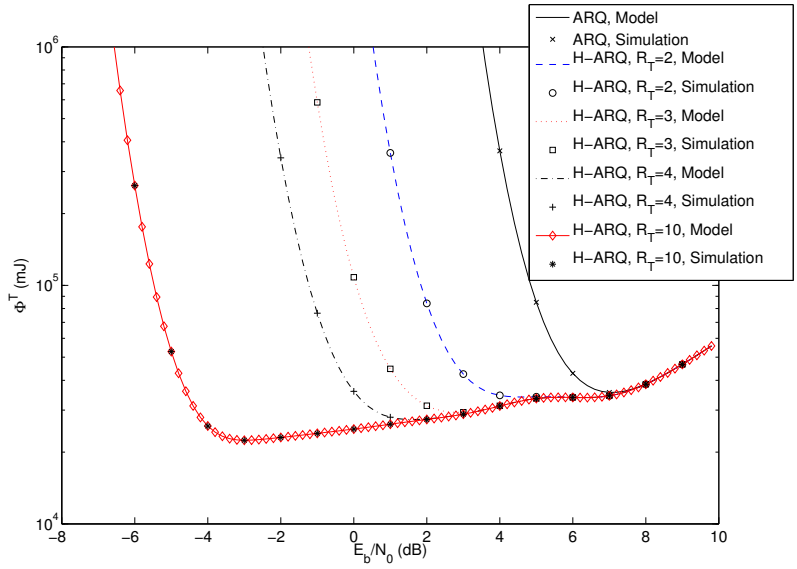

Figure 4.3: Φ^T performance for ARQ up to $R_T = 2$ and H-ARQ up to $R_T = 10$, regarding a distance of $d = 100$ m.

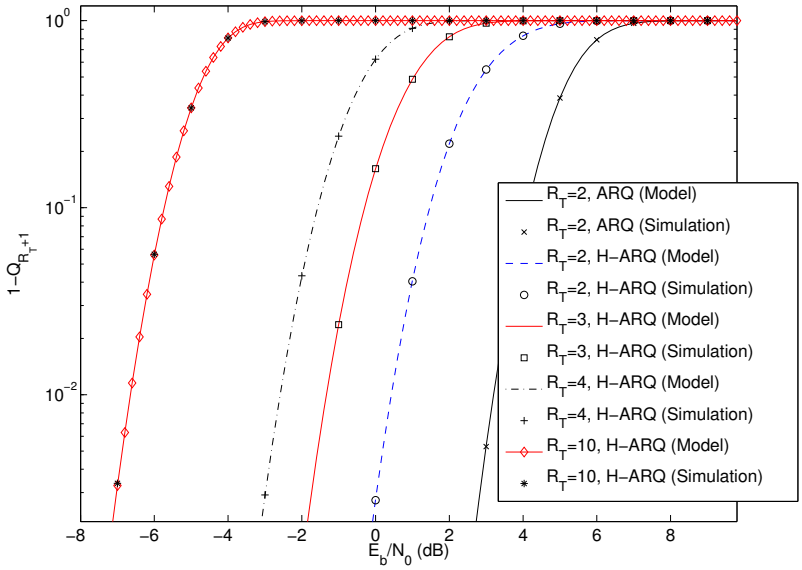

Figure 4.4: $1 - Q_{R_T+1}$ performance between conventional ARQ with $R_T = 2$ and H-ARQ with DC.

correctly is lower which leads to a lower Φ^T value for longer distances proving that H-ARQ is energy efficient when compared to conventional ARQ.

Figure 4.6, illustrates the analytical values of the Φ^T model concerning the H-ARQ system for a maximum of $R_T = 10$ transmissions. The values were plotted in function of the distance d, in meters, and E_b/N_0, in dB. As observed, with distances below $d \simeq 18$ m, the H-ARQ system is not energy efficient when compared to an ARQ system. For these distances the packet retransmission cost is too high and the minimum Φ^T value is reached for a packet success probability near one at the first transmission attempt ($p_{suc}^{(1)} \simeq 1$). For distances above 18m the H-ARQ system proves its energy efficiency, since it minimizes Φ^T for multiple transmissions per packet. Notice that for ARQ, the success rate is almost zero for E_b/N_0 below 3dB (see Fig. 4.4) and the minimum Φ^T for ARQ follows approximately the Φ^T values

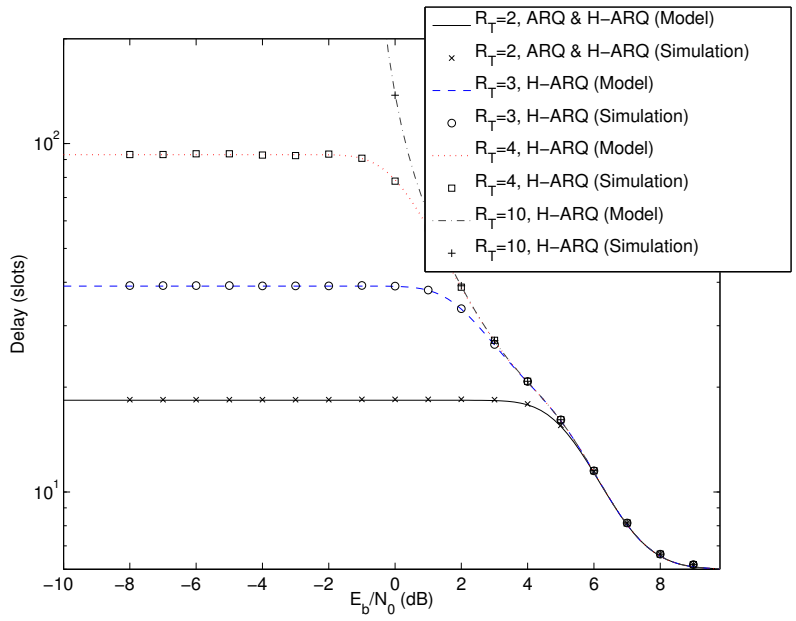

Figure 4.5: Delay performance between conventional ARQ with $R_T = 2$ and H-ARQ, for $\lambda = \frac{1}{40}$.

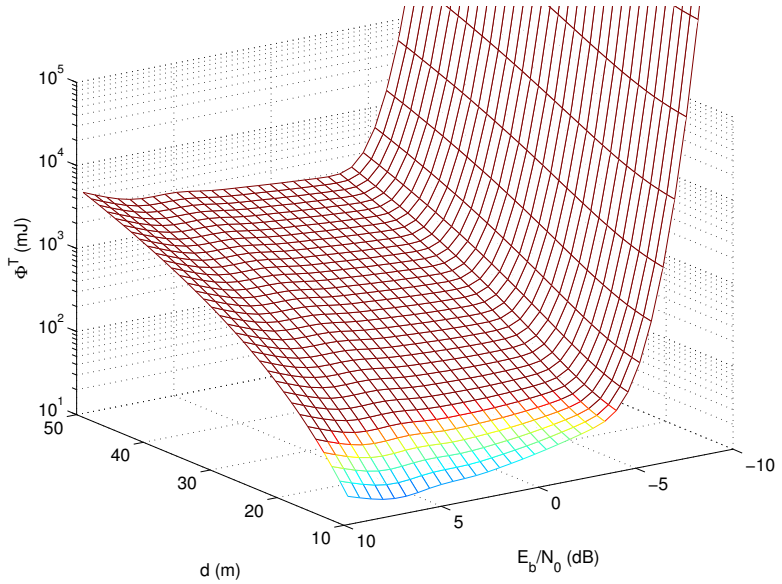

Figure 4.6: Analytical Φ^T for H-ARQ with $R_T = 10$.

for H-ARQ without errors when $E_b/N_0 = 10$ dB.

4.4.2 Multi-rate Coding for an AWGN Channel

A QPSK multi-rate code receiver for an AWGN scenario, that regards a HAP topology, is studied and its respective results are analyzed.

Receiver Model

The multi-rate coding scheme in this section is based on the $1/15$ rate turbo-code from [DP95]. The turbo-code consists of the parallel concatenation of two recursive convolutional codes separated by a pseudorandom interleaver (represented by the permutation function Π_1) as shown in Figure 4.7. Therefore, the same data block is applied at the input of both constituent encoders but one of them sees an interleaved version of the data block. Each encoder generates a sequence of parity bits which are transmitted alongside with the systematic bit. The transfer function of the 16-state constituent recursive convolutional codes is defined as

$$G(D) = \left[1, \frac{g_1(D)}{g_0(D)}, \frac{g_2(D)}{g_0(D)}, \frac{g_3(D)}{g_0(D)}, \frac{g_4(D)}{g_0(D)}, \frac{g_5(D)}{g_0(D)}, \frac{g_6(D)}{g_0(D)}, \frac{g_7(D)}{g_0(D)}\right],$$

where

$$\begin{aligned}
g_0(D) &= 1 + D^3 + D^4, \\
g_1(D) &= 1 + D^4, \\
g_2(D) &= 1 + D^2 + D^4, \\
g_3(D) &= 1 + D^2 + D^3 + D^4, \\
g_4(D) &= 1 + D + D^4, \\
g_5(D) &= 1 + D + D^3 + D^4, \\
g_6(D) &= 1 + D + D^2 + D^4, \\
g_7(D) &= 1 + D + D^2 + D^3 + D^4.
\end{aligned}$$

To achieve higher coding rates, puncturing is performed on the parity bits of both constituent encoders according to a predefined puncturing pattern. At the receiver a basic turbo decoder is used, as shown in Figure 4.8, where $\hat{b}$ denotes the estimated information bits sequence, $\hat{b}_\Pi$ the respective interleaved sequence, y^s the systematic observations and $y^{p,1}$ and $y^{p,2}$ the parity observations sequences of the two component encoders. Each soft-input soft-output block implements a trellis decoding algorithm (like the Maximum a Posteriori (MAP) algorithm [BCJR74]) for the respective component encoder. In addition to the systematic and parity observations weighed by the channel reliability factor $L_c = 4\ E_c/N_0$ (E_c as the expended energy per coded bit), each decoder also receives the *a priori* information obtained from the other decoder which is represented in the form

$$L_{ap}(b_t) = \log\left(\frac{\mathbb{P}[b_t = +1]}{\mathbb{P}[b_t = -1]}\right). \tag{4.25}$$

The output of the soft-input soft-output decoders is the sequence of log-likelihood ratios of the information bits which can be written as the sum of three terms

$$\begin{aligned}
L(b_t) &= \log\left(\frac{\mathbb{P}[b_t = +1|\text{observations}]}{\mathbb{P}[b_t = -1|\text{observations}]}\right) \\
&= L_c y_t^s + L_{ap}(b_t) + L_{l|2}^e(b_t)
\end{aligned} \tag{4.26}$$

In this expression $L_{l|2}^e$ is the extrinsic information produced by either decoder 1 or 2. While the first two terms are inputs to the component decoders, this third term represents new information derived in the decoder, which is used as *a priori* information, $L_{ap}(b_t)$ by the other decoder. To obtain $L_{l|2}^e(b_t)$,

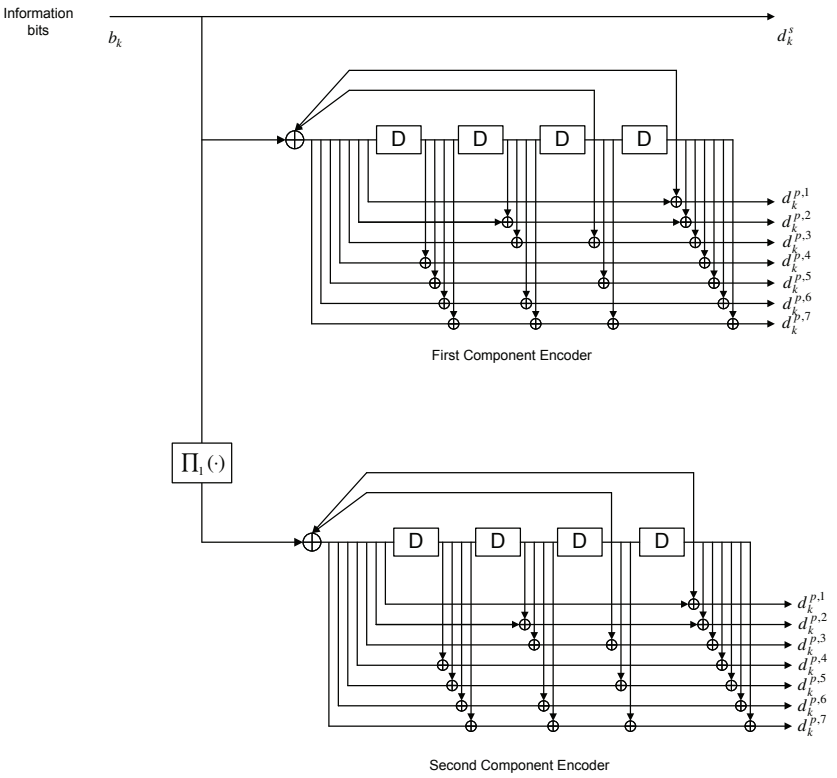

Figure 4.7: Encoding structure.

it is only necessary to subtract the weighed systematic observation and the *a priori* information from the output of the decoder. After passing this information to the interleaver (or de-interleaver, depending on the target decoder), the other decoder uses this extrinsic information as new *a priori* information and computes new estimates for the log-likelihoods of the information bits. The exchange of extrinsic information between the two decoders can proceed until a predefined maximum number of iterations is achieved. The output of the second decoder is then interleaved; a decision function can be applied to obtain the final estimates of the information bits.

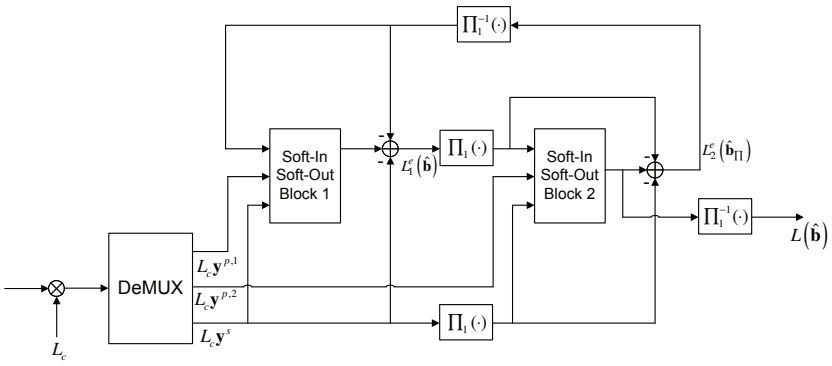

Figure 4.8: Turbo decoder block diagram.

Model Performance

The current section presents a performance analysis of the proposed system model. It is assumed that a TDMA frame lasts $(L_T + 1) = 8$ slots, where the wireless terminals generate packets with a constant length of $M = 1024$ bits based on a Poisson process where $\lambda = 1/40$ packets/slot. Table 4.2 presents the parameters list that are considered for the energy model, which follow the experimental parameters defined on the *StratXX* project [TWT08].

Parameter	Value
ϖ	0.35
T_{on}	0.205 ms
M	1024 bit
G_1	30 dB
d	20 Km
κ	2
M_l	40 dB
B	2.5 MHz
σ_C^2	-174 dBm/Hz

Table 4.2: Simulation parameters for a HAPN.

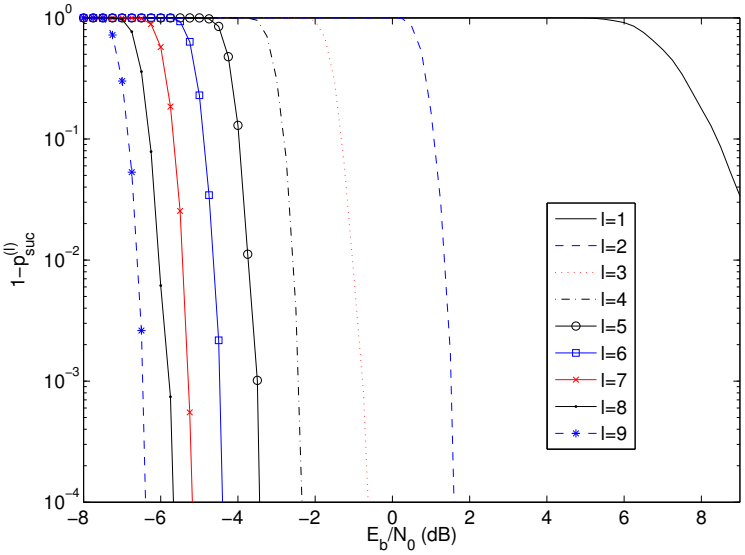

Figure 4.9: $1 - p_{suc}^{(l)}$ performance for conventional ARQ with $R_T = 2$ and H-ARQ up to $R_T = 9$ transmissions.

The model's performance is compared with simulation results based on the ns-2 simulator [Inf07]. $p_{suc}^{(l)}$ is a mean-ergodic process, where the PER is modeled up to 9 transmissions per packet. For each simulation, $p_{suc}^{(l)}$ was used as an input matrix parameter for a given value of E_b/N_0. The PER's results are shown in figure 4.9, showing a gain of roughly 6 dB with a single retransmission ($R_T = 2$) for a $PER = 10^{-1}$. The additional gain decreases for the subsequent retransmissions, leading to a total of 14dB with $R_T = 9$ transmissions per packet.

Figure 4.10 illustrates the variation of Φ^T with E_b/N_0 for a transmission distance of $d = 20$ km. The figure depicts the analytical and simulated values for the conventional ARQ technique, using up to $R_T = 2$ transmissions of the same packet, and for the H-ARQ technique with $R_T = [2, 3, 4, 9]$ transmissions. Results show that the simulated values follow the analytical model, therefore proving the model accuracy.

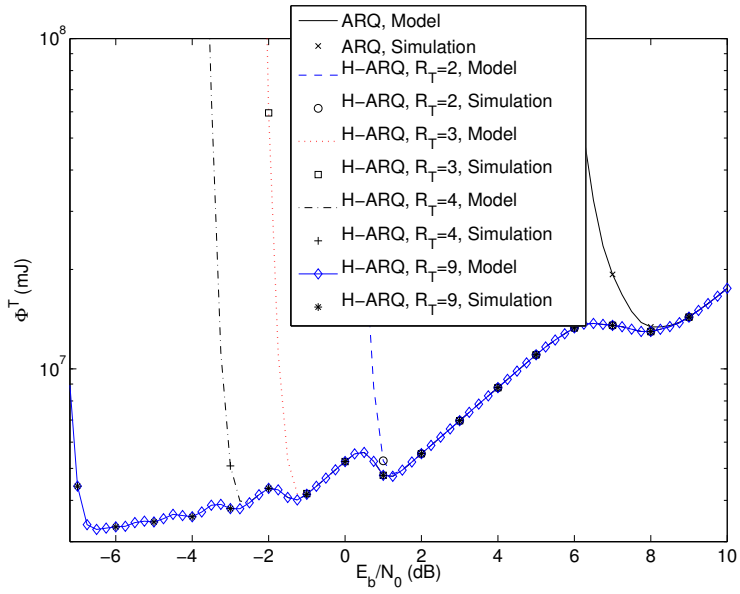

Figure 4.10: Φ^T for ARQ up to $R_T = 2$ and H-ARQ up to $R_T = 9$ for $d = 20$ km.

It is also possible to conclude that the H-ARQ technique allows a significant Φ^T reduction, since it attains the minimum Φ^T for lower E_b/N_0 values; the statement is valid as long as the number of transmissions R_T increases. As before, for H-ARQ and a given R_T the minimum $EPUP$ occurs for the minimum E_b/N_0 value where almost no errors occur (see Fig. 4.11). When $R_T > 1$ the variation of Φ^T with E_b/N_0 is non-monotonous - it has local minimums for the E_b/N_0 values that minimize Φ^T up to $(R_T - 1)$ transmissions.

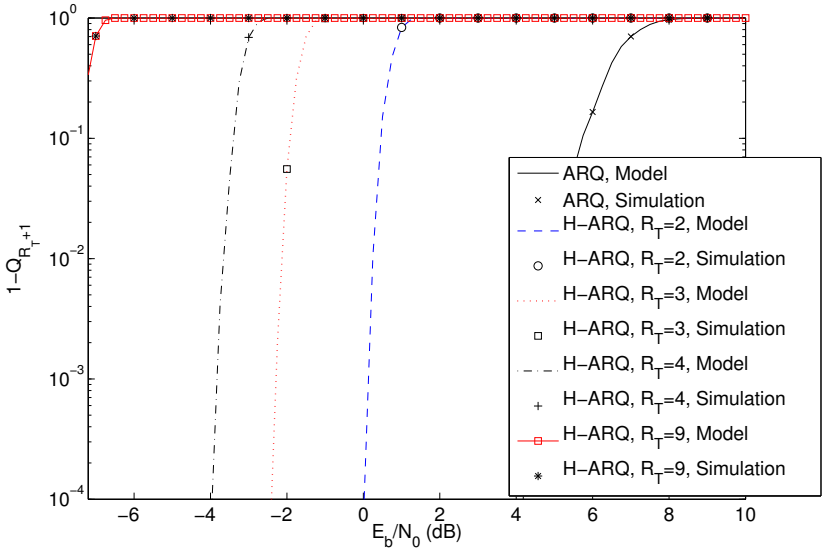

Figure 4.11: $1-Q_{R_T+1}$ performance between conventional ARQ up to $R_T = 2$ and H-ARQ up to $R_T = 9$.

Figure 4.11, shows the performance of the success probability $1 - Q_{R_T+1}$, and figure 4.12 illustrates the performance of $\mathbb{E}[\mathcal{D}^T]$. Once more, it is noticeable that the analytical values are accurate enough to model the proposed system. It is perceivable that the delay for ARQ and for the proposed H-ARQ system with $R = 2$ is the same; as before, the success probability $1 - Q_{R_T+1}$ is different, favoring the H-ARQ

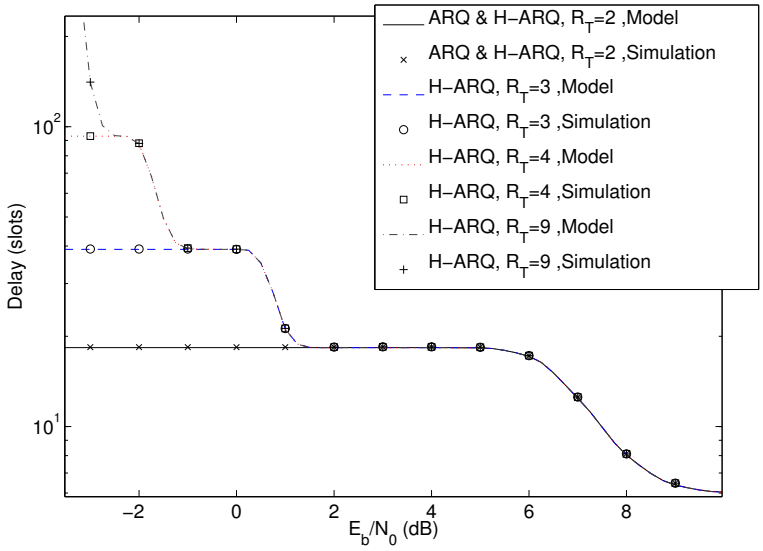

Figure 4.12: Delay performance between conventional ARQ up to $R_T = 2$ and H-ARQ up to $R_T = 9$, where $\lambda = \frac{1}{40}$ packets/slot.

system. It should be taken into account that as R_T increases for the proposed model, the expected delay for a given packet is also higher; nonetheless, the gain of receiving a packet correctly is higher leading to a lower Φ^T.

4.5 Conclusions

The current chapter conducted an extensive analysis of an H-ARQ TDMA MAC performance model for several metrics: the EPUP, the goodput and the packet delay. The model was then used to define the optimal parameters that guarantee a minimum EPUP and at the same time satisfying a given QoS. The model performance was very accurate when compared against simulation values for two simulation contexts: a WSN topology using a BPSK DC receiver for an AWGN channel and a HAP topology using a QPSK multi-code rate receiver for an AWGN channel .

The results show that significant gains can be obtained using a diversity combining H-ARQ scheme when compared to a classical ARQ scheme for longer distances and when retransmissions are tolerated by the application - especially for energy constrained topologies such as a WSN, where the H-ARQ EPUP is enhanced for longer distances, which translates into lower transmission power and an extended MT lifetime. Furthermore, by increasing the number of transmissions per packet, the EPUP also decreases for a lower E_b as long as no losses occur, especially for a HAP topology.

Chapter 5

H-ARQ Direct Sequence Code Division Multiple Access

5.1 Introduction

High data-rate broadband systems require an effective way to cope with highly dispersive channels at the uplink. As aforementioned in chapter 2, prefix-assisted DS-CDMA is a viable transmission technique for this context, where data symbols are spread in the time-domain with the aid of an orthogonal spreading code. At the receiver the equalization is made with FDE techniques [AGTT05, TA07].

For an infrastructured random access channel, managed by a BS that coordinates the channel in a slotted manner, prefix-assisted DS-CDMA brings benefits to the channel access. DS-CDMA can multiplex several MTs at the uplink channel, by assuming all MTs use unique orthogonal spreading codes.

At the BS, packets may be received with errors, due to high noise or interference levels, implying additional transmissions from the MTs; to avoid discarding packets, the BS can store the failed packet copies and combine them to successfully retrieve the data symbols - basically applying Type II H-ARQ with DC to the failed packet copies to take advantage of the time diversity of each packet transmission. If the BS is unable to retrieve the received data packets with success, due to a deep-fade that persists for several slots in the wireless channel, the BS can improve data reception through FDE techniques. With the aid of a non-linear iterative equalization method such as IB-DFE, the BS can diminish high channel interference or residual interference between MTs to enhance data reception. The PHY layer in this chapter extends the IB-DFE technique from chapter 3 for a prefix-assisted DS-CDMA context based on the works from [SD06, DS06b, DSG07a].

Most works that study prefix-assisted DS-CDMA with H-ARQ at the uplink are either too focused on the PHY layer or sparingly thin in terms of the MAC layer performance presenting only throughput results. In addition, MAC layer models that study the system performance with H-ARQ usually assume simplistic PER models based on the SINR, since PHY layer simulations are very time-consuming to extract PER results for the MAC layer simulations/model.

This chapter presents a PHY-MAC cross-layer model suited for a prefix-assisted DS-CDMA system that employs DC H-ARQ. The model reveals a strong inter-dependence between the PHY and MAC layer, since the MAC layer model strongly depends on the success probability of receiving a packet at each slot and at the same time the PHY layer model needs information from the system state, i.e. how many MTs

are concurrently accessing the channel as well as the number of the packet retransmissions already attempted.

The proposed model in this chapter distinguishes itself from existing works in the literature, since it defines a DC H-ARQ prefix-assisted DS-CDMA uplink system with MUD supported by an IB-DFE receiver. Based on the Discrete Time Markov Chain (DTMC) MAC-layer model states, the packet error rate at each state combination (the number of concurrent MTs and their respective retransmissions) is retrieved and therefore used to quantify the DTMC's steady state. Assuming a uniform average load, it is possible to measure the system's throughput, delay and expended EPUP.

The work in this chapter was partially published in [GVBD13].

The current chapter is structured as follows: section 5.2 characterizes the DS-CDMA H-ARQ system; section 5.3 analyses the IB-DFE receiver design; section 5.4 describes the DTMC wireless access model; section 5.5 shows the proposed model results; and section 5.6 briefs this chapter's conclusions.

5.2 System Description

The system model assumes an infrastructured wireless system, with full-duplex communication, where a BS coordinates the wireless uplink access in a time slotted manner. For the sake of simplicity, perfect synchronization is assumed with time advance mechanisms for the same reasons as in chapter 3 - for a prefix-assisted DS-CDMA system, timing errors can be absorbed by the cyclic prefix since the cyclic prefix is longer than the symbols' duration, and as long as the channel estimates are accurate enough.

For a DS-CDMA spreading factor K, each uplink slot should support up to K simultaneous transmissions thanks to the MUD receiver in section 5.3, assuming that the wireless medium has $J \leq K$ MTs contending the channel; a data packet at the uplink has the same size of an uplink slot. The BS is capable of detecting the number of MTs transmitting in an uplink slot.

Figure 5.1 displays the frame structure of each slot, composed by a SYNC signal at the downlink and data symbols with their respective cyclic prefix at the uplink. The SYNC signal transmitted at the beginning of each slot by the BS, signals all MTs registered at the BS with packets to transmit that they are allowed to transmit data in a synchronous way. The SYNC signal also indicates which packets were successfully received at the previous slot, requesting retransmissions from packets that were not received with success. MTs with data packets to transmit will send data packets with N modulated QPSK symbols with their respective cyclic prefix. If MTs do not have packets to transmit, these will remain silent until packets arrive to their queues. At the end of the slot the BS verifies all packets for errors using the IB-DFE technique from section 5.3, acknowledging at the beginning of the next slot all packets that were successfully received; packets with errors will be retransmitted in the next slot for H-ARQ purposes. Any MT whose packet is transmitted $R_C + 1$ times will discard it from the queue, either with or without errors.

It should be noted that the signal information received from MTs whose packets that were successfully received, or after R_C retransmissions, are removed from the BS memory. Since the BS uses a MUD scheme, it holds information from previously received packets with decoding errors and their respective transmissions, and also discards previously received signals that are not needed (either because MTs reached R_C retransmissions or effectively transmitted their packets with success); MTs with packets to transmit do not need to wait for unresolved transmissions from other MTs to conclude.

Once again, it should be clearly explained that the BS keeps track of how many retransmissions per MT have occurred, assuming that each transmission has a duration of one time slot. The BS groups MTs

with the same number of transmissions per packet into an H-ARQ stage. If (some or) all of the MTs for a given stage fail to transmit their packets then the BS will assign those MTs to the following H-ARQ stage. If MTs succeed transmitting their packets then the BS removes them from that H-ARQ stage.

Assuming perfect channel estimation, the BS performs H-ARQ by means of time diversity, i.e. for a given packet, the BS combines the received packets to enhance packet reception. It is also assumed that the BS can store up to $R_C + 1$ failed transmissions from all MTs, keeping track of which MTs are on the lth H-ARQ stage, where $0 \leq l \leq R_C$; $l = 0$ represents a stage with only one transmission.

For notation purposes, the number of idle users in a slot will be accounted as I and the number of users in a given slot performing at the l-th H-ARQ stage is ϑ_l, i.e. the number of MTs that have retransmitted a packet l times. ϑ_0 denotes the number of MTs that have only transmitted a single packet copy, i.e. without retransmissions.

5.2.1 Descriptive Example

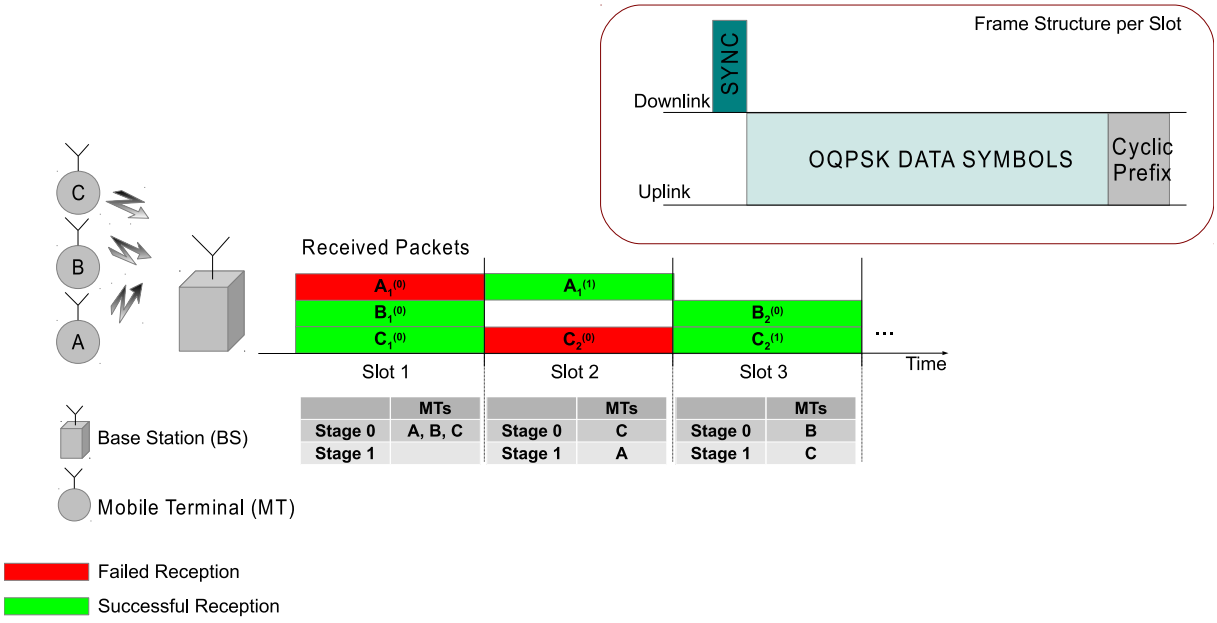

Figure 5.1: H-ARQ prefix-assisted DS-CDMA Reception scheme example and frame structure per slot.

Figure 5.1 presents a brief example of the modeled system, where three MTs A, B and C transmit data packets to a BS, assuming a retransmission limit of $R_C = 1$. A packet from any given MT, A for instance, is denoted in the figure as $A_i^{(r)}$, where $i = \{1, 2, ...\}$ denotes A's packet identifier and $r = \{0, 1, 2, ..., R_C\}$ the rth transmission. The BS at the end of each slot acknowledges packets that were successfully received and marks the beginning of the next slot. At the first slot, the three MTs transmit data to the BS, where B and C packets were received by the BS with success, while A's packet, $A_1^{(0)}$, has errors. To recover from $A_1^{(0)}$'s errors, MT A retransmits the same packet now denoted as $A_1^{(1)}$, and the BS will henceforth combine both $A_1^{(0)}$ and $A_1^{(1)}$ using the IB-DFE technique. During the second slot, MT C also transmits a second packet, $C_2^{(0)}$, though received with errors; in similar fashion, MT C retransmits the same packet, denoted as $C_2^{(1)}$. At the end of the third slot the BS recovers C's packet alongside with a successful reception from MT B's new packet.

5.2.2 Problem Introduction

This section briefs this chapter's PHY layer notations, although these are an extension of chapter 3. A data block from MT p, where $0 < p \leq \sum_{r=0}^{R_C} \vartheta_r$, with N symbols in the time domain is $\{s_{0,p}, \ldots, s_{N-1,p}\}$, and its respective DFT is $\{S_{0,p}, \ldots, S_{N-1,p}\}$.

For a spreading factor, K, a *Walsh-Hadamard* sequence assigned to a MT p is $\mathbf{c}_p = [c_{1,p}, \ldots, c_{K,p}]$ and its respective DFT is $\mathbf{C}_p = [C_{1,p}, \ldots, C_{K,p}]$ (see [SD06, DS06b]).

Time-domain spreading is done over the modulated data block where a cyclic-prefix is then added at the end of the same block. For $k \in [0, ..., N-1]$ any transmitted symbol from MT p is a vector $\mathbf{C}_p^T S_{k,p}$ with size $K \times 1$; this is roughly equivalent to have K diversity replicas of $S_{k,p}$.

Since each k-th symbol takes K channel realizations at the frequency domain for any lth transmission from MT p, where $0 < l \leq L$ and $L = \max_{l \leq R_C+1}\{\vartheta_l > 0\} + 1$, the channel realizations are depicted as

$$\mathbf{H}_{k,p}^{(l)\,\dagger} = \left[H_{k,p}^{(1,l)\dagger}, H_{k,p}^{(2,l)\dagger}, \ldots, H_{k,p}^{(K,l)\dagger} \right]. \tag{5.1}$$

For the sake of simplicity of subsequent mathematical operations, as in [SD06],

$$\mathbf{H}_{k,p}^{(l)\,\ddagger} = \left[H_{k,p}^{(1,l)\dagger} C_{1,p}, \ldots, H_{k,p}^{(K,l)\dagger} C_{K,p} \right], \tag{5.2}$$

where the total channel realizations for the spread symbol transmissions are

$$\mathbf{H}_{k,p}^{C} = \left[\mathbf{H}_{k,p}^{(1)\,\ddagger}, \ldots, \mathbf{H}_{k,p}^{(L)\ddagger} \right]^T. \tag{5.3}$$

Note that for any MT p that is in the lth H-ARQ stage, its channel realizations $\left[\mathbf{H}_{k,p}^{(l+1)\,\ddagger}, \ldots, \mathbf{H}_{k,p}^{(L)\ddagger} \right]$ are nil, since MT p has only retransmitted l copies.

The channel noise at the BS at the frequency domain for an lth transmission is

$$\mathbf{N}_{k}^{(l)\ddagger} = \left[N_{k}^{(1,l)}, \ldots, N_{k}^{(K,l)} \right]. \tag{5.4}$$

Grouping the channel realizations from all $P = \sum_{l=0}^{L} \vartheta_l$ MTs, results $\mathbf{H}_k^C = \left[\mathbf{H}_{k,1}^C, \ldots, \mathbf{H}_{k,P}^C \right]^T$.

The received signals at the frequency domain at the BS are $\left[\mathbf{Y}_0^C, \ldots, \mathbf{Y}_{N-1}^C \right]$, where

$$\mathbf{Y}_k^C = \left[\mathbf{Y}_k^{(1)\ddagger}, \ldots, \mathbf{Y}_k^{(L)\ddagger} \right]^T, \tag{5.5}$$

while the channel noise is $\mathbf{N}_k^C = \left[\mathbf{N}_k^{(0)\ddagger}, \ldots, \mathbf{N}_k^{(L)\ddagger} \right]^T$. So

$$\mathbf{Y}_k^C \;\; = \;\; \mathbf{H}_k^{C^T} \mathbf{S}_k + \mathbf{N}_k^C. \tag{5.6}$$

5.3 Receiver Design and Performance Analysis

This section extends the IB-DFE receiver design from chapter 3, under the same assumptions, for a QPSK modulation.

Regarding the IB-DFE receiver operation, it decodes the received data packets in an iterative manner, removing channel noise and interference between users up to N_{iter} iterations. The de-spreading operation, as in [SD06, DS06b], is already implicit within the IB-DFE receiver, since the receiver already works with the spread channel realizations and the estimates of the received symbols that are based on the same realizations. Even though the presented receiver removes errors based on MMSE estimation, it does not completely orthogonalize the MTs signals (especially for the first iteration); as a consequence of the iterative nature of the presented receiver, the Inter-Chip Interference (ICI) is diminished for subsequent iterations.

The IB-DFE receiver works with all transmissions that are on-going up to the current slot, where with the aid of the feedforward coefficients and feedback coefficients it diminishes channel interference and residual MAI. In addition, for a severely dispersive channel with rich multipath propagation, the receiver design does not consider the interleaving and de-interleaving of data bits since decision errors do not have a bursty nature.

An estimated data symbol from MT p at the output of the IB-DFE receiver for iteration $i < N_{iter}$ is

$$\tilde{S}_{k,p}^{(i)} = \left({}^{C}\mathbf{F}_{k,p}^{(i)} \right)^{T} \mathbf{Y}_{k}^{C} - {\mathbf{B}_{k,p}^{(i)}}^{T} \bar{\mathbf{S}}_{k}^{(i-1)}, \tag{5.7}$$

where for a given number of transmissions $L = \max_{l \leq R_C+1}\{\vartheta_l > 0\} + 1$,

$$\left({}^{C}\mathbf{F}_{k,p}^{(i)} \right)^{T} = \left[{}^{(i)}\mathbf{F}_{k,p}^{(1)}, \ldots, {}^{(i)}\mathbf{F}_{k,p}^{(L)} \right] \tag{5.8}$$

are the feedforward coefficients used to remove channel interference, where

$${}^{(i)}\mathbf{F}_{k,p}^{(l)} = \left[{}^{(i)}F_{k,p}^{(1,l)}, \ldots, {}^{(i)}F_{k,p}^{(K,l)} \right]. \tag{5.9}$$

and ${\mathbf{B}_{k,p}^{(i)}}^{T} = \left[B_{k,p}^{(i,1)}, \ldots, B_{k,p}^{(i,P)} \right]$ are the feedback coefficients that remove the residual interference for $P = \sum_{r=0}^{R_C} \vartheta_r$ contending MTs.

$\bar{\mathbf{S}}_{k}^{(i-1)} = \left[\bar{S}_{k,1}^{(i-1)}, \ldots, \bar{S}_{k,P}^{(i-1)} \right]^{T}$ are the soft decision estimates from the previous iteration for all users. $\bar{\mathbf{S}}_{k}^{(i-1)}$ can be related to the symbols' hard decisions, $\hat{\mathbf{S}}_{k}^{(i-1)}$, where

$$\bar{\mathbf{S}}_{k}^{(i-1)} \simeq \mathbf{P}^{(i-1)} \hat{\mathbf{S}}_{k}^{(i-1)}, \tag{5.10a}$$

$$\hat{\mathbf{S}}_{k}^{(i-1)} = \mathbf{P}^{(i-1)} \mathbf{S}_{k} + \mathbf{\Delta}_{k}, \tag{5.10b}$$

as in chapter 3. Furthermore, $\mathbf{P}^{(i-1)} = diag\left(\rho_1^{(i-1)}, \ldots, \rho_P^{(i-1)} \right)$ is the correlation matrix and $\mathbf{\Delta}_k = \left[\Delta_k^{(1)}, \ldots, \Delta_k^{(P)} \right]^{T}$ is a zero mean error vector that is independent from the $\mathbf{S}_k$ vector. It should be noted that the soft decision estimates are calculated this way, since by considering severely time dispersive channels with multipath propagation, the error bursts overlap themselves, which leads to an equivalent Gaussian noise without a clear bursty nature. For the first iteration, i.e. $i = 1$, $\bar{\mathbf{S}}_{k}^{(i-1)}$ is a null vector and

$\mathbf{P}^{(i-1)}$ is a null matrix.

Assuming that $\mathbf{R}_S$, $\mathbf{R}_N$ and $\mathbf{R}_\Delta$, are respectively, the correlation of $\mathbf{S}_k$, $\mathbf{N}_k^C$ and $\mathbf{\Delta}_k$, and considering that σ_S^2 is the symbol's variance and σ_N^2 is the noise variance then as in chapter 3 results

$$\mathbf{R}_S = \mathbb{E}\left[\mathbf{S}_k \mathbf{S}_k^H\right] = 2\sigma_S^2 \mathbf{I}_P, \tag{5.11a}$$

$$\mathbf{R}_N = \mathbb{E}\left[\mathbf{N}_k^C \mathbf{N}_k^{C\,H}\right] = 2\sigma_N^2 \mathbf{I}_{L\times K}, \tag{5.11b}$$

$$\mathbf{R}_\Delta = \mathbb{E}\left[\mathbf{\Delta}_k \mathbf{\Delta}_k^H\right] \simeq 2\sigma_S^2 \left(\mathbf{I}_P - \mathbf{P}^{(i-1)} \mathbf{P}^{(i-1)^T}\right). \tag{5.11c}$$

To compute the optimum feedforward and feedback coefficients of the IB-DFE receiver scheme, based on the MMSE results

$$\alpha_{k,p}^{(i)} = {}^C\mathbf{F}_{k,p}^{(i)} \mathbf{H}_k^{C^T} - \mathbf{B}_{k,p}^{(i)} \mathbf{P}^{(i-1)} \mathbf{P}^{(i-1)^T} - \mathbf{\Gamma}_p, \tag{5.12a}$$

$$\beta_{k,p}^{(i)} = \mathbf{B}_{k,p}^{(i)^T} \mathbf{P}^{(i-1)}, \tag{5.12b}$$

where $\mathbf{\Gamma}_p$ is a $P \times 1$ vector filled with zeros except at the p-th position, with a single one. Assuming that $\vec{0}_{1\times p}$ is a $1 \times p$ vector filled with zeros, then

$$\mathbf{\Gamma}_p = \left[\vec{0}_{1\times(p-1)}, 1, \vec{0}_{1\times(P-p)}\right]^T. \tag{5.13}$$

The MSE of $S_{k,p}$ for an i-th iteration is

$$\begin{aligned} \mathbb{E}\left[\left|S_{k,p} - \tilde{S}_{k,p}^{(i)}\right|^2\right] &= \alpha_{k,p}^{(i)^*} \mathbf{R}_S \alpha_{k,p}^{(i)^T} + \left({}^C\mathbf{F}_{k,p}^{(i)}\right)^H \mathbf{R}_N \, {}^C\mathbf{F}_{k,p}^{(i)} + \\ &\quad \beta_{k,p}^{(i)^*} \mathbf{R}_\Delta \beta_{k,p}^{(i)^T}. \end{aligned} \tag{5.14}$$

To minimize the MSE, the optimal coefficients ${}^C\mathbf{F}_{k,p}^{(i)}$ and $\mathbf{B}_{k,p}^{(i)}$ must be computed, so the MSE is subjected to $\gamma_p^{(i)} = \frac{1}{N}\sum_{k=0}^{N-1}\sum_{l=1}^{L}\sum_{n=1}^{K} {}^{(i)}F_{k,p}^{(n,l)} H_{k,p}^{(n,l)\,\dagger} C_{n,p} = 1$, which is formally equivalent to the gradient of the Lagrange function applied to (5.14), where $\mathcal{L}_{k,p}^{(i)} = \mathbb{E}\left[\left|S_{k,p} - \tilde{S}_{k,p}^{(i)}\right|^2\right] + \left(\gamma_p^{(i)} - 1\right)\lambda_p^{(i)}$. Therefore the gradient operation is applied to $\mathcal{L}_{k,p}^{(i)}$ where

$$\nabla \mathcal{L}_{k,p}^{(i)} = \nabla\left(\mathbb{E}\left[\left|S_{k,p} - \tilde{S}_{k,p}^{(i)}\right|^2\right] + \left(\gamma_p^{(i)} - 1\right)\lambda_p^{(i)}\right), \tag{5.15}$$

Evaluating the following set of equations

$$\begin{cases} \nabla_{{}^C\mathbf{F}_{k,p}^{(i)}} \mathcal{L} = 0 \\ \nabla_{\mathbf{B}_{k,p}^{(i)}} \mathcal{L} = 0 \\ \nabla_{\lambda_p^{(i)}} \mathcal{L} = 0 \end{cases}, \tag{5.16}$$

after some mathematical calculus $\nabla_{{}^{C}\mathbf{F}_{k,p}^{(i)}}\mathcal{L}=0$ is

$$\mathbf{H}_k^{C\,H}\mathbf{R}_S\mathbf{H}_k^C\left({}^{C}\mathbf{F}_{k,p}^{(i)}\right)-\mathbf{H}_k^{C\,H}\mathbf{R}_S\mathbf{P}^{(i-1)}\mathbf{P}^{(i-1)^T}\mathbf{B}_{k,p}^{(i)}-\mathbf{H}_k^{C\,H}\mathbf{R}_S+ \\ +\mathbf{R}_N\,{}^{C}\mathbf{F}_{k,p}^{(i)}+\frac{1}{N}\mathbf{H}_k^{C\,H}\lambda_p^{(i)}\mathbf{\Gamma}_p=0, \tag{5.17}$$

$\nabla_{\mathbf{B}_{k,p}^{(i)}}\mathcal{L}=0$ is

$$\left(\mathbf{P}^{(i-1)}\mathbf{P}^{(i-1)^T}\mathbf{R}_S+\mathbf{R}_\Delta\right)\mathbf{B}_{k,p}^{(i)}=\mathbf{R}_S\mathbf{H}_k^C\left({}^{C}\mathbf{F}_{k,p}^{(i)}\right)-\mathbf{R}_S\mathbf{\Gamma}_p, \tag{5.18}$$

and $\nabla_{\lambda_p^{(i)}}\mathcal{L}$ is $\gamma_p^{(i)}=1$. So the optimal coefficients are

$$\begin{cases}\mathbf{B}_{k,p}^{(i)}=\mathbf{H}_k^C\left({}^{C}\mathbf{F}_{k,p}^{(i)}\right)-\mathbf{\Gamma}_p \\ {}^{C}\mathbf{F}_{k,p}^{(i)}=\mathbf{\Lambda}_{k,p}^{(i)}\mathbf{H}_k^{C\,H}\mathbf{\Theta}_{k,p}^{(i)}\end{cases}. \tag{5.19}$$

$\mathbf{\Lambda}_{k,p}^{(i)}=\left(\mathbf{H}_k^{C\,H}\left(\mathbf{I}_P-\mathbf{P}^{(i-1)}\mathbf{P}^{(i-1)^T}\right)\mathbf{H}_k^C+\frac{\sigma_N^2}{\sigma_S^2}\mathbf{I}_{L\times K}\right)^{-1}$ and $\mathbf{\Theta}_{k,p}^{(i)}=\left(\mathbf{I}_P-\mathbf{P}^{(i-1)}\mathbf{P}^{(i-1)^T}\right)\mathbf{\Gamma}_p-\frac{\lambda_p^{(i)}}{2\sigma_S^2N}\mathbf{\Gamma}_p$.

From (5.14), and using the optimal ${}^{C}\mathbf{F}_{k,p}^{(i)}$ and $\mathbf{B}_{k,p}^{(i)}$ coefficients from (5.19), it is possible to compute the MMSE. Defining

$$\sigma_p^{2(i)}=\frac{1}{N^2}\sum_{k=0}^{N-1}\mathbb{E}\left[\left|S_{k,p}-\tilde{S}_{k,p}^{(i)}\right|^2\right], \tag{5.20}$$

and the Gaussian error function, $Q(x)$, the BER of user p at the ith iteration for a QPSK constellation is

$$BER_p^{(i)}\simeq Q\left(\frac{1}{\sigma_p{}^{(i)}}\right). \tag{5.21}$$

Since a severely time dispersive channel with multipath propagation is being considered, bit errors can be considered independent, therefore for an uncoded system with independent and isolated errors, the PER for a fixed packet size of M bits is

$$PER_p^{(i)}\simeq 1-\left(1-BER_p^{(i)}\right)^M. \tag{5.22}$$

5.4 DTMC Access Model

The current section describes the DTMC model based on the assumptions of section 5.2. For this model it is assumed a network of J MTs that transmit data to a single BS, and that the spreading sequences that the MTs use are enough for all of them (i.e. $K\geq J$ without any method to decrease the number of MTs simultaneously accessing the medium such as random contention mechanisms). MTs transmit data according to a *Poisson* distribution with rate λ. The BS is able to store up to (R_C+1) transmissions from all MTs, otherwise it drops all packet copies from any MT whose data is retransmitted R_C times and still cannot recover its content, or in the occasion of a successful reception. It is also assumed that MTs are able to store an infinite number of packets in their queues. In addition, it is assumed that the BS decodes data packets for a maximum number of iterations, N_{iter} - this information is omitted in the paragraphs below for the sake of simplicity of the DTMC model.

5.4.1 Steady-state Probability Distribution

Throughout this chapter the binomial Probability Density Function (PDF) is defined as $f_b(J,x,p) = \binom{J}{x}p^x(1-p)^{N-x}$. Since a severely time-dispersive channel with rich multipath propagation is considered, channel errors can be considered independent for each channel realization, therefore the use of the binomial PDF is valid under these circumstances. It should be noted that a highly variable channel that has a high multipath diversity brings non-negligible influence on the received power in terms of power fluctuations at the BS, therefore the channel barely influences channel errors from block-to-block transmission.

The system state for a given slot, $\chi \in \Omega$, is defined by a collection of random values

$$\chi = \{\chi_e, \chi_0, \chi_1, \ldots, \chi_{R_C}\};$$

χ_e stands for the random variable of the number of idle MTs and χ_l, $l \in [0, R_C]$, for the random variable of the number of MTs in the lth H-ARQ stage in a slot. The state space of χ is defined by the values $\vartheta = \{I, \vartheta_0, \vartheta_1, ..., \vartheta_{R_C}\}$, where I and ϑ_l, $l \in [0, R_C]$, are respectively the values of the number of idle MTs (where $\chi_e = I$) and transmitting MTs at the lth H-ARQ stage (where $\chi_l = \vartheta_l$); these values are conditioned by the number of MTs that are registered within the BS area, J, where $I + \sum_{l=0}^{R_C} \vartheta_l = J$.

So, the universe of system states, assuming that $\emptyset$ represents a non-existing one, can be described by

$$\Omega = \left\{\emptyset, \left\{\chi_e = I, \chi_0 = \vartheta_0, \chi_1 = \vartheta_1, \ldots, \chi_{R_C} = \vartheta_{R_C}; \left(\{I, \vartheta_l\} \in \mathbb{N}_{[0,J]}, l \in [0, R_C], I + \sum_{l=0}^{R_C} \vartheta_l = J\right)\right\}\right\}. \tag{5.23}$$

As an example, a state with J idle MTs can be described as $\chi = \{\chi_e = J, \chi_0 = 0, \ldots, \chi_{R_C} = 0\}$. From the aforementioned χ state, if n MTs out of J have a packet to transmit, then χ will be described as $\chi = \{\chi_e = J - n, \chi_0 = n, \chi_1 = 0, \ldots, \chi_{R_C} = 0\}$. The new system state can fork to several others, where for example: all MTs transmit with success and go back to the initial state ($\chi = \{\chi_e = J, \chi_0 = 0, \ldots, \chi_{R_C} = 0\}$); all MTs transmit with success but transmit a new packet at the following slot ($\chi = \{\chi_e = J - n, \chi_0 = n, \ldots, \chi_{R_C} = 0\}$); n_1 MTs fail to transmit a packet while the remaining MTs $n - n_1$ go back to the idle state ($\chi = \{\chi_e = J - n_1, \chi_0 = 0, \chi_1 = n_1, \ldots, \chi_{R_C} = 0\}$); etc..

A random process $\{\chi^1, \chi^2, ..., \chi^n\}, \forall n \epsilon \mathbb{N}$, can be defined, where $\chi^n \in \Omega$ and $\chi^n = \vartheta^n \equiv \{\chi_e^n = I^n, \chi_0^n = \vartheta_0^n, \chi_1^n = \vartheta_1^n, ..., \chi_R^n = \vartheta_{R_C}^n\}$. Assuming that $p_{err}^l(\vartheta^n)$ is the average packet error rate of the MTs at the lth H-ARQ stage at slot n, computed from equation (5.22), the probability that ϑ_{l+1}^{n+1} MTs from the l-th H-ARQ stage transit to the $(l+1)$-th stage at the following slot is

$$\mathbb{P}\left[\chi_{l+1}^{n+1} = \vartheta_{l+1}^{n+1} | \chi^n = \vartheta^n\right] = f_b\left(\vartheta_l^n, \vartheta_{l+1}^{n+1}, p_{err}^l\left(\vartheta^n\right)\right), 0 < l \leq R_C, \vartheta_{l+1}^{n+1} \leq \vartheta_l^n. \tag{5.24}$$

In addition, assuming that p_{QE}^C is the probability of a MT having an empty queue, the probability that there will be I^{n+1} idle MTs considering that there are I^n idle MTs; $\vartheta_{R_C}^n$ MTs at the last H-ARQ stage; and $\sum_{l=0}^{R_C-1}\left(\vartheta_l^n - \vartheta_{l+1}^{n+1}\right)$ successfully received packets is

$$\mathbb{P}\left[\chi_e^{n+1} = I^{n+1} | \chi^n = \vartheta^n\right] = f_b\left(I^n + \vartheta_{R_C}^n + \sum_{l=0}^{R_C-1}\left(\vartheta_l^n - \vartheta_{l+1}^{n+1}\right), I^{n+1}, p_{QE}^C\right), \forall l, \vartheta_{l+1}^{n+1} \leq \vartheta_l^n. \tag{5.25}$$

Based on the last two equations, the state transition probability can be described as

$$\mathbb{P}\left[\chi^{n+1}=\vartheta^{n+1}|\chi^{n}=\vartheta^{n}\right]= \tag{5.26}$$
$$\begin{cases} 0, \quad \text{if} \quad \vartheta_{l+1}^{n+1}>\vartheta_{l}^{n}, \text{for } 0<l\leq R_C-1 \\ \left(\prod_{l=0}^{R_C-1} f_b\left(\vartheta_l^n,\vartheta_{l+1}^{n+1},p_{err}^{l}\left(\vartheta^n\right)\right)\right)\times f_b\left(I^n+\vartheta_{R_C}^n+\sum_{l=0}^{R_C-1}\left(\vartheta_l^n-\vartheta_{l+1}^{n+1}\right),I^{n+1},p_{QE}^{C}\right), \\ \qquad\qquad\qquad\qquad\qquad\qquad\qquad\qquad\qquad\qquad\qquad\qquad \text{otherwise.} \end{cases}$$

For a *Poisson* rate λ, the p_{QE}^{C} probability can be computed with the following approximation from [Tak62]

$$p_{QE}^{C}\approx 1-min\left(\lambda\mathbb{E}\left[N_{sys}^{C}\right],1\right), \tag{5.27}$$

where $\mathbb{E}\left[N_{sys}^{C}\right]$ is the expected number of packet transmissions whose calculus is referred below in equation (5.28). Assuming Tx as the number of retransmissions for a given packet, then

$$\mathbb{E}\left[N_{sys}^{C}\right]=\sum_{l'=1}^{R_C+1} l'\times\mathbb{P}\left[Tx=l'-1|Tx\geq 0\right], \tag{5.28}$$

$\mathbb{P}\left[Tx=l|Tx\geq 0\right]$ is the probability of retransmitting a packet l times, conditioned by the fact that there is at least one transmission, where $\mathbb{P}\left[Tx=l|Tx\geq 0\right]=\frac{\Xi(l)}{\Upsilon}$ and

$$\Xi(l)=\begin{cases} \sum_{\forall\vartheta^n\in\Omega,\vartheta_l^n>0}\mathbb{P}\left[\chi^n=\vartheta^n\right]\sum_{k=1}^{\vartheta_l^n} k\times f_b(\vartheta_l^n,k,1-p_{err}^{l}(\vartheta^n)) & \text{if} \quad l<R_C \\ \sum_{\forall\vartheta^n\in\Omega,\vartheta_{R_C-1}^n>0}\mathbb{P}\left[\chi^n=\vartheta^n\right]\sum_{k=1}^{\vartheta_{R_C-1}^n} k\times f_b(\vartheta_{R_C-1}^n,k,p_{err}^{R_C-1}(\vartheta^n)) & \text{if} \quad l=R_C \end{cases}; \tag{5.29}$$

$$\Upsilon=\sum_{l=0}^{R_C}\Xi(l). \tag{5.30}$$

The second order moment, $\mathbb{E}\left[{N_{sys}^{C}}^2\right]$, can be computed in a similar way with l'^2 in (5.28).

Based on the aforementioned expressions, the steady-state probability distribution is computed below in equation (5.31).

$$\pi_\chi=\mathbb{P}\left[\chi\right]=\lim_{n\to\infty}\mathbb{P}\left[\chi^n=\chi\right]. \tag{5.31}$$

The steady-state distribution is independent of the first state, χ^0, and can be computed in an iterative manner using (5.26).

5.4.2 Delay

The mean packet delay, $\mathbb{E}\left[\mathcal{D}^C\right]$, can be computed, based on the *Pollaczek-Khinchine* formula from [Tak62] for infinite queues, where

$$\mathbb{E}\left[\mathcal{D}^C\right]=\mathbb{E}\left[N_{sys}^{C}\right]+\frac{\lambda\mathbb{E}\left[{N_{sys}^{C}}^2\right]}{2p_{QE}^{C}}. \tag{5.32}$$

5.4.3 Average Throughput

The average throughput per MT, S, can be obtained based on the system's steady-state probability distribution, as the ratio of the number of successful packet receptions over the average number of transmissions from all MTs. Denoting $\mathbb{1}$ as the indicator function then

$$S \approx \frac{1}{J \times \mathbb{E}\left[N_{sys}^{C}\right]} \sum_{\forall \vartheta \in \Omega} \mathbb{P}\left[\chi = \vartheta\right] \sum_{l=0}^{R_C} \mathbb{1}_{\vartheta_l > 0} \sum_{k=1}^{\vartheta_l} k \times f_b\left(\vartheta_l, k, 1 - p_{err}^{l}(\vartheta)\right) \tag{5.33}$$

5.4.4 Success Rate

The system's success rate, p_{suc}^{C}, i.e. the probability of transmitting data with success until the last R_C H-ARQ stage, can be computed based on the system's steady-state probability distribution as the complementary ratio of the failed transmitted packets over the number of transmitting MTs, where

$$p_{suc}^{C} = 1 - \frac{\sum_{\forall \vartheta \in \Omega \wedge (\vartheta_R > 0)} \mathbb{P}\left[\chi = \vartheta\right] \times \sum_{k=1}^{\vartheta_R} k \times f_b\left(\vartheta_R, k, p_{err}^{R_C}(\chi)\right)}{\sum_{\forall \vartheta \in \Omega} \mathbb{P}\left[\chi = \vartheta\right] \sum_{l=0 \wedge (\vartheta_l > 0)}^{R_C} \vartheta_l} \tag{5.34}$$

5.4.5 Energy per Useful Packet

The EPUP, Φ^C, can be obtained as shown in section 4.2.2. Assuming that the energy from the electrical circuitry is negligible for long distances as verified in section 4.4, then

$$E_p \approx (1 + \beta_T) G_1 d^{\kappa} M_l M E_b. \tag{5.35}$$

So based on the expected number of packet transmissions to successfully deliver a packet, $\mathcal{N}^C = \frac{\mathbb{E}\left[N_{sys}^{C}\right]}{p_{suc}^{C}}$, using (5.28) and (5.34), Φ^C can be computed as

$$\Phi^C = \mathcal{N}^C \times E_p = \frac{\mathbb{E}\left[N_{sys}^{C}\right] E_p}{p_{suc}^{C}}. \tag{5.36}$$

5.5 Performance Results

Table 5.1: Channel & Transmission Parameters

Description	Parameter
Channel Multipath components	64
Spacing between components	Symbol-Spaced
Fading type	Uncorrelated Rayleigh fading per path and per user channel
Number of packet symbols	256
Constellation	QPSK
Symbol transmission time	4μs
Spreading sequence technique	Walsh-Hadamard

The results throughout this section's figures use lines as the model's results and markers as the respective simulations; results were obtained using the *MATLAB* software [Mat11]. A severely time dispersive channel was considered, with rich multipath propagation and uncorrelated Rayleigh fading for each path and user, but with channel correlation between each packet retransmission. Table 5.1 describes the

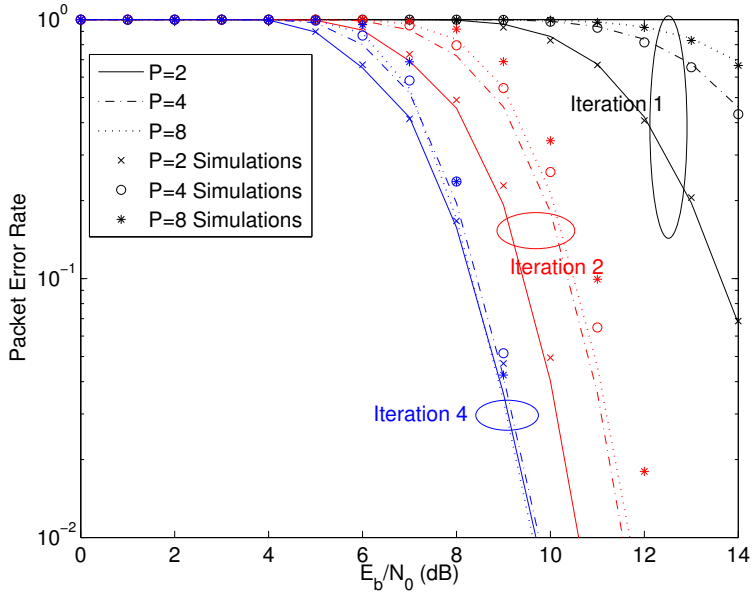

Figure 5.2: IB-DFE receiver PER performance for a single transmission, where $P = [2, 4, 8]$, with $K = P$.

channel parameters used in this section. To cope with channel correlation for each retransmission, the SP technique from section 3.3 was considered, where each retransmitted block has a different cyclic shift.

Terminals scattered inside the BS coverage area transmit uncoded data blocks with $N = 256$ symbols selected from a QPSK constellation for a transmission time of $4\mu s$. As a remark, the presented results only show spreading factors $K = [2, 4, 8]$ for simplicity purposes due to the receiver complexity and respective simulations' time. The presented results are general and their conclusions can be applied to any spreading factor, as long as the simulations conditions are accordingly scaled. In addition the EPUP results are multiplied by $(1/E_p) \times (E_b/N_0)$ to remove any dependencies on the distance, path loss, antenna parameters (see (5.35)), and to show the variation of Φ^C with DS-CDMA and DC H-ARQ configuration parameters, taking solely in consideration the average power received at the BS.

5.5.1 Receiver Performance

The current section presents PER results of the IB-DFE receiver constrained to a given bit energy, E_b, over the noise, N_0, ratio. Figure 5.2 presents the IB-DFE PER receiver performance for $P = [2, 4, 8]$ MTs for a single transmission and $N_{iter} = 1, 2, 4$ iterations, where $K = P$. The system model is accurate, although it is noticeable that for an increasing number of MTs and iterations there is a slight mismatch between the simulations and the model, showing that the receiver model is optimistic. In terms of performance, the IB-DFE receiver design performs well for an increasing number of iterations, since the system PER is considerably diminished. Carefully observing the results at the fourth iteration, the PER is almost the same for any number of MTs up to eight, even though the channel noise is higher for an increasing number of MTs. This demonstrates how good the IB-DFE technique is for a high number of iterations even if the channel is overloaded with a high number of users; the IB-DFE technique is able to effectively remove the MAI with a high number of users. Furthermore, for a PER of 10^{-1}, the IB-DFE technique can save at least 6dB in terms of transmission power for a single transmission.

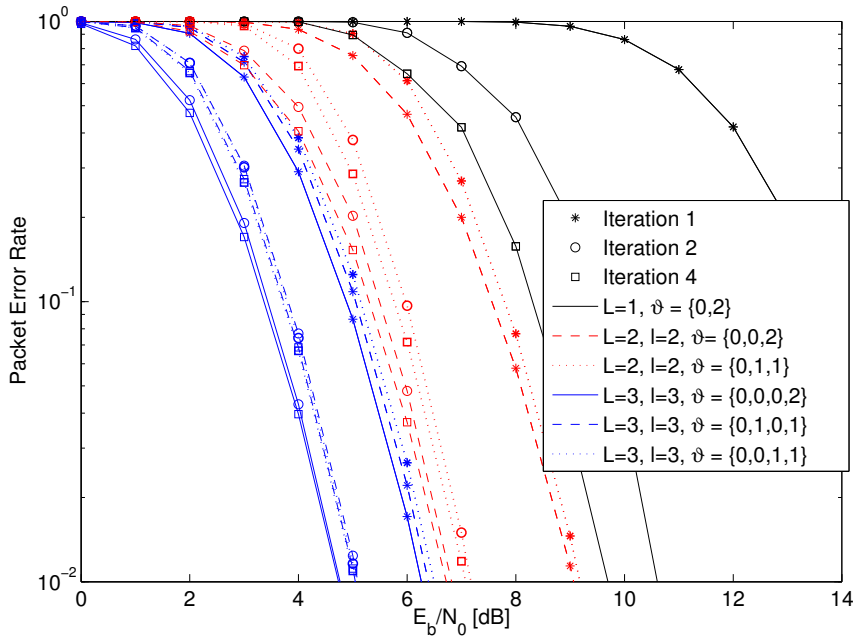

Figure 5.3: IB-DFE receiver PER performance for two MTs, with $K = 2$, contending the channel up to $L = 3$ transmissions under various simulation scenarios.

Figure 5.3 presents the IB-DFE PER receiver performance, up to $N_{iter} = 4$ iterations, for a scenario of $P = 2$ MTs sending data to a BS and up to $L = 3$ transmissions, i.e. with two additional H-ARQ retransmissions. The l variable stands for the $(l-1)$-th H-ARQ stage. $\vartheta = \{0, 2\}$ stands for two MTs with only one transmission; $\vartheta = \{0, 0, 2\}$, for two MTs with two transmissions; $\vartheta = \{0, 0, 0, 2\}$ for two MTs with three transmissions; $\vartheta = \{0, 1, 1\}$ for one MT with two transmissions and another one with only one; $\vartheta = \{0, 1, 0, 1\}$ for one MT with three transmissions and another one with only one; $\vartheta = \{0, 0, 1, 1\}$ for one MT with three transmissions and another one with only two. For any ϑ scenario, the IB-DFE PER performance is improved for each succeeding iteration, demonstrating the receiver's feasibility for lower E_b/N_0 values. For an increasing number of packet transmissions the receiver's PER performance is also improved due to the additional diversity when several packets are combined, showing that for an increasing number of transmissions the required E_b/N_0 to transmit a packet lowers; the combination of packets through DC H-ARQ increases the available energy of a given packet copy, requiring smaller E_b/N_0 values for succeeding transmissions. The DC H-ARQ effect allows greater gains in terms of the E_b/N_0 for succeeding transmissions where the feedforward coefficients of the IB-DFE receiver help to diminish channel interference; on succeeding iterations there is a smaller gain in terms of the E_b/N_0 ratio, especially due to the feedback coefficients that diminish the residual MAI.

5.5.2 Wireless Access: Variable E_b/N_0

The results in this section present the wireless access performance for a variable range of E_b/N_0, with $J = [2, 4]$ MTs, $K = J$, and a fixed data rate of $\lambda J = 0.4$ packets/slot, although there is one figure at the end of this section which considers a saturated load (i.e. $p_{QE}^{C} = 0$, there is always a packet in a MT's queue to transmit).

Figure 5.4 illustrates the necessary number of average transmissions to deliver a packet up to $R_C = 2$ H-ARQ retransmissions for $N_{iter} = 4$ and $\lambda J = 0.4$ packets/slot. There is a perfect match between these values, demonstrating the accuracy of the model. Regarding the performance of the H-ARQ DS-CDMA

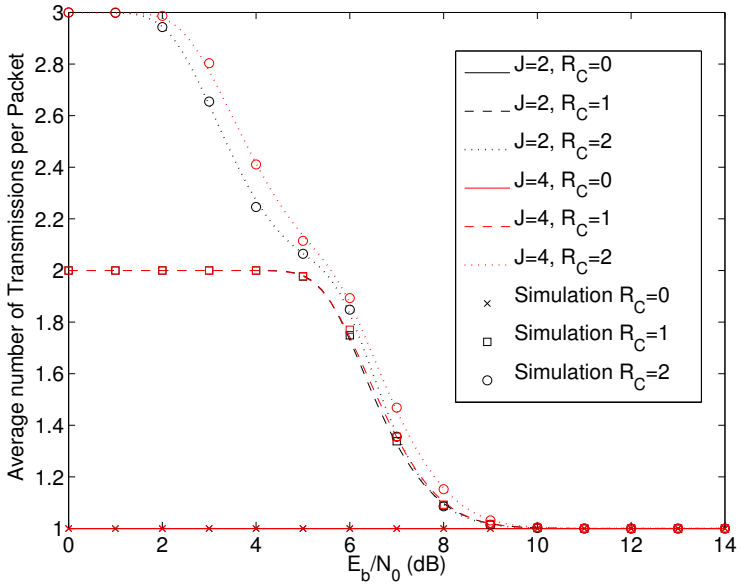

Figure 5.4: Average number of transmissions for $J = [2, 4]$ MTs, considering an H-ARQ scenario up to two additional retransmissions and $\lambda J = 0.4$.

system, as the number of allowed H-ARQ transmissions increases the required E_b/N_0 to transmit a packet for a succeeding retransmission is lower. Comparing the values between $J = 2$ MTs and $J = 4$ MTs it is observable that the required number of transmissions is higher for $J = 4$ MTs due to the additional interference between MTs.

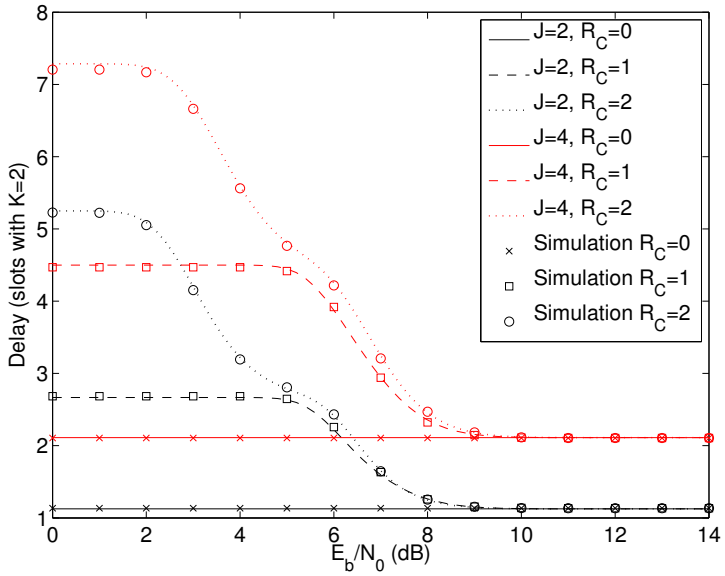

Figure 5.5: System delay for $J = [2, 4]$ MTs, considering an H-ARQ scenario up to two additional retransmissions and $\lambda J = 0.4$.

Figure 5.5 displays the system delay for $J = [2, 4]$ MTs, with a system load of $\lambda J = 0.4$ packets/slot for $N_{iter} = 4$ iterations and up to $R_C = 2$ H-ARQ retransmissions. For fairness reasons, the delay results were normalized to the slot duration for $K = 2$. The simulations and model's results are close to each other, showing the accuracy of the proposed system model. As expected, the system delay

does increase for lower E_b/N_0 up to a lower bound that meets the maximum number of retransmissions. E_b/N_0 values below this bound lead to a higher PER, though the delay remains constant given that the failed packets are dropped. The delay also increases with a higher number of H-ARQ transmissions that ensure the correct packet reception at the BS. Furthermore, it is also noticeable that a higher number of MTs introduces a higher delay because of the increased slot size.

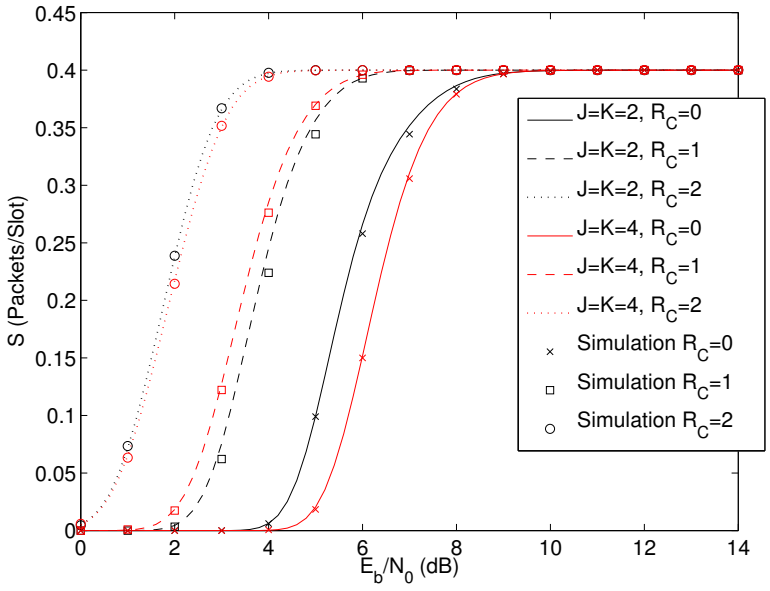

Figure 5.6: System throughput for $J = [2, 4]$ MTs, considering an H-ARQ scenario up to two additional retransmissions and $\lambda J = 0.4$.

Figure 5.6 demonstrates the system throughput for $J = [2, 4]$ MTs, with a system load of $\lambda J = 0.4$ packets/slot for $N_{iter} = 4$ iterations and up to $R_C = 2$ H-ARQ retransmissions. The system model performs well, although there is a slight mismatch between the simulations and the model's results, the system model can be observed as optimistic. Concerning the system performance, for an increasing number of transmissions, the H-ARQ behavior enhances the system throughput, decreasing the necessary E_b/N_0 ratio to attain a given system throughput for a fixed data rate; this way MTs, independently of the system delay, can save their batteries for a higher number of transmissions. For $R_C = 0$ and $R_C = 2$ retransmissions, the system throughput for $J = 4$ MTs is lower than for $J = 2$, mostly because the interference for $J = 4$ MTs does not allow higher throughput gains; this difference would be more evident if the number of iterations of the IB-DFE receiver was smaller.

Figure 5.7 demonstrates the saturated system throughput for $Q = [2, 4]$ MTs for $N_{iter} = 4$ iterations and up to $R_C = 2$ H-ARQ retransmissions. Once more the model results are very close to the simulation results. Concerning the system performance, for an increasing number of transmissions, the H-ARQ behavior enhances the system throughput, decreasing the necessary E_b/N_0 ratio to attain a given throughput value. It also shows that the system throughput for $J = 4$ is usually higher when compared to $J = 2$. However, without additional retransmissions, the system throughput for $J = 4$ is lower when compared to $J = 2$ for $E_b/N_0 \leq 7$ dB, which could be explained by the fact that without H-ARQ the additional redundancy from a spreading factor $K = 4$ does not introduce a significant gain to overturn the channel interference of four simultaneous MTs; another reason would be that the number of iterations is not enough to diminish the channel interference.

Figure 5.8 illustrates the necessary energy to transmit a packet with success (Φ^C), where $J = [2, 4]$

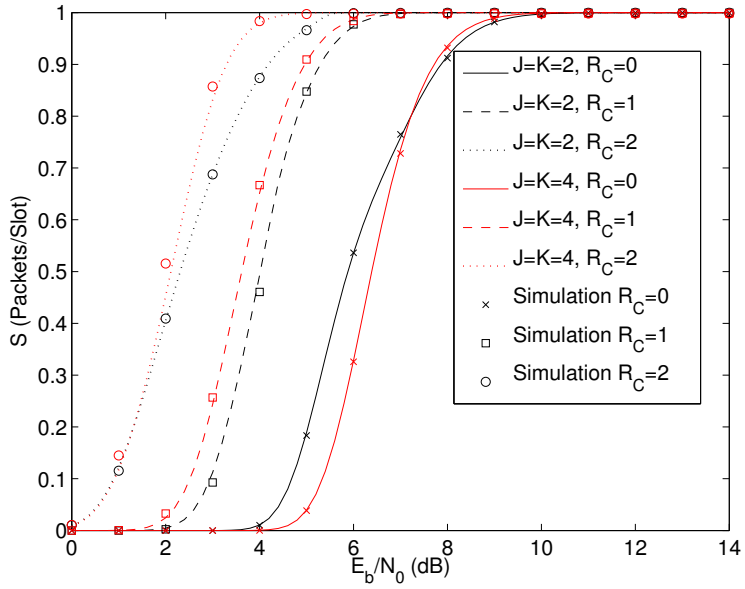

Figure 5.7: Saturated system throughput for $J = [2, 4]$ MTs, considering an H-ARQ scenario up to two additional retransmissions.

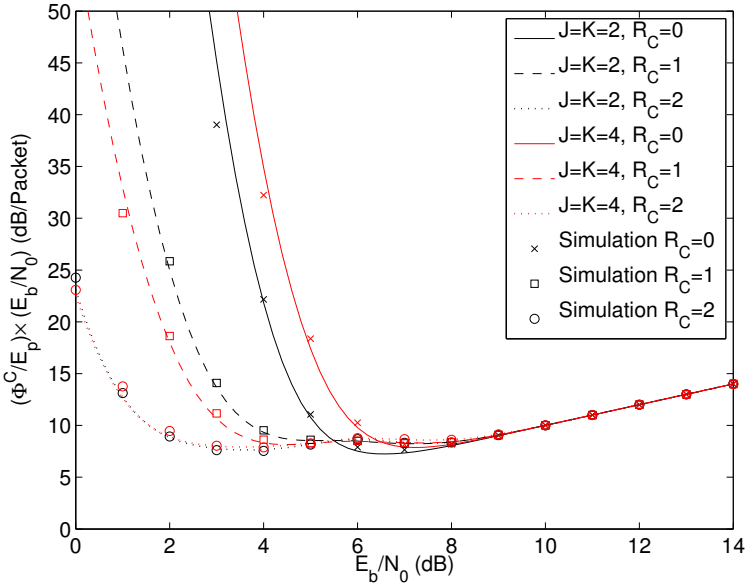

Figure 5.8: A MT's EPUP, Φ^C, for $J = [2, 4]$ MTs, considering an H-ARQ scenario up to two additional retransmissions and $\lambda J = 0.4$.

MTs, $N_{iter} = 4$, $\lambda J = 0.4$ packets/slot and up to $R_C = 2$ H-ARQ retransmissions. The system model performs well, although there is a slight mismatch between the simulations and the model's results. For an increasing number of H-ARQ transmissions it is noticeable that Φ^C diminishes for lower E_b/N_0 values, except for $E_b/N_0 =]5, 8[$ dB, although it is possible to attain a lower Φ^C value as the number of H-ARQ transmissions increases. For $E_b/N_0 =]5, 8[$ dB, the higher packet transmission energy is compensated by the associated PER decrease, which reduces the number of packet transmissions required to have a successful reception. Furthermore this plot shows that in general the higher the number of packets combined, the lower the E_b/N_0 per packet is needed, since the individual energy of

each packet transmission contributes for a better IB-DFE output estimation.

5.5.3 Wireless Access: Variable Load

The results in this section present the wireless access performance for a variable range of the system load for $J = [2, 4]$ MTs, $K = J$ and $E_b/N_0 = [0, 4, 6, 8]$ dB. Although, the results for $E_b/N_0 = 0$ dB account for a null throughput ($PER_p^{(i)} \approx 1$), these are presented in terms of the average number of transmissions and the system delay.

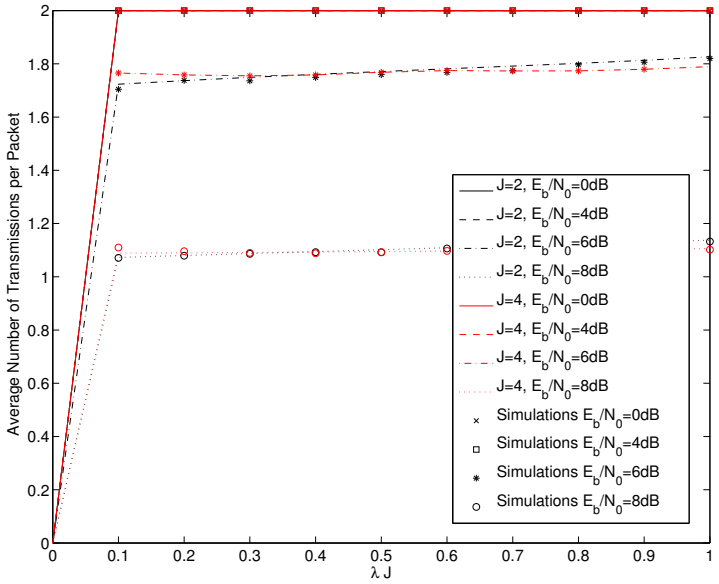

Figure 5.9: Average number of transmissions for $J = [2, 4]$ MTs, considering an H-ARQ scenario for one additional retransmission and $E_b/N_0 = [0, 4, 6, 8]$ dB.

Figure 5.9 portrays the average number of transmissions per packet according to a variable range of the system load for $E_b/N_0 = [0, 4, 6, 8]$ dB, $J = [2, 4]$ MTs and up to $R_C = 1$ H-ARQ retransmission. As observed, the model performance matches the simulations results. Regarding the MAC performance and as expected, the average number of transmissions increases as the system load increases. It is also observed that the number of average transmissions decreases as E_b/N_0 increases. The performance for both $J = 2$ MTs and $J = 4$ MTs is slightly the same, although the system performance is more sensible to the load variation with lower J values. The results of $E_b/N_0 = 0$dB and $E_b/N_0 = 4$ dB are almost the same since the system reached the maximum number of retransmissions. An higher number of MTs, or a higher system load, or a lower E_b/N_0 contribute to a higher number of system transmissions to deliver a packet with success, where the first two (the number of MTs and the system load) contribute with a higher MAI while the last one (E_b/N_0) contributes with a higher channel interference.

Figure 5.10 portrays the average delay per packet according to a variable range of the system load for $E_b/N_0 = [0, 4, 6, 8]$ dB, $Q = [2, 4]$ MTs and $R_C = 1$ H-ARQ retransmission. Once again, the delay results are scaled according to a common denominator of $K = 2$ slots. The model performance almost matches the simulation results. Regarding the MAC performance, the average delay increases as the system load increases; the delay also increases as E_b/N_0 decreases. It can be observed that the system is saturated (infinite delay) for $J = 2$ MTs for $E_b/N_0 = 0$dB, as well as for an E_b/N_0 of 4 dB and 6 dB when the system

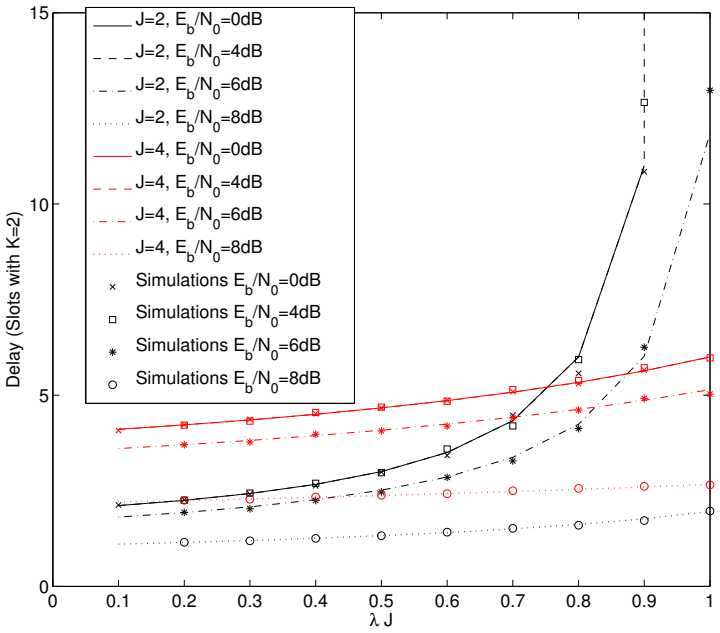

Figure 5.10: Average system delay for $J = [2, 4]$ MTs, considering an H-ARQ scenario for one additional retransmission and $E_b/N_0 = [0, 4, 6, 8]$ dB.

load is higher than 0.9 for $J = 2$. However, the system does not saturate for $J = 4$ MTs because the individual MTs load is halved when compared to $J = 2$ MTs with the same total load. Therefore, for a given total load regarding a K spreading sequence, saturation is less likely to occur for a larger number of MTs. On the other hand, since the system delay is scaled up for $K = J = 4$ the slot duration is larger for higher J, leading to longer effective delays for unsaturated conditions. Furthermore, the same conclusions from the previous figure also apply in this one where a higher number of MTs, or a higher system load, or a lower E_b/N_0 contribute to a higher delay, since there is a higher MAI and/or higher channel interference.

Figure 5.11 portrays the system throughput according to a variable range of the system load for $E_b/N_0 = [4, 6, 8]$ dB, $J = [2, 4]$ MTs and $R_C = 1$ H-ARQ retransmission. The model performance almost matches the simulation results. Regarding the system performance, the throughput follows the system load while the number of transmissions is below the maximum number of retransmissions, after that, it has a slow linear increase due to the PER - to prevent such effect from happening an higher R_C would have to be used for $J = 2$ MTs and $E_b/N_0 = 4$dB. As expected the throughput also increases as E_b/N_0 increases. The throughput performance of $J = 4$ MTs is practically the same as $J = 2$ MTs for $E_b/N_0 \geq 6$ dB since the E_b/N_0 ratio is more than enough to transmit a packet with success.

Figure 5.12 portrays the EPUP according to a variable range of the system load for $E_b/N_0 = [4, 6, 8]$ dB, $J = [2, 4]$ MTs and $R_C = 1$ H-ARQ retransmission. The model performance has similar results against the simulation results, however the model cannot faithfully portrait the simulation results for higher load rates, low E_b/N_0 and J values. As for the system performance, the EPUP does increase for higher load rates, but not vertiginously; as expected it also increases for lower E_b/N_0 values. Looking in-depth at the figure, the system has a lower EPUP for $J = 4$ MTs, since the number of packets per MT is lower than for $J = 2$ MTs, therefore having less interference per each slot access. In general it is plausible to assume that the EPUP is not greatly affected by the system load for a small number of MTs, allowing a

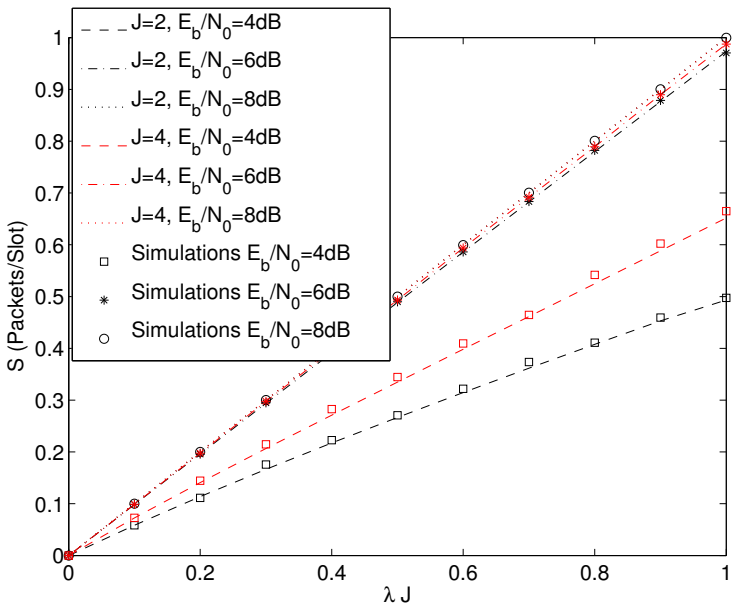

Figure 5.11: System throughput for $J = [2, 4]$ MTs, considering an H-ARQ scenario for one additional retransmission and $E_b/N_0 = [4, 6, 8]$ dB.

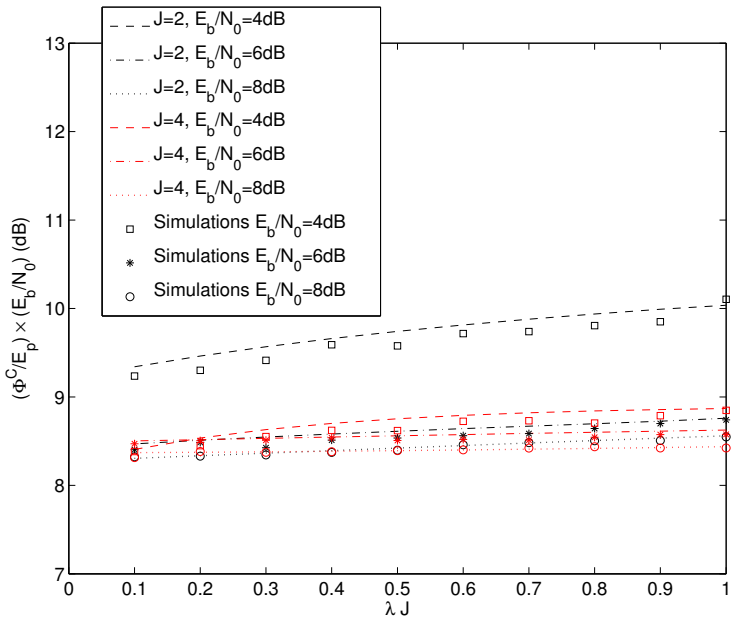

Figure 5.12: EPUP for $J = [2, 4]$ MTs, considering an H-ARQ scenario for one additional retransmission and $E_b/N_0 = [4, 6, 8]$ dB.

greater degree of freedom to adjust the QoS parameters.

5.6 Conclusions

This chapter proposed a wireless PHY-MAC DC prefix-assisted DS-CDMA model, based on an IB-DFE receiver design, that accounts the MTs channel interference and channel noise simultaneously. The

wireless access was characterized with DTMC, where the delay, throughput and EPUP were extracted. The model exhibits high accuracy when compared against the simulation values. Results show that the H-ARQ prefix-assisted DS-CDMA system with IB-DFE has a good performance when compared with a DS-CDMA system without H-ARQ interference cancellation schemes. Energy efficiency is improved for a higher number of allowed retransmissions, enabling the fulfilling of delay and throughput requirements for lower E_b/N_0, thus with a lower retransmission power. It is also shown the influence of the spreading factor (and the number of concurrent transmissions), which increases the average delay, but makes the system more tolerable to higher loads.

Chapter 6

H-ARQ Network Diversity Multiple Access

6.1 Introduction

A MUD technique can be helpful in decoding data packets from different MTs accessing the channel, where the signals associated to a sequence of multiple collisions can be used to separate the packets - assuming that the MAC layer is aware of such PHY layer capability. In the case of NDMA, the protocol forces all users involved in a collision of P packets to retransmit their packets $P-1$ times; the P transmissions are required to effectively separate the colliding packets. Originally, NDMA was only suitable for flat-fading channels [TZB00], but it was extended to multi-path time-dispersive channels in [ZT02]. The residual interference levels with the NDMA technique can be high and/or can have significant noise, but can be overcome with the FDE MUD reception scheme from chapter 3.

The NDMA MAC protocol is unfortunately unsuitable for low SNR scenarios. In this chapter, the advantages of having a MAC protocol that can adapt to lower SNR scenarios, using DC H-ARQ, are explored (e.g., due to fading or shadowing effects). H-ARQ techniques are an efficient way to cope with high noise levels, thus achieving higher throughputs at the cost of a higher number of transmissions.

The current chapter applies the H-ARQ concept to NDMA, i.e. instead of only asking for P packets from P MTs, a BS could ask for additional redundancy, where the BS only asks for additional transmissions from packets with errors. The proposed system, in order to work, it must use a MUD receiver - the ones in chapter 3 can be used in this context. In addition, the EPUP model from section 4.2.2 is extended for the NDMA context. In [MV05b] it was verified that NDMA achieves energy efficiency, but the energy model does not consider packet retransmissions for multiple epochs due to errors; there is not an analysis of the optimal transmission conditions to achieve energy efficiency for a given delay and throughput.

The system level performance of DC H-ARQ NDMA, named H-ARQ NDMA (H-NDMA), is analyzed and an analytical model that describes the system's behavior with unsaturated/saturated load is proposed; the throughput and the delay are analyzed for Poisson traffic. The proposed model differs from most of the related work, by studying H-NDMA's impact on energy consumption for a given system load and maximum average delay, as well as considering the importance of packet detection errors, i.e. the mis-detection and/or the false reception of packets. In addition, the optimal load at the BS and the transmission power that minimize the MTs' energy consumption are identified for a given average delay

requirement.

The work presented in this chapter was published in [GPB+11a, GPB+13].

The current chapter is organized as follows: The system overview, including the multi-packet reception technique and the MAC protocol, is presented in section 6.2; the system's performance is analyzed in section 6.3; a set of performance results is presented in section 6.4; and the chapter's conclusions in section 6.5.

6.2 System Characterization

The H-NDMA system characterization is made in this section where section 6.2.1 states the system assumptions and section 6.2.2 describes the protocol operation.

6.2.1 System assumptions

SC-FDE is used at the uplink, where MTs are low resource battery operated devices that send data to the BS, where the latter is a high resource device. To support multiple MTs in the wireless a channel, a MUD receiver should be used; the MUD equalization techniques from chapter 3 can be adopted.

In terms of system assumptions, the system operates with a full-duplex radio where MTs send data packets using the time slots defined by the BS; packets associated to each MT have the same duration. Furthermore, the BS controls the maximum number of MTs, J, using the wireless channel; so the BS detects collisions and uses a broadcast downlink channel to signal them, requesting the involved MTs to resend their packets.

Perfect channel estimation and synchronization between local oscillators, as in previous chapters, is also assumed. For an SC-FDE context, an extended cyclic prefix can be used to absorb residual time-of-arrival errors provided that a good channel estimation exists, as explained in chapter 3. In addition, the IB-DFE technique when well applied, can cancel residual carrier synchronization errors, leading seamlessly to the same performance as MTs with perfect synchronization - also explained in chapter 3.

Furthermore, on a collision event, each data packet in each slot arrives simultaneously, and a perfect average power control and time advance mechanisms exist to compensate different propagation times and attenuations. The assumption of uniform average power at the receiver means that the BS measures the same average E_b/N_0 from all MTs, thus reducing the complexity of the performance analysis.

6.2.2 Medium Access Control Protocol

H-NDMA is a slotted random access protocol with gated access, where the uplink slots are organized as a sequence of epochs. The BS broadcasts a synchronization control packet, SYNC, via the downlink channel setting the beginning of each epoch, allowing any MT with data packets to transmit in the next slot. MTs that do not transmit in the first epoch's slot are forbidden to send data until the end of the epoch.

A BS is capable of discerning all colliding data packets, DATA, using user-specific orthogonal ID sequences. During the first slot of an epoch, the BS detects collisions and uses a broadcast control downlink channel to send a collision signal, requesting all MTs involved to resend their data packets.

When $P > 1$ MTs are involved in the collision, the BS asks for $P - 1$ retransmissions for an effective separation of the P packets. After this initial set of P slots, the BS acknowledges the reception of the data packets, and it may request up to R_N additional retransmissions on an H-ARQ basis, intended for the packets that were received with errors. This request uses an ACK control packet, that is broadcasted via the downlink channel, that defines which MTs should retransmit.

To conduct DC H-ARQ of the received packets, it is assumed that the BS uses a suitable error detection scheme, such as Cyclic Redundancy Check (CRC). The epoch ends when all data packets are correctly received or after $P + R_N$ transmission slots for a collision of P MTs. The SYNC control packet also acknowledges the good reception of the data packets.

Two types of MTs' identification errors are considered in this chapter: detection error or mis-detection error, and false-alarm error. A mis-detection occurs when the BS cannot identify the colliding MTs during the initial slot, therefore ending the epoch after the first slot. A false alarm error happens when noise in the wireless channel is erroneously confused as a MT's signal.

For data reception purposes, the knowledge of the number of MTs that are trying to transmit in a given slot is required, as well as which are transmitting data. In practical applications this information can be obtained with the help of appropriate orthogonal-specific IDs. This information only needs to be transmitted by the MTs once, provided that the MTs are successfully identified. The size of these IDs grows with the number of MTs (the situation can be particularly serious if a channel estimate for each MT is needed [SDSC08]). To reduce the inherent overheads to these IDs the number of MTs that can register to a given slot must be limited, so that the wireless medium is not crowded.

Since the estimation of the MTs involved in a collision is not free of errors, the system model's performance should take into account the associated probability of false alarm p_F (i.e., the probability of assuming that a given MT is trying to transmit in a given slot when it is not) and the mis-detection probability $(1-p_D)$ (i.e., the probability of assuming that a given terminal is not trying to transmit in a given slot when it is trying to transmit). The values of these probabilities can be parametrized by the estimation technique from [SDSC08].

The focus of this chapter only regards the performance of the H-NDMA protocol, therefore the estimation of the p_F and p_D probabilities is not considered. In addition two assumptions were made for the sake of simplicity: it was assumed that when any MT tries to transmit at the beginning of the epoch, if the detection conditions are difficult (e.g. due to a deep fade) it is assumed that the BS cannot decode the transmitted packets; and when MTs do not transmit data, but the BS detects that there is data in the wireless medium from a MT, i.e. false alarm, then the BS asks for another retransmission, where it is assumed that at the second transmission the BS will end the epoch due to inexistent data in the wireless channel.

Figure 6.1 illustrates various cases with the H-NDMA access scheme for $R_N = 1$, where up to $J = 2$ MTs contend for the uplink channel by transmitting data packets right after the reception of a SYNC packet from the BS; the SYNC packet is represented by a dark bar. Slots may be empty, or may have up to two MTs transmitting data. A sequence of seven epochs illustrates the different scenarios that may occur in an epoch: an empty epoch (first slot); epochs two and three show that the H-NDMA behaves like a standard DC H-ARQ scheme when a single MT transmits during an epoch; the last four epochs illustrate MUD scenarios, where two MTs collide in the first slot. The packets may be received after the two initial slots (epochs four and seven), or after an additional slot where one or both MTs transmit (epochs five and six). For an H-ARQ recovery period, the MTs receive the feedback from the previous slot before the beginning of the next slot.

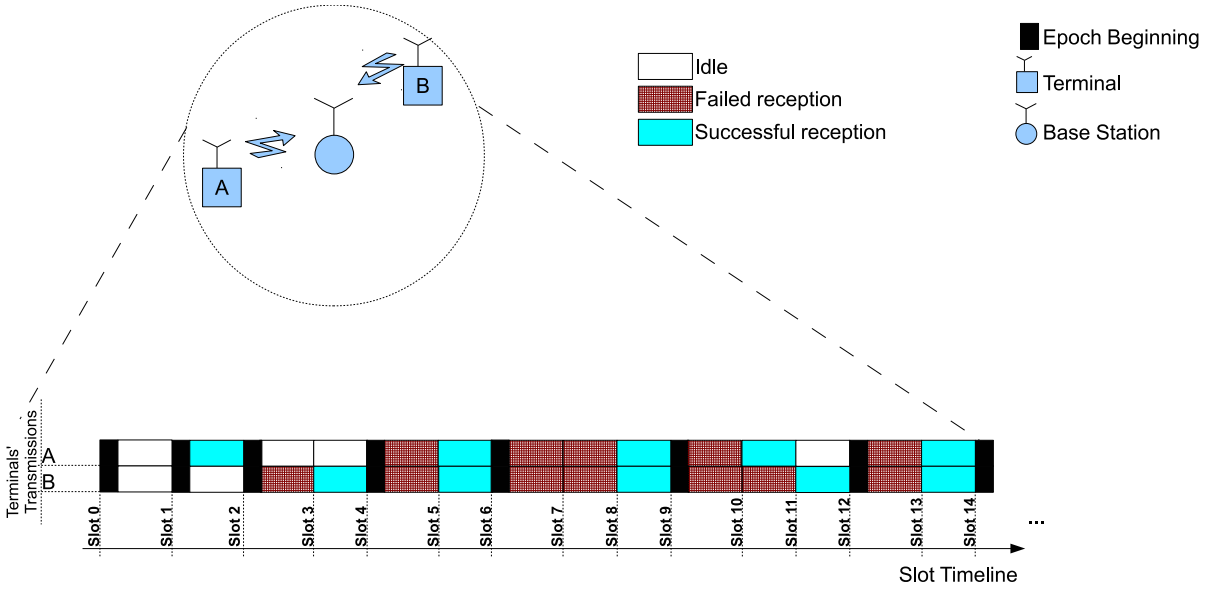

Figure 6.1: H-ARQ NDMA reception scheme.

6.3 Analytical Model

This section studies how the throughput, delay and energy consumption of an H-NDMA system are influenced by the PER, where the following modeling conditions were considered:

a) Finite Population: A finite number of J independent MTs are transmitting one time-unit (slot) long packets to a BS. MTs can store an infinite number of packets.

b) The BS is able to discern up to J colliding packets. So, it is assumed that P MTs access simultaneously the channel and $P \leq J$, for the sake of simplicity.

c) Immediate feedback: By the end of each slot the MTs are immediately informed, without errors at the downlink, of the outcome of the transmission, as in [TZB00] and [YG05].

d) Poisson arrivals: The buffer of each MT receives packets that are generated according to a Poisson source with rate λ.

e) Uniform average power: Perfect power control is assumed, where the average power received from each MT at the BS is equal.

Due to the nature of a full-duplex system communication, no spacing is used between each transmission slot. For the sake of simplicity, the duration of the PHY layer headers on the uplink and of the ACK and SYNC packets on the downlink communication is not considered in the analysis.

6.3.1 Epoch Analysis

The MTs' behavior can be approximately modeled by a sequence of epochs; an epoch can be defined as an empty slot, or a set of two empty slots due to a false alarm or a set of slots where MTs send the same packet due to a BS request. When P MTs access the first slot of an epoch, the BS forces the MTs to consecutively retransmit $P-1$ copies of the packets, except when a mis-detection occurs. A mis-detection leads to a useless epoch lasting a single slot.

When packets are successfully detected, the P packet copies are decoded using a MUD receiver, such as the one in chapter 3. If packets are received with errors at the end of P copies, the BS requests additional packet transmissions in an H-ARQ basis. The BS may ask up to R_N retransmission slots involved during this phase, which will be denoted as an interference cancellation phase.

The system state in an epoch with P MTs accessing the first slot and being correctly detected by the BS could be defined by the last slot that each MT uses, after the initial set of P transmission slots. However, this would produce a large state space, up to $(1+R_N)^P$ states for all possible combinations of ending slots for P MTs. For the particular scenario of this epoch model, with perfect power control that leads to a constant average SNR value for all MTs, the state space dimension can be reduced. It is irrelevant which MTs stopped transmitting; it is easier to model the number of MTs whose packets were successfully received and altogether stopped transmitting at each retransmission slot. Therefore, without detection errors the system state for an epoch up to retransmission slot $l \leq R_N$ is denoted by the vector $\Psi^{(l)} = \{\psi_k^{(l)}, k = 0...l\}$, which defines the number of MTs that stopped transmitting due to successful packet reception at each of the retransmission slots $k = 0, ..., l$ (assuming l slots in the interference cancellation phase, *slot* 0 covers the last slot of the NDMA phase).

The random variables $\psi_k^{(l)}$ satisfy $\sum_{k=0}^{l} \psi_k^{(l)} = P$, for all $l \in [0, R_N]$, since the total number of MTs transmitting during the epoch is equal to P. The state space of $\Psi^{(l)}$, denoted by the set $\Omega_P^{(l)}$, contains all the vector elements $K^{(l)}$ (with dimension $l+1$) that satisfy $\sum_{k=0}^{l} K_k^{(l)} = P$.

Each state $\Psi^{(l)} = \left\{\psi_0^{(l)} = K_0^{(l)}, ..., \psi_l^{(l)} = K_l^{(l)}\right\}$ defines the set of transmission sequences where $K_0^{(l)}$ MTs stopped transmitting after the initial P NDMA slots, $K_1^{(l)}$ MTs stopped transmitting after H-ARQ slot 1, and so on until $K_l^{(l)}$ MTs stopped transmitting at the last H-ARQ slot l. The number of transmission sequences associated to the state value $K^{(l)}$ is equal to the multinomial coefficient value $\frac{P!}{\prod_{k=0}^{l} K_k^{(l)}!}$ [Tau63], which counts the number of MTs combinations for the $K^{(l)}$ vector.

Without mis-detection or false alarm errors, the epoch ends when all packets are correctly received at the BS, or after R_N interference cancellation slots. When R_N interference cancellation slots are needed, the value of $\psi_{R_N}^{(R_N)}$ contains both the successful transmissions and unsuccessful transmissions at slot R_N. The epoch is then characterized by $\Psi^{(R_N)}$. $\Psi^{(0)}$ is constant and equal to P since $l = 0$, which means that all MTs transmitted P times. $\Psi^{(l)}$ is a random vector whose probability mass function depends on the packet error probability of the previous slot.

The probability mass function for $\Psi^{(R_N)}$ can be recursively defined using the probability mass functions of $\Psi^{(l)}$ for $l = 1, ..., R_N$. $\varepsilon_P\left(\Psi^{(l)}\right)$ denotes the average packet error rate at slot l during the H-ARQ interference cancellation phase of an epoch, with P MTs, for a given $\Psi^{(l)} = K^{(l)}$. The average packet error rate value is computed using the analytical models from chapter 3, so depending on the channel response for a given epoch state, results

$$\varepsilon_P\left(\Psi^{(l)}\right) = \frac{1}{P}\sum_{k=1}^{P} PER_k\left(\Psi^{(l)}\right). \tag{6.1}$$

The $(P+l) \times P$ matrix with the channel response, $\mathbf{H}_k$, has coefficients with value zero for the slots of the epoch where the MTs did not transmit. At the end of slot l, MTs with unsuccessful transmissions will try again in slot $l+1$, and MTs with successful transmissions are counted by $\psi_l^{(x)}$ for $x = l+1, ..., R_N$.

The conditional probability mass function for $\psi^{(l+1)}$ given $\psi^{(l)}$ follows

$$\mathbb{P}\left[\Psi^{(l+1)} = \left\{\psi_0^{(l+1)} = K_0^{(l)}, \ldots, \psi_{l-1}^{(l+1)} = K_{l-1}^{(l)}, \psi_l^{(l+1)} = n, \psi_{l+1}^{(l+1)} = K_l^{(l)} - n\right\} \mid \Psi^{(l)} = K^{(l)}\right] = f_b\left(K_l^{(l)}, n, 1 - \varepsilon_P\left(\Psi^{(l)}\right)\right) , \quad (6.2)$$

$\psi_l^{(l+1)} = n \in \left[0, K_l^{(l)}\right]$ represents the number of packets successfully received during slot l. The probability mass function for $\Psi^{(l)}$ can be explicitly written as

$$\mathbb{P}\left[\Psi^{(l)} = K^{(l)}\right] = \frac{P!}{\prod_{n=0}^{l} K_n^{(l)}!} \prod_{j=0}^{l-1} \left(\left(1 - \varepsilon_P\left(\Psi^{(j)}\right)\right) \prod_{i=0}^{j-1} \varepsilon_P\left(\Psi^{(i)}\right)\right)^{K_j^{(l)}} \left(\prod_{i=0}^{l-1} \varepsilon_P\left(\Psi^{(i)}\right)\right)^{K_l^{(l)}} , \quad (6.3)$$

where

$$\psi_j^{(i)} = \begin{cases} \psi_j^{(l)} = K_j^{(l)} & j < i < l \\ \psi_i^{(i)} = \sum_{n=i}^{l} K_n^{(l)} & j = i < l \end{cases} . \quad (6.4)$$

Equation (6.2) can be used to calculate the probabilities for all possible values of $K^{(R)}$ in $\Omega_P^{(R)}$, by running the recursive algorithm in a tree rooted in $K_0^{(0)} = P$, with R layers. For each layer, a node with $K_l^{(l)} = n$ has $(n+1)$ branches in the next sublayer: $\left(K_l^{(l+1)} = 0, K_{l+1}^{(l+1)} = n\right)$ (where reception failed for all packets at retransmission slot l), up to $\left(K_l^{(l+1)} = n, K_{l+1}^{(l+1)} = 0\right)$ (where all packets were successfully received after retransmission slot l). For instance, $K_0^{(0)} = P$ has $(P+1)$ branches: $\left(K_0^{(1)} = 0, K_1^{(1)} = P\right)$, $\left(K_0^{(1)} = 1, K_1^{(1)} = P - 1\right)$, up to $\left(K_0^{(1)} = P, K_1^{(1)} = 0\right)$. The full vector $K^{(R)}$ that corresponds to entire collection of tree branches (i.e. state of $\Omega_P^{(R_N)}$) can be obtained using (6.4).

The maximum number of slots in the H-ARQ interference cancellation phase (R_N parameter) does not define the actual epoch duration; it bounds the maximum epoch duration. The epoch duration is defined by the last slot with a packet transmission, so the epoch duration for state $K^{(R_N)}$ is denoted by

$$\Delta\left(\Psi^{(R_N)} = K^{(R_N)}\right) = \min_l \left\{\forall k > l, \sum_{k=l+1}^{R_N} K_k^{(R_N)} = 0\right\}, \quad (6.5)$$

where $K_{R_N+1}^{(R_N)} = 0$. The n-th order moment of the epoch expected duration with P MTs transmitting without detections errors, $\Delta\left(\Omega_P^{(R_N)}\right)$, can be computed as follows

$$\mathbb{E}\left[\Delta\left(\Omega_P^{(R_N)}\right)^n\right] = 1 - p_D + p_D \left(\sum_{K^{(R_N)} \in \Omega_P^{(R_N)}} \mathbb{P}\left[\Psi^{(R_N)} = K^{(R_N)}\right] \Delta\left(\Psi^{(R_N)}\right)^n\right). \quad (6.6)$$

The expected duration is $\mathbb{E}\left[\Delta\left(\Omega_P^{(R_N)}\right)\right] = \mathbb{E}\left[\Delta\left(\Omega_P^{(R_N)}\right)^1\right]$. The conditional probability of an epoch

duration equal to l given that all P MTs are correctly detected (D_P condition) is

$$\mathbb{P}\left[\Delta\left(\Omega_P^{(R_N)}\right) = l \mid D_P\right] = \sum_{K^{(R_N)} \in \Omega_P^{(R_N)} \mid \Delta\left(\Psi^{(R_N)} = K^{(R_N)}\right) = l} \mathbb{P}\left[\Psi^{(R_N)} = K^{(R_N)}\right]. \tag{6.7}$$

The average number of slots used by a MT to transmit a packet during an epoch where $\Psi^{(R_N)} = K^{(R_N)}$ is $tx\left(\Psi^{(R_N)} = K^{(R_N)}\right) = \sum_{l=0}^{R_N}(1 + \frac{l}{P})K_l^{(R_N)}$. So, the expected number of slots used by a MT to transmit a packet during an epoch with P MTs is denoted by $\mathbb{E}\left[tx\left(\Omega_P^{(R_N)}\right)\right]$. It can be calculated using a Bayesian approach for all $K^{(R_N)}$ in $\Omega_P^{(R_N)}$, assuming all MTs are correctly detected, where

$$\mathbb{E}\left[tx\left(\Omega_P^{(R_N)}\right)\right] = 1 - p_D + p_D\left(\sum_{K^{(R_N)} \in \Omega_P^{(R_N)}} Pr\left\{\Psi^{(R)} = K^{(R_N)}\right\} tx\left(\Psi^{(R_N)} = K^{(R_N)}\right)\right). \tag{6.8}$$

A packet is not correctly received if it is transmitted in all epoch slots and its reception also fails for the last slot, or if the transmission is not detected. Consequently, the expected number of packets received with errors during an epoch where $\Psi^{(R_N)} = K^{(R_N)}$ is $\mathbb{E}\left[err\left(\Psi^{(R_N)} = K^{(R_N)}\right)\right] = K_{R_N}^{(R_N)}\varepsilon_P\left(\Psi^{(R_N)}\right)$.

Assuming that packet failures are independent, the packet error probability for an epoch $\Omega_P^{(R_N)}$ is given by

$$\varepsilon_\Omega\left(\Omega_P^{(R_N)}\right) = 1 - p_D + \frac{p_D}{P}\sum_{K^{(R_N)} \in \Omega_P^{(R_N)}} \mathbb{P}\left[\Psi^{(R_N)} = K^{(R_N)}\right]\mathbb{E}\left[err\left(\Psi^{R_N} = K^{(R_N)}\right)\right]. \tag{6.9}$$

6.3.2 Queue Analysis

The MT's queue behavior can be approximately modeled by a sequence of *relevant epochs*, in which packets belonging to the MT are sent, and *irrelevant epochs*, in which the MT is silent. The number of packets in the buffer at the beginning of each epoch is denoted by q_m, where the subscript m denotes the epoch. The sequence $q_m, q_{m+1}, q_{m+2}, \ldots$ constitutes a Markov Chain. If a packet is always resent, the Markov Chain is defined by

$$q_{m+1} = \begin{cases} v & q_m = 0 \\ q_m - 1 + v & (q_m > 0) \ \wedge \overline{Err} \\ q_m + v & (q_m > 0) \ \wedge \ Err \end{cases}, \tag{6.10}$$

where Err is the packet error event at the end of an epoch and v is the number of packets arriving during the mth epoch ($x \wedge y$ denotes "x AND y" and $\overline{Err}$ denotes NOT Err). As lost packets are resent, the queue length, q_m, is not decreased. An approximate expression for the MT's buffer being empty at the beginning of an epoch can be

$$P_e^N = lim_{m\to\infty}\mathbb{P}\left[q_m = 0\right] \tag{6.11}$$

Assuming that epochs are independent and that errors are uncorrelated with q_m, the number of MTs contending in each epoch, P, can be approximated by the binomial distribution with a transmission probability equal to $(1 - P_e^N)$. Therefore, the packet error probability is

$$\varepsilon_{sys} = \sum_{k=0}^{J-1} f_b\left(J-1, k, 1-P_e^N\right) \varepsilon_\Omega\left(\Omega_{k+1}^{(R)}\right). \tag{6.12}$$

The following lemma, for (6.10), was proved in [DCB+09] and proposed as follows:

Lemma 1. *If the MT's buffer is fed by a Poisson source with rate λ, the probability generating function of q_m in the steady state, $Q(z)$, is given by*

$$Q(z) = \mathbb{E}\left[z^{q_m}\right] = P_e^N \frac{z \times F(z) - (z \times \varepsilon_{sys} + 1 - \varepsilon_{sys}) G(z)}{z - (z \times \varepsilon_{sys} + 1 - \varepsilon_{sys}) G(z)}, \tag{6.13}$$

where $F(z) = \lim_{m\to\infty} E\left[z^v \mid q_m = 0\right]$ and $G(z) = lim_{m\to\infty} E\left[z^v \mid q_m > 0\right]$ are the conditional probability generating functions of the queue length distribution for the irrelevant and relevant epochs, respectively.

Proof. Using (6.10), $Q_{m+1}(z)$ is expressed as

$$\begin{aligned} Q_{m+1}(z) = \mathbb{E}\left[z^{q_{m+1}}\right] = \mathbb{P}\left[q_m = 0\right] \mathbb{E}\left[z^v \mid q_m = 0\right] + \\ \left(1 - \mathbb{P}\left[q_m = 0\right]\right) \left(\left(1-\varepsilon_{sys}\right) z^{-1} + \varepsilon_{sys}\right) \mathbb{E}\left[z^{q_m} \mid q_m > 0\right] \mathbb{E}\left[z^v \mid q_m > 0\right]. \end{aligned} \tag{6.14}$$

Since

$$\mathbb{E}\left[z^v \mid q_m > 0\right] = \frac{\left(\mathbb{E}\left[z^{q_m}\right] - \mathbb{P}\left[q_m = 0\right]\right)}{\left(1 - P_e^N\right)}, \tag{6.15}$$

by letting $m \to \infty$ and using $G(z)$ and $F(z)$ as defined below, as well as solving $Q(z)$, in (6.13), the desired result is achieved. □

The conditional probability generating functions $F(z)$ and $G(z)$ can be calculated for stationary Poisson sources and assuming independence between epochs and MTs errors, where

$$\begin{aligned} G(z) = \sum_{k=0}^{J-1} f_b\left(J-1, k, 1-P_e^N\right) \\ \left(\left(1-p_D\right) e^{\lambda(z-1)} + p_D \sum_{l=0}^{R_N} \mathbb{P}\left[\Delta\left(\Omega_{k+1}^{(R_N)}\right) = l \mid D_{k+1}\right] e^{(k+1+l)\lambda(z-1)}\right), \end{aligned} \tag{6.16}$$

and

$$\begin{aligned} F(z) = \left(\left(1-p_F\right) e^{\lambda(z-1)} + p_F e^{2\lambda(z-1)}\right) {P_e^N}^{J-1} + \sum_{k=1}^{J-1} f_b\left(J-1, k, 1-P_e^N\right) \\ \left(\left(1-p_D\right) e^{\lambda(z-1)} + p_D \sum_{l=0}^{R_N} \mathbb{P}\left[\Delta\left(\Omega_k^{(R_N)}\right) = l \mid D_k\right] e^{(k+l)\lambda(z-1)}\right). \end{aligned} \tag{6.17}$$

It is assumed that a false alarm error during the first slot of an epoch (p_F) is always detected at the second slot of an epoch, producing an irrelevant epoch with a duration of two slots.

Evaluating (6.13) for $z = 1$, a relationship between P_e^N and λ is obtained, which takes into account the

error probability.

Proposition 1. *P_e^N is the solution in [0,1] of*

$$1 - \varepsilon_{sys} - G'(1) - P_e^N \left(1 + F'(1) - \varepsilon_{sys} - G'(1)\right) = 0. \tag{6.18}$$

Proof. Evaluating (6.13) for $z = 1$ and applying *L'Hopital*'s rule, results

$$1 = Q(1) = P_e^N \frac{1 + F'(1) - \varepsilon_{sys} - G'(1)}{1 - \varepsilon_{sys} - G'(1)} \tag{6.19}$$

□

For the H-NDMA system, equation (6.18) can be calculated replacing $G'(1)$ and $F'(1)$ respectively with

$$G'(1) = \lambda \sum_{k=0}^{J-1} f_b\left(J-1, k, 1 - P_e^N\right) \mathbb{E}\left[\Delta\left(\Omega_{k+1}^{(R_N)}\right)\right], \tag{6.20}$$

and

$$F'(1) = \lambda\left(1 + p_F\right) {P_e^N}^{J-1} + \lambda \sum_{k=1}^{J-1} f_b\left(J-1, k, 1 - P_e^N\right) \mathbb{E}\left[\Delta\left(\Omega_k^{(R_N)}\right)\right]. \tag{6.21}$$

Equation (6.18) has at least one solution for $P_e^N \in [0,1]$, since its left part is equal to $-\lambda\left(1 + p_F\right)$ for $P_e^N = 1$ and it is equal to $1 - \varepsilon_{sys} - \lambda \mathbb{E}\left[\Delta\left(\Omega_J^{(R_N)}\right)\right]$ for $P_e^N = 0$, which is positive for a non-saturated system. Note that for $R_N = 0$, $p_D = 1$ and $p_F = 0$, equations (6.16) and (6.17) are reduced to the ones considered in [DCB+09]. This section extends [DCB+09] NDMA results, providing a model for the H-NDMA system.

6.3.3 Throughput Analysis

The throughput is calculated with the ratio of the number of packets received per epoch to the average epoch duration

$$S = \frac{\sum_{k=1}^{J} f_b(J, k, 1 - P_e^N) \sum_{j=1}^{k} j \; f_b\left(k, j, 1 - \varepsilon_\Omega\left(\Omega_k^{(R_N)}\right)\right)}{\left(1 + p_F\right) {P_e^N}^J + \sum_{k=1}^{J} f_b(J, k, 1 - P_e^N) \mathbb{E}\left[\Delta\left(\Omega_k^{(R_N)}\right)\right]}. \tag{6.22}$$

6.3.4 Delay Analysis

The delay of a packet may contain (part of) the duration of an irrelevant epoch, denoted by h_{ir} (it might be the state when the packet arrives to be transmitted), or it can happen that the MT is transmitting other packets at that instant. The analysis also considers the relevant epochs, h_r, necessary to successfully transmit the packet (including previous packets in the queue and lost packets). From the property of M/G/1 queue with vacation [BG92, pp. 194], the average system delay for a data packet is expressed as

$$\mathcal{D} = \overline{h_r} + \frac{\lambda \overline{h_r^2}}{2(1 - \lambda \overline{h_r})} + \frac{\overline{h_{ir}^2}}{2\overline{h_{ir}}}, \tag{6.23}$$

where $\overline{h_r}$ and $\overline{h_r^2}$ are the first and second moments of a relevant epoch's duration, and $\overline{h_{ir}}$ and $\overline{h_{ir}^2}$ are the first and second moments of an irrelevant epoch's duration. The moments of an irrelevant epoch are calculated from (6.17). Using *Little*'s theorem, $\overline{h_{ir}} = F'(1)/\lambda$ and $\overline{h_{ir}^2} = F''(1)/\lambda^2$, where the value of the second derivative of $F(z)$ for $z = 1$ is

$$F''(1) = \lambda^2 \left(1 + 3p_F\right) {P_e^N}^{J-1} + \lambda^2 \sum_{k=1}^{J-1} f_b\left(J-1, k, 1-P_e^N\right) E\left[\Delta\left(\Omega_k^{(R_N)}\right)^2\right]. \tag{6.24}$$

The relevant epochs' moments are

$$\overline{h_r} = \sum_{i=1}^{\infty} i\left(1-\varepsilon_{sys}\right)\left(\varepsilon_{sys}\right)^{i-1}\overline{h_1} = \frac{G'(1)}{\lambda\left(1-\varepsilon_{sys}\right)} \tag{6.25}$$

and

$$\overline{h_r^2} = \sum_{i=1}^{\infty} i^2\left(1-\varepsilon_{sys}\right)\left(\varepsilon_{sys}\right)^{i-1}\overline{h_1^2} = \frac{\left(1+\varepsilon_{sys}\right)G''(1)}{\lambda^2\left(1-\varepsilon_{sys}\right)^2}, \tag{6.26}$$

where $\overline{h_1}$ and $\overline{h_1^2}$ are the first and second moments of a single relevant epoch, and are given by $\overline{h_1} = G'(1)/\lambda$ and $\overline{h_1^2} = G''(1)/\lambda^2$. The value of the second derivative of $G(z)$ for $z = 1$ is

$$G''(1) = \lambda^2 \sum_{k=0}^{J-1} f_b\left(J-1, k, 1-P_e^N\right) \mathbb{E}\left[\Delta\left(\Omega_{k+1}^{(R_N)}\right)^2\right]. \tag{6.27}$$

6.3.5 System Stability

The system is stable when the network utilization for each node, $\rho^N = \lambda\overline{h_r} < 1$. Therefore, the stability condition is defined by $G'(1) < 1 - \varepsilon_{sys}$.

6.3.6 Energy Analysis

MTs transmit packets to the uplink channel, which arrive at the BS with a uniform average reception power due to the use of perfect average power control. The EPUP model for an H-NDMA context is proposed, it only considers the transmission energy and neglects the energy consumption related to electrical circuitry for long distances, based on the same reasoning as in section 5.4.5.

The EPUP, denoted by Φ^N, measures the necessary energy to successfully receive a packet at the BS. Φ^N depends on the expected number of epochs required to correctly receive a packet at the BS, $E\left[N_\Omega\right]$, and on the expected energy consumption during each epoch. In subsection 6.3.2, it was shown that the probability of a MT not having a packet to transmit during an epoch (P_e^N) can be calculated using (6.18) and that the average packet error probability (ε_{sys}) is given by (6.12). Therefore, the average number of epochs to transmit a packet with success is

$$\mathbb{E}\left[N_\Omega\right] = \sum_{k=0}^{\infty}(k+1)\left(\varepsilon_{sys}\right)^k\left(1-\varepsilon_{sys}\right) = \frac{1}{1-\varepsilon_{sys}}\ . \tag{6.28}$$

The average number of slots that a MT uses during an epoch, $E\left[tx_\Omega\right]$, can be calculated using a

Bayesian approach, where the conditional probability for having k MTs transmitting is

$$\mathbb{E}\left[tx_{\Omega}\right] = \sum_{k=1}^{J} \frac{f_b(J,k,1-P_e^N)}{1-f_b(J,0,1-P_e^N)} \mathbb{E}\left[tx\left(\Omega_k^{(R_N)}\right)\right]. \tag{6.29}$$

Finally, the EPUP is given by

$$\Phi^N(J,R,P_e^N) = \mathbb{E}\left[tx_{\Omega}\right]\mathbb{E}\left[N_{\Omega}\right]E_p = \frac{E_p}{1-\varepsilon_{sys}} \sum_{k=1}^{J} \frac{f_b(J,k,1-P_e^N)}{1-f_b(J,0,1-P_e^N)} \mathbb{E}\left[tx\left(\Omega_k^{(R_N)}\right)\right] . \tag{6.30}$$

6.3.7 Transmission Power Tuning

The BS is responsible for defining the average E_b/N_0 value that must be received from all MTs, regardless of their distance to the BS. This subsection proposes a method for the BS to tune the transmission power in such way that it minimizes the individual MTs energy consumption per packet (ignoring the different E_p values required to compensate the different distances and propagation conditions) subject to some working requirements. Only packet errors are considered for the sake of simplicity, i.e. for detection errors purposes only the PER is considered ($1-p_D = p_F = 0$). Therefore, $(1-p_D)$ and (p_F) are not considered.

Analyzing (6.30), it is observable that Φ^N varies with the value of E_b/N_0 and also with the load on the system. Over the range of E_b/N_0 there is a minimum Φ^N, though Φ^N tends to infinity for very low and for very high E_b/N_0 values: for very low E_b/N_0, ε_{sys} tends to one and more packets have to be sent; for very high E_b/N_0 the ε_{sys} is approximately zero, so the increase on transmission power increases Φ^N. For intermediate values of E_b/N_0 the increase on the transmission power can be compensated by a reduction of the error rate (ε_{sys}), or the mean number of packet transmissions ($\mathbb{E}\left[N_{\Omega}\right]\mathbb{E}\left[tx_{\Omega}\right]$). The sensitivity of Φ^N with the increase of the load is not so trivial: for low values of E_b/N_0, MTs are *forced* to transmit packets more times due to populated epochs; for low values of E_b/N_0, ε_{sys} can be reduced for higher loads, because the MUD receiver from chapter 3 is more efficient for a higher number of MTs involved in a collision. In addition, the E_b/N_0 value that minimizes Φ^N may not satisfy the application requirements.

The optimization process at the BS, described below, sets the best E_b/N_0 value for the measured load, complying with a maximum value for the packet delay and the maximum energy level that a MT can use to transmit data. The best value is the one that minimizes Φ^N regarding the system application requirements and conditions.

In terms of energy, if J MTs are considered, the maximum energy the BS can ask from the MTs has to be the lowest energy provided by the *weakest* MT signal received at the BS (note that the distance is also a parameter). Consider $(E_b/N_0)^p|_{P_{max}}$ the average E_b/N_0 value at the BS for MT p transmitting with maximum power. Thus, the maximum possible value for E_b/N_0 that the BS can require is

$$\left(\frac{E_b}{N_0}\right)_{max} = \min\left\{ \left.\frac{E_b}{N_0}^p\right|_{max} \text{ for terminal } p = 1...J \right\} . \tag{6.31}$$

The relation between the value of the E_b/N_0 and the throughput is not straightforward. The optimization procedure has to guarantee that the throughput is enough for the system load and it can never be higher than the saturation throughput, S_{sat}^N, with $P_e^N = 0$ ($S_{sat}^N \geq S = \lambda J$).

So, considering J MTs with a known uniform load λ packets/slot/MT, regarding a uniform E_b/N_0 at the BS, for a maximum delay value ($\mathcal{D} \leq D_{max}$), with the guarantee that the load is served, and using (6.12), (6.18), (6.22), (6.23), and (6.30), the optimization model can be written as

$$\begin{aligned} \text{Minimize:} \quad & \Phi^N \left(\frac{E_b}{N_0} \right) \\ \text{Subject to:} \quad & S \left(\frac{E_b}{N_0} \right) = \lambda J \ , \mathcal{D} \left(\frac{E_b}{N_0} \right) \leq D_{max} \text{ and } \frac{E_b}{N_0} \leq \left(\frac{E_b}{N_0} \right)_{max} . \end{aligned}$$

The optimization process can be implemented by looking for the value of E_b/N_0 that minimizes Φ^N when $S = \lambda J$ for a given J. To reduce the computation time, the implementation uses a two step process: the first step is to lookup over a list of precomputed values of Φ^N and delay for a set of $\{\lambda J,\ E_b/N_0\}$ pairs. If the load is identical to λJ then a pair is selected. If not, the nearest two pairs are selected; the second step implements a search method of the best pairs with fine adjustments to the load, and new calculations of Φ^N and delay - as the function is monotonic this search is bounded in time.

A list of precomputed values forms a coarse grid of $\{\lambda J,\ E_b/N_0\}$ and is used as a fast approximation to the solution with a precision dependent on the step size of the grid. The transmission power used by a given MT, P_t, can then be calculated using (4.4), (4.5) and the MT's channel state information.

For finer adjustments, the BS could introduce idle (sleep) slots. In practical terms, the BS would increase the load on the remaining epochs forcing the system to work at levels where Φ^N would be lower. The process would be similar to the one explained above except that the selected pair in the first step would have a slightly higher load and a lower Φ^N (in this case, the throughput optimization condition would be rewritten to $S \left(\frac{E_b}{N_0} \right) \geq \lambda J$).

6.4 Performance Analysis

The system model performance is analyzed in this section, considering the PER, throughput, energy and delay. A severely time dispersive channel was considered, with rich multipath propagation and uncorrelated Rayleigh fading for each path and user, but with channel correlation between each packet retransmission. Under these conditions, the SP technique for a linear equalization receiver from chapter 3 was considered. MTs scattered inside the BS coverage area transmit uncoded data blocks with $N = 256$ symbols selected from a QPSK constellation for a transmission time of $4\mu s$. Results in this section were obtained with the *MATLAB* software [Mat11].

The analytical values, represented by curves in the figures, were compared with simulations represented by the $\times$, $\square$ and $\circ$ markers; figure 6.13 is the only one without simulation values. The simulation results were averaged from a period of 25000 slots.

Φ^N results are not directly shown but multiplied by $(1/E_p)(E_b/N_0)$. The reason is to remove the dependencies on the distance, path loss and antenna parameters (see (5.35)), and to show the variation of Φ^N with NDMA and H-NDMA configuration parameters, taking solely in consideration the average power received at the BS.

Section 6.4.1 illustrates the H-NDMA performance over E_b/N_0, where the H-NDMA approach is also compared with NDMA; section 6.4.2 presents the performance results of the H-NDMA approach over the network load λJ; section 6.4.3 overviews the H-NDMA performance based on the number of the existing

MTs J that compete for the wireless channel; section 6.4.4 overviews the H-NDMA performance for a variable range of the p_F and p_D probabilities; finally section 6.4.5 analyzes the H-NDMA transmission power tuning performance.

6.4.1 E_b/N_0 Performance Results

The current subsection presents the performance over E_b/N_0, with four MTs and up to $R_N = 4$ retransmissions. All figures related to the MAC performance contain results for ideal and non-ideal detection conditions, i.e. $1 - p_D = p_F = 0$, and $p_D = 0.7$ and $p_F = 0.2$, respectively; in addition the simulated network load for a non-saturated scenario is $\lambda J = 0.4$.

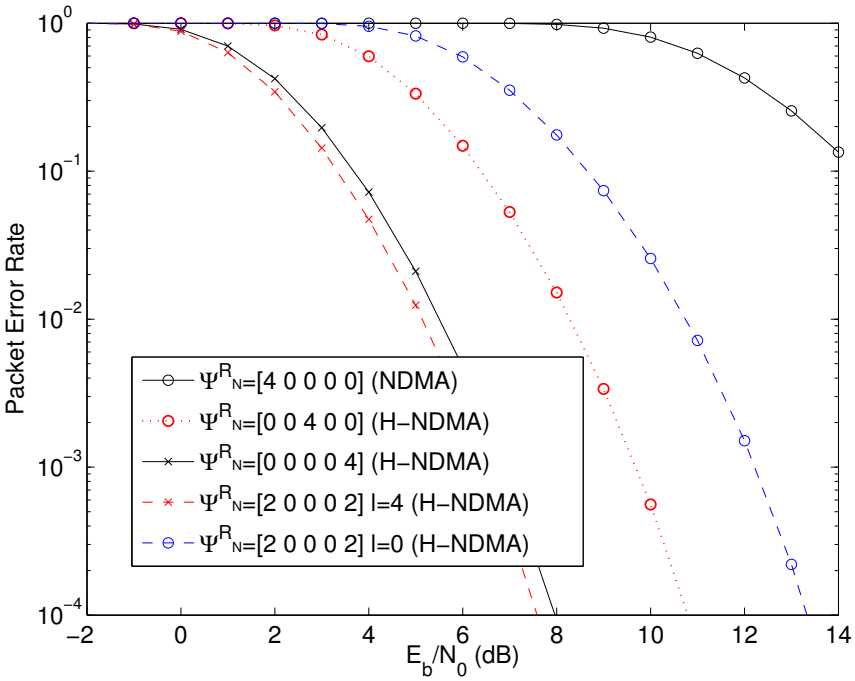

Figure 6.2: Packet Error Rate analytical results over E_b/N_0 for $P = 4$ MTs comparing different Ψ^{R_N} values.

Figure 6.2 reproduces the PER analytical results for $P = 4$ MTs, based on the SC-FDE linear receiver from chapter 3, comparing different Ψ^{R_N} values for $R_N = 4$, where the x-axis is a range of E_b/N_0 values. This figure shows that the H-NDMA protocol introduces a significant average PER gain compared to the classical NDMA protocol (represented by $\Psi^{R_N} = [40000]$) where all MTs only transmit during the four NDMA slots. It also shows that when only two MTs transmit during the four additional slots due to errors (for $\Psi^{R_N} = [20002]$, $l = 4$), the average PER for those MTs is slightly better than for the case of all four MTs transmitting their packets eight times ($\Psi^{R_N} = [00004]$), since the existing interference is inferior. Therefore, the H-NDMA approach performs better than the NDMA approach for all P packets involved in a collision.

To understand the maximum achievable throughput with this system, a saturated wireless network was considered for figure 6.3, where MTs always have a packet to transmit (i.e. $P_e^N = 0$). The analytical model follows the same pattern as the simulation values in this figure, though the model is fairly optimistic for an increasing number of transmissions. The throughput increments for higher R_N values when $E_b/N_0 < 11$dB, where the incremental step becomes smaller for bigger R_N. The throughput S for

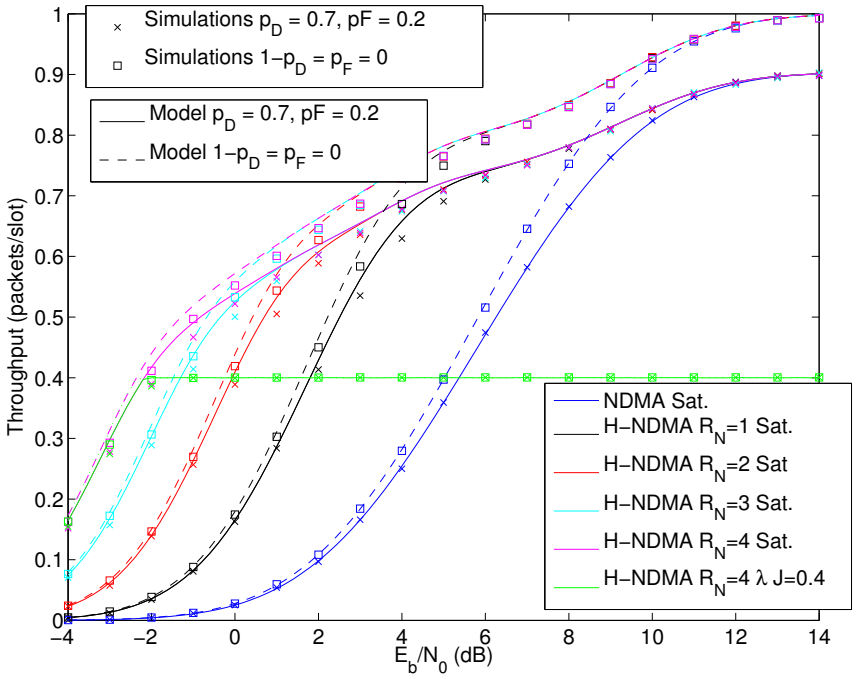

Figure 6.3: Throughput over E_b/N_0 for $J = 4$ MTs comparing saturation with different R_N values and non-saturation scenario.

$\lambda J = 0.4$ packets/slot is also represented, showing that S is equal to 0.4. Note that for $E_b/N_0 < -1$dB the system is already saturated. It is visible that the introduction of additional transmissions enhances the system reception performance and hence the throughput of the system. Additionally, the results for non-ideal detection conditions, i.e. $p_D = 0.7$ and $p_F = 0.2$, show a slight degradation compared to $(1 - p_D) = p_F = 0$. The variation is much lower than for $(1 - p_D) = 0$ due to the short duration of the epochs with detection errors. The p_F value is irrelevant, since there are no idle slots in saturation.

Figure 6.4 depicts the average packet delay using (6.23). The analytical model performs fairly better with $1 - p_D = p_F = 0$ than with $p_D = 0.7$ and $p_F = 0.2$, when compared to the simulation results. The analytical model could be considered pessimistic for non-ideal detection conditions. The figure shows that with a total network utilization of 40% the H-NDMA improves the delay for $E_b/N_0 < 14$dB. For $R_N = 4$ it is even possible to have an average delay below 30 slots for $E_b/N_0 \leq 1$dB. Delay is not influenced by R_N for $E_b/N_0 > 14$dB. These results are explained by the fact that on severe channel conditions, the use of additional transmissions improves the success of receiving packets without errors and therefore improving the system delay. The figure also shows the combined effect of $p_F = 0.2$ introducing longer irrelevant epochs along with $p_D = 0.7$ leading to slightly longer delays for non-ideal detection conditions.

Figure 6.5 depicts the average $(\Phi^N/E_p)(E_b/N_0)$ using (6.30). The analytical results are approximately the same as the simulation values, though the model is slightly optimistic for $R_N = 0$ and $E_b/N_0 > 6$dB. The figure shows that a higher R_N value never degrades the Φ^N for the same network conditions: it either improves when the additional retransmissions reduce the PER (e.g. for $E_b/N_0 = 0$dB), or maintains it (e.g. $R_N = 4$ follows $R_N = 2$ for $E_b/N_0 \geq 10$dB). The use of H-NDMA has the great benefit of combining the energy of several transmissions without requiring additional transmission power from the MTs. These results also show that under non-ideal conditions such as $p_D = 0.7$ and $p_F = 0.2$ the Φ^N performance is quite similar to ideal detection conditions, i.e. $(1 - p_D) = p_F = 0$. This figure

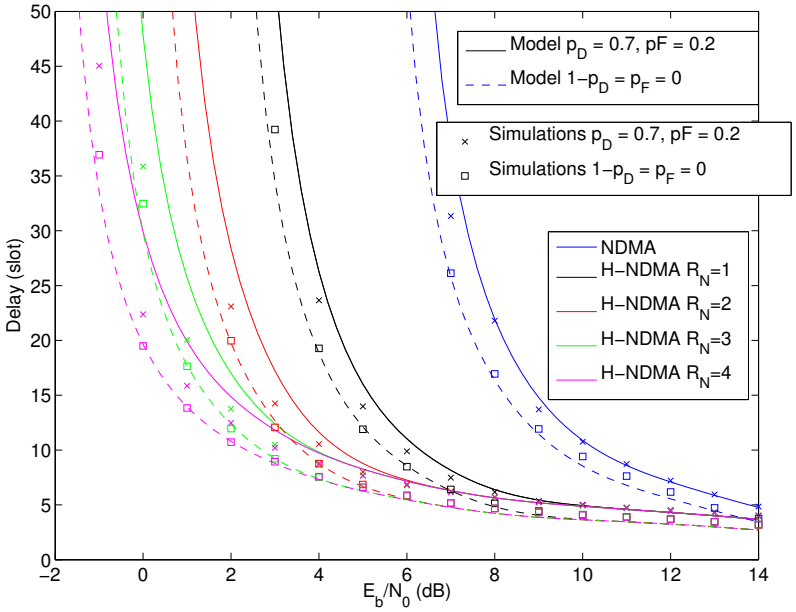

Figure 6.4: Delay over E_b/N_0 for J=4 MTs and $\lambda J = 0.4$ packets/slot comparing different R_N values.

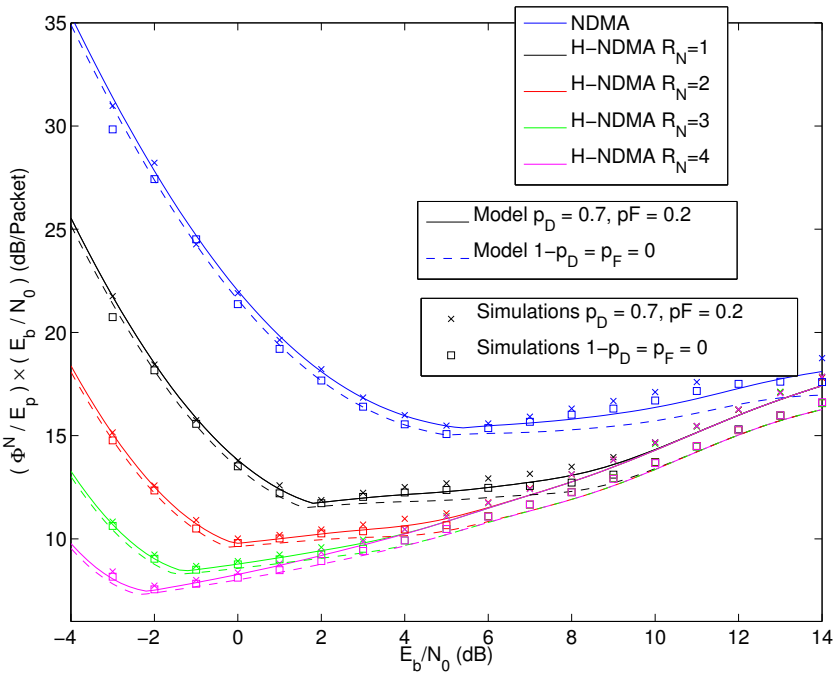

Figure 6.5: $(\Phi^N/E_p) \times E_b/N_0)$ over E_b/N_0 for J=4 MTs and $\lambda J = 0.4$ packets/slot comparing different R_N values.

illustrates the variation of Φ^N for a constant load, showing that it exhibits a minimum value, which can be found using the process described in section 6.3.7. Note that the delay in figure 6.4 must be taken into consideration to provide a lower E_b/N_0 bound. These results confirm that H-NDMA outperforms NDMA by allowing an higher redundancy of retransmissions (R_N).

6.4.2 Network Load Performance Results

The current subsection presents the performance over the network load λJ, with four MTs, $R_N = 4$ retransmissions and values of E_b/N_0 between -2dB and 4dB. All figures contain results for ideal and non-ideal detection conditions, i.e. $(1 - p_D) = p_F = 0$, and $p_D = 0.7$ and $p_F = 0.2$, respectively.

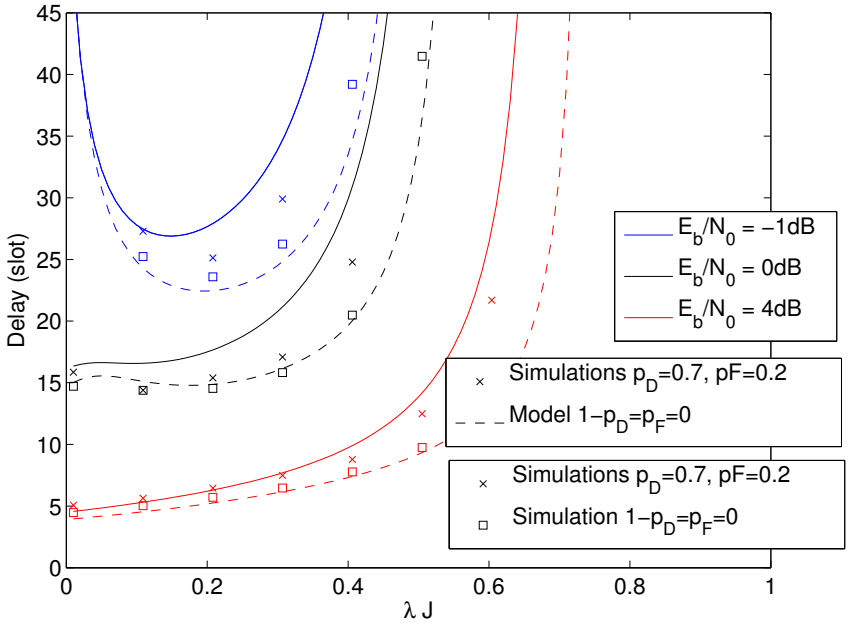

Figure 6.6: System delay versus the network utilization with $J = 4$, $R_N = 4$ and different E_b/N_0.

Figure 6.6 shows the total packet delay that includes transmissions in several consecutive epochs until the successful reception of the packet at the BS. The analytical results are close to the simulation values under ideal transmission conditions, i.e. $(1-p_D) = p_F = 0$, making the model slightly optimistic. For non-ideal conditions, where $p_D = 0.7$ and $p_F = 0.2$, the model has a visible deviation and underestimates the simulations' results.

For $E_b/N_0 = -1$dB and $(1 - p_D) = p_F = 0$, the delay decreases for a network utilization up to about 20%. Therefore, for low E_b/N_0, the delay can be reduced by slightly increasing the network utilization. The reason is that the conditions are so poor that more retransmissions are needed. For slightly higher loads, more MTs transmit in average per slot, producing up to $J + R_N$ transmissions per packet (when J MTs transmit in an epoch) and therefore the performance of the MUD mechanism improves with extra competing packets, which leads to a reduction of the overall delay. An higher R_N would generate the same effect, but R_N is bounded by complexity or delay restrictions. In conclusion, this effect happens for very low E_b/N_0 values. Above 20% of the network utilization, especially for $E_b/N_0 = -1$dB, there is a higher delay since the MUD technique cannot decode the receiving packets, mostly due to the poor propagation conditions with a high number of competing MTs. This same reasoning applies for the remaining curves of the plot.

Figure 6.7 plots $(\Phi^N/E_p)(E_b/N_0)$ versus the network utilization. Herein this figure, the analytical values are once more close to the simulated ones with a slight deviation, making the analytical model optimistic in general. Here once more the results for $(1 - p_D) = p_F = 0$ are better than $p_D = 0.7$ and $p_F = 0.2$. For $E_b/N_0 = 4$dB and $\lambda J < 0.75$, Φ^N grows with the network utilization and stabilizes for a higher load since the number of required transmissions per epoch is also stable. For $E_b/N_0 < 0$dB Φ^N decreases as the

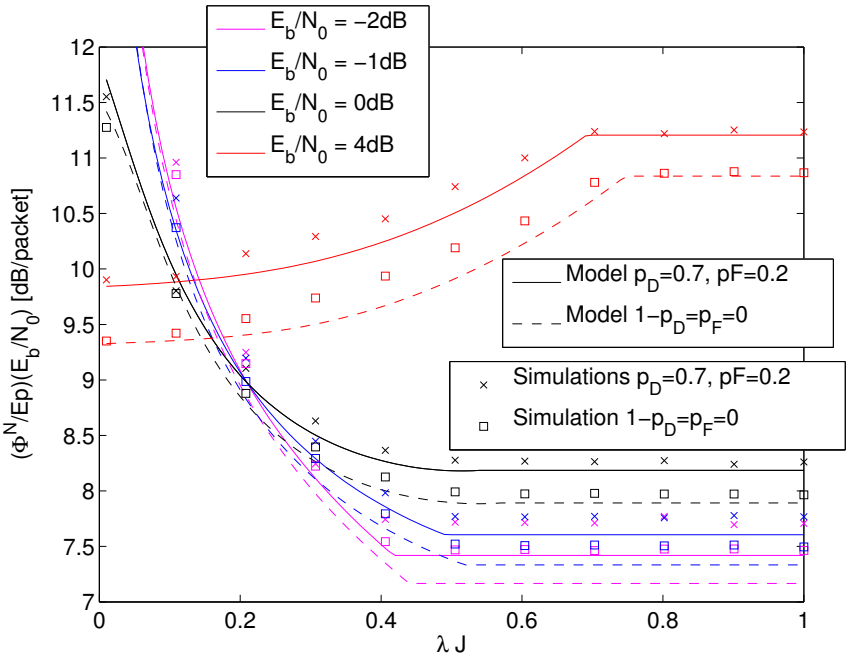

Figure 6.7: $(\Phi^N/E_p)(E_b/N_0)$ versus the network utilization with $J = 4$, $R_N = 4$ and different E_b/N_0.

network utilization increases, clearly showing that the dominant factor for Φ^N with low E_b/N_0 values is the number of epochs required to successfully transmit a packet: when the network utilization increases, the probability of having more MTs transmitting in the same slot also increases, thus producing lower PER values.

For all scenarios with ideal transmission conditions, when the network saturates, $(\Phi^N/E_p)(E_b/N_0)$ is constant and equal to $\frac{\mathbb{E}\left[tx\left(\Omega_J^{(R_N)}\right)\right]}{(1-\varepsilon_{sys})}$, which corresponds to the absolute minimum for $E_b/N_0 < 0$dB. However, this is not useful for our purposes because the delay is not bounded in a saturated network – the useful range of λJ values for a given E_b/N_0 is constrained by the non-saturation condition. Clearly, Φ^N is minimized using lower E_b/N_0 values, but the BS has to be sensitive to the application requirements in terms of network utilization and delay. The minimum achievable delay decreases and the saturated network capacity increases with the increase of E_b/N_0. Low delay and a high network utilization (e.g. a delay below 5 slots for a network utilization above 90% for ideal transmission conditions) are only achievable for high E_b/N_0 values, forcing a higher transmission energy per packet.

6.4.3 Impact from the number of MTs J

The current subsection presents the performance over J for $R_N = 4$ retransmissions, $\lambda J = 0.4$ and three values of E_b/N_0 (0dB, 4dB, 8dB). All figures related to the MAC network performance contain results for ideal and non-ideal detection conditions, i.e. $(1-p_D) = p_F = 0$, and $p_D = 0.7$ and $p_F = 0.2$, respectively.

Figure 6.8 shows the packet delay. The delay model has close results when compared to the simulations, having an optimistic behavior for $1 - p_D = p_F = 0$ and pessimistic for $p_D = 0.7$ and $p_F = 0.2$. Results show that the delay decreases when J increases for the same network utilization (a total throughput of 40%), almost stabilizing on a delay dependent of the E_b/N_0 value. The improvement is quite remarkable with poor propagation conditions. Similar to other figures the performance for $(1-p_D) = p_F = 0$ is better than for $p_D = 0.7$ and $p_F = 0.2$.

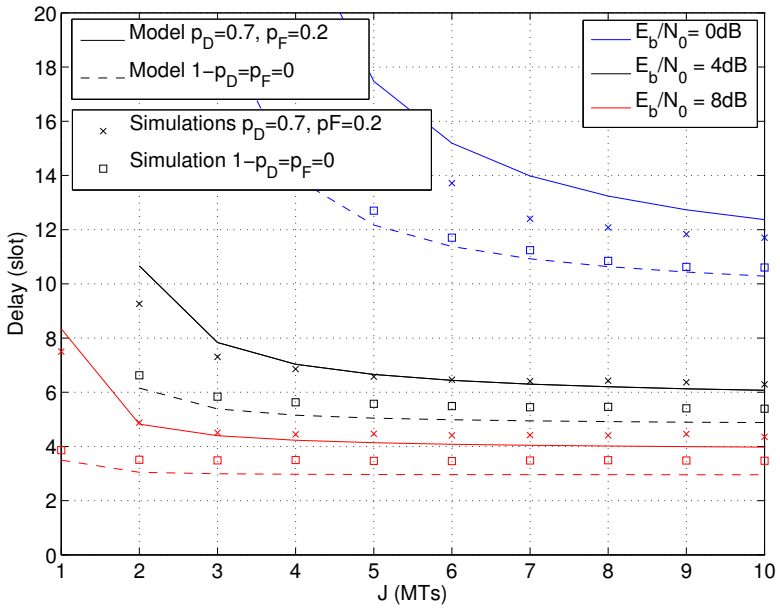

Figure 6.8: Scalability of the delay over J for $R_N = 4$ retransmissions, $\lambda J = 0.4$ and different E_b/N_0 values.

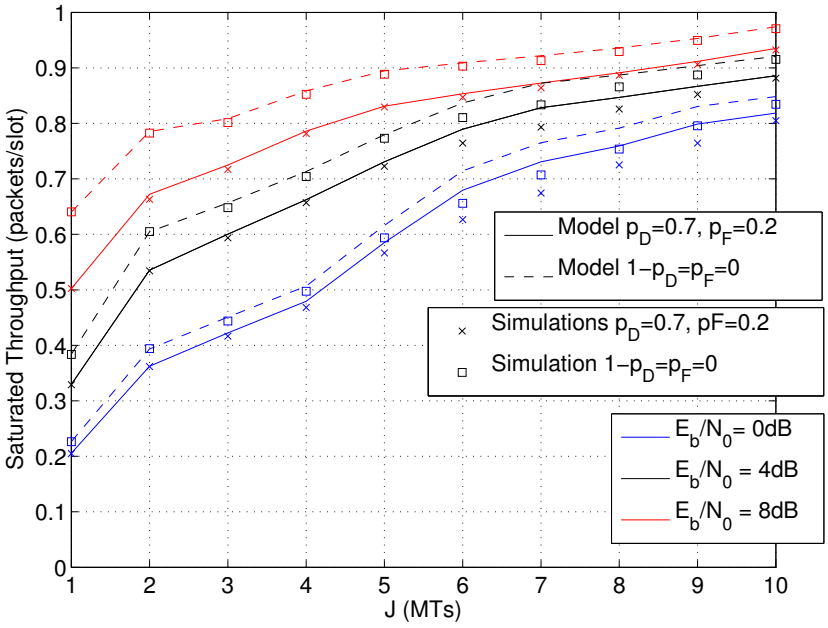

Figure 6.9: Scalability of the saturated throughput over J for R_N=4 retransmissions and different E_b/N_0 values.

Figure 6.9 illustrates the saturation throughput. The analytical model has close results to the simulation values, presenting itself as optimistic, especially for low E_b/N_0 values (e.g. $E_b/N_0 = 0$ dB). The saturated throughput reduction due to non-ideal detection conditions is lower when compared against ideal simulation conditions. The network capacity increases with J in result of diluting the packet retransmission overhead over a larger number of MTs. The network capacity increases up to to 95% for $E_b/N_0 = 8$dB under ideal transmission conditions. As expected, lower E_b/N_0 values reduce the average

throughput network capacity. This experiment can also be used to evaluate the performance of a classical DC H-ARQ system (with a single MT) against the H-NDMA system: the value $J = 1$ corresponds to a single MT transmitting in each slot using H-ARQ. All in all, greater values of J correspond to H-NDMA having a greater network capacity.

6.4.4 p_F and p_D Performance Results

The current subsection presents the performance results for a variable range of the p_F and p_D probabilities, where $p_D \in [0, 1]$ and $p_F = \{0; 0.4; 0.9\}$. It was also assumed that there is only $R_N = 1$ retransmission slot for each H-NDMA epoch. The results were extracted for a wireless topology of four MTs competing for the wireless medium, where the BS measures $E_b/N_0 = 20$dB. The simulated system rate is $\lambda J = 0.4$ for all figures except for figure 6.12 that illustrates the saturated system throughput. All figures illustrate the curves as the model's performance and the markers as the system simulations.

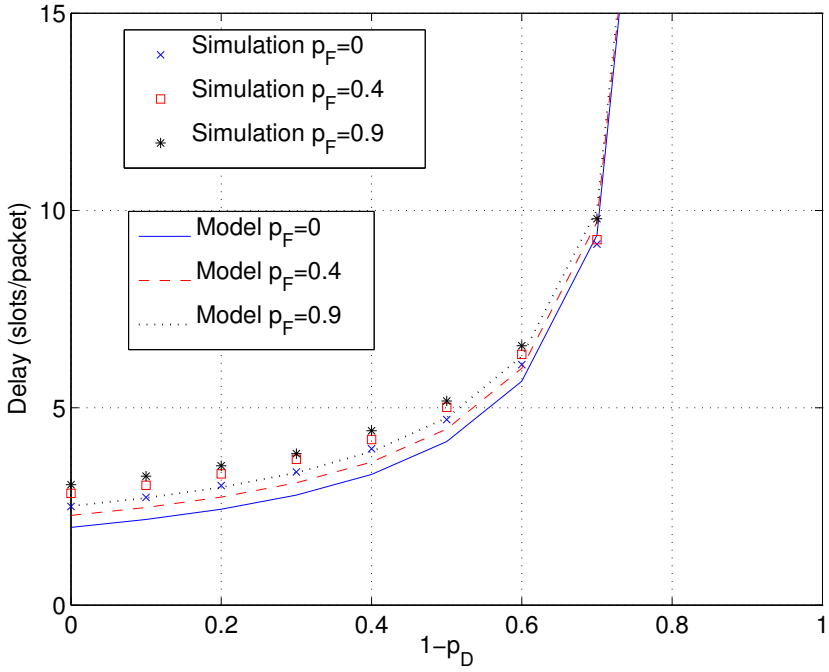

Figure 6.10: Delay over $1 - p_D$ for $J = 4$ and different p_F values.

Figure 6.10 illustrates the system delay performance. The model performance is slightly optimistic for higher p_D values, though following with better precision as p_D decreases. The mis-detection probability influences the system performance, where the delay doubles from five slots for $1 - p_D = 0.5$ to ten slots for $1 - p_D = 0.7$.

Figure 6.11 illustrates the $(\Phi^N/E_p)(E_b/N_0)$ performance. Similarly to the previous figure, the model performance is slightly optimistic for higher p_D values, though having better precision for lower p_D values. The mis-detection probability has a noticeable influence on $(\Phi^N/E_p)(E_b/N_0)$ performance, regardless of the p_F value, increasing monotonically with $1 - p_D$.

Figure 6.12 illustrates the saturated system throughput performance. The model performance matches seamlessly with the simulation values. Also, it is immediately recognizable that the mis-detection probability heavily influences the system performance, diminishing the system throughput as $1-p_D$ increases.

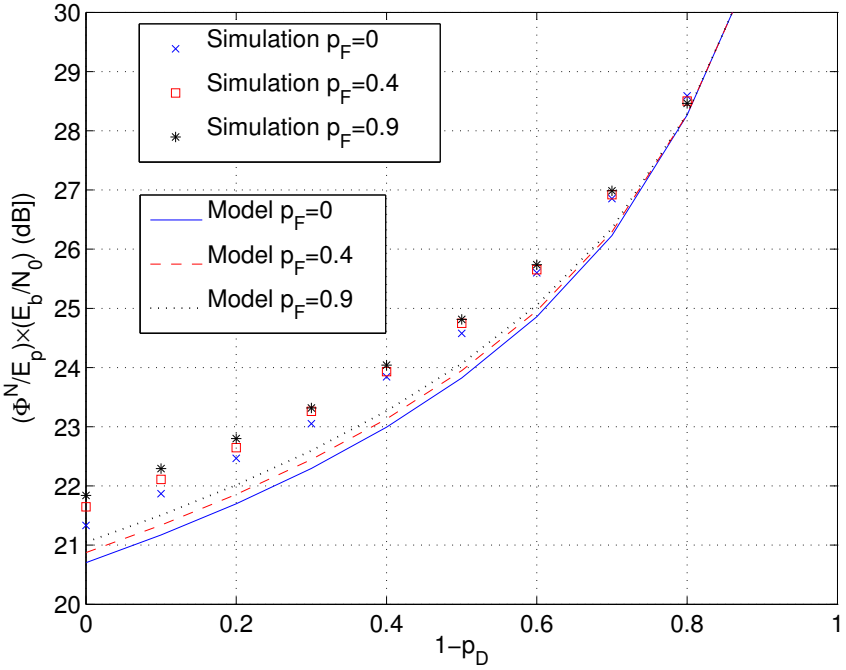

Figure 6.11: $(\Phi^N/E_p) \times (E_b/N_0)$ over $1 - p_D$ for $J = 4$ and different p_F values.

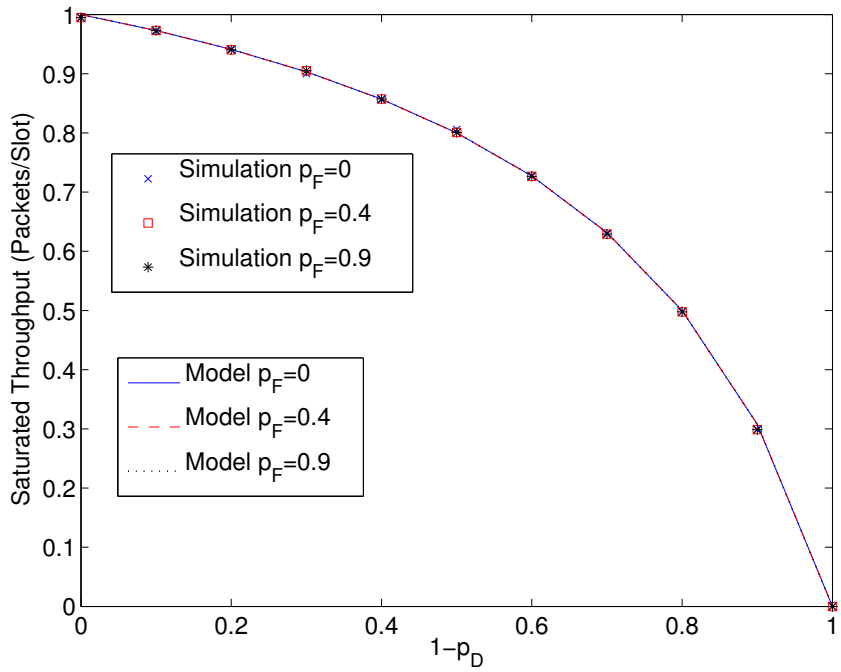

Figure 6.12: Saturated throughput over $1 - p_D$ for $J = 4$ and different p_F values.

The saturated throughput reduction is initially small compared to the value of $1 - p_D$, but approaches 0 as $1 - p_D$ tends to 1.

In all figures it is possible to observe that the p_F probability, as was defined in this analysis, has only a marginal influence in the system performance, since it only affects idle slots, leading to slightly longer

irrelevant epochs. Thus introducing a slightly longer delay and more MTs transmitting per epoch.

6.4.5 H-NDMA Power Tuning Optimization

The current sub-section presents the H-NDMA power tuning optimization performance under optimal detection conditions based on analytical results over the system network load for $J = 4$ MTs and $R_N = 4$ retransmissions.

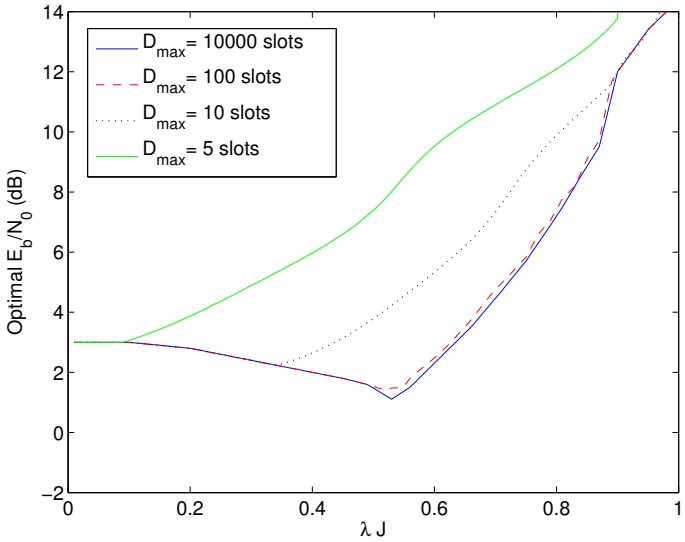

Figure 6.13: Optimal E_b/N_0 over the network utilization with $J = 4, R_N = 4$ and different maximum delays D_{max}.

Figure 6.13 contains four curves (one for each value of delay). Each curve represents the variation of the optimal E_b/N_0 versus the load calculated using the optimization process described in section 6.3.7 - i.e., for each value of the load, λ, the optimal E_b/N_0 (that minimizes Φ^N) that complies with a certain value of delay ($\mathcal{D} \leq D_{max}$) was calculated. The figure is plotted with a step of 0.01 regarding the system load. The figure shows that when low average delay is a concern, the optimal E_b/N_0 value grows linearly with the network utilization, and the energy efficiency is maximized when the load is minimal. However, when the delay is not a concern, the best energy efficiency happens for a network utilization around 55% and E_b/N_0 below 2dB. Although E_b/N_0 is below 2dB, the average total energy per bit available at the receiver is above 2dB, since the signals from the multiple transmissions of the same packet are combined.

Energy efficiency can be further improved by letting the BS control the MTs access to the epochs' slots, freeing some of the slots and possibly increasing the load on the remaining slots, as explained at the end of section 6.3.7.

6.5 Conclusions

A new protocol, H-NDMA, was described in this chapter. It was designed to improve a scheme with MUD in terms of network capacity through means of DC H-ARQ. An analytical model for H-NDMA was derived for the system throughput, energy consumption and packet delay. The H-NDMA performance

was evaluated for a linear SC-FDE receiver and the results show that H-NDMA improves the network capacity, reduces the packet delay and the energy consumption when compared to the basic NDMA MAC protocol, or to the classical H-ARQ protocol. Results also show that a small performance degradation is introduced by constrained detection and false-alarm errors. Based on the system results H-NDMA can be a good option for future very-high data rate cellular networks.

Chapter 7

H-ARQ Schemes Comparison

7.1 Introduction

The previous chapters studied three H-ARQ implementations, each applied to different structured access schemes: TDMA, slotted prefix-assisted DS-CDMA and NDMA. In general H-ARQ schemes, more specifically DC H-ARQ, enhance packet reception at the BS. Besides better packet reception, DC H-ARQ also improves energy efficiency, since each packet can be retransmitted with a lower E_b/N_0 - other advantages include: higher throughput and in some cases a lower delay.

The implementation of DC H-ARQ brings several advantages, although using it efficiently is a completely different matter, especially when comparing different access schemes. DC H-ARQ applied to TDMA is somewhat inefficient in terms of the system delay, since MTs have to wait an entire system frame to retransmit their packets; for a slotted prefix-assisted DS-CDMA protocol, MTs might use too much redundancy when the wireless channel is lightly used, therefore wasting channel capacity and packet energy for additional retransmissions; H-NDMA in the other hand needs a highly loaded channel to become efficient enough for low E_b/N_0 values. Each of these problems are quite distinguishable between the three access schemes, especially for low E_b/N_0 since more retransmissions are needed to deliver a packet with success using DC H-ARQ - this is heavily conditioned by the maximum number of allowed retransmissions for each access scheme.

Based on the previous chapters' results, there are traits that characterize each of the MAC control schemes with DC H-ARQ. TDMA for instance should be the most energy efficient protocol, since the BS only asks for a single packet retransmission (when needed) for each TDMA frame; slotted prefix-assisted DS-CDMA should achieve the lowest delay and need the least number of packet transmissions, since it uses additional redundancy from the spreading code; H-NDMA should have the best overall performance for higher system loads.

The current chapter studies the performance of the previously presented MAC access schemes using the IB-DFE receiver from chapter 3. The performance results illustrate the number of expected transmissions per packet, the success rate, the throughput, delay and the EPUP. The structure of this chapter is as follows: section 7.2 states this chapter's normalization conditions regarding each system's parameters; section 7.3 analyzes the three systems' performance; and section 7.4 states this chapter's conclusions.

7.2 Normalization Conditions

Section 3.2 compared the three MAC schemes from a PHY layer perspective regarding each protocol's redundancy - i.e. the number of packet transmissions (L) and/or the spreading gain (K). However, the studied MAC protocols have different behaviors and cannot be *fairly* compared since all of them have their own traits.

The current section normalizes the cross-layered protocols by the maximum redundancy per packet, i.e. number of transmissions and/or code spreading gain. L_Ω is defined in this chapter as the normalized maximum redundancy per packet.

For a TDMA protocol that employs DC H-ARQ, L_Ω is equivalent to the maximum number of packet transmissions, i.e. $L_\Omega = R_T$; regarding a slotted prefix-assisted DS-CDMA system it is equivalent to $(R_C + 1) = L_\Omega / K$; while for H-NDMA it should be $L_\Omega = (J + R_N)$.

For example, if $L_\Omega = 4$ and the BS supports $J = 4$ MTs, then $R_T = 4$, $R_C = 0$ for $K = 4$ and $R_N = 0$. On the other hand for $L_\Omega = 8$, for the same number of MTs, it corresponds to $R_T = 8$, $R_C = 1$ for $K = 4$ and $R_N = 4$.

Dependent of the system load, the three schemes will behave differently even though the three employ the same L_Ω.

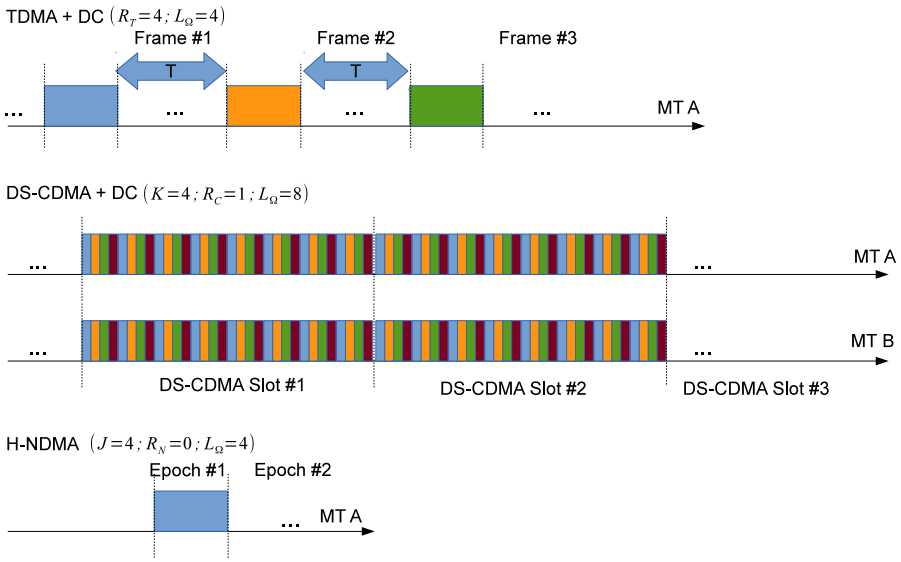

Figure 7.1: Example of the protocols' behavior for different constraints.

Figure 7.1 exemplifies the protocols behaviors, where TDMA only uses the amount of transmissions it needs to receive a packet with success (i.e. the access scheme does not need to reach the available L_Ω transmissions); DS-CDMA might use more redundancy than it needs for lighter traffic loads due to its spreading gain (in practice the access scheme could use less redundancy than its maximum); and H-NDMA in lighter traffic loads might not use as many transmissions as L_Ω (e.g. For $J > 1$, an epoch with a single MT does not have as much data diversity as L_Ω).

Figure 7.2 illustrates the dynamic behavior of H-NDMA against DS-CDMA. For each epoch in NDMA, MTs only transmit as many times as necessary (depending on the number of MTs) and have the chance to retransmit more than J packets if $R_N > 0$; DS-CDMA, on the other hand, has a fixed behavior since it cannot change the amount of redundancy used per packet transmission, where the protocol always uses K redundant replicas.

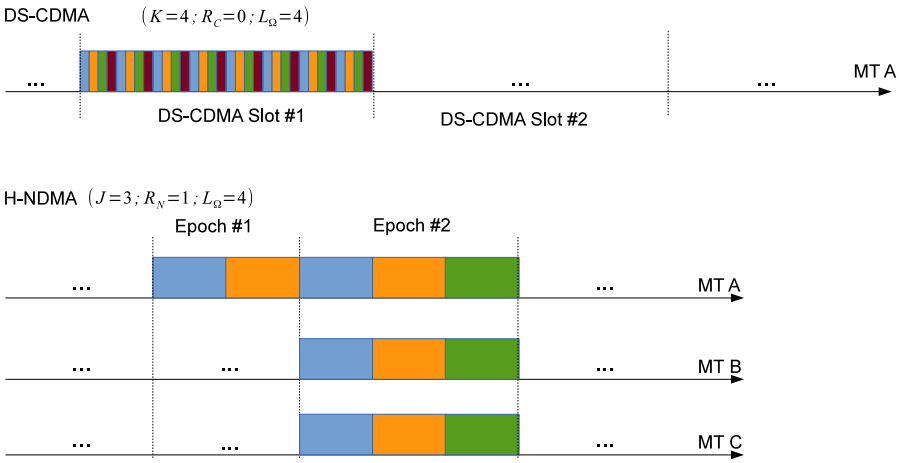

Figure 7.2: DS-CDMA's fixed behavior and H-NDMA's dynamic behavior.

For a *fairer* comparison between the three protocols, the DS-CDMA's number of packet transmissions (N_{sys}^{C}) and respective delay ($\mathcal{D}^{C}$) should be scaled according to the code spreading gain K, since DS-CDMA has the advantage of using more diversity replicas than the other protocols. Therefore $N_{sys}^{C^*} = K \times N_{sys}^{C}$ and $\mathcal{D}^{C^*} = K \times \mathcal{D}^{C}$ are respectively the normalized number of packet transmissions and packet delay for a DS-CDMA context. Since the number of packet transmissions is normalized for a DS-CDMA context, the EPUP should be normalized as well, where $\Phi^{C^*} = K \times \mathcal{N}^{C} E_p$ is the normalized EPUP for DS-CDMA.

7.3 Performance Analysis

A performance analysis is made in this section, where TDMA, slotted prefix-assisted DS-CDMA and H-NDMA are compared using DC H-ARQ. TDMA and H-NDMA results use the IB-DFE model from chapter 3, while DS-CDMA results use the IB-DFE model from chapter 5. The results in this section only use the performance models presented in the previous chapters.

Table 7.1: PHY layer parameters

Description	Parameter
Channel Multipath components	64
Fading type	Uncorrelated Rayleigh fading per path/user channel
Number of packet symbols (N)	256
Constellation	QPSK
Symbol transmission time	4μs
Transmission technique	SP technique
Spreading sequence technique (DS-CDMA)	Walsh-Hadamard
IB-DFE iterations (N_{iter})	4

Table 7.1 lists the PHY layer parameters for the performance results. A severely time dispersive channel was considered, with 64 multipath rays and uncorrelated Rayleigh fading for each path and user, but with channel correlation between each packet retransmission. To cope with channel correlation for each retransmission, the SP technique from chapter 3 was considered. Terminals scattered inside the BS's coverage area transmit uncoded data blocks with $N = 256$ symbols selected from a QPSK constellation during a transmission time of $4\mu s$. For all protocols, the IB-DFE receiver removes any channel interference and MAI up to four iterations.

Two scenarios were considered for this chapter, with $J = 4$ MTs receiving packets in their queues for a *Poisson* system rate of $\lambda J = \{0.1; 0.4; 0.8\}$. The first scenario uses $L_\Omega = 4$ and the other one $L_\Omega = 8$. Regarding a DS-CDMA context and for the sake of simplicity the code spreading gain is the same as the maximum number of MTs ($K = J$) that can access the wireless channel. Furthermore the TDMA performance model considers that there are $(L_T + 1)$ slots per TDMA frame, where $J = L_T - 1$. Table 7.2 displays the MAC normalization parameters for the considered scenarios.

Table 7.2: MAC normalization parameters for $J = 4$

Normalization Parameters	TDMA ($L_T = J + 1$)	DS-CDMA ($K = J = 4$)	H-NDMA
$L_\Omega = 4$	$R_T = 4$	$R_C = 0$	$R_N = 0$
$L_\Omega = 8$	$R_T = 8$	$R_C = 1$	$R_N = 4$

For the first scenario, $L_\Omega = 4$, a MT in TDMA should be able to retransmit a packet three times; while for DS-CDMA there is only one transmission, i.e. $R_C = 0$; and for H-NDMA this means that for $J = 4$ MTs there are at most four transmissions in an epoch, then $R_N = 0$.
For the second scenario, $L_\Omega = 8$, a MT in TDMA retransmits a packet up to seven times; in DS-CDMA MTs might retransmit their packets only once; and in H-NDMA, for $J = 4$ MTs there should be at most $R_N = 4$ retransmissions.

Regarding the EPUP results, the expended energy from the electrical circuitry was removed for all protocols, as in chapters 5 and 6. Furthermore, each protocol's EPUP was multiplied by $(1/E_p)(E_b/N_0)$. The reason is to remove the dependencies on the distance, path loss and antenna parameters (see (5.35)), and to show the variation of the EPUP with the protocols' configuration parameters, taking solely in consideration the average power received at the BS. For the sake of simplicity, the EPUP is denoted as Φ in this chapter.

As for TDMA, based on the goodput expression from (4.9), its normalized throughput shall be treated as the success probability over the number of necessary transmissions ratio to receive a packet, where

$$S^T = \frac{1 - Q_{R_T+1}}{N_{sys}^T}. \tag{7.1}$$

All results are illustrated for a given range of the bit energy over the noise ratio E_b/N_0, where black lines illustrate results for $L_\Omega = 4$ data replicas and red lines for $L_\Omega = 8$. The $+$ marker represents the results for TDMA with DC H-ARQ, the $*$ marker the results for DS-CDMA with DC H-ARQ and the $\square$ marker the results for H-NDMA.

Figure 7.3 illustrates the average number of transmissions per packet. As observed DS-CDMA in general, with or without H-ARQ, has the highest number of packet transmissions, due to the fact that it uses too much redundancy for each packet transmission. While DS-CDMA is slightly unaffected by λJ, H-NDMA is greatly affected, since a higher load implies a larger number of transmissions per epoch. TDMA is unaffected by the system load since MTs are not competing for the system channel. A higher diversity for TDMA, $L_\Omega = 8$, implies a larger number of packet transmissions for low E_b/N_0 values, especially for $E_b/N_0 =]0, 2[$ dB and as expected for higher values out of this interval the performance remains the same for $L_\Omega = 4$ or $L_\Omega = 8$. H-NDMA has an higher number of packet transmissions for $L_\Omega = 8$, as well as for higher loads, since it needs to cope with channel interference from all MTs, despite that it performs close to TDMA when $L_\Omega = 8$. Furthermore, H-NDMA outperforms TDMA and DS-CDMA for $L_\Omega = 4$, $\lambda J = \{0.1, 0.4\}$ and $E_b/N_0 =]0, 8[$dB, which means that H-NDMA has an higher diversity gain to deliver a packet than TDMA and DS-CDMA under these conditions.

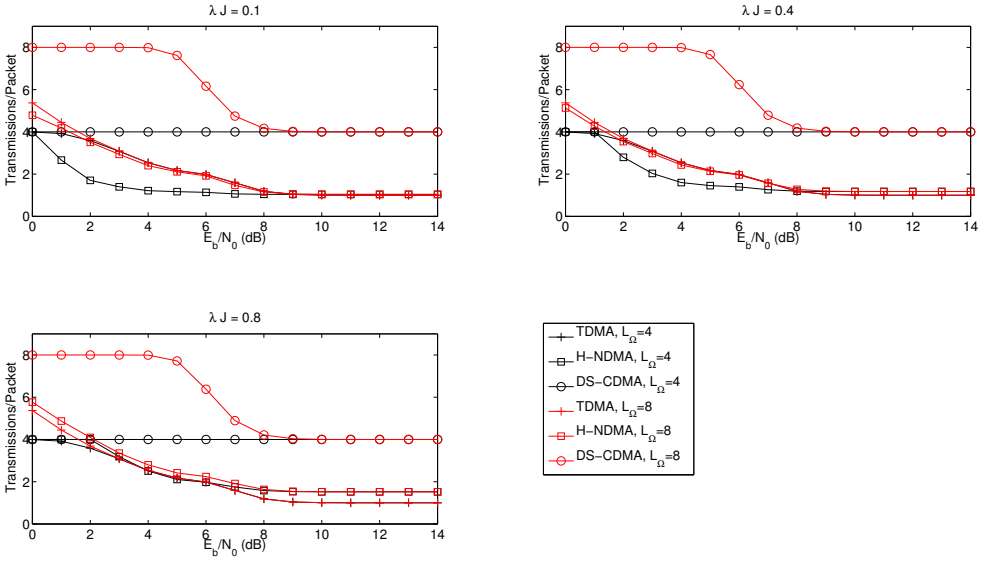

Figure 7.3: Average number of Packet Transmissions.

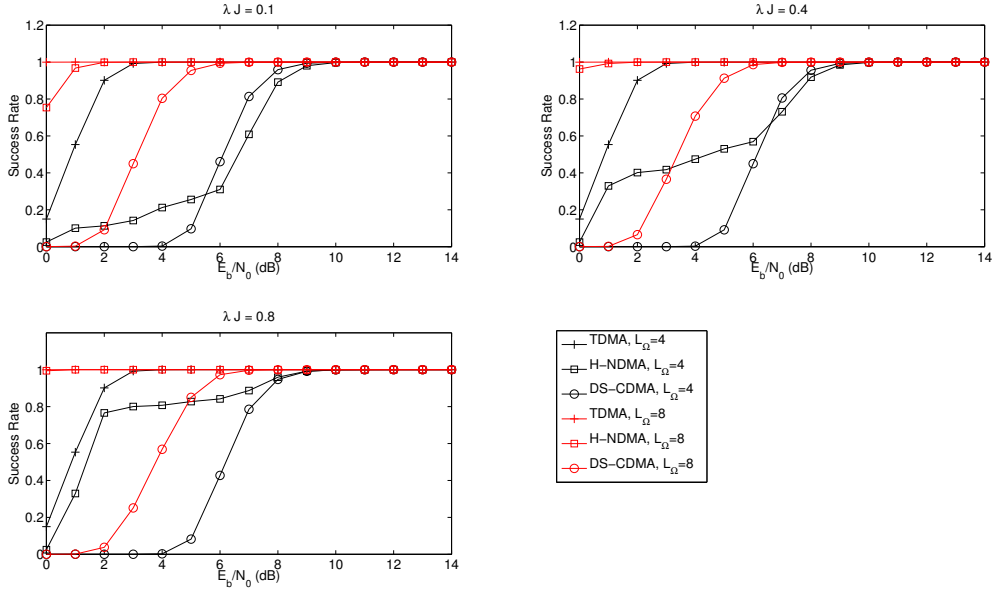

Figure 7.4: Success rate of delivering a packet at the BS.

Figure 7.4 illustrates the probability of delivering a packet with success at the BS. DS-CDMA, in general, has the worst performance for low E_b/N_0 values, only outperforming H-NDMA for $L_\Omega = 4$, $E_b/N_0 =]5, 7[$ dB and $\lambda J = \{0.1, 0.4\}$; this can be explained by the fact that DS-CDMA's code spreading gain can surpass the existing channel interference and MAI between MTs. H-NDMA for heavier loads, i.e. $\lambda J = 0.8$, performs almost as good as TDMA, since heavier loads imply a higher number of retransmissions to achieve a successful packet delivery at the BS although suffering from MAI. Since TDMA does not suffer any kind of MAI between transmissions, it has a higher chance of delivering a packet with success, therefore having the best overall performance in terms of the success probability.

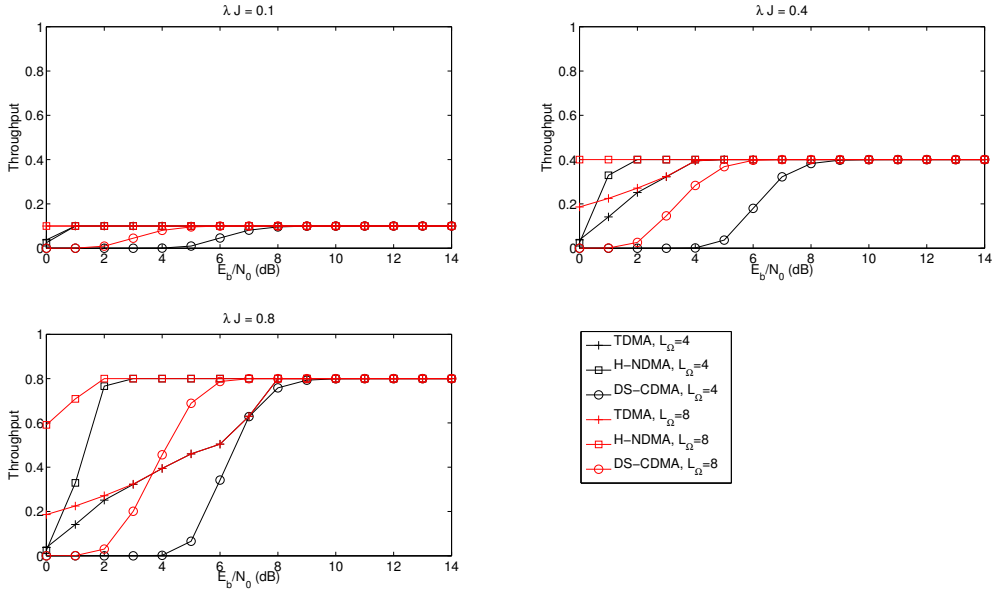

Figure 7.5: Average Throughput.

Figure 7.5 illustrates the throughput of the three protocols. Once more and similarly to the previous figure the DS-CDMA protocol, with or without H-ARQ, has the worst performance, except for $L_\Omega = 8$ and $\lambda J = 0.8$; contrarily, H-NDMA has the best performance since in general MTs need fewer transmissions to deliver a packet - the additional redundancy of having more MTs in an epoch ensures a better reception at the BS. TDMA in general performs well, except when more packet transmissions are necessary to deliver a packet, since more slots are used to transmit a single packet than in other protocols - in other protocols the MTs transmissions are easily diluted, since more MTs are involved.

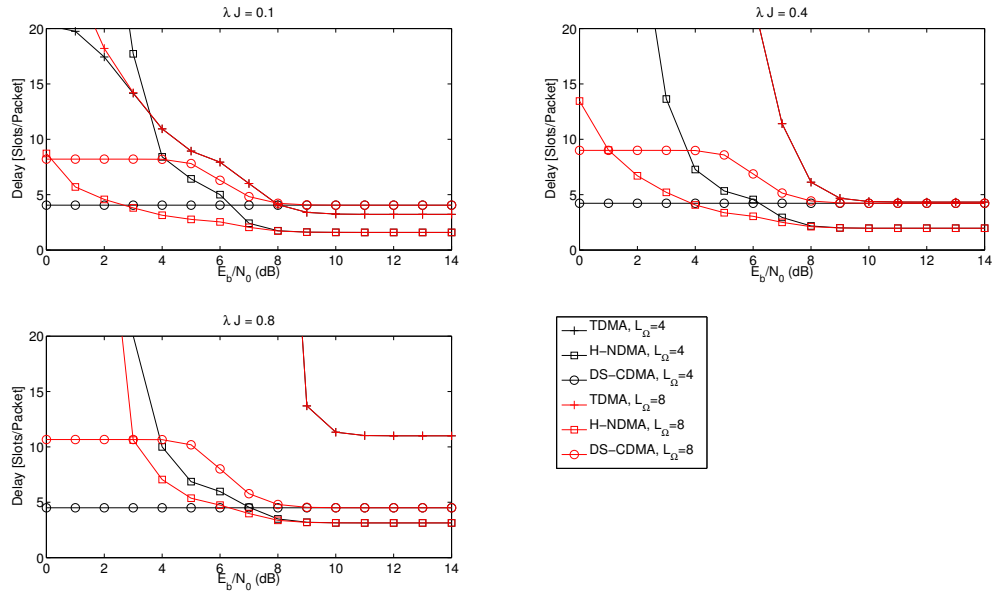

Figure 7.6: Average Delay.

Figure 7.6 illustrates the average packet delay. For $L_\Omega = 4$, DS-CDMA in general has the best per-

formance for $E_b/N_0 = [0,6[$ dB, since it requires less transmissions per packet; in addition, once DS-CDMA's queue receives a data packet it transmits it immediately and does not have to wait for an extended time period. H-NDMA, in general has to wait for the end of an epoch, or in the case of TDMA, a MT might have to wait for almost an entire TDMA frame. For $E_b/N_0 > 6$ dB, DS-CDMA looses to H-NDMA due to the use of excessive redundancy, but holds well against TDMA. TDMA in general has the worst performance for $E_b =]4,14[$dB, mostly because each MT has to wait up to an entire TDMA frame. H-NDMA, either with or without redundant transmissions, can outperform other protocols especially for higher loads and/or higher L_Ω - below 4 dB, H-NDMA cannot handle the existing interference as well as TDMA and DS-CDMA.

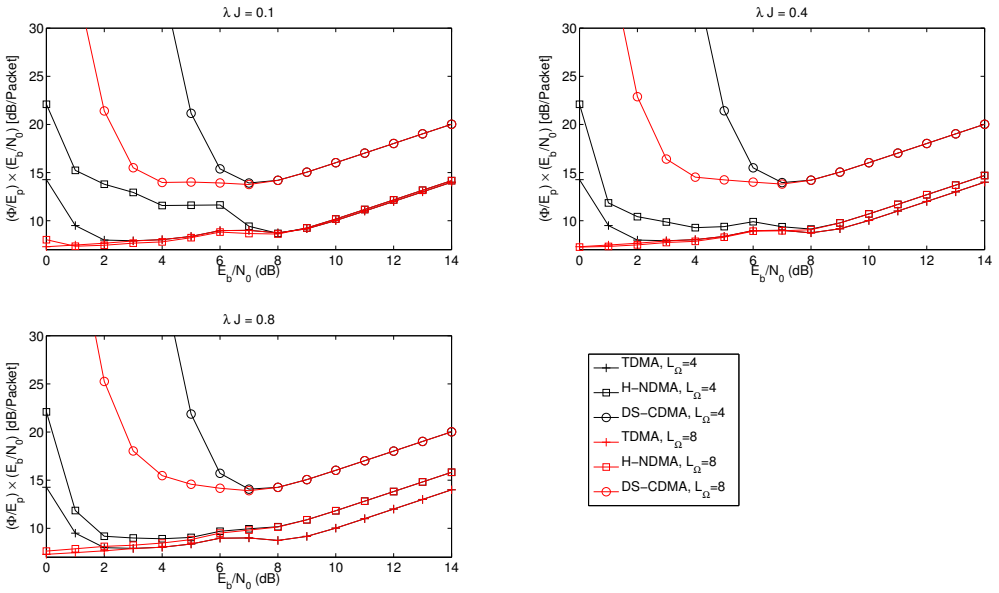

Figure 7.7: Average Normalized Energy per Useful Packet $(\Phi/E_p) \times (E_b/N_0)$.

Figure 7.7 illustrates the $(\Phi/E_p)(E_b/N_0)$ ratio. Through a careful observation, it is noticeable that TDMA outperforms both DS-CDMA and H-NDMA, both of them with or without H-ARQ. DS-CDMA, with or without H-ARQ in general, has the worst performance of the three - regardless of the network load; this fact is due to the MAI between users that aggravate the packets reception at the BS and also the data spreading that is overly redundant. H-NDMA performs almost as good as TDMA for high λJ values, as well as for high E_b/N_0 when $L_\Omega = 4$, demonstrating the flexibility of the NDMA protocol that forces retransmissions according to the number of MTs contending for the wireless channel.

7.4 Conclusions

The current chapter compares the performances of TDMA, slotted prefix-assisted DS-CDMA and H-NDMA, where the three protocols employ DC H-ARQ. The three protocols were benchmarked with an IB-DFE receiver, for a multipath dispersive channel, at the PHY layer; despite sharing the same receiver structure, the three protocols have different traits that make them harder to compare, especially with DS-CDMA that employs fixed additional redundancy from the code spreading gain - the DS-CDMA system was normalized to make the comparison as *fair* as possible.

Table 7.3 enumerates this chapter's results, where TDMA with DC H-ARQ shows a good performance

Table 7.3: Pros and Cons of TDMA with DC H-ARQ, DS-CDMA with DC H-ARQ and H-NDMA.

Protocol	Pros	Cons
TDMA with DC H-ARQ	- Most energy efficient; - Highest success rate.	- Higher delay to recover packets; - Lower throughput for low E_b/N_0 values.
DS-CDMA with DC H-ARQ	- Good delay;	- Least energy efficient; - Lowest throughput; - Wastes too much redundancy.
H-NDMA	- Highest overall throughput; - Great overall performance for high λJ.	- Underperforms for lower λJ.

in terms of energy efficiency and highest success rate, although it suffers of a lower throughput for lower E_b/N_0 values and as expected a higher delay to recover packets at the BS. DS-CDMA with DC H-ARQ is the least energy efficient of the three protocols in general and also suffers of a lower throughput at low E_b/N_0 values, despite that it performs well in terms of packet delay. Finally, H-NDMA shows that it performs quite well in most situations as long as λJ is high, even though it stands as a good choice for low λJ values; in addition H-NDMA has in general the best throughput of the three protocols. It should be noted that in terms of general performance, the H-NDMA protocol has the best results, since it shows enough flexibility in terms of data redundancy for each epoch contention period.

Chapter 8

Conclusions

Wireless communications have been an hot topic for the last decades, not only due to scientific breakthroughs, but from mass market demand. Wireless handsets, either laptop computers or cellphones, have become a commonality in people's lives - it becomes natural that the wireless communications' industry must push forward for new standards that respond to users' needs.

Reliability in today's wireless communications is expected from the moment a mobile terminal is connected to the Internet. However, this reliability is not trivial in a wireless context, wireless communications are subjected to channel errors or interference; better reliability in a wireless communications context can also quickly deplete a mobile terminal's battery.

Three wireless medium access protocols were chosen and extended to be energy efficient without sacrificing the necessary reliability for a wireless communications context. To achieve such feat for very high data rates, a broadband receiver that takes advantage of channel diversity was chosen and modeled for this purpose.

Chapter 2 overviewed a comprehensive set of PHY layer and MAC layer techniques that tackle channel errors and/or MAI when several MTs access the wireless medium. Chapter 2 also studied that for a broadband context, FDE is ideal to tackle with a highly dispersive channel. Besides, from a MT's point of view, in a structured wireless network, using SC-FDE is excellent in terms of energy efficiency due to its low PAPR.

SC-FDE when combined with a proper equalization technique such as IB-DFE with time diversity mechanisms, it can reduce channel errors and MAI altogether, therefore improving data reception at the BS. To take advantage of time diversity mechanisms, the PHY layer becomes dependent of the MAC layer to actually obtain additional data replicas in the time domain, since a BS's MAC protocol coordinates the wireless medium. On top of this, a wireless MAC protocol becomes truly effective when well coordinated with the PHY layer, therefore a cross-layered PHY-MAC protocol becomes a better solution to enhance the overall performance in a wireless medium, especially when difficult transmission conditions are met due to channel interference and/or MAI.

Two options for PHY-MAC protocols that employed time diversity through means of DC H-ARQ control had a special emphasis in chapter 2 : TDMA and slotted prefix-assisted DS-CDMA. Both of these techniques are great to consider for a bounded delay and/or jitter, though both techniques can waste idle resources. NDMA is a step-up from these protocols, since it only uses as many slots as the number of users that contend for a structured wireless channel that is controlled by a BS. When difficult transmission conditions persist, a combination of NDMA with DC H-ARQ can be very fruitful for strict QoS. In

addition and unfortunately, the modeling of a cross-layered PHY-MAC is usually difficult to implement, since the two layers are strongly connected; previous research usually emphasizes one layer over the other, i.e. a higher focus on the PHY layer but sparse results on the MAC layer, or a simplified PHY layer but highly focused on the MAC layer.

Based on the aforementioned facts, this thesis researched a proper (and general) PHY layer model for an SC-FDE receiver structure that took advantage of time diversity mechanisms (DC H-ARQ) and applied it to TDMA, slotted prefix-assisted DS-CDMA and especially to NDMA. The following conclusions correspond to these cross-layered techniques.

Chapter 3 proposed an analytical model for two SC-FDE equalization schemes: linear and iterative equalization methods. The model was proposed with the purpose to *ease* the process of evaluating a cross-layered PHY-MAC protocol without the need of computing PHY layer simulations beforehand. Since several cross-layered protocols were studied in this thesis, the analytical model had to be versatile and simple. The BER and PER performances for DC and/or MUD schemes can be employed in various scenarios, including scenarios with nonhomogeneous transmitting powers for each MT. Results showed that the analytical model provided accurate BER and PER results, although presenting some inaccuracy for iterative schemes, because of residual errors that were unaccounted in the analytical model. All in all, the proposed model can be used to study the impact of using DC and MUD techniques.

Chapter 4 studied a cross-layered H-ARQ TDMA MAC performance model. The studied model portrays the protocol behavior for several metrics: the EPUP, the goodput and the packet delay. An optimization problem was also posed, based on the performance model, to compute the optimal parameters that guarantee a minimum EPUP and at the same time satisfying a given QoS. Results showed accurate predictions for a WSN topology and a HAP topology. In addition and as expected, the use of a DC scheme provides better EPUP gains for a given QoS, especially for energy constrained topologies and longer distances.

Chapter 5 studied a wireless PHY-MAC DC prefix-assisted DS-CDMA model, using an FDE receiver design with iterative equalization (IB-DFE). The wireless access was analyzed with DTMC. From here several metrics were extracted: the delay, throughput and EPUP. The model exhibited a high accuracy and results showed that the H-ARQ prefix-assisted DS-CDMA system with IB-DFE has a good performance to diminish both channel interference and MAI. Energy efficiency is also improved for a higher number of retransmissions for a given QoS, especially when considering lower E_b/N_0 values.

Chapter 6 proposed a new NDMA protocol variant, named H-NDMA. The protocol was designed to improve the network capacity of NDMA through additional DC H-ARQ transmissions. An analytical model was derived for the system throughput, EPUP and packet delay. H-NDMA improves the network capacity, reduces the packet delay and the energy consumption when compared to a basic NDMA scheme. Results also showed that a small performance degradation is expected for constrained detection and false alarm errors.

Chapter 7 compared the performances of TDMA, slotted prefix-assisted DS-CDMA and H-NDMA, employing DC H-ARQ. The three protocols were normalized to make the comparison as *fair* as possible; at the PHY layer, the protocols used an IB-DFE receiver, assuming a multipath dispersive channel. TDMA with DC H-ARQ showed the best performance in terms of energy efficiency and success rate, although suffering of a lower throughput for lower E_b/N_0 values and as expected a higher delay to recover packets at the BS. DS-CDMA with DC H-ARQ was the least energy efficient, suffering of a lower throughput at low E_b/N_0 values, despite performing well in terms of packet delay. H-NDMA, in the other hand, showed the best overall performance, especially for a high system load; H-NDMA also showed good results for

lower system loads.

8.1 Future Work

The various models and results of this document can be used for future work of cross-layered applications that still have a long research lifespan regarding energy efficiency and QoS.

The PHY layer model from chapter 3 can be extended for other cross-layered PHY-MAC protocols that make use of it, especially applications that require interference mitigation and the simulation of a MAC protocol that supports non-uniform transmission powers received at the BS - a PHY layer model that supports non-uniform transmission powers can be also useful for cognitive radio protocols. Furthermore, the PHY layer model could be extended to consider the use of channel coding and imperfect channel estimations.

Regarding the TDMA model from chapter 4, applied to an LTE channel, it could be extended to regard the interference from other surrounding networks - this scenario could *ideally* benefit from the PHY layer model in chapter 3. Other scenarios could reflect a MUD TDMA system for several TDMA frames that are concurrently working, each one with a distinct transmission power at the BS.

The DS-CDMA model could be also extended/reformulated for various scenarios. For example, the model could consider backoff mechanisms to study the system behavior with H-ARQ mechanisms; otherwise, it would be meaningful to study the MAC system performance for an overloaded system, i.e. with a spreading code gain lower than the number of contending MTs, using DC H-ARQ and the IB-DFE receiver to solve the packet collisions. In addition, the use of an adaptive spreading code, could be studied, to solve the energy inefficiency of DS-CDMA.

Finally, the H-NDMA concept could be optimized to ensure that the system is always loaded, from a performance perspective, by introducing idle slots/epochs. The H-NDMA concept can be further extended to allow multiple concurrent epochs, either with CDMA spreading codes or multiple transmission powers. Epochs could be distributed according to QoS requirements for instance.

Bibliography

[Abr70] N. Abramson. The ALOHA System: Another Alternative for Computer Communications. In *AFIPS Fall Joint Computer Conference, Houston, Texas*, pages 281–285, November 17–19 1970.

[Abr73] N. Abramson. *The ALOHA System, Computer Communication Networks*. Prentice Hall, 1973.

[ACD88] M. Aciardi, G. Casalino, and F. Davoli. Independent Stations Algorithm for the Maximization of One-Step Throughput in a Multiple Access Channel. *IEEE Transactions on Communications*, 35(8):795–800, August 1988.

[AD04] T. Araújo and R. Dinis. Iterative Equalization and Carrier Synchronization for Single-Carrier Transmission over Severe Time-Dispersive Channels. In *IEEE Globecom, Dallas, Texas, USA*, volume 5, pages 3103–3107, November 29–December 3 2004.

[AGTT05] F. Adachi, D. Garg, S. Takaoka, and K. Takeda. BROADBAND CDMA TECHNIQUES. *IEEE Wireless Communications*, 12(2):8–18, April 2005.

[AK97] A. S. Acampora and S. V. Krishnamurthy. A New Adaptive MAC Layer Protocol for Wireless ATM Networks in Harsh Fading and Interference Environments. In *IEEE International Conference on Universal Personal Coomunications Record, San Diego, California, USA*, volume 2, pages 410–415, October 12–16 1997.

[Ala98] S. Alamouti. A simple transmit diversity technique for wireless communications. *IEEE Journal on Selected Areas in Communications*, 16(8):1451–1458, October 1998.

[Ami92] N. Amitay. Resource Auction Multiple Access (RAMA): Efficient Method for Fast Resource Assignment for Decentralized Wireless PCS. *IET Electronic Letters*, 28(8):799–801, April 1992.

[Ami93] N. Amitay. Distributed Switching and Control with Fast Resourcre Assignment/Handoff for Personal Communication Systems. *IEEE Journal on Selected Areas in Communications*, 11(6):842–849, August 1993.

[ASO97] F. Adachi, M. Sawahashi, and K. Okawa. Tree-structured generation of orthogonal spreading codes with different lengths for forward link of DS-CDMA mobile radio. *IET Electronics Letters*, 33(1):27–28, January 1997.

[BBFM97] G. Bianchi, F. Borgonovo, L. Fratta, and L. Musumeci. C-PRMA: A Centralized Packet Reservation Multiple Access for Local Wireless Communications. *IEEE Transactions on Vehicular Technology*, 46(2):422–426, May 1997.

[BC10] F. Babich and M. Comisso. Theoretical Analysis of Asynchronous Multi-Packet Reception in 802.11 Networks. *IEEE Transactions on Communications*, 58(6):1782–1794, June 2010.

[BCJR74] L. R. Bahl, J. Cocke, F. Jelinek, and J. Raviv. Optimal decoding of linear codes for minimizing symbol error rate. *IEEE Transactions on Information Theory*, 20(2):284–287, March 1974.

[BDFT10] N. Benvenuto, R. Dinis, D. Falconer, and S. Tomasin. Single Carrier Modulation With Nonlinear Frequency Domain Equalization: An Idea Whose Time Has Come–Again. *IEEE Proceedings*, 98(1):69–96, January 2010.

[BDMP95] S. Benedetoo, D. Divsalar, G. Montorsi, and F. Pollara. Bandwidth-efficient parallel concatenated coding schemes. *IET Electronics Letters* , 31(24):2067–2069, November 23 1995.

[BDN97] R. Bolla, F. Davoli, and C. Nobile. A RRA-ISA Multiple Access Protocol with and without Simple Priority Schemes for Real-Time and Data Traffic in Wireless Cellular Systems. *Springer Journal of Mobile Networks and Applications*, 2(1):35–53, July 1997.

[Bea03] N. Beaulieu. Introduction to "Linear Diversity Combining Techniques". *IEEE Proceedings*, 91(2):328–330, February 2003.

[Ben85] G. Benelli. An ARQ Scheme with Memory and Soft Error Detectors. *IEEE Transactions on Communications*, 33(3):285–288, March 1985.

[Ber68] E.R. Berlekamp. *Algebraic Coding Theory*. McGraw-Hill, 1968.

[BF78] F. Borgonovo and L. A. Fratta. SRUC: A technique for packet transmission on multiple access channels. *IEEE International Conference on Computer Communications, Kyoto, Japan*, pages 601–607, September 1978.

[BG92] D. Bertsekas and R. Gallager. *Data Networks*. Prentice-Hall, 1992.

[BGB97] A. Bigloo, T. Gulliver, and V. Bhargava. Maximum-Likelihood Decoding and Code Combining for DS/SSMA Slotted ALOHA. *IEEE Transactions on Communications*, 45(12):1602–1612, December 1997.

[BGT93] C. Berrou, A. Glavieux, and P. Thitimajshima. Near Shannon limit error-correcting coding and decoding. *IEEE International Conference on Communications, Geneva, Switzerland*, pages 1064–1070, May 1993.

[Bha97] V. Bharghavan. A New Protocol for Medium Access in Wireless Packet Networks. See `http://timely.crhc.uiuc.edu/publications.html`, 1997.

[Bla83] R. E. Blahut. *Theory and Practice of Error Correcting Codes*. Addison-Wesley, 1983.

[BLZ08] L. Badia, M. Levorato, and M. Zorzi. Markov analysis of selective repeat type II hybrid ARQ using block codes. *IEEE Transactions on Communications*, 56(9):1434–1441, September 2008.

[BOP+07] L. Bernardo, R. Oliveira, M. Pereira, M. Macedo, and P. Pinto. A Wireless Sensor MAC Protocol for bursty data traffic. In *IEEE Personal Indoor and Mobile Radio Communications, Athens, Greece*, pages 1–5, September 3–7 2007.

[Bre55] D. G. Brennan. On the maximal signal-to-noise ratio realizable from several noisy signals. *Proceedings of the Institute of Radio Engineers*, 43:1530, October 1955.

[Bre04] M. Breiling. A logarithmic upper bound on the minimum distance of turbo codes. *IEEE Transactions on Information Theory*, 50(7):1692–1710, July 2004.

[BT02] N. Benvenuto and S. Tomasin. Block iterative dfe for single carrier modulation. *IET Electronics Letters*, 38(19):1144–1145, September 2002.

[CAISV12] H. Chafnaji, T. Ait-Idir, S. Saoudi, and A.V. Vasilakos. Low complexity frequency domain hybrid-ARQ chase combining for broadband MIMO CDMA systems. *EURASIP Journal on Wireless Communications and Networking*, 2012(1):134, April 2012.

[CC09] A. Carlson and P. Crilly. *Communication Systems*. McGraw-Hill, 2009.

[CDM11] F. Coelho, R. Dinis, and P. Montezuma. Estimation of the Feedback Reliability for IB-DFE Receivers. *ISRN Communications and Networking Journal*, 2011(30):1–7, June 2011.

[Cea96] B. Crow and et al. Performance aspects of IEEE 802.11 Wireless Local Area Networks. *SPIE Proceedings*, 2917:480–491, November 1996.

[CF07] Daniel J. Costello and G. David Forney. Channel Coding: The Road to Channel Capacity. *IEEE Proceedings*, 95(6):1150–1177, June 2007.

[CFea10] C. Chae, A. Forenza, and R. Heath et al. Adaptive MIMO transmission techniques for broadband wireless communication systems. *IEEE Communications Magazine*, 48(5):112–118, May 2010.

[CFRP00] E. Cianca, S. De Fina, M. Ruggieri, and R. Prasad. On the satellite diversity in CDMA based mobile satellite systems. In *IEEE International Symposium on Personal, Indoor, Mobile and Radio Communications, London, England*, volume 2, pages 1080–1084, 2000.

[CGB05] Shuguang Cui, A.J. Goldsmith, and A. Bahai. Energy-constrained modulation optimization. *IEEE Transactions on Wireless Communications*, 4(5):2349–2360, September 2005.

[CGdRH07] Enrico Casini, Riccardo De Gaudenzi, and Oscar del Rio Herrero. Contention Resolution Diversity Slotted ALOHA (CRDSA): An Enhanced Random Access Scheme for Satellite Access Packet Networks. *IEEE Transactions on Wireless Communications*, 6(4):1408–1419, April 2007.

[Cha85] D. Chase. Code Combining-A Maximum-Likelihood Decoding Approach for Combining an Arbitrary Number of Noisy Packets. *IEEE Transactions on Communications*, 33(5):385–393, May 1985.

[CHIW98] D.J. Costello, J. Hagenauer, H.J. Imai, and S.B.H. Wicker. Applications of error-control coding. *IEEE Transactions on Information Theory*, 44(6):2531–2560, June 1998.

[CL93] K. C. Chen and C. H. Lee. RAP - A Novel Medium Access Protocol for Wireless Data Networks. In *IEEE Globecom, Houston, Texas, USA*, volume 3, pages 1713–1717, 1993.

[CS88] J. H. Conway and N. J. A. Sloane. *Sphere Packings, Lattices and Groups*. Springer, 1988.

[CW10] C. Caicedo and M. Weiss. The viability of spectrum trading markets. In *IEEE Symposium on New Frontiers in Dynamic Spectrum, Singapore*, April 6–9 2010.

[CZKM10] Guner D. Celik, Gil Zussman, Wajahat F. Khan, and Eytan Modiano. MAC for Networks with Multipacket Reception Capability and Spatially Distributed Nodes. *IEEE Transactions on Mobile Computing*, 9(2):226–240, February 2010.

[DAPN10] R. Dinis, T. Araújo, P. Pedrosa, and F. Nunes. Joint Turbo Equalization and Carrier Synchronisation for SC-FDE schemes. *Wiley European Transactions on Telecommunications*, 21(2):131–141, February 2010.

[DCB+07] R. Dinis, P. Carvalho, L. Bernardo, M. Serrazina, and P. Pinto. Frequency-Domain Multipacket Detection: A High Throughput for SC-FDE Systems. *IEEE Globecom, Washington, USA*, pages 4619–4624, November 26–30 2007.

[DCB+09] R. Dinis, P. Carvalho, L. Bernardo, R. Oliveira, M. Pereira, and P. Pinto. A High Throughput Technique for SC-FDE Systems. *IEEE Transactions on Wireless Communications*, 8(7):3798–3807, July 2009.

[DCM08] R. Dinis, P. Carvalho, and J. Martins. Soft Combining ARQ Techniques for Wireless Systems Employing SC-FDE Schemes. *IEEE International Conference on Computer Communications and Networks, St. Thomas, US Virgin Islands*, pages 1–5, August 3–7 2008.

[DCM09] R. Dinis, P. Carvalho, and M. Martins. SC-FDE with soft packet combining ARQ techniques for interference-limited UWB systems. In *International Conference on Signal Processing and Communication Systems, Omaha, Nebraska, USA*, pages 1–6, September 28–30 2009.

[DeV93] J. M. DeVile. A Reservation-based Multiple Access Scheme for Future Universal Mobile Telecommunications System. In *IEE Conference Mobile and Personal Communications, Brighton, UK*, pages 210–215, December 13–15 1993.

[DGE03] R. Dinis, A. Gusmão, and N. Esteves. On broadband block transmission over strongly frequency-selective fading channels. In *IEEE Wireless Proceedings, Calgary, Canada*, July 2003.

[DGea02] R. Derryberry, S. Gray, and D. Ionescu et al. Transmit diversity in 3G CDMA systems. *IEEE Communications Magazine*, 30(4):68–75, April 2002.

[DH93a] A. Duel-Hallen. A Familiy of Multi-User Decision-Feedback Multi-User Detector for Synchronous Code-Division Multiple Access Channel. *IEEE Transactions on Communications*, 43(2):421–434, February 1993.

[DH93b] A. Duel-Hallen. Decorrelating Decision-Feedback Multi-User Detector for Synchronous Code-Division Multiple Access Channel. *IEEE Transactions on Communications*, 41(2):285–290, February 1993.

[DMB+09] R. Dinis, P. Montezuma, L. Bernardo, R. Oliveira, M. Pereira, and P. Pinto. Frequency-Domain Multipacket Detection: A High Throughput for SC-FDE Systems. *IEEE Transactions on Wireless Communications*, 8(7):3798–3807, July 2009.

[DMSS10] R. Dinis, P. Montezuma, N. Souto, and J. Silva. Iterative Frequency-Domain Equalization for General Constellations. In *IEEE Sarnoff Symposium, Princeton, New Jersey, USA*, April 12–14 2010.

[DP95] D. Divsalar and F. Pollara. On the Design of Turbo Codes. Technical report, Stanford, 1995.

[dRHG08] Oscar del Rio Herrero and Riccardo De Gaudenzi. A High Efficiency Scheme for Quasi-Real-Time Satellite Mobile Messaging Systems. In *International Workshop on Signal Processing for Space Communications, Rhodes Island, Greece*, pages 1–9, October 6–8 2008.

[DS03] G. Dimic and N. Sidiropoulos. Frequency-hopped network diversity multiple access for semi-ad-hoc wireless networks. In *IEEE International Conference on Acoustics, Speech, and Signal Processing*, volume 4, April 6–10 2003.

[DS06a] R. Dinis and P. Silva. A Frequency-Domain Receiver for Asynchronous Systems Employing CP-Assisted DS-CDMA Schemes. In *IASTED International Conference on Signal and Image Processing, Honolulu, Hawaii*, August 14–16 2006.

[DS06b] R. Dinis and P. Silva. An Iterative Detection Technique for DS-CDMA Signals with Strong Nonlinear Distortion Effects. In *IEEE Vehicular Technology Conference Fall, Montreal, Quebec*, pages 1–5, September 25–28 2006.

[DSG07a] R. Dinis, P. Silva, and A. Gusmão. IB-DFE receivers with space diversity for CP-assisted DS-CDMA and MC-CDMA systems. *Springer European Transactions on Telecommunications*, 8(7):791–802, June 2007.

[DSG07b] R. Dinis, P. Silva, and A. Gusmão. IB-DFE receivers with space diversity for CP-assisted DS-CDMA and MC-CDMA systems. *Springer European Transactions on Telecommunications*, 8(7):791–802, June 2007.

[DV06] S. Das and H. Viswanathan. A Comparison of Reverse Link Access Schemes for Next-Generation Cellular Systems. *IEEE Journal on Selected Areas in Communications*, 24(3):684–692, March 2006.

[ea90] R. Kohno et al. Combination of an Adaptive Array Antenna and a Canceller of Interference for Direct-Sequence Spread-Spectrum Multiple-Access System. *IEEE Journal on Selected Areas in Communications*, 8(4):675–682, April 1990.

[ea99] V. Erceg et al. A Model for the Multipath Delay Profile of Fixed Wireless Channels. *IEEE Journal on Selected Areas in Communications*, 17(3):399–410, March 1999.

[ECSN07] Yiftach Eisenberg, Keith Conner, Mathew Sherman, and Joshua Niedzwiecki. MUD Enabled Media Access Control For High Capacity, Low Latency Spread Spectrum Communications. In *IEEE MILCOM, Orlando, Florida, USA*, pages 1–7, October 29–31 2007.

[Eli54] P. Elias. Error-free coding. *IRE Transactions on Information Theory*, 4(4):29–37, September 1954.

[Eli55] P. Elias. Coding for noisy channels. *IRE Conv. Rec.*, 3(4):34–76, 1955.

[ER10] K. Etemad and M. Riegel. Topics and updates on 4G technologies. *IEEE Communications Magazine*, 48(8):38–39, August 2010.

[ETS95] ETSI. HIPERLAN Functional Specification. Technical report, ETSI, July 1995.

[FAea02] D. Falconer, S. Ariyavisitakul, and A. Benyamin-Seeyar et al. Frequency domain equalization for single-carrier broadband wireless systems. *IEEE Communications Magazine*, 40(4):58–66, April 2002.

[GA06] D. Garg and F. Adachi. Packet Access Using DS-CDMA With Frequency-Domain Equalization. *IEEE Journal on Selected Areas in Communications*, 24(1):161–170, January 2006.

[Gal63] R. Gallager. *Low-Density Parity-Check Codes*. PhD thesis, MIT, 1963.

[Gal68] R. G. Gallager. *Information Theory and Reliable Communication*. Wiley, 1968.

[Gal05] R. G. Gallager. *Introduction to Coding for noisy channels*. MIT Press, 2005.

[GBB+13] Francisco Ganhão, Gonçalo Barros, Luis Bernardo, Rui Dinis, P. Carvalho, José Vieira, Rodolfo Oliveira, and Paulo Pinto. A soft-handover scheme for LEO satellite networks. In *IEEE Vehicular Technology Conference (VTC) Fall, Las Vegas, Nevada, USA*, pages 1–5, September 2–5 2013.

[GBD+12] Francisco Ganhão, Luis Bernardo, Rui Dinis, Gonçalo Barros, Eduardo Santos, António Furtado, Rodolfo Oliveira, and Paulo Pinto. Energy-Efficient QoS Provisioning in Demand Assigned Satellite NDMA Schemes. In *IEEE International Conference on Computer Communications and Networks (ICCCN), Munich, Germany*, pages 1–8, July 30–August 2 2012.

[GC08] R. Gau and K. Chen. Probability Models for the Splitting Algorithm in Wireless Access Networks with Multipacket Reception and Finite Nodes. *IEEE Transactions on Mobile Computing*, 7(12):1519–1535, December 2008.

[GCCC81] Jr. G. C. Clark and J. B. Cain. *Error-Correction Coding for Digital Communications*. Plenum, 1981.

[GDBO12] Francisco Ganhão, Rui Dinis, Luis Bernardo, and Rodolfo Oliveira. Analytical ber and per performance of frequency-domain diversity combining, multipacket detection and hybrid schemes. *IEEE Transactions on Communications*, 60(8):2353 – 2362, 2012.

[GDE99] A. Gusmão, R. Dinis, and N. Esteves. Adaptive HARQ schemes using punctured RS codes for ATM-compatible broadband wireless technologies. In *IEEE Vehicular Technology Conference - Fall, Amsterdam, Netherlands*, volume 5, pages 2530–2535, September 19–22 1999.

[GdRH09] Riccardo De Gaudenzi and Oscar del Rio Herrero. Advances in Random Access protocols for satellite networks. *IEEE International Workshop on Satellite and Space Communications, Tuscany, Italy*, pages 331–336, September 9–11 2009.

[Gea89] D. J. Goodman and et al. Packet Reservation Multiple Access for Local Wireless Communications. *IEEE Transactions on Communications*, 37(8):885–890, July 1989.

[GJV13] Maruti Gupta, Satish C. Jha, and Rath Vannithamby. Energy impact of emerging mobile internet applications on LTE networks: issues and solutions. *IEEE Communications Magazine*, 51(2):90–97, February 2013.

[GL00] Ajay Chandra V. Gummala and John O. Limb. Wirelesss Medium Access Control Protocols. *IEEE Communications Surveys and Tutorials*, 3(2):2–15, February 2000.

[GPB+10a] Francisco Ganhão, Miguel Pereira, Luis Bernardo, Rui Dinis, Rodolfo Oliveira, and Paulo Pinto. Energy Per Useful Packet Optimization on a TDMA WSN Channel. In *IEEE International Conference on Computer Communications and Networks, Zurich, Switzerland*, pages 1–6, August 2–5 2010.

[GPB+10b] Francisco Ganhão, Miguel Pereira, Luis Bernardo, Rui Dinis, Nuno Souto, João Silva, Rodolfo Oliveira, and Paulo Pinto. Energy Per Useful Packet Optimization on a TDMA HAP Channel. In *IEEE Vehicular Technology Conference (VTC) Fall, Ottawa, Canada*, pages 1–6, September 6–9 2010.

[GPB+11a] Francisco Ganhão, Miguel Pereira, Luis Bernardo, Rui Dinis, Rodolfo Oliveira, and Paulo Pinto. Performance of Hybrid ARQ for NDMA Access Schemes with Uniform Average Power Control. *ACN Journal of Communications*, 6(9):691–699, December 2011.

[GPB+11b] Francisco Ganhão, Miguel Pereira, Luis Bernardo, Rui Dinis, Rodolfo Oliveira, and Paulo Pinto. Performance of Hybrid ARQ for Network Diversity Multiple Access Schemes. In *International Conference on Computer Communications and Networks (ICCCN), Maui, Hawaii*, pages 1–6, July 31–August 4 2011.

[GPB+13] Francisco Ganhão, Miguel Pereira, Luis Bernardo, Rui Dinis, Rodolfo Oliveira, and Paulo Pinto. Performance Analysis of an Hybrid ARQ Adaptation of NDMA Schemes. *IEEE Transactions on Communications*, 61(8):3304 – 3317, August 2013.

[GS87] D. J. Goodman and A. Saleh. The Near/Far Effect in Local ALOHA Radio Communications. *IEEE Transactions on Vehicular Technology*, 36(1):19–27, February 1987.

[GTDE07] A. Gusmão, P. Torres, R. Dinis, and N. Esteves. A Turbo FDE Technique for Reduced-CP SC-Based Block Transmission Systems. *IEEE Transactions on Communications*, 55(1):16–20, January 2007.

[GVBD13] Francisco Ganhão, José Vieira, Luis Bernardo, and Rui Dinis. Type II Hybrid-ARQ for DS-CDMA: A Discrete Time Markov Chain Wireless MAC Model. In *International Conference on Next Generation Wired/Wireless Advanced Networking, St. Petersburg, Russia*, pages 1–12, August 28–30 2013.

[GVS88] Sylvie Ghez, Sergio Verdú, and Stuart C. Schwartz. Stability Properties of Slotted Aloha with Multipacket Reception Capability. *IEEE Transactions on Automatic Control*, 33(7):640–649, July 1988.

[GWW09] Ming-Fei Guo, Xinbing Wang, and Min-You Wu. On the Capacity of κ-MPR Wireless Networks. *IEEE Transactions on Wireless Communications*, 8(7):3878–3886, July 2009.

[HA93] R. J. Haines and A. H. Aghavami. Indoor Radio Environment Considerations in Selecting a Media Access Control Protocol for Wideband Radio Data Communications. In *IEEE International Conference on Communications, Geneva, Switzerland*, volume 2, pages 990–994, May 23–26 1993.

[Hag88] J. Hagenauer. Rate-compatible Punctured Convolutional Codes and Their Applications. *IEEE Transactions on Communications*, 36(4):389–400, April 1988.

[Ham50] R. W. Hamming. Error Detecting and Correcting Codes. Technical report, Bell, 1950.

[Hol94] J. M. Holtzman. DS/CDMA Successive Interference Cancellation. In *IEEE Symposyum on Spread Spectrum Techniques and Applications, Oulu, Finland*, volume 1, pages 69–78, July 4–6 1994.

[HP97] S. Hara and R. Prasad. Overview of multicarrier CDMA. *IEEE Communications Magazine*, 35(12):126–133, December 1997.

[Inf07] Information Sciences Institute. Ns-2 network simulator (version 2.34). Software Package retrieved from http://www.isi.edu/nsnam/ns/, 2007.

[Int02] International Telecommunications Union. *Handbook on Satellite Communications, Third Edition*. Wiley, April 2002.

[JB95] P. Jung and J. Blanz. Joint Detection with Coherent Receiver Antenna Diversity in CDMA Mobile Radio Systems. *IEEE Transactions on Vehicular Technology*, 44(1):76–88, January 1995.

[JBSQNHea05a] S. Jun-Bae, L. Seung-Que, P. Nam-Hoon, and et al. Performance analysis of a type-II hybrid-ARQ in a TDMA system over a non-stationary channel. In *IEEE International Symposium on Personal, Indoor and Mobile Radio Communication, Berlin, Germany*, pages 1530–1534, September 11–15 2005.

[JBSQNHea05b] S. Jun-Bae, L. Seung-Que, P. Nam-Hoon, and et al. Queueing behavior of a type-II hybrid-ARQ in a TDMA system over a Markovian channel. In *IEEE International Conference on Wireless Networks, Communications and Mobile Computing*, volume 1, pages 362–367, June 13–16 2005.

[JZ99] R. Johannesson and K. S. Zigangirov. *Fundamentals of Convolutional Coding*. IEEE Press, 1999.

[Kal90] S. Kallel. Analysis of a type II hybrid ARQ scheme with code combining. *IEEE Transactions on Communications*, 38(8):1133–1137, August 1990.

[Kar90] P. Karn. MACA - A New Channel Access Method for Packet Radio. In *ARRL Computer Networking Conference, London, Ontario, Canada*, 1990.

[KHI83] R. Kohno, M. Hatori, and H. Imai. Cancellation Techniques of Co-Channel Interference in Asynchronous Spread Specturm Multiple Access Systems. *Electronics and Communications in Japan*, 66(5):20–29, September 1983.

[KKB96] A. Klein, G. K. Kaleh, and P. W. Baier. Zero Forcing and Minimum Mean-Square Error Equalization for Multi-User Detection in Code-Division Multiple Access Channels. *IEEE Transactions on Vehicular Technology*, 45(5):276–287, May 1996.

[KLE95] M. J. Karol, Z. Liu, and K. Y. Eng. *An Efficient Demand Assignment Multiple Access Protocol for Wireless Packet (ATM) Networks*, volume 1. Baltzer Science Publishers, 1995.

[Koh94] R. Kohno. Spatial and Temporal Filtering for Co-Channel Interference in CDMA. *IEEE International Symposyum on Spread Spectrum Techniques and Applications, Oulu, Finland*, pages 51–61, July 4–6 1994.

[LC04] S. Lin and D.J. Costello. *Error Correcting Coding: Fundamentals and Applications*. Prentice-Hall, 2004.

[LE05] Jie Luo and A. Ephremides. On the Throughput, Capacity and Stability Regions of Random Multiple Access over Standard Multi-Packet Reception Channels. In *IEEE International Symposium on Information Theory, Adelaide, Australia*, pages 2256–2260, September 4–9 2005.

[Lia] C. Liang. Explosive mobile data growth paves the way for LTE. See `http://www.bridgewatersystems.com/Assets/Downloads/Articles/Explosive%20mobile%20data%20growth%20paves%20the%20way%20for%20LTE_12Sep10.pdf`.

[Lin70] S. Lin. *An Introduction to Error-Correcting Codes*. Prentice-Hall, 1970.

[LJC85] Jr. L. J. Cimino. Analysis and Simulation of a Digital Mobile Channel Using Orthogonal Frequency Division Multiplexing. *IEEE Transactions on Commuications*, 33(7):665–675, July 1985.

[LL07] J. Li and X. Liu. A Frequency Diversity Technique for Interference Mitigation in Co-existing Bluetooth and WLAN. In *IEEE International Conference on Communications, Glasgow, Scottland*, pages 5490–5495, June 24–28 2007.

[LM02] K.B. Letaief and Y.F. Melanie. Performance Analysis of Wireless Multimedia DS/CDMA Communications with Power Control and Hybrid ARQ. In *IEEE Wireless Personal Communications, Ottawa, Ontario, Canada*, volume 3, pages 2197–2201, May 18–21 2002.

[LP05] R. Lin and A. Petropulu. A New Wireless Network Medium Access Protocol Based on Cooperation. *IEEE Transactions on Signal Processing*, 53(12):4675–4684, December 2005.

[LS04] K.-C. Lai and J. J. Shynk. Analysis of the Linear SIC for DS/CDMA Signals with Random Spreading. *IEEE Transactions on Signal Processing*, 52(12):3417–3428, December 2004.

[LWZ04] B. Lu, X. Wang, and J. Zhang. Throughput of CDMA Data Networks With Multiuser Detection, ARQ, and Packet Combining. *IEEE Transactions on Wireless Communications*, 3(5):1576–1589, May 2004.

[LY82] S. Lin and P. Yu. A Hybrid ARQ Scheme with Parity Retransmission for Error Control of Satellite Channels. *IEEE Transactions on Communications*, 30(7):1701–1719, July 1982.

[LZ09] M. Levorato and M. Zorzi. On the Performance of Ad Hoc Networks with Multiused Detection, Rate Control and Hybrid ARQ. *IEEE Transactions on Wireless Communications*, 30(7):1701–1719, July 2009.

[Mat87] E. Matricciani. Orbital Diversity in Resource-Shared Satellite Communication Systems Above 10Ghz. *IEEE Journal on Selected Areas in Communications*, 5(4):714–723, April 1987.

[Mat11] Mathworks. MATLAB. See `http://www.mathworks.com/products/matlab/`, April 2011.

[Mea98] Jo. Mikkonen and et al. The MAGIC WAND - Functional Overview. *IEEE Journal on Selected Areas in Communications*, 16(6):953–972, June 1998.

[MLG06] H. Myung, J. Lim, and D. Goodman. Single carrier FDMA for uplink wireless transmission. *IEEE Vehicular Technology Magazine*, 1(3):30–38, March 2006.

[MN95] D. J. C. MacKay and R. M. Neal. Good codes based on very sparse matrices. In *IMA Conference on Cryptography Coding*, pages 110–111, 1995.

[Mos96] S. Moshavi. Multi-user detection for DS-CDMA communications. *IEEE Communications Magazine*, 34(10):124–136, October 1996.

[MS77] F. J. MacWilliams and N. J. A. Sloane. *The Theory of Error-Correcting Codes*. Elsevier, 1977.

[MS98] J. Medbo and P. Schramm. Channel models for HIPERLAN/2 in different indoor scenarios. Technical report, ETSI, 1998.

[MV05a] M. Madueño and J. Vidal. Joint physical-MAC Layer design of the broadcast protocol in ad hoc networks. *IEEE Journal on Selected Areas in Communications*, 23(1):65–75, January 2005.

[MV05b] M. Madueño and J. Vidal. PHY-MAC performance of a MIMO network-assisted multiple access scheme. In *IEEE Workshop on Signal Processing Advances in Wireless Communications, Barcelona, Spain*, Month 5–8 2005.

[Nan90] S. Nanda. Analysis of Packet Reservation Multiple Access: Voice and Data Integration for Wireless Networks. In *IEEE Globecom, San Diego, California, USA*, volume 3, pages 1984–1988, December 2–5 1990.

[NGEG07] Young-Han Nam, Praveen Kumar Gopala, and Hesham El-Gamal. Resolving Collisions Via Incremental Redundancy: ARQ Diversity. In *IEEE INFOCOM, Barcelona, Spain*, pages 285–293, May 6–12 2007.

[NY95] P. Narasimhan and R. D. Yates. A New Protocol for the Integration of Voice and Data over PRMA. *IEEE Journal on Selected Areas in Communications*, 14(4):623–631, April 1995.

[ÖD06] B. Özgül and H. Deliç. Wireless Access With Blind Collision-Multiplicity Detection and Retransmission Diversity for Quasi-Static Channels. *IEEE Transactions on Communications*, 54(5):858–867, May 2006.

[PBD+09] M. Pereira, L. Bernardo, R. Dinis, R. Oliveira, P. Carvalho, and P. Pinto. A MAC Protocol for Half-Duplex Multi-Packet Detection in SC-FDE Systems. In *IEEE Vehicular Technology Conference Spring, Barcelona, Spain*, pages 1–6, April 26–29 2009.

[PBD+10] M. Pereira, L. Bernardo, R. Dinis, R. Oliveira, P. Carvalho, and P. Pinto. Performance of packet combining ARQ error control in a TDMA SC-FDE system. *IEEE Wireless Communications and Networking Conference, Sydney, Australia*, pages 1–6, April 18–21 2010.

[PBD+12] Miguel Pereira, Luis Bernardo, Rui Dinis, Rodolfo Oliveira, Paulo Carvalho, and Paulo Pinto. Performance of Diversity Combining ARQ Error Control in a TDMA SC-FDE System. *IEEE Transactions on Communications*, 60(3):735–746, March 2012.

[PDN10] P. Pedrosa, R. Dinis, and F. Nunes. Analytical Performance Evaluation of a Class of Receivers with Joint Equalization and Carrier Frequency Synchronization. In *IEEE Sarnoff Symposyum, Princeton, New Jersey, USA*, April 12–14 2010.

[Pet61] W.W. Peterson. *Error-Correcting Codes*. MIT Press, 1961.

[Pet96] D. Petras. Performance Evaluation of Medium Access Control Protocols for Mobile Broadband Systems. See `http://www.comnets.rwth-aachen.de/petras/Publications`, January 1996.

[Pey99] Hassan Peyravi. Medium Access Control Protocols Performance in Satellite Communications. *IEEE Communications Magazine*, 37(3):62–71, March 1999.

[PH94] P. Patel and J. Holtzman. Performance Comparison of a DS/CDMA System Using a Successive Interference Cancellation (IC) Scheme and a Parallel IC Scheme under Fading. In *IEEE International Conference on Communications, New Orleans, Louisiana, USA*, pages 510–514, May 1–5 1994.

[PJ72] W. W. Peterson and E. J. Weldon Jr. *Error-Correcting Codes*. MIT Press, 1972.

[PM96] A. L. A. Pinheiro and J. R. B. De Marca. Fair Deterministic Packet Access Protocol: F-RAMA. *IET Electronic Letters*, 32(25):2310–2311, December 1996.

[PRC86] C. Parvey, R. Rice, and E. Cummins. A performance evaluation of the PDAMA satellite access protocol. In *IEEE INFOCOM, Miami, Florida, USA*, pages 580–589, April 1986.

[PV00] R. Prakash and V.V. Veeravalli. Analysis of code division random multiple access systems with packet combining. In *Asilomar Conference on Signals, Systems & Computers, Pacific Grove, California, USA*, volume 2, pages 1225–1229, October 29 - November 1 2000.

[QSCea05] S. Quaglieri, M. De Sanctis, E. Cianca, and et al. Performance and Energy Efficiency of Hybrid ARQ Over Ground-HAP Links. In *IEEE Aerospace Conference, Big Sky, Montana, USA*, pages 1313–1321, March 5–12 2005.

[Qur85] S. U. H. Qureshi. Adaptive Equalization. *IEEE Proceedings*, 17(9):399–410, September 1985.

[RGS87] B. Ramamurthi, D. J. Goodman, and A. Saleh. Perfect Capture for Local Radio Communications. *IEEE Journal on Selected Areas in Communications*, 5(5):806–813, June 1987.

[Rob72] L. G. Roberts. ALOHA Packet Systems with and Without Slots and Capture. *ARPANET System Note 8*, June 1972.

[RSU01] T. J. Richardson, A. Shokrollahi, and R. Urbanke. Design of capacity approaching irregular low-density parity-check codes. *IEEE Transactions on Information Theory*, 47(2):619–637, February 2001.

[RU08] T. Richardson and R. Urbanke. *Modern Coding Theory*. Cambridge Univ. Press, 2008.

[Sch79] K. S. Schneider. Optimum Detection of Code Division Multiplexed Signals. *IEEE Transactions on Aerospace Electrical Systems*, 15(1):181–185, January 1979.

[SD06] P. Silva and R. Dinis. Frequency-Domain Multiuser Detection for CP-Assisted DS-CDMA Signals. In *IEEE Vehicular Technology Conference Spring, Melbourne, Australia*, pages 2103–2108, May 7–10 2006.

[SD11] P. Silva and R. Dinis. Frequency-Domain Multiuser Detection for Highly Overloaded DS-CDMA Systems. In *IEEE Vehicular Technology Conference Fall, San Francisco, California, USA*, September 5–8 2011.

[SDSC08] N. Souto, R. Dinis, J.C. Silva, and P. Carvalho. A High Throughput Technique for OFDM Systems. In *IEEE Wireless Communications and Networking Conference, Las Vegas, Nevada, USA*, pages 301–306, March 31–April 3 2008.

[SG01] P. Struhsaker and K. Griffin. Analysis of PHY Waveform Peak to Mean Ratio and Impact on RF Amplification. Technical report, IEEE, 2001.

[Sha48] C.E. Shannon. A Mathematical Theory of Communication. Technical report, Bell, 1948.

[Sha06] Jacob Sharony. Introduction to Wireless MIMO - Theory and Applications, see `http://www.ieee.li/pdf/viewgraphs/wireless_mimo.pdf`. Technical report, CEWIT, 2006.

[SKJ94] H. Sari, G. Karam, and I. Jeanclaude. Frequency-Domain Equalization of Mobile Radio and Terrestrial Broadcast Channels. In *IEEE Globecom, San Francisco, California, USA*, pages 1–5, November 28–December 2 1994.

[SKJ95] H. Sari, G. Karam, and I Jeanclaude. Transmission Techniques for Digital Terrestrial TV Broadcasting. *IEEE Communications Magazine*, 33(2):100–109, February 1995.

[SR82] B. Saeki and I. Rubin. An Analysis of a TDMA Channel Using Stop-and-Wait, Block, and Select-and-Repeat ARQ Error Control. *IEEE Transactions on Communications*, 30(5):1162–1173, May 1982.

[SRGM06] Ramiro Samano-Robles, Mounir Ghogho, and Des.C. McLernon. P-Persistent Stabilisation for Wireless Network Diversity Multiple Access Protocol. In *IEEE Signal Processing Advances in Wireless Communications*, pages 1–5, July 2–5 2006.

[SRGM07] Ramiro Samano-Robles, Mounir Ghogho, and D.C. McLernon. Quality of Service in Wireless Network Diversity Multiple Access Protocols Based on a Virtual Time-Slot Allocation. In *IEEE International Conference on Communications, Glasgow, Scottland*, pages 5843–5848, June 24–28 2007.

[SRGM08a] Ramiro Samano-Robles, Mounir Ghogho, and D.C. McLernon. A Multiaccess Protocol assisted by Retransmission Diversity and Multipacket Reception. *IEEE International Symposyum on Wireless Pervasive Computing, Las Vegas, Nevada, USA*, pages 189–193, March 31–April 4 2008.

[SRGM08b] Ramiro Samano-Robles, Mounir Ghogho, and D.C. McLernon. An Infinite User Model for Random Access Protocols assisted by Multipacket Reception and Retransmission Diversity. In *IEEE Workshop on Signal Processing Advances in Wireless Communications, Recife, Brasil*, pages 111–115, July 6–9 2008.

[SRGM08c] Ramiro Samano-Robles, Mounir Ghogho, and D.C. McLernon. Cooperative and Sequential User Detection for Wireless Network Diversity Multiple Access Protocols. In *IEEE International Symposyum on Wireless Pervasive Computing, Santorini, Italy*, pages 189–193, July 6–9 2008.

[SRGM09] Ramiro Samano-Robles, Mounir Ghogho, and D.C. McLernon. Wireless Networks With Retransmission Diversity and Carrier-Sense Multiple Access. *IEEE Transactions on Signal Processing*, 57(9):3722–3726, April 2009.

[SRK03] Sanjay Shakkotai, Theodore S. Rappaport, and Peter C. Karlsson. Cross-Layer Design for Wireless Networks. *IEEE Communications Magazine*, 41(10):74–80, October 2003.

[SS96] M. Sipser and D. A. Spielman. Expander codes. *IEEE Transactions on Information Theory*, 42(6):1645–1646, November 1996.

[SS05] E. Sofer and Y. Segal. Tutorial on Multi Access OFDM (OFDMA) Technology. Technical report, DOC: IEEE 802.22-05-0005r0, 2005.

[SS07] Y. Sun and J. Shi. Retransmission Diversity in Large CDMA Random Access Systems. *IEEE Transactions on Signal Processing*, 55(7):3471–3483, July 2007.

[Stü00] G. Stüber. *Principles of Mobile Communication, Second Edition*. Springer, 2000.

[SW95] S. Souissi and S.B. Wicker. A Diversity Combining DS/CDMA System with Convolutional Encoding and Viterbi Decoding. *IEEE Transactions on Vehicular Technology*, 44(2):304–312, May 1995.

[TA07] K. Takeda and F. Adachi. HARQ Throughput Performance of Multicode DSCDMA with MMSE Turbo Equalization. In *IEEE Vehicular Technology Conference Spring, Dublin, Ireland*, pages 1603–1607, April 22–25 2007.

[Tak62] L. Takács. *Introduction to the Theory of Queues*. Oxford University Press, 1962.

[Tan81] R. M. Tanner. A recursive approach to low complexity codes. *IEEE Transactions on Information Theory*, 27(5):533–547, September 1981.

[Tan03] Andrew S. Tanenbaum. *Computer Networks, Fourth Edition*. Prentice Hall, 2003.

[Tau63] S. Tauber. On Multinomial Coefficients. *The America Mathematical Monthly*, 70(10):1058–1063, December 1963.

[Tim11] Financial Times. Verizon profits surge to $ 1.4bn. See `http://www.ft.com/cms/s/0/41d7cb5a-6c1d-11e0-b36e-00144feab49a.html#axzz1MoogtwSP`, April 21 2011.

[TK75] F. A. Tobagi and L. Klienrock. Packet Switching in Radio Channels: Part II - The Hidden Terminal Problem in Carrier Sense Multiple Access and the Busy Tone Solution. *IEEE Transactions on Communications*, 23(12):1417–1433, December 1975.

[TWT08] J. Thornton, A.D. White, and T.C. Tozer. A WiMAX Payload for High Altitude Platform Experimental Trials. *EURASIP Journal on Wireless Communications and Networking*, 2008.

[TZB00] M. Tsatsanis, R. Zhang, and S. Banerjee. Network Assisted Diversity for Random Access Wireless Networks. *IEEE Transactions on Signal Processing*, 48(3):702–711, March 2000.

[Ung82] G. Ungerboeck. Channel coding with multilevel/phase signals. *IEEE Transactions on Information Theory*, 28(1):55–67, January 1982.

[VA90] M. K. Varanasi and B. Aazhang. Multistage detection in asynchronous code-division multiple access communications. *IEEE Transactions on Communications*, 38(4):509–519, April 1990.

[Ver86] S. Verdu. Minimum probability of error for asynchronous Gaussian multiple-access channels. *IEEE Transactions on Information Theory*, 32(1):85–96, January 1986.

[VGB+13] José Vieira, Francisco Ganhão, Luis Bernardo, Rui Dinis, Marko Beko, Rodolfo Oliveira, and Paulo Pinto. Energy-Efficient QoS Provisioning in Random Access Satellite NDMA Schemes. In *IEEE International Conference on Computer Communications and Networks, Nassau, The Bahamas*, pages 1–9, July 30–August 2 2013.

[Vit90] A. J. Viterbi. Very Low Rate Convolutional Codes for Maximum Theoretical Performance of Spread-Spectrum Multiple-Access Channels. *IEEE Journal on Selected Areas in Communications*, 8(4):641–649, April 1990.

[VST+05] E. Visotsky, Y. Sun, V. Tripathi, M. Honig, and R. Peterson. Reliability-based incremental redundancy with convolutional codes. *IEEE Transactions on Communications*, 53(6):987–997, June 2005.

[VSW05] N. Varnica, E. Soljanin, and P. Whiting. LDPC code ensembles for incremental redundancy hybrid ARQ. In *IEEE International Symposyum on Information Theory, Adelaide, Australia*, pages 995–999, September 4–9 2005.

[WDH96] H. Y. Wu and A. Duel-Hallen. Performance Comparison of Multi-User Detectors with Channel Estimation for Flat Rayleigh Fading CDMA. *Springer Journal of Wireless Personal Communications*, 6:137–160, 1996.

[Wea66] G. Wu and et al. An R-ISMA Integrated Voice/Data Wireless Information System with Different Packet Generation Rates. In *IEEE International Conference on Communications, Dallas, Texas, USA*, volume 3, pages 1263–1269, June 23–27 1966.

[WG93] W. C. Wong and D. J. Goodman. Integrated Data and Speech Transmission using Packet Reservation Multiple Access. In *IEEE International Conference on Communications, Geneva, Switzerland*, volume 1, pages 172–176, May 23–26 1993.

[WHY06] Qin Wang, M. Hempstead, and W. Yang. A Realistic Power Consumption Model for Wireless Sensor Network Devices. In *IEEE Sensor and Ad Hoc Communications and Networks, Reston, Vancouver*, volume 1, pages 286–295, September 28 2006.

[WJ65] J. M. Wozencraft and I. M . Jacobs. *Principles of Communication Engineering*. Wiley, 1965.

[WMF93] G. Wu, K. Mukumoto, and A. Fukuda. An Integrated Voice and Data transmission System with Idle Signal Multiple Access - Dynamic Analysis. *IEEE Transactions on Communications*, 76(11):1398–1407, November 1993.

[WPS09] M.Z. Win, P.C. Pinto, and L.A. Shepp. A Mathematical Theory of Network Interference and Its Applications. *IEEE Proceedings*, 97(2):205–230, February 2009.

[XSR90] Z. Xie, R. T. Short, and C. K. Rushforth. A Family of Suboptimum Detectors for Coherent Multi-User Communications. *IEEE Journal on Selected Areas in Communications*, 8(4):683–690, April 1990.

[YG05] Yingqun Yu and Georgios B. Giannakis. SICTA: A 0.693 Contention Tree Algorithm Using Successive Interference Cancellation. In *IEEE INFOCOM, Miami, Florida, USA*, volume 3, pages 1908–1916, March 13–17 2005.

[YH05] L. Yang and L. Hanzo. Performance of Broadband Multicarrier DS-CDMA Using Space–Time Spreading-Assisted Transmit Diversity. *IEEE Wireless Communications Magazine*, 4(3):885–894, March 2005.

[YMG08] Jennifer Yick, Biswanath Mukherjee, and Dipak Ghosal. Wireless Sensor Network Survey. *ACM Computer Networks*, 52(12):2292–2330, August 2008.

[YMMZ09] Raymond Yim, Neelesh B. Mehta, Andreas F. Molisch, and Jinyun Zhang. Dual Power Multiple Access with Multipacket Reception using Local CSI. *IEEE Transactions on Wireless Communications*, 8(8):4078–4088, August 2009.

[YYL+10] J. Yao, X. Yang, J. Li, Z. Li, and Y. Zhang. Blind Collision Resolution Using Cooperative Transmission. In *IEEE Vehicular Technology Conference Spring, Taipei, Taiwan*, pages 1–5, May 16–19 2010.

[ZA91] Z. Zhang and A. S. Acampora. Performance of a Modified Polling Strategy for Broadband Wireless Lans in a Harsh Fading Environment. In *IEEE GLOBECOM, Phoenix, Arizona*, volume 2, pages 1141–1146, December 2–5 1991.

[Zha10] Ying Jun Angela Zhang. Multi-Round Contention in Wireless LANs with Multipacket Reception. *IEEE Transactions on Wireless Communications*, 9(4):1503–1513, April 2010.

[ZLC08] Ying Jun Angela Zhang, Soung Chang Liew, and Da Rui Chen. Delay Analysis for Wireless Local Area Networks with Multipacket Reception under Finite Load. In *IEEE Globecom, New Orleans, Louisiana*, November 30 – December 4 2008.

[ZT02] R. Zhang and M. Tsatsanis. Network-Assisted Diversity Multiple Access in Dispersive Channels. *IEEE Transactions on Communications*, 50(4):623–632, April 2002.

[ZT03] Qing Zhao and Lang Tong. A Multiqueue Service Room MAC Protocol for Wireless Networks with Multipacket Reception. *IEEE/ACM Transactions on Networking*, 11(1):125–137, February 2003.

[ZT04] Qing Zhao and Lang Tong. A Dynamic Queue Protocol for Multiaccess Wireless Networks with Multipacket Reception. *IEEE Transactions on Wireless Communications*, 3(6):2221–2231, November 2004.

[ZWL99] Q. Zhang, T. F. Wong, and J. S. Lehnert. Performance of type-II hybrid ARQ protocol in slotted DS-SSMA packet radio systems. *IEEE Transactions on Communications*, 47(2):281–290, February 1999.

[ZZL09] Y. Jun Angela Zhang, Peng Xuan Zheng, and Soung Chang Liew. How Does Multiple-Packet Reception Capability Scale the Performance of Wirelesss Local Area Networks. *IEEE Transactions on Mobile Computing*, 8(7):923–935, July 2009.